Cambridge/Boston, Massachusetts

CSW2018

COMPOUND SEMICONDUCTOR WEEK 2018

45th International Symposium on Compound Semiconductors

30th International Conference on Indium Phosphide and Related Materials

Massachusetts Institute of Technology

CSW2018 CAMBRIDGE BOSTON

IEEE

Office of Naval Research ONR Science & Technology

MTL microsystems technology laboratories

MAY 29-JUNE 1, 2018

Massachusetts Institute of Technology

Cambridge, MA, USA

NSF

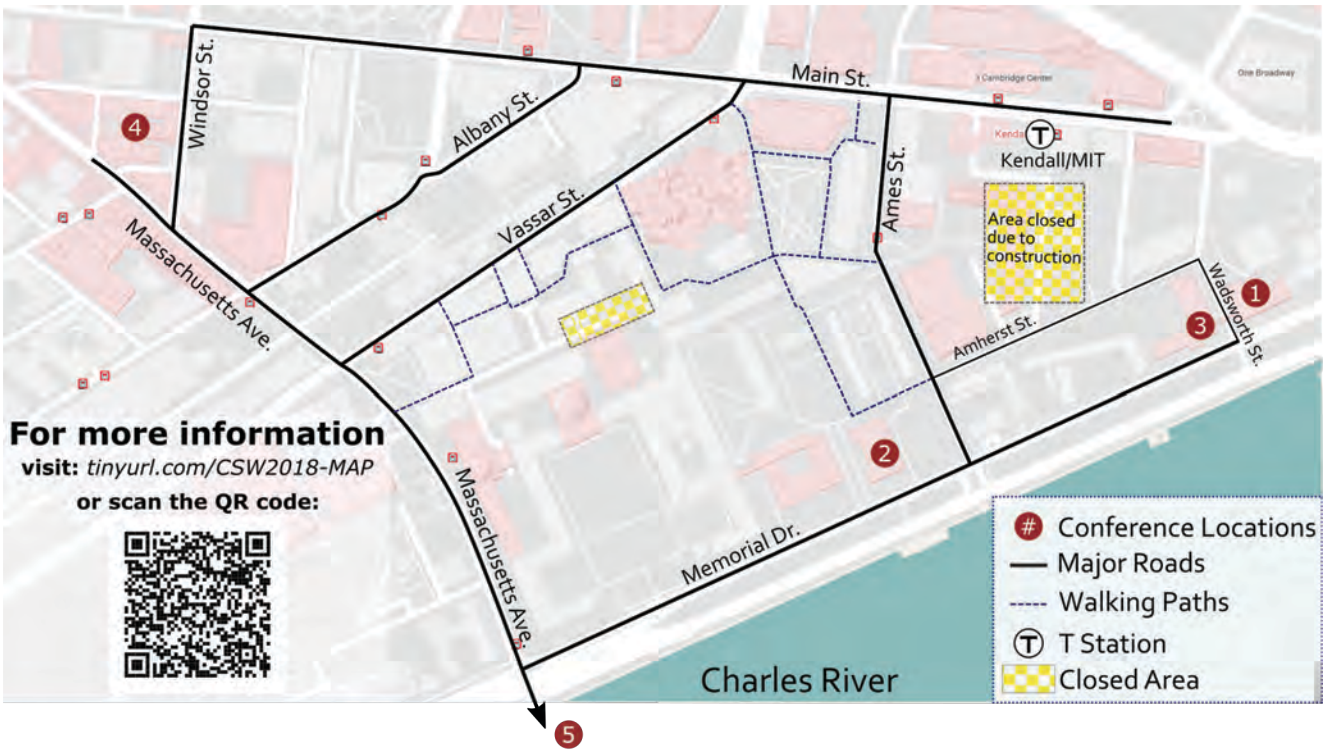

1. Samberg Conference Center (Bldg. E52)

50 Memorial Dr, Cambridge, MA

- Invited and Contributed Talks in Salon M and T (7th floor), and DR3&4 and DR5&6 (6th floor)
- Industrial Exhibition (Wed-Fri) in Salon I (7th floor)

2. Walker Memorial (Bldg. 50)

142 Memorial Dr, Cambridge, MA

- Plenary (Tues) in Morss Hall
- Poster Sessions (Wed and Fri) in Morss Hall

3. Tang Center (Bldg. E51)

2 Amherst St, Cambridge, MA

- Invited and Contributed Talks (Thurs) for session B5 and B6 in Wong Auditorium
- Rump Session (Wed) in Wong Auditorium

4. MIT Museum (Bldg. N51)

265 Massachusetts Ave, Cambridge, MA

- Welcome Reception (Tues)

5. Fenway Park

4 Yawkey Way, Boston, MA

- Conference Banquet (Thur)

Table of Contents

WELCOME

On behalf of the entire Organizing Committee, we would like to welcome you to the Compound Semiconductor Week (CSW) 2018 in Cambridge, Massachusetts. As in previous years, CSW 2018 will bring together the *45th International Symposium on Compound Semiconductors (ISCS)* and the *30th International Conference on Indium Phosphide and Related Materials (IPRM)*. It aims to be the premier forum for the dissemination of research findings on all aspects of compound semiconductors. In this way, it continues the tradition of the successful CSW 2017 in Berlin, Germany, and CSW 2016 in Toyama, Japan.

CSW 2018 will start on Tuesday morning, May 29th, with a short course on "*Materials and Devices for Neuromorphic Applications*," organized by Professor Jeehwan Kim from MIT. The short course will be followed by the official opening of the conference and the plenary session. We are very fortunate to have four outstanding plenary speakers this year: Prof. Hiroshi Fujioka of the University of Tokyo with a talk on *Sputtering Epitaxial Growth of III Nitrides and Its Device Applications*; Prof. Evelyn Hu of Harvard University, who will speak about *Semiconductors at the Frontiers of Quantum Technologies*; Prof. Mark Rodwell, of the University of California, Santa Barbara, who will present his vision on *Transistors: mm-Wave and Low-Power VLSI* and lastly Dr. Dario Gil of IBM, who will discuss *The Physics of AI and Quantum Computing*. The plenary session will be followed by the ISCS/IPRM Award ceremony and reception.

From Wednesday through Friday, CSW will highlight the state-of-the-art in compound semiconductors thanks to 48 invited talks, 147 contributed oral presentations, and 140 poster presentations. On Wednesday evening, Prof. Eugene Fitzgerald (MIT) will chair a lively rump session on the future of III-V semiconductors. On Friday, the conference will also host a Focus Session on *Ga_2O_3 Materials and Devices,* organized by Dr. Masataka Higashiwaki (NICT). For those attendees who signed up for it, Thursday afternoon will feature an excursion to beautiful downtown Boston and the conference banquet at historic Fenway Park.

We extend our sincere thanks and appreciation to members of the Program Committee and International Steering Committees for their tireless efforts in assembling a high quality technical program. We also thank the exhibitors and sponsors for their participation and support, and gratefully acknowledge the support provided by the Office of Naval Research and the National Science Foundation.

We wish you all a pleasant stay in the Cambridge/Boston area, and an enjoyable week attending CSW 2018, mingling with your colleagues, and pushing the limits of Compound Semiconductors.

Tomás Palacios
Conference Chair

Srabanti Chowdhury
Publication Chair

Grace (Huili) Xing
Technical Program Chair

Jeehwan Kim
Short Course Organizer

Masataka Higashiwaki
Ga_2O_3 Focus Session Organizer

Yong-Hang Zhang
Regional Chair for America

Tetsuya Suemitsu
Regional Chair for Asia and Australia

Eva Monroy
Regional Chair for Europe and Africa

GENERAL INFORMATION

Welcome to the Massachusetts Institute of Technology! The campus community has joined in an effort to make your stay a pleasant and rewarding experience. We hope that you will take the opportunity to explore the campus and local area, and that you will enjoy your time here.

CSW PROGRAM SCHEDULE

Please refer to this program book for details regarding session location and special events. You can find a campus map behind the program cover with specific information about the conference.

GUIDEBOOK APP (CSW 2018)

CSW 2018 will feature an iOS and Android App for all registered attendees accessible through your mobile devices. This App will come in handy to easily bookmark and attend the sessions/talks of your interest. The App also contains information regarding CSW evening events, hotels and restaurants nearby. Attendees can easily download this App from the App store in their iOS or Android devices. First, search for the "Guidebook" app, enter the 'passphrase' (security code) which will be provided during the confernce. Once you are logged in, you can access the CSW 2018 app.

REGISTRATION HOURS

Short Course Registration:
Tuesday, May 29, 2018 8am-10am
Samberg Conference Center (Building E52 6th floor, 50 Memorial Drive, Cambridge, MA)

MAIN REGISTRATION:
Tuesday, May 29, 2018 from 12:30pm-5pm
Walker Memorial (Building 50 1st floor, 142 Memorial Drive, Cambridge, MA)
There are two entrances into Walker Memorial, the Main Entrace (142 Memorial Drive) which faces the Charles River, and the back entrance, closer to Amherst Street (★Registration begins here).

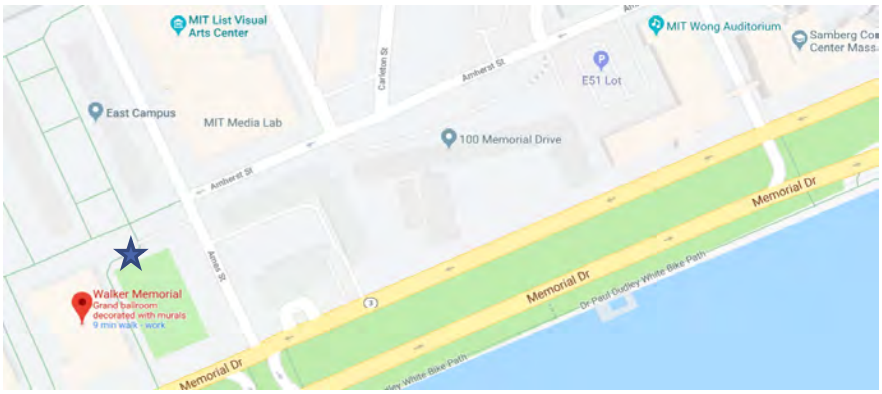

Wednesday-Friday, May 30-June 1, 2018 8am-5pm
Samberg Conference Center (Building E52 7th floor, 50 Memorial Drive, Cambridge, MA)

INTERNET ACCESS:

The MIT GUEST Wireless Network

Internet access can be found through the MIT Guest Network at the Samberg Conference Center and most other locations on campus.

This network does not require authentication and is not encrypted. The network is provided for visitors and short-term guests and has limited access to the Internet and MIT resources.

It is easy to connect to the MIT GUEST wireless network with a wireless device. Since there are no restrictions to connecting, your device should be able to "see" the network as one of the open wireless options and connect instantly.

Eduroam Network

Visitors to MIT from eduroam-participating institutions may connect to the on-campus "eduroam" WiFi network using their credentials for their home institution.

TRANSPORTATION: *BOSTON T-LINE AND BUS LINE*

Public transportation in Cambridge and Boston works very well and, most of the times, it is the fastest transportation method. The closest T-stop (ie. metro stop) to MIT is the Kendall/MIT station along the Red line. It is located at 300 Main Street, Cambridge, less than 5 min walk from the Samberg Conference Center. The Red line connects MIT to Downtown Boston, the Green Line, and Harvard University.

The #1 bus line connects MIT to Boylston Street and Harvard (opposite direction) routinely stops at 77 Massachusetts Avenue (one of the main entrances to MIT). This is the best way to reach MIT for attendees staying at the Sheraton hotel.

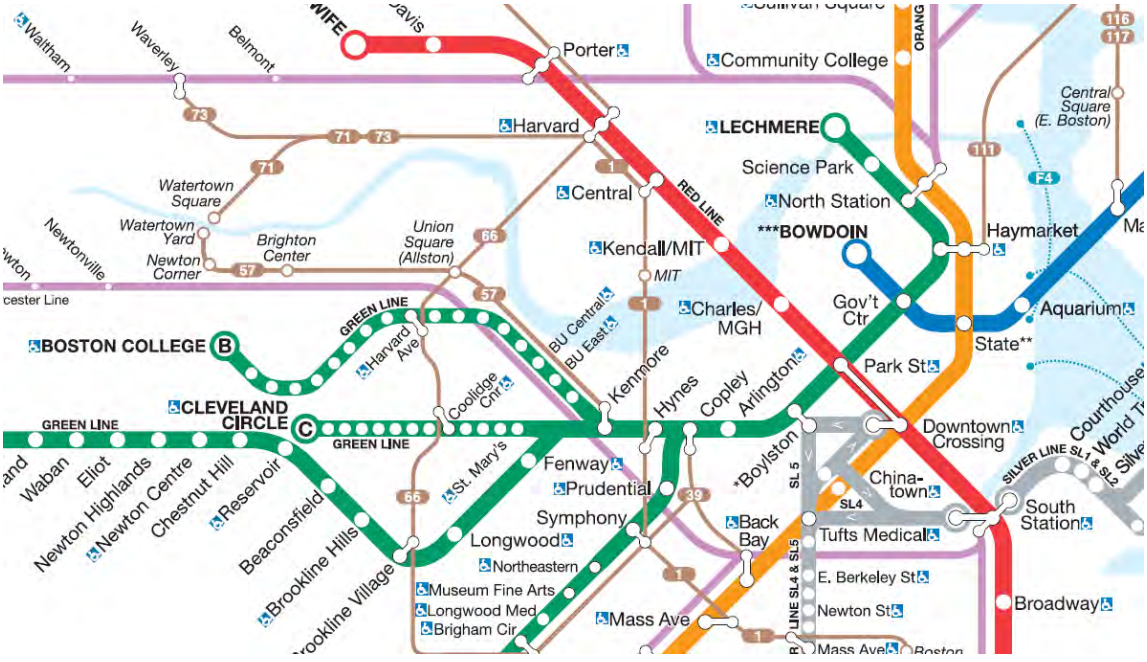

TRANSPORTATION TO AIRPORT

Airport shuttles: The Sheraton Hotel offers a shuttle service that departs from the Hynes Convention Center from 5:00am to 9:00pm. The shuttle costs $7.50 with credit card (no cash), or $3 through an MBTA pass. No advance reservations can be made.

If you have enough time for the trip (~1 hour), you can go to the airport by taking the Red T-line to South Station, and there the Silver bus line to the airtport. This will cost $2.25. If you prefer to take a taxi from MIT, it will take you around 20 min and approximately $35.

Uber/Lyft are very efficient and economical ways to move around Boston and/or go to the airport (approximately $20 from MIT). You can download the apps by scanning the QR code below**.**

iOS devices

UBER QR code

LYFT QR code

Android devices

UBER QR code

LYFT QR code

PARKING INFORMATION

Parking in Cambridge/Boston is expensive and traffic can be bad during rush hour. Therefore, we strongly advise you not to get a car while in Boston. However, if you have a car and need parking while at the conference, these are some parking garages nearby.

Parking Structure Location-Name	Distance from Samberg Conference Center
1 Memorial Drive	0.16 km, 0.1 miles
5 Cambridge Center – East Garage	0.48 km, 0.3 miles
4 Cambridge Center	0.64 km, 0.4 miles
7 Cambridge Center – West Garage	0.80 km, 0.5 miles
10 Cambridge Center – North Garage	0.80 km, 0.5 miles
245 Riverview Garage	1.29 km, 0.8 miles
55 Franklin Street Garage – University Park	1.77 km, 1.1 miles

MEALS

Your conference registration fee includes the Welcome/Award Reception on Tuesday evening, daily refreshment breaks and catered lunches on Wednesday, Thursday and Friday, hors d'oeuvre and finger food during the Wednesday poster session, and Breakfast during the Friday poster session. The Banquet Thursday evening requires the purchase of an additional ticket for $50. *Please see registration desk if tickets are still available.

ADDITIONAL DINING OPTIONS

Below you can find information on several restaurants recommended by the CSW organizers:

Restaurant Name	Cuisine	Distance (from Samberg)	Location (all in Cambridge)	Takeout or Sitdown	Price
Saloniki	Greek	1.29 km, 0.8 miles	181 Mass. Ave	Both, Casual	$
Bailey and Sage	Vegetarian (Lunch only)	0.48 km, 0.3 miles	355 Main St	Both, Casual	$
Flour	Pastry, Coffee, Sandwiches	1.45 km, 0.9 miles	190 Mass. Ave	Both, Casual	$
Chipotle	Mexican	0.32 km,0.2 miles	50 Broadway	Both, Casual	$
Za	Pizza	0.48 km, 0.3 miles	350 Third St	Sitdown	$$
Thelonius Monkfish	Asian Fusion	0.48 km, 0.3 miles	524 Mass Ave	Sitdown	$$
Asmara	Ethiopian	2.25 km, 1.4 miles	739 Mass. Ave	Sitdown	$$
Legal Sea Foods	Seefood	0.64 km, 0.4 miles	355 Main St	Sitdown	$$$
Catalyst Restaurant	American, Dessert, Breakfast/Brunch	1.28 km, 0.8 miles	300 Technology Square,	Sitdown	$$$

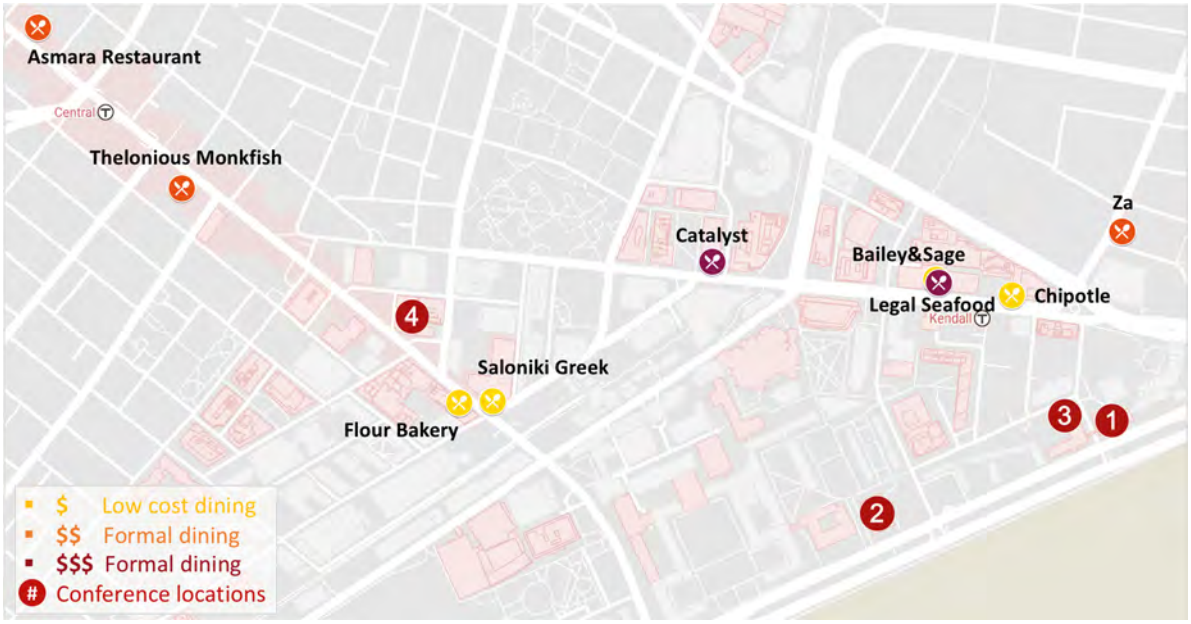

EXHIBITION SCHEDULE

The exhibit area will be located in the Samberg Conference Center on the 7th floor, Salon I
Our exhibitors play a key role in supporting the conference. Please stop by their tables and say thank you!

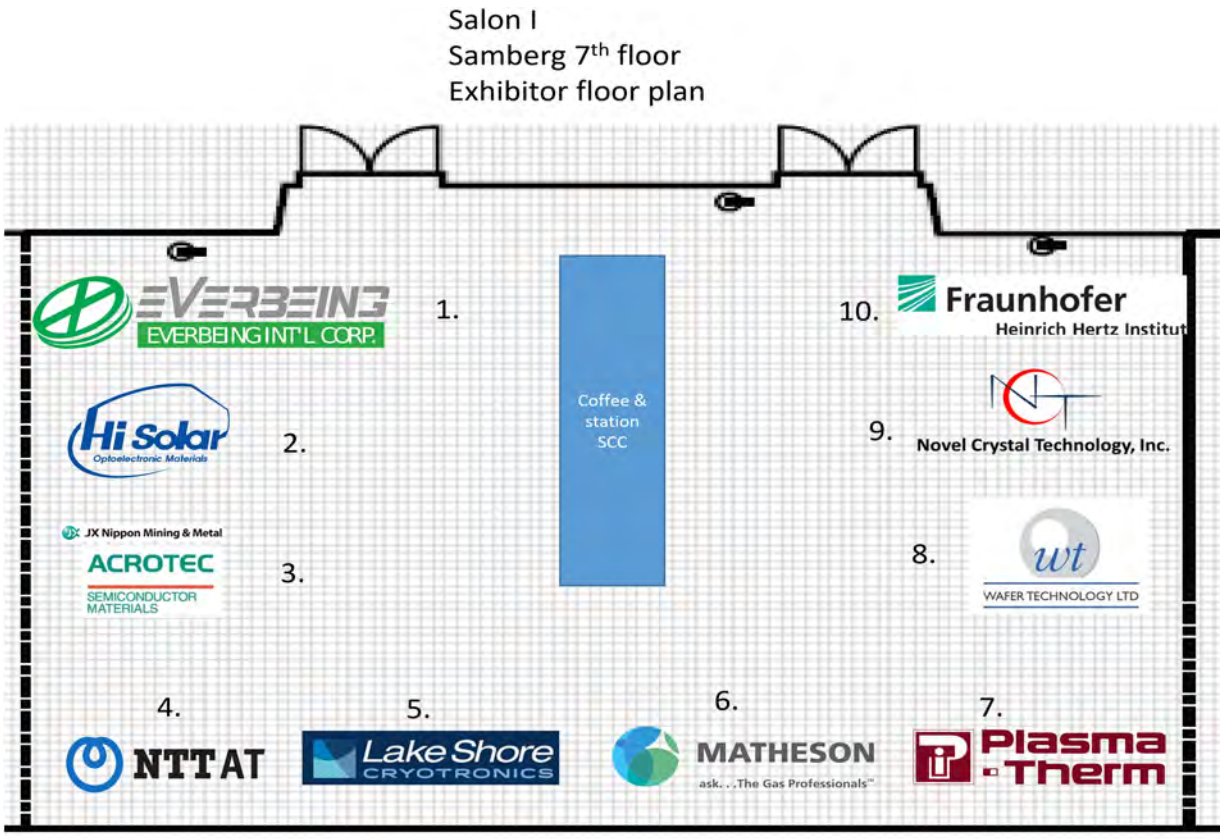

Wednesday, May 30th	8:30AM - 5:00PM	Samberg Conference Center 7th floor (Salon **I**)
Thursday, May 31th	8:30AM - 1:00PM	Samberg Conference Center 7th floor (Salon **I**)
Friday, June 1st	10:00AM - 1:30PM	Samberg Conference Center 7th floor (Salon **I**)

FULL CSW 2018 ABSTRACTS

The full 2-page abstracts for all the papers presented at CSW 2018 are available through the CSW2018 app. This app can be downloaded from the Android and Apple App Stores as discussed in page 6. The conference proceedings with the full 2-page abstracts can also be downloaded from the following link: https://www.csw2018.org/proceedings.

CSW WELCOME/AWARD RECEPTION

We will hold the CSW Welcome/Award Reception at the MIT Museum (265 Massachusetts Ave, Cambridge, MA 02139) on Tuesday, May 29th, from 6:30pm to 8:30pm. We will all be walking there together after the Award ceremony and group photograph. It is about a 15 min walk. There will also be buses available for those attendees who prefer to take the bus.

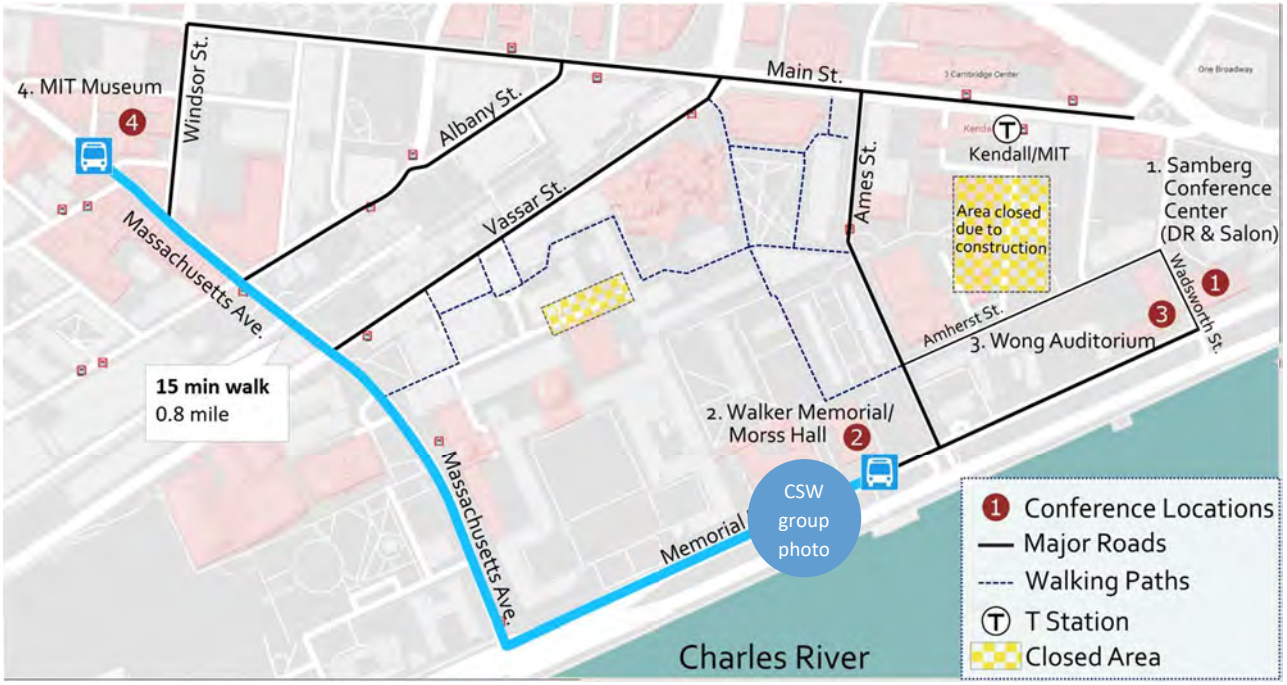

The MIT Museum has just over a million objects in its collections, including the world's most comprehensive collection of holograms, the Hart Nautical Collection, and the Institute's Architecture and Design Collection, as well as one of the largest collections of robots in the world.

In addition to its regular exhibition, the MIT Museum is holding an exciting special exhibit this month that we urge you to attend called "*The Beautiful Brain: The Drawings of Santiago Ramón y Cajal.*" Santiago Ramón y Cajal was a Spanish scientist who made monumental discoveries regarding the brain and nervous system. He won the Nobel Prize in 1906. Not only was he a founder of the neuroscience field we know today, but he was also an artist who created detailed drawings of the brain's structure to better understand its function.

TECHNICAL PROGRAM

The scientific program of CSW 2018 consists of plenary and invited talks as well as contributed oral and poster presentations. Plenary talks are 45 minutes each, while invited talks will be divided into 25 minutes of presentation and 5 minutes for questions and discussion. The contributed oral presentation will be divided into 12 minute presentations with additional 3 minutes for questions and discussion.

POSTER SESSION

Two (2) Poster sessions are scheduled for Wednesday afternoon and Friday morning. We will have 4 posters per easle, two on each side. The maximum dimensions for each poster are 42 in x 42 in (106 cm x 106cm). Both sessions will take place at the **Walker Memorial Building (50-140)** in 142 Memorial Dr, Cambridge, MA. Poster presenters should set up their posters 30 min before the session and take them down inmediately after the session.

First (1st) Poster presentation	Second (2nd) Poster presentation
Walker Memorial Hall (50-140)	**Walker Memorial Hall (50-140)**
Wednesday, May 30th	Friday, June 1st
5pm-6:30pm	8:30am-10am
Poster set up: 4:30pm, 5/30	Poster set up: 8am, 6/1
Poster take out: 6:30pm, 5/30	Poster take out: 10am, 6/1

FOCUS SESSION ON GA_2O_3

Nowadays, gallium oxide (Ga_2O_3) has gained great attention as a new ultra-wide bandgap semiconductor. The big appeal of Ga_2O_3 from the viewpoint of material properties is its extremely large bandgap of over 4.5 eV. The availability of large melt-grown Ga_2O_3 bulk single crystals is another important benefit, because low-cost mass production of high-quality, large-diameter native Ga_2O_3 wafers becomes possible.

Thanks to the leadership of Dr. Masataka Higashiwaki from NICT, this year's CSW conference will have a Focus Session on Ga_2O_3 Materials and Devices on Friday, June 1st. It will introduce current status and future prospects of Ga_2O_3 technologies, covering a variety of topics such as epitaxial growth of thin films and heterostructures, material characterization, and device processing and characterization of field-effect transistors and diodes.

EXCURSION (Thursday, May 31st)

For those attendees that have purchased a ticket for the walking tours of Boston for Thurday, May 31st, buses will leave the Samberg Conference Center in the front steps of 50 Memorial Drive. They are the double exit doors located on the ground floor facing the Charles River and Boston. Each excursion is 90 minutes long. Please be on time as our buses leave promptly!

Excursion #1 (bus excursion and guided walking tour leaving at 12:40PM for 1PM tour).

Excursion #2 (bus excursion and guided walking tour leaving at 3:10PM for 3:30PM tour).

In these tours you will see highlights of Boston which include the beauty and grace of Copley Square, the cobblestone drives and gaslights of historic Beacon Hill, the 19th century Back Bay area and the Boston Public Garden, the Freedom Trail from Faneuil Hall to Boston Common, and the quirky, vibrant architecture and streets of old Downtown Boston. *Please see registration desk if tickets are still available.

CONFERENCE BANQUET (Thursday, May 31st)

The CSW 2018 Banquet will take place the evening of Thursday, May 31, 2018 from 6:30PM – 9:30PM at Fenway Park, "America's Most Beloved Baseball Park." We will gather at the State Street Pavilion Club, the largest club space in the park, which overlooks the ballpark, with a view of Boston's skyline. During the reception prior to the dinner, there will be private tours of the Park. Buses will take you there and back leaving the Samberg Conference Center at 5:45PM. Please be on time as our buses leave promptly!

NOTE: If you have NOT registered for the banquet, please see the front desk of Samberg Center for more details. (Fenway Park, 20 Jersey Street, Boston, MA)

CSW 2018 ISSUE IN *physica status solidi* (a)

Selected papers from CSW 2018 will be published as peer reviewed articles in *physica status solidi (a)*. The guest editors for this issue will be Prof. Tomás Palacios, Prof. Srabanti Chowdhury, and Prof. Grace (Huili) Xing. Manuscripts in MS Word or PDF format must be submitted by June 30, 2018. The full call-for-papers can be found here:
https://www.csw2018.org/s/Call-for-Papers_Compound-Semiconductors_CSW2018-final.pdf

Call for papers – Invitation to authors

Topical section in physica status solidi a

Compound Semiconductors

pss (a) – applications and materials science

Materials and characterization, narrow bandgap materials, nanostructures, novel materials (nanocarbon, 2D materials, and Ga_2O_3 other related oxides) & characterization, wide bandgap materials, devices and technologies, high-frequency devices, power electronics, semiconductor lasers, optoelectronics: devices and integration, physics and emerging devices, semiconductor physics, organic semiconductors and flexible electronics, other novel device concepts including ferroelectrics, spintronics, etc.

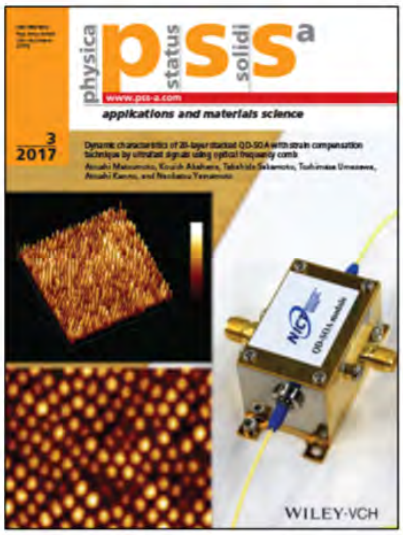

Guest Editors: Srabanti Chowdhury, Tomas Palacios, Grace (Huili) Xing

Submission Deadline: **June 30th, 2018**

Submission at ***pss (a):*** **www.editorialmanager.com/pssa-journal**

AWARDS

During the Compound Semiconductor Week, both the International Symposium for Compound Semiconductors (ISCS) and the International Conference on Indium Phosphide and Related Materials (IPRM) present their annual awards:

- Welker Award
- ISCS Quantum Device Award
- IPRM Award
- ISCS Young Scientist Award
- CSW 2018 Best Student Paper Award

Presentation of the Awards will be made at a special CSW Award Ceremony at 5pm on Tuesday, June 29, 2018. This will be right after the CSW Plenary session in Walker Memorial.

The Welker Award was established in 1976 by Siemens AG in honor of Heinrich Welker, a pioneer in the field of III-V compound semiconductors. The award is now supported by Osram GmbH and selected by the ISCS awards committee. It is presented for outstanding and pioneering research in the area of III-V compound semiconductors.

The ISCS Quantum Device Award was initiated by Fujitsu Quantum Devices Ltd. in 2000 and is now sponsored by the Japanese Section of the ISCS Steering Committee. The award honors pioneering contributions to the field of compound semiconductor and quantum/nanostructure devices which have made a major impact in the past two decades. New device concepts and structures, device physics and modeling as well as device realization and characterization are areas included in the award.

The IPRM Award was initiated by the Indium Phosphide and Related Materials (IPRM) Conference in 1993, as The Michael Lunn Award. During the first three years following its introduction (1993-1995), the award was given for the best paper presented at IPRM. The award criteria were revised in 1996 to recognize individuals who have made "outstanding contributions to the InP community". In 2007, the award was renamed the IPRM Award and has since been sponsored by the IPRM international steering committee to recognize individuals or organizations who have made an outstanding contribution to the InP and related materials community, especially in the areas of materials growth, integrated photonic components, and high frequency electronics.

The ISCS Young Scientist Award was established in 1986, and it acknowledges technical achievements in the field of compound semiconductors by a scientist younger than 40 years on the first day of the conference.

The CSW Best Student Paper will be selected by members of the program committee among the student papers at CSW 2018. The award will be presented during the closing ceremony on Friday, June 1st, 2018.

Previous recipients of the Welker Award

Nick Holonyak, Jr., Cyril Hilsum, Hisayoshi Yanai, Gerald L. Pearson, Herbert Kroemer, Izuo Hayashi, Heinz Beneking, A.Y. Cho, Zhores I. Alferov, Jerry M. Woodall, Don W. Shaw, Greg Stillman, Lester F. Eastman, Harry C. Gatos, James Turner, Federico Capasso, Isamu Akasaki, Ben G. Streetman, M. George Craford, Takashi Mimura, Claude Weisbuch, James S. Harris (2000), Karl Hess (2001), Hiroyuki Sakaki (2002), Klaus Ploog (2003), James J. Coleman (2004), Hans Melchior (2005), Marc Ilegems (2006), Kenichi Iga (2007), Gunter Weimann (2008), P. Daniel Dapkus (2009), Pallab Bhattacharya (2010), Yasuhiko Arakawa (2011), Umesh K. Mishra (2012), Tom Foxon (2013), and Gerald Bastard (2014), Dieter Bimberg (2015), Joe C. Campbell (2016), Chennupati Jagadish (2017).

Previous recipients of the ISCS Quantum Device Award

Emilio E. Mendez and Gerald Bastard (2000), Leo P. Kouwenhoven, Mark A. Reed and Seigo Tarucha (2001), Yasuhiko Arakawa (2002), Pallab Bhattacharya (2003), Jean-Pierre Leburton (2004), Pierre Petroff (2005), Carlo Sirtori (2006), Umesh K. Mishra and James S. Speck (2007), Jean-Michel Gerard (2008), Joe Campbell (2009), Chennupati Jagadish (2010), Alan C. Seabaugh (2011), David Gershoni (2012), Yoshiro Hirayama (2013), and Connie Chang-Hasnain (2014), Maurice Skolnick (215), Kazuhiko Hirakawa (2016), Nicolas Grandjean (2017).

Previous recipients of the ISCS Young Scientist Award

Russell D. Dupuis, Naoki Yokoyama, W.T. Tsang, Russ Fischer, Yasuhiko Arakawa, Sandip Tiwari, Umesh K. Mishra, Kai Chang, Michael A. Haase, John D. Ralston, Nikolai Ledentsov, Fred Kish, Steven P. Den Baars, Jerome Faist, Kohiki Mukai (2000), Masahiko Kondow (2001), Diana Huffaker (2002), Mike Larson (2003), Toshihide Kikkawa (2004), Nils Weimann (2005), Andrea Fiore (2006), Masataka Higashiwaki (2007), Jonathan J. Finley (2008), Seth R. Bank (2009), Tomás Palacios (2010), Yoshitaka Taniyasu (2011), Debdeep Jena (2012), Sanjay Krishna (2013), and Huili (Grace) Xing (2014), Zetian Mi (2015), Srabanti Chowdhury (2016), Masahiro Nomura (2017).

Previous recipients of the IPRM Award

Osamu Wada (2007), Andre Scavennec (2008), Mark Rodwell (2009), Hajime Asahi (2010), F. J. Tegude (2011), Brad Boos (2012), Yuichi Matsushima (2013), and Abderrahim Ramdane (2014), Larry Coldren (2015), Takatomo Enoki (2016), Sebastian Lourdudoss (2017).

Previous recipients of the Michael Lunn Memorial Award

Shigehisa Arai (2000), Gregory Olsen (2001), Dwight Streit (2002), Hideki Hasegawa (2003), Drew Nelson (2004), Masami Tatsumi (2005), and George Antypas (2006)

Previous recipients of the CSW Best Student Paper Award

Georg Rossbach (2011), Jordan Lang and Adam Scofield (2012), Noelia Vico Trivino (2013), and Ya Zhang (2014), Moritz Baier and Justin Iveland and Fanglu Lu (2015), Takuya Inoue and Bernhard Loitsch and Daisuke Inoue (2016), Wenjie Lu and Stefano Moroni and Jaan Freudenfeld (2017).

2018 CSW - ISCS/IPRM COMMITTEES

Conference Chair
Tomás Palacios, *Massachusetts Institute of Technology, USA*

Technical Program Chair
Grace (Huili) Xing, *Cornell University, USA*

Publication Chair
Srabanti Chowdhury, *University of California, Davis, USA*

Jeehwan Kim, MIT - Short Course Organizer

Masataka Higashiwaki, NICT - Focus Session Organizer

Yong-Hang Zhang, Arizona State University (USA) - Regional Chair for America

Tetsuya Suemitsu, Tohoku University (Japan) - Regional Chair for Asia and Australia

Eva Monroy, CEA-Grenoble (France) - Regional Chair for Europe and Africa

Joseph Baylon, MIT – Conference Coordinator

Student Organizers (MIT): Ahmad Zubair, Marek Hempel**,** Mantian Xue, Mengyang Yuan, Nadim Chowdhury, Yuhao Zhang, Elaine McVay, Qingyun Xie, Joshua A. Perozek

Technical Program Subcomittees

0. ***Focus Session on Ga_2O_3***
Chair: Masataka Higashiwaki, NICT; Oliver Bierwagen, PDI; Zbigniew Galazka, IKZ Berlin; Gregg Jessen, AFRL; Debdeep Jena, Cornell Univ.; Marko Tadjer, NRL

1. **Materials and Characterization**

1.1. ***Narrow bandgap materials***
Chair: Amy Liu, IQE; Tim Ashley, Univ. of Warwick; Volker DAumer, Fraunhofer Institute; Takaaki Koga, Hokkaido University; Jerry Meyer, NRL; Michael Santos, Univ. of Oklahoma; Hongqi Xu, Beijing Key Laboratory of Quantum Devices

1.2. ***Nanostructures***
Chair: Lutz Geelhaar, Paul Drude Institute; Kris Bertness, NIST; Xiuling Li, U. of Illinois; Stefano Sanguinetti, Como/Milan Univ.; Katsuhiro Tomioka, Hokkaido Univ.

1.3. ***Novel materials (nanocarbon, 2D materials, and non-Ga_2O_3 oxides) and characterization***
Chair: Randal Feenstra, Carnegie Mellon Univ.; Matthias Batzill, Univ. of South Florida; Holger Eisele, Tech. Univ. of Berlin; Petra Reinke, U. of Virginia; Rainer Timm, Lund Univ.; Shiro Tsukamoto, Anan Nat. College of Tech.

1.4. ***Wide bandgap materials***
Chair: Zetian Mi, University of Michigan; Elaheh Ahmadi, U. of Michigan; Srabanti Chowdhury, UC Davis; Hideki Hirayama, RIKEN; Woongje Sung, SUNY Poly; Andreas Waag, TU Braunschweig; Xinqiang Wang, PKU; Tao Wang, U. Sheffield

2. **Devices and Technologies**

2.1. ***High-frequency devices***
Chair: Miguel Urteaga, Teledyne; Eduardo Chumbes, Raytheon; Gerry Mei, Northrop Grumman; Kozo Makiyama, Fujitsu; Nils Weimann, Univ. of Duisburg

2.2. ***Power electronics***
Chair: Sameer Pendharkar, Texas Instruments; Kevin Chen, KHUST; Elison Matioli, EPFL; Rudiger Quay, Fraunhofer IAF; Tom Tsay, TSMC

2.3. ***Semiconductor lasers*** (Chair: Nelson Tansu, Lehigh University; Daniel Feezell, U. of New Mexico; Luke J. Mawst, UW-Madison; Roberto Paiella, Boston U.)

2.4. ***Optoelectronics: devices and integration*** (Chair: Eva Monroy, CEA Grenoble; Sarath D. Gunapala, NASA JPL; James Gupta, NRC; Euijoon Yoon, Seoul Natl. Univ.; Val Zwiller, KTH)

3. **Physics and Emerging Devices**

3.1. ***Semiconductor physics*** (Chair: Farhan Rana, Cornell University; Linyou Cao, NCSU; Debdeep Jena, Cornell Univ.; Jacob Khurgin, John Hopkins Univ.; Ermin Malic, Chalmers Univ.; André Schleife, UIUC)

3.2. ***Organic semiconductors and flexible electronics*** (Chair: David Gundlach, NIST; Emily Bittle, NIST; Chris Giebink, PennState Univ.; Oana Jurchescu, Wake Forest Univ.; John Kymissis, Columbia Univ.)

3.3. ***Other novel device concepts including ferroelectrics, spintronics etc.*** (Chair: Steven Koester, Univ. of Minnesota; Aaron Franklin, Duke Univ.; Nazila Haraitpour, Intel; Roland Kawakami, OSU; Tony Low, UMN)

ISCS International Steering Committee

Yasuhiko Arakawa (Univ. Tokyo, Japan), Chair
Oliver Ambacher (Univ. Freiburg, Germany)
Colombo Bolognesi (Swiss Federal Institute of Technology, Switzerland)
James Coleman (Univ. Illinois at Urbana Champaign, USA)
Shizuo Fujita (Kyoto Univ., Japan)
Nicolas Grandjean (Ecole Polytechnique Federale de Lausanne, Switzerland)
James S. Harris (Stanford Univ., USA)
Yoshiro Hirayama (Tohoku Univ., Japan)
Diana Huffaker (UCLA, USA)
Heonsu Jeon (Seoul National Univ., South Korea)
Umesh Mishra (UCSB, USA)
Henning Riechert (Paul-Drude-Institut, Germany)
Tom Tiedje (Univ. British Columbia, Canada)
Eric Tournie (Univ. Montpellier, France)
Charles Tu (UCSD, USA)

IPRM International Steering Committee

Henning Riechert (Paul-Drude-Institut, Germany), Chair
Shigehisa Arai (Tokyo Inst. of Technology, Japan)
Hajime Asahi (Osaka Univ., Japan)
Sophie Bouchoule (CNRS-LPN, France)
Takatomo Enoki (NTT, Japan)
Norbert Grote (Fraunhofer HHI, Germany)
Sebastian Lourdudoss (Royal Institute of Technology, Sweden)
Yuichi Matsushima (Waseda Univ., Japan
Yasuyuki Miyamoto (Tokyo Inst. of Technology, Japan)
Yoshiaki Nakano (Univ. Tokyo, Japan)
Tomás Palacios (MIT, USA),
Abderrahim Ramdane (CNRS-LPN, France)
Mark Rodwell (UCSB, USA)
Andre Scavennec (Alcatel Thales III-V Lab, France)
Osamu Wada (Kobe Univ., Japan)

SHORT COURSE: *MATERIALS AND DEVICES FOR NEUROMORPHIC APPLICATIONS*

Short Course Organizer: Prof. Jeehwan Kim (Massachusetts Institute of Technology)

Welcome remarks and description of Short Course

8:45-9:00 AM, DR 5 & 6 (Samberg Conference Center, 6th floor)

Lecture #1 **Neuromorphic computing with memristive devices and arrays**

9:00-10:00 AM, DR 5 & 6 (Samberg Conference Center, 6th floor)

Lecturer: Prof. J. Joshua Yang, Department of Electrical and Computer Engineering, University of Massachusetts, Amherst

Prof. Joshua Yang is a professor in the Department of Electrical and Computer Engineering at the University of Massachusetts, Amherst. Before joining UMass in 2015 he spent over 8 years at HP Labs, leading the memristive materials and device team. His current research interests are Nanoelectronics and Nanoionics, especially for energy and computing applications, where he authored and co-authored over 100 papers in peer-reviewed academic journals, and holds 77 granted and over 70 pending US Patents. He obtained his B.A. degree in mechanical engineering from Southeast University in China and PhD from the University of Wisconsin – Madison in Material Science Program in 2007.

Lecture #2 **Materials for neuromorphic computing**

10:15-11:15 AM, DR 5 & 6 (Samberg Conference Center, 6th floor)

Lecturer: Ilia Valov, Research Centre Jülich

Dr. Ilia Valov is a Principle Investigator at the Research Centre Juelich and RWTH-Aachen University, Germany. He studied physical chemistry/electrochemistry (M.Sc.) in Sofia, Bulgaria working on the electrode reaction kinetics of arsenic from low concentrated solutions. After the graduation he continues his research at the Institute of Physical Chemistry, Bulgarian Academy of Science on the mechanism and electrode reaction kinetics of cathodic deposition of rare-earth metal oxides from non-aqueous electrolytes. In 2006 becomes Dr. rer. nat (Ph.D.) with summa cum laude at the Institute of Physical Chemistry, Justus-Liebig-University, Germany in the field of physical chemistry of solids, defect chemistry and solid state electrochemistry. Since 2009 he works on fundamental processes at an atomic and nano-scale. His research interests and activities now are concentrated on electrochemical and, in general, physicochemical phenomena at the nano and sub-nanoscale, such as mass and charge transport, point defects, surfaces and interfaces with a focus on resistive switching memories, memristive devices and energy conversion and electro- catalysis (water splitting).

Lecture #3 **Analog arrays and algorithms**

11:30-12:30 PM, DR 5 & 6 (Samberg Conference Center, 6th floor)

Lecturer: Dr. Wilfried Haensch, IBM

Dr. Wilfried Haensch received his Ph.D. in 1981 from the Technical University of Berlin, Germany in the field of theoretical solid state physics. He started his career in Si technology 1984 at SIEMENS corporate research Munich. There he worked on high field transport in MOSFETs and later in DRAM development and manufacturing. In 2001 he joined the IBM TJ Watson Research Center to lead a group for novel devices and applications. He was responsible for the exploration of device concepts for future technology nodes and new concepts for memory and logic circuits, including 3D integration, early FinFET work and the exploration of Carbon Nanotubes for VLSI circuits. He also was active in CMOS integrated Silicon Photonics to provide high bandwidth low cost links for future compute systems. He is currently responsible for novel technologies for neuromorphic computation with emphasis on exploring memristive elements (like PCM, RRAM, FeRAM, etc) in neural network arrays. He is the author of a text book on transport physics and author/co-author of more than 150 publications. He was awarded the Otto Hahn Medal for outstanding Research in 1983. He was named IEEE Fellow in 2012.

PLENARY SPEAKERS

Prof. Hiroshi Fujioka (Professor, University of Tokyo)

Professor Hiroshi Fujioka a Professor in the Department of Materials and Environmental of the Institute of Industrial Science (IIS), University of Tokyo. His research interests are in the areas of PLD and sputtering growth of III-V semiconductors and their heterostructures for high-speed electronic and optoelectronic devices. His current research projects include sputtering growth of InGaN for large area optical and electron devices.

Professor Fujioka has authored or co-authored over 200 journal papers. Dr. Fujioka is a member of Japanese Society of Applied Physics and the Chemical Society of Japan. He has been serving as a vice president of Japanese Association of Crystal Growth from 2012. He has been also serving as a chairman of the Japan Society for the Promotion of Science 161 committee from 2012.

Prof. Evelyn Hu (Harvard University)

Evelyn L. Hu is Gordon McKay Professor of Applied Physics and Electrical Engineering at Harvard University. Prof. Evelyn Hu's research focuses on high-resolution fabrication of compound semiconductor electronic and optoelectronic devices, candidate structures for the realization of quantum computation schemes, and on novel device structures formed through the heterogeneous integration of materials. Recently her work has involved increasing the efficiency blue emission from GaN, manipulating defect centers in GaN and silicon carbide, developing metallic resonators to enhance spontaneous emission, and engineering Zinc Oxide for optoelectronics applications.

Hu is a member of the National Academy of Engineering, the Academica Sinica of Taiwan, a recipient of an NSF Distinguished Teaching Fellow award, an AAAS Lifetime Mentor Award, a Fellow of the IEEE, APS, and the AAAS, and holds an honorary Doctorate of Engineering from the University of Glasgow. She was selected UCSB Faculty Research Lecturer in 2005.

Dr. Dario Gil (Vice President, Science and Solutions, Thomas J. Watson Research Center, IBM)

Dr. Gil is a leading technologist and senior executive at IBM. As Vice President of Science and Solutions of IBM Research, Dr. Gil is responsible for IBM's Artificial Intelligence research efforts and for IBM's commercial quantum computing program (IBM Q). Prior to his current position, Dr. Gil was the VP of Science and Solutions, directing a global organization of ~1,500 researchers across 12 laboratories, where he had direct responsibility for IBM's science agenda, with a broad portfolio of activities spanning the physical sciences, the mathematical sciences, and industry solutions based on AI, IoT, Blockchtain and Quantum technologies.

Dr. Gil's research results have appeared in over 20 international journals and conferences and he is the author of numerous patents. Dr. Gil is an elected member of the IBM Academy of Technology. He received his Ph.D. in Electrical Engineering and Computer Science from the Massachusetts Institute of Technology.

Prof. Mark Rodwell (University of California – Santa Barbara)

Mark Rodwell holds the Doluca Family Endowed Chair in Electrical and Computer Engineering at UCSB. He directs the SRC/DARPA Center for Converged TeraHertz Communications and Sensing, and manages the UCSB Nanofabrication Lab. His research group develops nm and THz transistors, and mm-wave/sub-mm-wave ICs.

Prof. Rodwell received the 2010 IEEE Sarnoff Award and the 2009 IEEE IPRM Conference Award for the development of InP-based bipolar IC technology, at both the device and the circuit design levels, for mm-wave and sub-mm-wave applications. His group's work on GaAs Schottky-diode ICs for picosecond / mm-wave instrumentation was awarded the 1997 IEEE Microwave Prize and the 1998 European Microwave Conference Microwave Prize. His group's collaborative development, with Prof. Madhow's group, of mm-wave line-of-sight MIMO received the 2012 IEEE Marconi Prize Paper Award. Prof. Rodwell was elected IEEE Fellow in 2003.

INVITED SPEAKERS

Author	Title	Date	Time	Room
Albrecht, Martin	Growth, Doping and Defects of Homoepitaxial β-Ga_20_3 Grown by Metal Organic Vapor Phase Epitaxy	6/1/18	2:00 PM	DR 5&6
Belkin, Mikhail	THz Difference-Frequency Generation in Quantum Cascade Lasers on Silicon	6/1/18	10:30 AM	Salon M
Boucaud, Philippe	III-nitride Microlasers on Silicon Integrated on a 2D Photonic Platform	6/1/18	12:00 PM	Salon M
Bowers, John	Quantum-Dot Lasers on Silicon	5/30/18	11:30 AM	Salon M
Bracker, Allan	Self-assembled InGaAs Quantum Dots for Quantum Nanophotonics	6/1/18	2:00 PM	DR 3&4
Calleja Pardo, Enrique	III-Nitride Nanostructures Grown by MBE: Basics and Applications	5/31/18	11:00 AM	Wong(E-51)
Chang-Hasnain, Connie	High-Contrast Gratings in VCSELs	5/30/18	4:00 PM	Salon M
Crawford, Mary	Materials Challenges of AlGaN-based Power Electronics and UV Lasers	5/30/18	2:00 PM	DR 3&4
Davanco, Marcelo	Heterogeneous Integration for On-Chip Quantum Photonics with Single InAs Quantum Dots	6/1/18	4:30 PM	Salon M
del Alamo, Jesus	III-V CMOS: Quo Vadis?	5/30/18	1:30 PM	Salon T
DeLongchamp, Dean	Microstructure and Morphology Measurements for Organic Electronics	5/30/18	3:30 PM	Salon T
Feezell, Daniel	A Decade of Nonpolar and Semipolar III-Nitrides: A Review of Successes and Challenges	5/31/18	9:00 AM	Wong(E-51)
Ferrari, Andrea	n/a	5/31/18	9:30 AM	Salon T
Fullerton, Susan	Electric Double Layer Dynamics in Graphene FETs: Using Ions to Control Transport in Two-Dimensional Materials	5/30/18	4:15 PM	DR 5&6
Gmachl, Claire	Mid-Infrared Quantum Cascade Lasers and Applications	5/31/18	8:30 AM	Salon M

Author	Title	Date	Time	Room
Harmand, Jean-Christophe	MBE Growth of GaAs Nanowires Observed in Situ by TEM	6/1/18	4:00 PM	DR 3&4
Heron, John	Pathways to Low Energy Control of Magnetism Using Multiferroics	5/31/18	11:30 AM	Salon T
Hersam, Mark	Transition Metal Dichalcogenide Memristors and Memtransistors	5/31/18	8:30 AM	Salon T
Higashiwaki, Masataka	Introduction of Gallium Oxide Technologies	6/1/18	10:30 AM	DR 5&6
Hinkle, Christopher	High Hole Mobility, 3D Vertical Integration Compatible WSe_2 FETs Grown by MBE on ALD Oxides	5/30/18	3:30 PM	DR 5&6
Howell, Robert	the Superlattice Castellated Field Effect Transistor (SLCFET): A Novel Low Loss, Broadband RF Switch Technology with an Fco Figure of Merit > 2 THz	5/31/18	9:30 AM	DR 5&6
Khan, Asif	Negative Capacitance Transistors: Physics, Materials and the State-of-Art	6/1/18	3:30 PM	Salon T
Kumagai, Yoshinao	Development of Halide Vapor Phase Epitaxy of Ga_2O_3 for Power Device Applications	6/1/18	11:30 AM	DR 5&6
Lauhon, Lincoln	Total Tomography of Nonplanar InGaAs Quantum Wells on GaAs Nanowires	6/1/18	2:30 PM	Salon T
Law, Stephanie	High-quality Growth of Chalcogenide Topological Insulators	5/30/18	2:30 PM	Salon M
Liu, Amy	Heterointegration of Photonics and IR Materials on Large-mismatched Substrates via Direct MBE Growth	6/1/18	1:30 PM	Salon M
Lyakh, Arkadiy	Quantum Cascade Lasers on Metamorphic Buffer Layer	5/31/18	10:30 AM	Salon M
Palmstrom, Chris	Growth and Electronic Properties of Heusler Epitaxial Thin Films	5/31/18	10:30 AM	Salon T
Peterson, Rebecca	Electronics on Anything' Using Wide Bandgap Amorphous Oxide Semiconductors	5/31/18	12:00 PM	DR 5&6
Rajan, Siddharth	Material and Device Engineering for Gallium Oxide Field Effect Transistors	6/1/18	12:00 PM	DR 5&6
Samarth, Nitin	Topological Spintronic Devices	6/1/18	4:30 PM	Salon T

Author	Title	Date	Time	Room
Sasaki, Kohei	Ga_2O_3 Vertical Trench SBDs and FETs	6/1/18	5:00 PM	DR 5&6
Shabani, Javad	Heterostructures of Narrow-Gap Semiconductor and Superconductors for Quantum Information Applications	5/30/18	8:30 AM	Salon M
Shojiki, Kanako	Fabrication of High-Quality AlN Template on Sapphire Using High-Temperature Annealing	5/30/18	9:00 AM	DR 3&4
Speck, James	Development of $(Al_xGa_{1-x})_2O_3/Ga_2O_3$ Heterostructures and Devices	6/1/18	10:45 AM	DR 5&6
Sun, Qian	GaN-on-Si Laser Diodes and Normally-Off HEMTs	5/30/18	11:00 AM	DR 3&4
Takahashi, Tsuyoshi	Enhancement in Fmax by Adopting an Extended Drain-Side Recess Structure in InAlAs/InGaAs HEMTs	5/30/18	8:30 AM	Salon T
Takahasi, Masamitu	Liquid-Solid Interface as Crystal Growth Front	6/1/18	1:30 PM	Salon T
Takeuchi, Tetsuya	Electrically-Injected GaN-based VCSELs	5/30/18	12:00 PM	DR 3&4
Tournié, Eric	Sb-based IR Detector and Emitter Materials	5/30/18	1:30 PM	Salon M
Uren, Michael	Leaky Dielectric Model for Dynamic R_{ON} in GaN/AlGaN Power Transistors	5/30/18	12:00 PM	DR 5&6
Wasige, Edward	Mm-wave/THz Multi-Gigabit Wireless Links and Microwave Interfaces - The iBROW Project	5/30/18	10:30 AM	Salon T
Watts, Michael	Silicon Photonics, Optical Phased Arrays, and LiDAR	6/1/18	3:30 PM	Salon M
Wernersson, Lars-Erik	III-V Nanowire MOSFETs: A Path Towards 10 nm High-Performance Transistors	6/1/18	11:15 AM	DR 3&4
Yu, Shui-Qing	Development of Si-based GeSn Laser	5/31/18	11:45 AM	Salon M
Zhang, Yong	RS-PbTe/ZB-CdTe (111) Heterostructure an Inter-Diffusion Free Interface with a High Mobility Two-Dimensional Electron Gas (2DEG) Showing Quantum Oscillations	5/30/18	9:30 AM	Salon M

TUESDAY

5/29/2018

TECHNICAL PROGRAM

IPRM
Est. 1989

Cambridge / Boston, Massachusetts

CSW2018

2018
iSCS

Tu1JP1: Joint Plenary I	
Time:	5/29/2018, 01:30 PM - 03:15 PM
Room:	Walker Memorial (Building 50-140)
Chair:	Tomás Palacios (Massachusetts Institute of Technology, United States) Huili Xing (Cornell University, United States)

Tu1JP1.1 **Welcome Remarks**

01:30 PM *Tomás Palacios (Massachusetts Institute of Technology, USA); Huili Xing (Cornell University, USA)*

Tu1JP1.2 **Sputtering Epitaxial Growth of III Nitrides and Its Device Applications**

01:45 PM *Hiroshi Fujioka (The University of Tokyo, Japan)*

PLENARY We have developed a new epitaxial growth technique named PSD (pulsed sputtering deposition) for fabrication of group III nitride devices. Advantages of PSD include a dramatic reduction in growth temperatures and suppression of interfacial reactions between nitrides and substrates. All of the nitride films were grown by PSD in a substrate temperature range from room temperature (RT) to 700 C. A record low resistivity for n-type GaN of 0.16 mΩcm was achieved with an electron mobility of 100 $cm^2V^{-1}s^{-1}$ at a carrier concentration of 3.9×10^{20} cm^{-3}. Hafnium foils, amorphous SiO_2 sheets, and polymer films were utilized for demonstration of large area devices on low cost substrates. We have found that our process is compatible with high Indium concentration InGaN growth which is necessary for fabrication of long wavelength light emitting devices: we have successfully fabricated RGB full color LEDs at a maximum process temperature of 480 C.

Tu1JP1.3 **Semiconductors at the Frontiers of Quantum Technologies**

02:15 PM *Evelyn Hu (Harvard University, USA)*

PLENARY Semiconductor "wires" and "point contacts" provided the first reasonably clean, controlled systems that let us explore non-intuitive ideas of quantized conductance. Ultra-thin oxides let us demonstrated devices that operated through quantum mechanical tunneling. Semiconductor "quantum wells" and "quantum dots" were test beds and validations of our simple ideas of quantum mechanical enhancement, and provided pathways to more efficient operation of LEDs and lasers. And today, we have the rich bounty of "defects" in semiconductors that may be potent qubits. As well, we have a new class of 2D semiconductors that also hold exiting promise as the platforms for quantum systems.

Tu2JP2: Joint Plenary II

Time:	5/29/2018, 03:30 PM - 05:00 PM
Room:	Walker Memorial (Building 50-140)
Chair:	Huili Xing (Cornell University, United States)

Tu2JP2.1 **The Physics of AI and Quantum Computing**

03:30 PM *Dario Gil (IBM, USA)*

PLENARY New materials and architectures driven by basic physical considerations are required to extend computing beyond the imminent limits of CMOS von Neumann machines. Although Machine Learning (ML) has made tremendous advances, especially after the development of deep learning, implementations typically employ standard CPU or GPU devices. I will review the specifications, microarchitectures and materials for new analog Non-Volatile Memory devices which promise to improve ML power/performance metrics orders of magnitude. Quantum computing is another game-changing approach to computation, including AI, which could solve problems we now simply can't even attempt. After an overview of key concepts, I will compare technologies for implementing quantum bits, or qubits, with a focus on our superconducting implementation.

Tu2JP2.2 **Transistors: mm-Wave and Low-Power VLSI**

04:15 PM *Mark J W Rodwell (University of California, Santa Barbara, USA)*

PLENARY With 70 years development, transistors now approach physical limits; we seek promising new research directions. One opportunity is wireless, with 5G poised to use 28, 38, and 71-86 GHz. The subsequent generation will use massive spatial multiplexing at 140, 220, and 340 GHz. For these, efficient, high-power GaN HEMT and InP HBT transmitters and sensitive InP HEMT receivers must be developed to increase link range and capacity. I will discuss prospects for improved THz InP HBTs and MOS-HEMTs; other groups now work to extend GaN to 220GHz. Another opportunity is low-power VLSI, potentially addressed by tunnel- and ferro-FETs; I will discuss prospects for high-speed, high-current TFETs using effective mass and field engineering.

WEDNESDAY

5/30/2018

TECHNICAL PROGRAM

IPRM
Est. 1989

Cambridge / Boston, Massachusetts

CSW2018

2018
iSCS

We1A1: Narrow Band Gap (Quantum)	
Time:	5/30/2018, 08:30 AM - 10:00 AM
Room:	Salon M (Samberg Conference Center, 7th floor) E52 (50 Memorial Dr.)
Chair:	Amy W. K. Liu (IQE Inc., United States)

We1A1.1

08:30 AM

INVITED

Salon M

Heterostructures of Narrow-Gap Semiconductor and Superconductors for Quantum Information Applications

Javad Shabani (NYU, USA)

Recently, advances in narrow-gap semiconductors have enabled a variety of new devices, including detectors, sensors, low noise amplifiers and new potential avenues for quantum computation. Currently superconducting qubit experiments have demonstrated single and two-qubit gate operations with fidelities exceeding 99%, placing fault tolerant quantum computation schemes within reach. On the other hand, semiconductor based devices have their own merits: fast manipulation, low-power consumption and a more direct path toward scalability. Hybrid superconductor and semiconductor devices could have advantages of both systems. We discuss the recent developments in epitaxial growth of Al on two-dimensional (2D) surface InAs quantum wells. This system is shown to yield a high quality superconductor-semiconductor system with uniformly transparent interfaces and a hard induced gap, indicted by strongly suppressed subgap tunneling conductance. We present transport properties of these density-controlled surface InAs quantum wells as well as demonstrate Josephson junctions with highly transparent contacts. These developments have lead to unprecedented control over proximity effect in semiconductors where electron densities can be tuned using a gate voltage. We discuss potential applications of this new material system that can serve as a platform for low power circuits, gate-based qubits as well as exploring topological superconductivity for computation.

We1A1.2

09:00 AM

Salon M

InAsSb/InAlAs Quantum Wells on GaAs Substrates for the Mid-Infrared Spectral Range

Eva Repiso (Lancaster University, United Kingdom (Great Britain)); Chris Broderick (Tyndall National Institute, Ireland); Maria de la Mata (Cadiz University, Spain); Reza Arkani (Tyndall National Institute, Ireland); Qi Lu and Andrew R J Marshall (Lancaster University, United Kingdom (Great Britain)); Sergio Molina (Cadiz University, Spain); Eoin O'Reilly (Tyndall Institute, Ireland); Peter Carrington and Anthony Krier (Lancaster University, United Kingdom (Great Britain))

We report on the optical and structural properties of InAsSb/InAlAs multi-quantum wells (MQWs) together with a theoretical study of the spontaneous emission spectra for such structures. The advantages of this QW system is that it exhibits a type I band alignment with high band offsets suitable for electronic confinement. The samples were grown using molecular beam epitaxy (MBE) on GaAs substrates using an InAlAs buffer layer to accommodate the lattice mismatch. Intense photoluminescence (PL) is observed up to room temperature in the 2.7-3.4 μm spectral range. An increase in the Sb content in the QWs shifts the emission peak to longer wavelengths but also leads to an unusual increase in emission intensity. Simulation of the emission spectra using an 8-band k.p model indicate that this is due primarily to the impact of the increase in the in-plane strain in the QW which reduces the hole effective mass.

We1A1.3

09:15 AM

Salon M

Analysis of Composition Profiles and Strain Across Heterovalent Non-Common-Atom CdTe/InSb Interfaces

Esperanza Luna (Paul-Drude-Institut für Festkörperelektronik, Leibniz-Institut im Forschungsverbund Berlin, Germany)

CdTe thin films are generating much current interest because of potential solar-cell applications. Epitaxial growth on (almost) lattice-matched InSb substrates provides an avenue towards achieving very high quality material, although unanswered questions remain about the interfacial region which must inevitably incorporate a mixture of II-V and/or III-VI bonds due to its heterovalent non-common-atom (NCA) character. In this work, we present an analysis of the composition profile across CdTe/InSb NCA interfaces carried out using a combination of (scanning) transmission electron microscopy (S)TEM imaging techniques. The use of the chemically sensitive 002 dark-field (DF) TEM imaging emphasizes the interface location by comparing differences in structure factors, and comparison of the CdTe-on-InSb experimental and simulated profiles reveals that the interface is structurally very abrupt. g002 DFTEM results would be correlated with interfacial strain data from geometric phase analysis on aberration-corrected STEM micrographs.

We1A1.4

09:30 AM

INVITED

Salon M

RS-PbTe/ZB-CdTe (111) Heterostructure An Inter-Diffusion Free Interface with a High Mobility Two-Dimensional Electron Gas (2DEG) Showing Quantum Oscillations

Yong Zhang (The University of North Carolina at Charlotte, USA)

RS-PbTe/ZB-CdTe (111) heterostructure is of great interest in multiple aspects, from developing new approaches for achieving inter-diffusion free hetero-interfaces to exploring new physical mechanisms for generating 2D electron or hole gases and related novel quantum physics. Because of the large miscibility gap, atomic inter-diffusion is nearly completely suppressed between PbTe and CdTe, leading to an abrupt heterostructure interface. The primary formation mechanism of the 2DEG in the RS-PbTe/ZB-CdTe (111) interface is distinctly different from other known systems. The mismatch in crystal structure between PbTe and CdTe leads to a mismatch in the bonding configurations of the valence electrons, which results in excess of valence electrons, thus a high density and high mobility 2DEG. Quantum oscillations are observed in electronic transport measurements at low temperature under magnetic field up to 60 T. A non-zero Berry phase suggests the Dirac fermion nature of the 2DEG and being a new candidate for 2D topological crystalline insulators.

We1B1: Wide Band Gap (AlGaN)

Time:	5/30/2018, 08:30 AM - 10:00 AM
Room:	DR 3 & 4 (Samberg Conference Center, 6th floor)
Chair:	Qian Sun (Suzhou Institute of Nano-Tech and Nano-Bionics, Chinese Academy of Sciences, P.R. China)

We1B1.1

08:30 AM

DR 3 & 4

Optical and Electrical Properties of Mg-doped High Al-content AlGaN Grown by Molecular Beam Epitaxy

Xianhe Liu (University of Michigan, Ann Arbor, USA; McGill University, Canada); Kishwar Mashooq, Jin Shin, David Laleyan and Ayush Pandey (University of Michigan, Ann Arbor, USA); Zetian Mi (University of Michigan, USA)

To date, it has remained extremely challenging to achieve efficient p-type conduction of AlN and Al-rich AlGaN. The underlying challenges include the very large p-type dopant (Mg) activation energy (up to 600 meV) in Al-rich AlGaN, the compensating defects, and the unintentional impurity incorporation. In this context, we have performed a detailed investigation of MBE growth of Mg-doped AlGaN with around 55% Al content. The samples were grown under nearly metal-rich conditions, achieving smooth surface morphology with RMS roughness smaller than 1 nm. Free hole concentrations at room temperature up to ~1×10^{18} cm^{-3} was measured, which is significantly higher than those reported previously by MOCVD. With increasing Mg concentration, the hole concentration increased with Mg concentration and then stays nearly constant, accompanied by a reduction in the hole mobility. Emission peaks related to the donor-acceptor pair transitions, conduction band to Mg acceptor transition and bound excitonic emission are clearly identified.

We1B1.2

08:45 AM

DR 3 & 4

High Quality Large Diameter AlN-on-sapphire Templates by High Temperature N2 Annealing

Akira Mishima, Yuji Tomita, Yuya Yamaoka, Yoshiki Yano, Toshiya Tabuchi and Koh Matsumoto (Taiyo Nippon Sanso Corporation, Japan); Mayank Bulsara (Matheson Tri-Gas; Taiyo Nippon Sanso, USA); Hideto Miyake (Mie University; Graduate School of Regional Innovation Studies, Japan)

High performance, low cost deep ultraviolet LEDs (DUVLEDs), require the development of high quality, large diameter AlN substrates. Bulk AlN substrates are expensive and are currently limited to one (1) or two (2) inch diameter. A proposed alternative is the development of high quality AlN thin films on large diameter sapphire, which could then serve as templates for subsequent device layer epitaxy and fabrication. The results of this study indicate that a MOCVD plus high temperature annealing sequence can be used to fabricate high quality, six-inch diameter AlN-on-sapphire templates.

We1B1.3

09:00 AM

INVITED

DR 3 & 4

Fabrication of High-Quality AlN Template on Sapphire Using High-Temperature Annealing

Kanako Shojiki, Xiaotong Liu and Shoya Kawai (Mie University, Japan); Hideto Miyake (Mie University; Graduate School of Regional Innovation Studies, Japan)

AlN films with thickness of 10-300 nm were deposited on c-plane sapphire substrates by sputtering.The radio frequency (RF) power and growth temperature were 700 W and 500-650°C, respectively. Subsequently, the sputtered AlN films were thermally annealed in N2 at 1300 - 1700°C for 1-3 h using Face-to-Face method. Both the (0002) and (10^{-12}) X-ray rocking curves (XRCs) of the AlN films had a single sharp peak after thermal annealing owing to the elimination of the tilt and twist components from the sputtered AlN films by high-temperature thermal annealing. FWHMs of the (0002) and (10^{-12}) XRCs were markedly reduced to 40-80 and 220-280 arcsec, respectively.The improved crystallinity is related to the solid-phase reactions that occur at high annealing temperatures. we have demonstrated the atomically flat surface of the AlN film on annealed sputter-deposited AlN/sapphire templates with low density of TDs. These results can be utilized to obtain highly efficient UV-LEDs and LDs on thermal annealed sputter-deposited AlN/sapphire templates.

We1B1.4

09:30 AM

DR 3 & 4

Extreme-high-temperature MOVPE Design and Practice for Nitrides

Kuang-Hui Li, Haiding Sun, Che-Hao Liao and Hsin-Hung Yao (KAUST, Saudi Arabia); William Holden, Tom Salagaj, Aaron Feldman, Gary Provost and Gary Tompa (SMI, USA); Xiaohang Li (KAUST, Saudi Arabia)

We design and build an extreme high temperature MOCVD (EHT MOCVD) that has improved heating efficiency and allows the gas inlet to be closer to the susceptor. Specifically, the induction coil was designed to surround the vertical cylinder of a T-shaped susceptor comprising the cylinder and a top horizontal plate holding the wafer substrate within the reactor. Therefore, the cylinder coupled most magnetic field to serve as the thermal source for the plate. Furthermore, the plate could block and thus significantly reduce the uncoupled magnetic field above the susceptor, thereby allowing the gas inlet to be closer. The reactor has a double quartz wall, stainless steel flange on the top and at the bottom, T-shaped susceptor, surrounding thermal insulation for heat confinement and protecting induction coil from thermal radiation, supporter at the bottom of the susceptor, heat shields for protecting bottom flange from thermal radiation, thermal couple and pyrometer.

We1B1.5 **Electrical and Optical Properties of Heavily Ge-Doped AlGaN**

09:45 AM *Rodrigo Blasco (Univesidad de Alcala, Spain); Akhil Ajay (CEA-Grenoble, France); Katharina Lorentz (IPFN, Portugal); Luís Manuel Cerqueira Lopes Alves (C2TN, Portugal); Eva Monroy (CEA-Grenoble, France)*

DR 3 & 4

The preferred n-type dopant for wurtzite GaN is silicon. However, in nanowire structures, the silicon radial distribution is inhomogeneous, and high doping levels tend to degrade the nanowire morphology. In response, the use of germanium as n-type dopant has been proposed as an alternative when dopant concentrations around or higher than the Mott transition 10^{19} cm^{-3}. Germanium can occupy the Ga lattice site causing less lattice distortion than Si.. In this work, we report the effect on the electrical and optical properties of germanium as n-type dopant in AlGaN layers grown by plasma assisted molecular-beam epitaxy, first varying the Ge concentration in the range of 10^{19} to 10^{21} cm^{-3} for relatively low Al compositions, and then with fixed Ge density ([Ge] = 1×10^{21} cm^{-3}) increasing the Al composition up to 0.66.attaining conductive layers with 64% of aluminum.

We1C1: RF (III-V)

Time:	5/30/2018, 08:30 AM - 10:00 AM
Room:	Salon T (Samberg Conference Center, 7th floor)
Chair:	Eduardo Chumbes (Raytheon, United States)

We1C1.1

08:30 AM

INVITED

Salon T

Enhancement in Fmax by Adopting an Extended Drain-Side Recess Structure in InAlAs/InGaAs HEMTs

Tsuyoshi Takahashi, Yoichi Kawano, Kozo Makiyama, Shoichi Shiba, Masaru Sato, Yasuhiro Nakasha and Naoki Hara (Fujitsu Laboratories Ltd., Japan)

We report an enhancement in fmax of 1.3 THz using InAlAs/InGaAs HEMTs with a gate length of 75 nm by adopting a widely extended drain-side recess length of 250 nm. The improvement in fmax is primarily due to the reduction in drain conductance. In addition, a double-sided doped structure facilitated the improvement of the fmax. Furthermore, a cavity structure was introduced to reduce the parasitic gate capacitance.

We1C1.2

09:00 AM

Salon T

Through Silicon via (TSV) Process for Suppression of Substrate Modes in a Transferred-Substrate InP DHBT MMIC Technology

Dimitri Stoppel, Michael Hrobak, Alexander Külberg, Saskia Schönfeld, Dirk Rentner, Olaf Krüger, Ksenia Nosaeva, Mohamed Brahem and Sebastian Boppel (Ferdinand-Braun-Institut, Germany); Nils Weimann (University of Duisburg-Essen, Germany)

For a commercial system implementation of the InP HBT transferred-substrate technology, it is necessary to thin down the chips and integrate through silicon vias (TSVs) to suppress parasitic parallel plate modes. In this abstract we report on the necessity (electromagnetic simulation) and implementation (process development) of TSVs for monolithic microwave integrated circuits (MMICs). In particular we show simulations of MMICs w/o TSVs and the impact on the transmission and reflection coefficient. Furthermore we describe a cost-effective via-first process with laser processed vias and the implementation into our transferred-substrate process.

We1C1.3 **Fin-Width Scaling of Highly-Doped InGaAs Fins**

09:15 AM *Alon Vardi and Jesús del Alamo (MIT, USA)*

Salon T We study the impact of fin width scaling on transport in highly doped InGaAs fins and the effect of digital etch. Our experiments suggest the existence of a 10 nm wide "deadzone" on each side of the fin that does not contribute to transport. The extent of the deadzone cannot be mitigated by digital etch nor sidewall passivation. Simulations suggest that Fermi level pinning and its associated subsurface depletion region alone cannot explain the relatively wide deadzone that is measured. We propose an explanation based on the combination of Fermi level pinning and mobility degradation as the fin width scales down leading to an apparent wider deadzone.

We1C1.4 **Vertical, High-Performance 12 nm Diameter InAs Nanowire MOSFETs on Si Using an All III-V CMOS Process**

09:30 AM

Salon T *Adam Jönsson, Johannes Svensson and Lars-Erik Wernersson (Lund University, Sweden)*

We present a streamlined process for co-integration of InAs(n-type) and GaSb(p-type) MOSFETs, utilizing a common gate-stack. Sub-100 nm gate-length devices with gm vales up to 2.7 mS/um where fabricated. A detailed evaluation of series resistance originating from the source contact is enabled via utilization of thin hydrogen silsequioxane (HSQ) based spacers for the InAs devices. The process is optimized for strong n-type performance, co-integrated with a functional p-type device. The processed MOSFETs are based on, gold seeded, vapor-liquid-solid (VLS) grown InAs-GaSb heterojunction nanowires1 with a, highly doped, overgrown InAs shell for improving etch selectivity and reducing contact resistance. The shell is later removed at the gate position to restore the proper channel material, namely InAs or GaSb core material, respectively.

We1C1.5 **Digital Etch for InGaSb p-Channel FinFETs with 10 nm Fin Width**

09:45 AM *Wenjie Lu and Jesús del Alamo (MIT, USA)*

Salon T III-V channel MOSFETs is considered as promising technology for future CMOS. In this work, we demonstrate a digital etch process for antimonide-based multi-gate transistors. We fabricated InGaSb p-channel FinFETs with smallest fin width of 10 nm. Scaling study on the OFF-state current shows multiple leakage paths within the devices, and the application of the digital etch process was able to improve the turn-off performance significantly. A record maximum transconductance per device footprint of over 700 μS/μm is obtained for FinFETs with 10 nm fin width. The results suggest potential for the InGaSb material system for future PMOS technology.

We1D1: Power (Bulk GaN)

Time:	5/30/2018, 08:30 AM - 10:00 AM
Room:	DR 5 & 6 (Samberg Conference Center, 6th floor)
Chair:	Elison Matioli (EPFL, Switzerland)

We1D1.1 **GaN Junction Barrier Schottky Diodes by Selective Ion Implantation**

08:30 AM

DR 5 & 6

Yuhao Zhang (Massachusetts Institute of Technology, USA); Zhihong Liu (Singapore-MIT Alliance for Research and Technology, Singapore); Marko Tadjer (Naval Research Laboratory, USA); Daniel Piedra (Massachusetts Institute of Technology, USA); Christopher Hatem (Applied Materials-Varian, USA); Xiang Gao (IQE LLC, USA); Travis Anderson, Lunet Luna, Andrew Koehler, Boris Feigelson and Karl Hobart (Naval Research Laboratory, USA); Tomás Palacios (Massachusetts Institute of Technology, USA)

This work demonstrates vertical GaN junction barrier Schottky (JBS) rectifiers fabricated with novel ion implantation techniques. We used two different methods to form the lateral pn grids below the Schottky contact: (a) Mg implantation into n-GaN to form p-wells and (b) Si implantation into p-GaN to form n-wells. Specific differential on-resistances (Ron) of 1.5-2.5 $m\Omega \cdot cm^2$ and 7-9 $m\Omega \cdot cm^2$ were obtained in the Mg-implanted and Si-implanted JBS rectifiers, respectively. A breakdown voltage of 500-600 V was achieved in both devices, with a leakage current at high reverse biases at least 100-fold lower than conventional vertical GaN Schottky barrier diodes. This work shows the feasibility of forming patterned pn junctions by novel ion implantation techniques, to enable high-performance vertical GaN power devices.

We1D1.2 **MBE Grown NPN GaN/InGaN HBTs on bulk-GaN Substrates**

08:45 AM

DR 5 & 6

Kazuki Nomoto (Cornell University, USA); Henryk Turski and Grzegorz Muziol (Institute of High Pressure Physics, PAS, Poland); Zongyang Hu and Shyam Bharadwaj (Cornell University, USA); Marcin Siekacz (Institute of High Pressure Physics, PAS, Poland); Czeslaw Skierbiszewski (Unipress, Poland); Debdeep Jena and Huili Xing (Cornell University, USA)

In this work, we demonstrate MBE grown GaN/InGaN/GaN n-p-n HBTs on bulk single-crystal GaN substrates with a low leakage current in each p-n junction. Good current saturation of the collector current with the collector-emitter voltage was observed. The common-emitter current gain is ~1.5 (VCB=0V). Visible light emission was observed from the B-C and E-B junctions at forward-bias from 3.5 to 7 V. Two EL peaks at 3.2 eV and 2.9 eV are seen. The origin of this photon peak at 3.2 eV is related with band to band radiative transition in the In~0.04Ga~0.096N base. Though recombination in the base of a HBT hurts its gain and performance, if the recombination is radiative, it also offers potential ways to cool the device, and to communicate with other devices. This first

demonstration of a MBE-grown HBT paves the way towards HBT based power electronic devices and circuits in the future.

We1D1.3

09:00 AM

DR 5 & 6

Investigation of the Origin of the Leakage of P-N Diodes on a Free-Standing GaN Substrate Using the 3DAP and LACBED Methods

Shigeyoshi Usami (Nagoya University, Japan); Yoshihiro Sugawara, Yong-Zhao Yao and Yukari Ishikawa (Japan Fine Ceramics Center, Japan); Norihito Mayama and Kazuya Toda (Toshiba Nanoanalysis Corpotration, Japan); Yuto Ando, Atsushi Tanaka, Kentaro Nagamatsu, Manato Deki, Maki Kushimoto, Shugo Nitta, Yoshio Honda and Hiroshi Amano (Nagoya University, Japan)

Dislocations that cause a reverse leakage current in vertical p-n diodes on a GaN free-standing substrate were investigated. Under a high reverse bias, dot-like leakage spots were observed using an emission microscope. Subsequent cathodoluminescence (CL) observation revealed that the leakage spots coincided with part of the CL dark spots, indicating that some of the dislocations cause reverse leakage. When etch pits were formed on dislocations by KOH etching, three types of etch pits were obtained (large, medium, and small). Among these etch pits, only the medium pits coincided with leakage spots. Additionally, transmission electron microscope observations revealed that pure screw dislocations are present under leakage spots. The results revealed that 1c pure screw dislocations are related to the reverse leakage in vertical p-n diodes.

We1D1.4

09:15 AM

DR 5 & 6

1.1 kV Regrown AlGaN/GaN Channel Based Vertical Trench MOSFET

Chirag Gupta, Silvia H Chan and Anchal Agarwal (University of California Santa Barbara, USA); Nirupam Hatui, Stacia Keller and Umesh Mishra (UCSB, USA)

Vertical GaN power devices have gained increased attention for high voltage/high current applications. Among many types of power MOSFET structures, trench MOSFET, is a favorable structure to reduce on-resistance due to the capability of high cell density and lack of junction-FET region. However, due to the formation of the channel on the etched sidewall, low channel mobility is observed in GaN trench MOSFETs resulting in either increased on-resistance and/or reliability issues. AlGaN/GaN hetero-junction based regrown channel have been explored in trench MOSFETs to improve channel mobility. So far, with MOS/MIS-gate, high performance AlGaN/GaN regrown channel based trench MOSFETs has not been demonstrated. In this work, we demonstrate a high performing normally-off, regrown AlGaN/GaN based vertical trench MOSFET with a low on-resistance of 3 $m\Omega \cdot cm^2$ and a breakdown voltage of 1.1 kV.

We1D1.5

09:30 AM

DR 5 & 6

High-Performance Vertical GaN P-N Diodes Fabricated with Epitaxial Lift-Off from GaN Substrates

Jingshan Wang and Lina Cao (University of Notre Dame, USA); Robert McCarthy (MicroLink Devices, USA); Chris Youtsey (MicroLink Devices, Inc., USA); Louis Guido (Virginia Tech, USA); Jinqiao Xie and Edward Beam (Qorvo, Inc., USA); Patrick Fay (University of Notre Dame, USA)

This is the first demonstration of high-performance vertical GaN-based p-n junction diodes fabricated using an epitaxial lift-off process from GaN substrates. The epitaxial GaN layers and a thin InGaN release layer were grown by MOCVD on bulk GaN substrates. A comparison study was performed on the devices after lift-off processing (after transfer to an Alumina carrier wafer) and nominally-identical control devices (without the buried release layer). It shows that devices after ELO have nearly identical electrical performance to those on full-thickness GaN substrates. The breakdown voltage, ideality factor and forward turn-on performance were found to be unchanged, indicating that the transfer process did not degrade the material quality. The devices exhibit turn-on voltages of 3.1 V at a current density of 100 A/cm^2, with specific on resistance of 0.2-0.5 mOhm-cm^2 at 4.8 V and breakdown voltage of 750-770V.

We1D1.6

09:45 AM

DR 5 & 6

Measurement of Electron and Hole Impact Ionization Coefficients in GaN P-N Junctions on Native GaN Substrates

Lina Cao, Jingshan Wang, Galen Harden, Anthony Hoffman and Patrick Fay (University of Notre Dame, USA)

GaN is attractive for power applications due to its wide bandgap and high critical electric field. The critical electric field is related to the onset of avalanche breakdown due to impact ionization, which puts an upper limit on the reverse blocking voltage. In this work, we experimentally characterize p-n junctions grown on single crystal bulk GaN substrates and extract the impact ionization coefficients for both electrons and holes. To our knowledge, this is the first report of the impact ionization coefficients of both electrons and holes from p-n junctions grown on native GaN substrates. Electron and hole impact ionization rates were measured using the photomultiplication method. The measured impact ionization rates presented here are in good general agreement with the theoretical impact ionization rates predicted using Monte Carlo simulation, indicating that defect and edge effects have been adequately suppressed.

We2A2: Lasers

Time:	5/30/2018, 10:30 AM - 12:30 PM
Room:	Salon M (Samberg Conference Center, 7th floor)
Chair:	Eric Tournié (Université de Montpellier, France)

We2A2.1

10:30 AM

Salon M

Single-Mode Buried InGaP Aperture VCSEL Emitting at 980 nm

Jiaxing Wang and Jonas Kapraun (University of California Berkeley, USA); Neil Cabello and Philippe Tingzon (University of the Philippines Diliman, USA); Kevin Cook, Jipeng Qi, Emil Kolev and Connie J. Chang-Hasnain (University of California Berkeley, USA)

We demonstrate a novel VCSEL design with lithographically defined InGaP layer as current aperture and a regrown high contrast grating (HCG) top mirror. This approach is promising to realize high power and high-speed VCSEL as it has many advantages compared to the conventional oxide aperture VCSEL. Firstly, the small index contrast between semiconductor and the InGaP aperture supports large-aperture single transverse mode devices with a smaller beam divergence (numerical aperture) facilitating high efficiency coupling with optical fiber and diffractive optics. The large current aperture can lead to potentially higher optical powers. The InGaP layer has a higher thermal conductivity providing an efficient path to dissipate heat off the device. In addition, concerns of structural integrity related to the porous oxide layer do not apply to our design. Lastly, a high degree of design freedom for high packing density of VCSEL arrays can be achieved via lithographic definition.

We2A2.2

10:45 AM

Salon M

Single Mode Operation of Multiple Phase-Shift Grating Membrane Buried Heterostructure Lasers Integrated on Silicon Nanowire Waveguide

Takuma Aihara (NTT Device Technology Laboratories, Japan); Tatsurou Hiraki (NTT, Japan); Koji Takeda, Koichi Hasebe, Takuro Fujii and Tai Tsuchizawa (NTT Corporation, Japan); Takaaki Kakitsuka (, Japan); Shinji Matsuo (NTT Corporation, Japan)

Silicon (Si) photonics technology based on a Si-on-insulator (SOI) substrate has great potential for constructing photonic integrated circuits (PICs) with reduced cost and size. Since laser sources are essential elements for PICs, it is important to fabricate PICs consisting of lasers and Si-based photonic devices. For this purpose, we have developed a heterogeneous integration technique, in which a membrane buried heterostructure (BH) including the III-V active region is heterogeneously integrated on a SOI substrate. We have already realized the integration of lasers and a Si nanowire waveguide, in which we used 200-nm-thick Si that is typically used in Si photonic devices. Since coupling coefficient of grating in membrane laser is relatively large involving spatial hole burning effect, we used a modulated grating to suppress the effect. In this paper, we show the design of the modulated grating, and demonstrate the experimentally obtained single mode lasing spectrum.

We2A2.3

11:00 AM

Salon M

Failure of the Current Modulation Driven Linewidth Broadening Factor for Analyzing the Optical Linewidth Behavior of Quantum Dot Lasers

Heming Huang (Télécom ParisTech; Université Paris-Saclay, France); Jianan Duan (Télécom ParisTech, Université Paris-Saclay, France); Jean-Guy Provost(III-V Lab, a joint laboratory Nokia Bell Labs France , Thales Research and Technology and CEA Leti, 1 avenueAugustin Fresnel, 91767 Palaiseau Cedex, France) ;Zhenguo Lu and Philip Poole (National Research Council Canada, Canada); Frédéric Grillot (Télécom Paristech, Université Paris-Saclay, France)

Narrow linewidth lasers can be engineered with self-assembled quantum dots (QD) as gain media. The optical linewidths of semiconductor lasers are often in the megahertz range and strongly increased above the Schawlow-Townes limit because of the linewidth broadening factor (αH-factor). In this work, we show that QD lasers can simultaneously exhibit a narrow optical linewidth (low αH-factor from the optical linewidth), while producing a much larger frequency chirp (high current αH-factor from the FM/AM). The FM/AM method reflects most likely a current modulation driven αH-factor, since the carrier fluctuations are perturbed by the current modulation while other methods show that QD lasers perturbed by the optical noise exhibits a smaller αH-factor. To sum, the FM/AM method overestimates the αH-factor and its application is limited when characterization of the phase noise is required such as in coherent communication systems.

We2A2.4

11:15 AM

Salon M

Temperature Tuning of Two-Color Lasing Using a Coupled GaAs/AlGaAs Multilayer Cavity by Current Injection

Xiangmeng LU and Yasuo Minami (Tokushima University, Japan); Naoto Kumagai (National Institute of Advanced Industrial Science and Technology, Japan); Ken Morita (Chiba University, Japan); Takahiro Kitada (Tokushima University, Japan)

We demonstrated the two-color lasing at room temperature (RT) and investigated the effects of temperature tuning on the lasing characteristics. The optical emission properties of three different devices A, B, and C were measured at RT using a pulsed-current source with a repetition rate of 1 kHz and a pulse duration of 0.5 μs. Two-color lasing was observed when the upper and lower cavity have equivalent thickness for device B. Only single lasing was observed when the thickness of upper and lower cavity are nonequivalent for device A and C. We carried out a temperature tuning on the device C ranged from RT to 85 °C in an ambient atmosphere. Two-color lasing of device C was realized at 85 °C. The optical thickness of lower cavity became equal to that of upper cavity as a result of the increment of refractive index due to thermal effect.

We2A2.5 **Quantum-Dot Lasers on Silicon**

11:30 AM *John E Bowers (University of California, Santa Barbara, USA)*

INVITED

Salon M

We present recent advances in InAs quantum dot (QD) lasers epitaxially grown on silicon. Advantages of QD over quantum well lasers on silicon are longer lifetime, lower reflection sensitivity and smaller linewidth enhancement factor. Our device and process design reduces threading dislocation densities from 3×10^{8} cm^{-2} to 7×10^{6} cm^{-2} using thermal cycle annealing and strained superlattices. Fabry-Perot QD lasers show a CW threshold current of 4.8 mA, extrapolated laser lifetimes more than 10 million hours at 35 °C, and direct modulation up to 12 Gbps. We have also demonstrated a single-section mode-locked QD laser on silicon that generates 490 fs optical pulses at a 31 GHz repetition rate, which is promising for potential applications such as wavelength division multiplexing systems. Finally, we show ultra-small micro ring QD lasers with a CW threshold of 0.5 mA and single-section mode-locked lasers with a 490 fs pulse width and 31 GHz repetition rate.

We2A2.6 **Improved Optical Properties in Plasmonic Silicon-doped InAs Using Bismuth Surfactants**

12:00 PM

Salon M

Dongxia Wei, Patrick Sohr and Stephanie Law (University of Delaware, USA)

InAs is a common III-V semiconductor used as designer plasmonic metals in the mid-infrared. However, the growth of high-quality heavily-doped InAs is challenging because silicon atoms tend to diffuse to the surface at high concentration. Here we report on the growth of highly silicon-doped InAs using bismuth as a surfactant. Our results show that a small amount of bismuth can lower the scattering rate and significantly improve the surface morphology of highly doped InAs films. Silicon atoms are also better incorporated into the lattice with the help of bismuth. The introduction of bismuth during the growth also allow us to grow highly doped InAs at higher temperatures (over 500℃) which make it easier to be integrated with other semiconductors. Surfactant-mediated growth therefore opens the door to integrating semiconductor plasmonic materials with other III-V optoelectronic structures.

We2A2.7

12:15 PM

Salon M

Enhancement of Thermoelectric Performance of Si Membrane by Al Silicide Nanodots

Masahiro Nomura (The University of Tokyo, Japan); Anthony George (The University of Tokyo); Ryoto Yanagisawa (The University of Tokyo, Japan); Sebastian Volz (CNRS, France)

On-chip thermoelectric generators (TEG) could provide a valid energy harvesting mechanism to devices for Internet of Things (IoT) if the power-cost ratio could somehow be improved. Si membranes are innately inexpensive, but offer limited thermoelectric efficiency. Recent our works have identified phonon surface scattering by nanodots as an important factor in lowering thermal conductivity and improving the ZT of nanostructured Si. This work demonstrates a low-cost large-area method for enhancing the performance of Si membrane TEG devices via single-nanometer Al thin film deposition. We fabricate Si membrane TEG devices with Al silicide nanodots, which was confirmed by TEM observation, and demonstrate that the thermoelectric performance was increased by 30% by the simple method.

We2B2: Wide Band Gap (GaN on Si)

Time:	5/30/2018, 10:30 AM - 12:30 PM
Room:	DR 3 & 4 (Samberg Conference Center, 6th floor)
Chair:	Hideto Miyake (Mie University, Japan)

We2B2.1
10:30 AM
DR 3 & 4

High Quality 200 mm GaN-on-Si Blue LED for uLED Display Application

Liyang Zhang, Kai Liu, Peng Xiang, Hongjing Huo, Ni Yin and Kai Cheng (Enkris Semiconductor, P.R. China)

Beyond general lighting, GaN based uLED technology has been considered as one of the most promising candidates for the next generation display applications. Large size, flat LED epi-wafers with a narrow wavelength bin range and low defect level are highly desired. A narrow wavelength bin range can avoid time consuming die binning process, and large size wafer can be transferred to a target backplane through wafer bonding technology if wafer is flat enough. A low defect level is critical to improve the final yield. In this report, we demonstrate high quality, crack-free GaN blue LED structures on 200 mm Si substrates. Large size GaN-on-Si LED wafer with a flat wafer bow of <30 µm, high IQE of ~90%, good wavelength uniformity (std 2.4 nm) and a low particle level of ~50 is one of the most promising technology roadmap for uLED display applications.

We2B2.2
10:45 AM
DR 3 & 4

Si Complies with GaN to Overcome Thermal Mismatches for the Heteroepitaxy of Thick GaN on Si

Atsunori Tanaka, Woojin Choi, Renjie Chen and Shadi Dayeh (University of California, San Diego, USA)

Heteroepitaxial growth of lattice mismatched materials has advanced through the epitaxy of thin coherently strained layers, the strain sharing in virtual and nanoscale substrates, and the growth of thick films with intermediate strain-relaxed buffer layers. However, the thermal mismatch is not completely resolved in highly mismatched systems such as in GaN-on-Si. In this paper, we report a way to dilate thermal stresses by utilizing geometrical effects and surface faceting in selectively grown epitaxial GaN layers on Si. The growth of thick 19 µm, crack-free, and pure GaN layers on Si with the lowest threading dislocation density of 1.1×10^7 cm^{-2} achieved to date in GaN-on-Si is demonstrated. With these advances, the first vertical GaN metal-insulator-semiconductor field-effect transistors on Si substrates with low leakage currents and high on/off ratios paving the way for a cost-effective high power device paradigm on an Si CMOS platform are demonstrated.

We2B2.3 **GaN-on-Si Laser Diodes and Normally-Off HEMTs**

11:00 AM *Qian Sun (Suzhou Institute of Nano-Tech and Nano-Bionics, Chinese Academy of Sciences, P.R. China)*

INVITED

DR 3 & 4

Direct growth of III-Nitride semiconductors on large-diameter cost-effective silicon is a promising game-changing technology to GaN-based optoelectronics and power electronics industry. However, hetero-epitaxial growth of GaN on Si encounters a large mismatch in both lattice constant and coefficient of thermal expansion, often resulting in a high density of defects and even micro-crack networks. By carefully engineering Al-composition step-graded AlN/AlGaN multilayer buffer between Si and GaN, we have not only successfully eliminated the crack formation, but also effectively reduced the dislocation density, as evidenced by both TEM and high resolution x-ray rocking curve measurements. Upon the high-quality GaN-on-Si platform, we have not only commercialized highly efficient blue, white, and UVA LEDs [1-2], but also realized the first electrically injected edge-emitting blue, violet, and UVA laser diodes [3-5]. In addition, room temperature electrically injected micro-disk laser diode directly grown on Si [6] will also be demonstrated. Meanwhile, normally-off HEMTs grown on Si with a p-GaN gate have also been fabricated through a selective removal of p-GaN for the access region with an etching-stop technology [7]. The as-fabricated enhancement mode HEMTs showed a decent performance with a good uniformity [8].

We2B2.4 **Realization of MOCVD GaN Tunnel Junction Contacts in Large Area LEDs**

11:30 AM *Abdullah Alhassan and Cheyenne Lynsky (University of California, Santa Barbara, USA); Ahmed Y. Alyamani (King Abdulaziz City for Science and Technology, Saudi Arabia); Shuji Nakamura (University of California Santa Barbara, USA); Steven DenBaars (University of California, Santa Barbara)*

DR 3 & 4

We demonstrate light-emitting diodes (LEDs) with tunnel junction (TJ) contacts grown entirely by metalorganic chemical vapor deposition (MOCVD). After the growth of the LED device structure where the growth stopped at the p-GaN layer, a pattern of a dielectric is deposited on the surface of the p-GaN. Then, a selective area regrowth of a tunnel junction by MOCVD is performed. After etching the mesa structure, a post anneal is carried out to fully activate the p-GaN through the lateral and vertical diffusion of hydrogen. In this work, we will discuss in details the effect of varying the patterns size, spacing between vias and annealing temperature on the performance of MOCVD TJ LEDs. Additionally, we explored different doping schemes to achieves high Si concentration while maintaining good surface morphology of the n++GaN layer.

We2B2.5

11:45 AM

DR 3 & 4

Fabrication of Nano-Cavity Patterned Sapphire Substrates and Their Application to the Growth of GaN

Donghyun Lee, Jehong Oh, Seungmin Lee, Giwoong Kim, Jongmyeong Kim, Jeonghwan Jang and Daeyoung Moon (Seoul National University, Korea); Yongjo Park (Advanced Institutes of Convergence Technology, Korea); Euijoon Yoon (Seoun National University, Korea)

We report the growth of GaN using the NCPSS which has hexagonally non-close-packed nano-cavity patterns on the sapphire substrate fabricated by the simple and cost-effective PS patterning process. The ELO of GaN on the NCPSS was achieved by the formation of relatively large GaN islands followed by enhanced lateral overgrowth of GaN over several nano-cavity patterns. The TDD of GaN calculated by the CL measurement was significantly reduced from 2.4×10^{8} cm^{-2} to 6.9×10^{7} cm^{-2} by using the NCPSS. The nano-cavities embedded in the GaN layer relaxed the residual compressive stress by 21%. Furthermore, the diffuse reflectance of GaN on the NCPSS was enhanced by 54% ~ 62% compared to that of GaN on the planar substrate. The enhancement is attributed to the increased refractive-index-contrast by introducing the cavity at the interface between GaN and the sapphire substrate and probability of light extraction through effective light scattering by nano-cavities.

We2B2.6

12:00 PM

INVITED

DR 3 & 4

Electrically-Injected GaN-based VCSELs

Tetsuya Takeuchi (Meijo University, Japan)

We have developed GaN-based VCSELs with AlInN/GaN DBRs, emitting 410 nm wavelength. By optimizing MOVPE growth conditions of the AlInN, more than 99% reflectivity of the DBR was achieved. So far RT-CW operations of the GaN-based VCSELs with the undoped DBRs were demonstrated. The threshold current was 5.2 mA, and the external differential quantum efficiency was 13 %. The corresponding maximum light output power was 4.2 mW. Up to 100°C, the GaN-based VCSEL was operated. In addition, we have developed conducting AlInN/GaN DBRs by using modulation doping of Si towards the GaN-based VCSELs with vertical carrier injections through the DBRs. Currently the conducting DBR-VCSEL shows not only the same threshold current but also a lower differential device resistance, less than 100 Ω.

We2C2: RF (Resonat Tunneling Diodes)

Time:	5/30/2018, 10:30 AM - 12:30 PM
Room:	Salon T (Samberg Conference Center, 7th floor)
Chair:	Nils Weimann (University of Duisburg-Essen, Germany)

We2C2.1

10:30 AM

INVITED

Salon T

Mm-wave/THz Multi-Gigabit Wireless Links and Microwave Interfaces - The iBROW Project

Edward Wasige (University of Glasgow, United Kingdom (Great Britain))

This paper reports on a novel, energy-efficient and compact ultra-broadband short-range wireless communication transceiver technology, which can be seamlessly interfaced with optical fibre networks and capable of addressing envisaged future network needs. The underpinning technology is the Resonant Tunnelling Diode (RTD). The RTD is the fastest demonstrated electronic device with fundamental oscillation frequencies of up to 1.98 THz reported recently, and is one of the promising solid-state technologies for compact and coherent sources for multi-gigabit wireless communication systems. On iBROW, RTD oscillators at both W-band and G-band with around 1 mW output power have been demonstrated. These have been used in laboratory wireless experiments and have supported data rates of over 10 Gb/s at both W-band and G-band using simple amplitude shift keying (ASK). RTDs can also be designed as photodetectors (PD). On iBROW, RTD-PDs have enabled microwave-photonic interfaces of up to 100 Mbaud optical data transmission using QPSK.

We2C2.2

11:00 AM

Salon T

Room Temperature Microwave Oscillators Enabled by Resonant Tunneling Transport in III-Nitride Heterostructures

Jimy Encomendero and Rusen Yan (Cornell University, USA); Amit Verma (Indian Institute of Technology, India); SM Islam and Vladimir Protasenko (Cornell University, USA); Sergei Rouvimov and Patrick Fay (University of Notre Dame, USA); Debdeep Jena and Huili Xing (Cornell University, USA)

In the present work, we report III-Nitride RTDs operating at room temperature, which exhibit record-high peak current densities up to ~ 220 kA/cm^2. When the diodes are biased within the negative differential conductance (NDC) region, self-oscillations build up in the biasing circuit. A maximum frequency of oscillation close to 1 GHz is reported. The oscillatory signal and output power is studied in two different RTD designs, showing that their robust negative dynamic conductance can be effectively used as gain element in high-frequency electronic oscillators.

We2C2.3

11:15 AM

Salon T

Triple Barrier RTD Integrated in a Slot Antenna for Mm-Wave Signal Generation and Detection

Khaled Arzi (University of Duisburg-Essen, Germany); Safumi Suzuki (Tokyo Institute of Technology, Japan); Daniel Erni and Nils Weimann (University of Duisburg-Essen, Germany); Masahiro Asada (Tokyo Institute of Technology, Japan); Werner Prost (University of Duisburg-Essen, Germany)

Mobile usage of (sub-) millimeter waves requires solid-state, compact, coherent, tunable, energy efficient, and hence preferably fundamental mode oscillators. The resonant tunneling diode is a promising candidate providing fundamental mode oscillation via an on-chip antenna up to 2 THz. The antenna requires a huge chip area and it is of fundamental interest to use a single antenna for both signal emission and detection. A triple barrier resonant tunneling diode provides at forward bias negative differential resistance for signal emission while at zero bias a blocking behavior is observed for signal detection. We present the experimental proof of signal emission and detection using one component: Biasing in the NDR yields an fundamental mode output signal of 90 µW at 260 GHz while at reverse bias a responsivity of R = 70 mV/µW was measured at f0 = 280 GHz. This concept is expected to reach sub-millimeter frequencies in the near future.

We2C2.4

11:30 AM

Salon T

Output Power Characteristics of Sub-THz Differential Oscillators Using an RTD Pair Topology

Maengkyu Kim (Korea Advanced Institute of Science and Technology, Korea); Se-Mi Kim and Jae-Hyung Jang (Gwangju Institute of Science and Technology, Korea); Kyounghoon Yang (KAIST, Korea)

In this work, we demonstrate an RTD-based sub-THz differential oscillator by using the RTD-pair topology to improve the output power of oscillation effectively in a sub-THz frequency range. the fabricated RTD-pair differential oscillator shows the oscillation frequency of 219 GHz with the maximum output power of 65 µW at each output port of Pdiff1 and Pdiff2.

We2C2.5

11:45 AM

Salon T

Experimental Demonstration of a Resonant Tunneling Diode Device Array with a Single Negative Differential Conductance Region

Abdullah Al-Khalidi (University of Glasgow, United Kingdom (Great Britain)); Jue Wang (University of Glasgow; University of Glasgow, United Kingdom (Great Britain)); Khalid Alharbi and Edward Wasige (University of Glasgow, United Kingdom (Great Britain))

In this paper, we report on a new device integration approach which extends the span of the negative differential conductance (NDC) region, through the use of an RTD array with terminal characteristics similar but larger compared to a single device. This approach employs resistors across the series integrated RTDs to act as voltage divider providing a constant voltage to the individual RTDs resulting in an NDC region with a single peak. Three RTDs integrated in series exhibit an NDC span with ΔV of 2V compared

to 0.7V of a single RTD. Since the output power of an RTD oscillator is directly proportional to the NDC span, this approach provides a potential route to high frequency RTD oscillators with high output power.

We2C2.6

12:00 PM

Salon T

Characterization of Nonvolatile Memory Operations Using GaN/AlN Resonant Tunneling Diodes

Masanori Nagase, Tokio Takahashi and Mitsuaki Shimizu (National Institute of Advanced Industrial Science and Technology (AIST), Japan)

A new nonvolatile memory using GaN/AlN resonant tunneling diodes (RTDs) was investigated to realize a high-speed nonvolatile random-access memory (RAM) operating at picosecond time scales. Based on the bistability of current-voltage characteristics caused by the intersubband transitions and electron accumulation in the quantum well, write/erase memory operations were performed using periodic pulse-voltage sequences. The error free operations during the repeated cycles of 8,000 and the ON/OFF current ratio above 3 dB were attained at room temperature. Also, the importance of realizing high-speed nonvolatile RAMs with the operation-speeds equivalent to those of SRAM and DRAM was discussed toward the realization of a new computing system with an ability of low power consumption.

We2C2.7

12:15 PM

Salon T

A Non-alloyed Au-free Ti/AlSiCu Ohmic Contact for n-InGaAs MOSFETs

Jen-Inn Chyi, Shan-Chun Hsu, Cheng-Han Tsou and Wei Jen Hsueh (National Central University, Taiwan); Szu Hung Chen (National Nano Device Laboratories, Taiwan)

In order to fabricate III-V devices in current Si manufacturing facilities, an Au-free ohmic contact is desirable. In this work, we experimentally demonstrate that Ti/AlSiCu metal stack, which is commonly used in Si industry, is well suited for the source/drain ohmic contacts of n-channel InGaAs MOSFETs. Specific contact resistivity as low as 2.85×10^{-7} Ω-cm^2 is obtained without any post metal annealing on an $In_{0.53}Ga_{0.47}As$ epilayer with carrier concentration of 4.1×10^{18} cm^{-3}. The non-alloyed contact also shows good stability with resistance variation less than 1% after current stress of $3.2\text{x}10^5$ A/cm^2 at room temperature for over 27 hours. Besides, the specific contact resistivity increases only slightly to 3.41×10^{-7} Ω-cm^2 after annealing in a furnace at 300°C for 15 min in forming gas.

We2D2: Power (GaN)

Time:	5/30/2018, 10:30 AM - 12:30 PM
Room:	DR 5 & 6 (Samberg Conference Center, 6th floor)
Chair:	Sameer Pendharkar (Texas Instruments, United States)

We2D2.1 **1-kV-class AlN Schottky Barrier Diodes on Sapphire Substrates**

10:30 AM

DR 5 & 6

Houqiang Fu (Arizona state University; Arizona State University, USA); Xuanqi Huang, Hong Chen, Izak Baranowski, Jossue Montes and Tsung-Han Yang (Arizona State University, USA); Yuji Zhao (Arizona state University, USA)

Ultra-wide bandgap (UWBG) semiconductor aluminum nitride (AlN) has recently been investigated as a promising candidate for high power and high voltage electronic applications, due to its large bandgap (6.2 eV) and high breakdown electric field (12 MV/cm). We recently demonstrated the first 1-kV-class AlN SBDs on cost-effective sapphire substrates grown by metal organic chemical vapor deposition (MOCVD). The device structure mimics the silicon-on-insulator (SOI) technology, consisting of thin n-AlN epilayer as the device active region and thick resistive AlN underlayer as the insulator. The devices show outstanding performances with a low turn-on voltage of 1.2 V, a high on/off ratio of ~10^5, and a low ideality factor of 5.5. The devices also exhibit excellent thermal stability up to 300 °C. This work presents a cost-effective route to high performance AlN based Schottky barrier diodes for high power, high voltage and high temperature applications.

We2D2.2 **High Performance 820V GaN-on-Si PiN Diodes**

10:45 AM

DR 5 & 6

Riyaz Mohammed Abdul Khadar (École Polytechnique Federale de Lausanne, Switzerland); Chao Liu (Ecole Polytechnique Fédérale de Lausanne (EPFL), Switzerland); Reza Soleiman Zadeh Ardebili (École Polytechnique Federale de Lausanne, Switzerland); Liyang Zhang, Peng Xiang and Kai Cheng (Enkris Semiconductor, P.R. China); Elison Matioli (EPFL, Switzerland)

GaN-on-Silicon offers a cost-effective platform for vertical power devices, due to its low cost, large-scale, and mature fabrication technology. However, their performance is much worse than that on GaN substrates, due to the challenging growth of thick GaN layers on Si. In this work we demonstrate GaN-on-Si p-i-n diodes with high breakdown voltage and state-of-the-art Baliga's Figure of Merit (BFOM). The growth and doping of the GaN drift layer were optimized, leading to a remarkable electron mobility of 720 cm^2/Vs for a Si doping level of 2×10^{16} cm^{-3}. With a 4 µm-thick drift layer, we achieved an excellent breakdown voltage of 820 V and ultra-low specific on-resistance of 0.33 mohm-cm^2. This results in a BFOM of 2.0 GW/cm^2, which is more than 6x-larger than the best value reported to date. These results reveal the excellent prospect of GaN-on-Si for cost-effective vertical power devices.

We2D2.3 **2 kV GaN-on-Si SBDs with a Slanted Tri-Gate Architecture**

11:00 AM *Jun Ma and Elison Matioli (École polytechnique fédérale de Lausanne (EPFL), Switzerland)*

DR 5 & 6

In this work we demonstrate slanted tri-gate GaN-on-Si SBDs with record voltage-blocking performance. The devices presented the highest breakdown voltage of 2000 V at 1 μA/mm, the lowest reverse leakage current of 5.5 ± 1.8 nA/mm at -650 V (or ~0.1 μA at -1200 V), a small turn-on voltage of 0.61 ± 0.03 V, and an excellent high-power figure-or-merit of 1.16 GW/cm^2, as compared with existing technologies. These results constitute a significant breakthrough for GaN-on-Si power SBDs, and can open enormous opportunities for future monolithic GaN power converters.

We2D2.4 **Vertical 18-Um-Thick GaN Trench Gate MISFETs on Si**

11:15 AM *Woojin Choi, Atsunori Tanaka, Renjie Chen and Shadi Dayeh (University of California, San Diego, USA)*

DR 5 & 6

Our recent work overcomes barriers for thick GaN growth due to the large mismatches in coefficient of thermal expansion (CTE) between GaN and Si, and we successfully demonstrated 18 μm thick vertical GaN MISFETs on Si through strain engineered selective area growth (SAG). The dislocation density in the grown layer was as low as 1.1E7 cm^{-2} at the surface, and we fabricated vertical trench gate MISFETs employing 18 μm thick GaN layers on a Si substrate. The fabricated device showed the threshold voltage of 8 V, the on/off drain current ratio of ~1E7, and the maximum drain current density of 20 mA/mm. These results showed a great potential in high-performance and low-cost vertical GaN devices on a Si substrate as well as a possible Si CMOS integration.

We2D2.5 **N-Polar GaN HEMTs for High Voltage Switching Applications Demonstrating Negligible Dispersion at 450 V Quiescent Bias**

11:30 AM *Onur Koksaldi, Jeffrey Haller, Haoran Li, Nirupam Hatui and Brian Romanczyk (University of California Santa Barbara, USA); Matthew Guidry (University of California, Santa Barbara, USA); Steven Wienecke, Jr, Stacia Keller and Umesh Mishra (University of California Santa Barbara, USA)*

DR 5 & 6

The development of III-Nitride devices has historically focused on the metal-polar crystal orientation (0001),and has achieved excellent results in both RF and power domains.The N-polar orientation (000-1) has gained momentum more recently,and demonstrated record performances in both application spaces.In this paper,we discuss the recent developments in N-Polar HEMTs for high voltage switching applications,that showed no increase in dynamic on-resistance (Ron) at 450 V,with a DC breakdown of >1300 V. N-Polar GaN epi-layers were grown by MOCVD on miscut SiC substrates.MOCVD regrown ohmic contacts were used.The devices were fabricated with three field plates(FP),one gate-connected FP and two source-connected FPs.The specific on-resistance (active-area) was 5.8 mΩ·cm^2 (14.4 Ω·mm),with a DC breakdown voltage of 1320 V.Dynamic R_{on} was measured 5 μs after the device was switched from the off-state to the on-

state.These transistors demonstrated record-low dispersion when measured up to 450 V drain stress,with no increase in dynamic R_{on} at 450 V.

We2D2.6 **Scaling of GaN HEMTs Thermal Transient Characteristics**

11:45 AM

DR 5 & 6

Adrien Cutivet (Universitὶé de Sherbrooke, Canada); Meriem Bouchilaoun (University of Sherbrooke, Canada); Bilal Hassan (Universitὶé de Sherbrooke, Canada); Christophe Rodriguez (University of Sherbrooke, Canada); Ali Soltani (IEMN - Université de Lille, France); François Boone and Hassan Maher (Université de Sherbrooke, Canada)

This work presents a study on the scaling of the GaN HEMTs thermal time constants with device periphery. The characterization technique used (gate resistance thermometry in frequency domain) enables to determine the transistor thermal impedance on a broad range of conditions (time scales and biasing conditions). From measurement on HEMTs with diverse gate widths, we show experimentally that the thermal impedance remains unchanged whether the device is in the linear or saturation region. Furthermore, thermal impedance normalized with total gate width is shown to be constant for frequencies above 30 kHz (equivalent to pulsed time less than 5 µs). Thorough analysis of the different transient regimes will be described during the oral presentation and final insights for the optimization of thermal management in transient operations.

We2D2.7 **Leaky Dielectric Model for Dynamic R_{ON} in GaN/AlGaN Power Transistors**

12:00 PM

INVITED

DR 5 & 6

Michael J Uren and Martin Kuball (University of Bristol, United Kingdom (Great Britain))

GaN-on-Si power switching devices are now commercially available and giving outstanding efficiency. However, delivering this performance has been surprisingly difficult as developers have sought to improve reliability and suppress stability issues. This work reviews the consequences of using a complex multilayer semi-insulating epitaxial buffer structure on key metrics such as dynamic R_{ON}, and shows that treating the buffer as a set of leaky dielectric layers allows many time and bias dependent effects to be understood and controlled.

We3A3: Narrow Band Gap

Time:	5/30/2018, 01:30 PM - 03:00 PM
Room:	Salon M (Samberg Conference Center, 7th floor)
Chair:	John E Bowers (University of California, Santa Barbara, United States)

We3A3.1 **Sb-based IR Detector and Emitter Materials**

01:30 PM *Eric Tournié (University of Montpellier)*

INVITED

Salon M

Sb-based materials rely on the GaSb, InAs, AlSb, InSb binary compounds and their quaternary or quinary alloys (AlGaAsSb, GaInAsSb, AlGaInAsSb,..). This technology exhibits several distinctive properties as compared to other semiconductors: type-I to type-III band alignments, giant band offsets, low effective masses of electrons and holes, direct bandgaps between 0.15 and 1.7 eV. In this presentation we review the epitaxial growth and properties of the Sb-based materials and show how they enable the development of a variety of optoelectronics devices operating in the IR range for photonic sensing and/or security and defense applications, including their integration on Si substrates.

We3A3.2 **High Quality InP Epitaxially Grown on (001) Silicon for On-Chip Lasers**

02:00 PM *Bei Shi (The Hong Kong University of Science and Technology, Hong Kong); Qiang Li and Kei May Lau (Hong Kong University of Science and Technology, Hong Kong)*

Salon M

We focus on lowering the defect density of InP epitaxially grown on (001) silicon to improve the optical properties of silicon-based lasers. For InP grown on planar Si (IoPS), we adopted the InAs quantum dots as dislocation filter layers. The surface threading dislocation density was lowered to 3e8 cm^{-2} based on plan-view TEM. Another integration scheme was the epitaxy of InP on V-grooved Si (IoVS). Utilizing the aspect ratio trapping effect, most of the defects can be confined in the bottom InP. The low defect density was verified by the two-fold reduction in the FWHM of XRD ω-rocking scan, as compared to the IoPS substrate. Based on the IoVS template, we grew and fabricated 1550 nm band electrical Fabry-Perot lasers on Si. These devices can operate beyond 60 ℃ under pulsed injection. The characteristic temperature T0 is 133 K, and the threshold current density is Jth=7.2 kA/cm^2 at room temperature.

We3A3.3 **Substrate-transferred Crystalline Coatings**

02:15 PM *Garrett Cole (Crystalline Mirror Solutions LLC; Crystalline Mirror Solutions GmbH, USA); David Follman, Paula Heu and Gar-Wing Truong (Crystalline Mirror Solutions LLC, USA); Christoph Deutsch, Dominic Bachmann, Tobias Zederbauer and Ashish Rai (Crystalline Mirror Solutions GmbH, Austria); Mark White (Crystalline Mirror Solutions LLC, USA); Markus Aspelmeyer (Crystalline Mirror Solutions GmbH, Austria)*

Salon M

Substrate-transferred crystalline coatings have emerged as a groundbreaking new concept in optical coatings, merging epitaxially-grown compound semiconductors with super-polished bulk optics. Initially pursued for the development of ultra-low Brownian noise optics for precision metrology, these novel single-crystal coatings display fundamental advantages over traditional amorphous coatings. With improvements in our manufacturing and inspection processes, we have now pushed the excess optical losses of these GaAs/AlGaAs-based single-crystal multilayers to well below 5 ppm. Recent results have demonstrated a cavity finesse exceeding 600,000 near 1550 nm (equivalent to a reflectivity >99.9995%) for GaAs/AlGaAs on a fused silica substrate at room temperature. Moreover, in the mid-infrared spectral region, we verify optical absorption values as low as 2 ppm near 3700 nm for epitaxial multilayers transferred to single-crystal silicon substrates. Taken together, our "semiconductor supermirrors" exhibit the lowest Brownian noise, the highest thermal conductivity, and the widest transparency window of any optical coating technology.

We3A3.4 **High-quality Growth of Chalcogenide Topological Insulators**

02:30 PM *Stephanie Law (University of Delaware, USA)*

INVITED

Salon M

Chalcogenide topological insulators (TIs), including Bi2Se3, Bi2Te3, and Bi2(Se(1-x)Tex)3, are of significant interest due to their unique band structure. These materials have a bulk bandgap crossed by surface states that exhibit linear dispersion and spin-momentum locking. The Dirac electrons in these surface states are low-mass, spin-polarized, and unable to backscatter, making them a tantalizing prospect for applications in optics, electronics, and spintronics. Unfortunately, many TI films exhibit significant bulk conductivity and unstable properties upon exposure to air, making it difficult to access the topological electrons and design real-world devices. In this talk, I will describe our recent results on the growth of chalcogenide TIs. By using a combination of chalcogenide cracking sources, annealing techniques, alloying, lattice-matched virtual substrates, and capping layers, we have been able to reduce the bulk carrier density by more than a factor of two in our films, allowing access to the topological surface electrons. Furthermore, our films are stable in air for over 60 days. I will present x-ray diffraction, atomic force microscopy, and optical data showing how the film quality depends on various growth parameters. Further refinements to our growth procedures may completely eliminate the bulk electrons, leading to long-awaited TI devices.

We3B3: Wide Band Gap

Time:	5/30/2018, 01:30 PM - 03:00 PM
Room:	DR 3 & 4 (Samberg Conference Center, 6th floor)
Chair:	Tetsuya Takeuchi (Meijo University, Japan)

We3B3.1

01:30 PM

DR 3 & 4

Anisotropic Strain and Linearly Polarized Photoluminescence of C-Plane GaN Layers on Stripe-Shaped Cavity-Engineered Sapphire Substrate

Jongmyeong Kim, Daeyoung Moon and Duyoung Yang (Seoul National University, Korea); Yongjo Park (Advanced Institutes of Convergence Technology, Korea); Euijoon Yoon (Seoun National University, Korea)

Anisotropic in-plane strain and resultant linearly polarized photoluminescence (PL) of c-plane GaN layers were realized by using a stripe-shaped cavity-engineered sapphire substrate (SCES). High resolution X-ray reciprocal space mapping measurements revealed that the GaN layers on the SCES were under significant anisotropic in-plane strain of -0.0140% and -0.1351% along the directions perpendicular and parallel to the stripe pattern, respectively. The anisotropic strain in the GaN layers was attributed to the anisotropic strain relaxation due to the anisotropic arrangement of cavity-incorporated membranes. The anisotropic in-plane strain altered valence band structures of GaN, resulting in the polarized PL from the c-plane GaN layers. The experimental results of peak shift and angle-dependent PL intensities were comparable with calculated value based on k·p perturbation theory. It was found that the polarized PL behavior was attributed to the modification of valence band structures induced by anisotropic strain in the GaN layers on the SCES.

We3B3.2

01:45 PM

DR 3 & 4

Carrier Transport and Deep Level Defects Lead to Delayed Cathodoluminescence in InGaN/GaN LEDs

Akshay Singh (Massachusetts Institute of Technology, USA); Zhibo Zhao (Massachusetts Institute of Technology`, USA); Silvija Gradecak (Massachusetts Institute of Technology, USA)

InGaN LEDs are the dominant solid state lighting solutions but suffer from efficiency droop at high injection currents. In this work, we use a combination of electron microscopy tools to investigate reduced-droop InGaN/GaN quantum well (QW) designs. We find that chip-scale efficiency is uncorrelated with extended well-width fluctuations observed in scanning transmission electron microscopy. Remarkably, delayed cathodoluminescence (CL) is observed from LEDs in which carriers are designed to easily escape from the QWs. We propose a model in which the electron beam (a) passivates deep level defect states and (b) drives charge carrier accumulation and subsequent reduction of the built-in field across the QW active region, resulting in delayed radiative recombination. Finally, we correlate CL rise dynamics with capacitance-voltage measurements, and show that certain early-time components of the CL dynamics are indicative of the open circuit carrier population within one or more QWs.

We3B3.3

02:00 PM

INVITED

DR 3 & 4

Materials Challenges of AlGaN-based Power Electronics and UV Lasers

Mary Crawford, Andrew Allerman, Andrew Armstrong, Robert Kaplar, Greg Pickrell, Jeramy Dickerson, Michael Smith and Karen Cross (Sandia National Laboratories, USA); Vincent Abate (Sandia National Laboratory, USA); Caleb Glaser and Michael Van Heukelom (Sandia National Laboratories, USA)

AlGaN alloys have emerged as highly-promising materials for applications including high-power electronics and ultraviolet optoelectronics. Despite their tremendous potential, materials challenges have impeded maturation of AlGaN-based devices. In this presentation, we will discuss several key challenges and overview recent advances to overcome them. A major challenge for both electronic and optoelectronic devices is the lack of a substrate option that is electrically-conducting and enables pseudomorphic growth of device heterostructures. We will present recent progress on AlGaN growth on patterned templates, including n-type GaN, to address this challenge. A second challenge is doping, particularly p-type doping in higher-Al-content alloys. We will present potential solutions including polarization-induced doping through composition-graded, Mg-doped AlGaN layers and Mg-doped short-period superlattices and describe their implementation in AlGaN-based power diodes. Finally, we will discuss challenges and potential solutions for reducing compensating point defects in AlGaN alloys and devices.

We3B3.4

02:30 PM

DR 3 & 4

Comparative Study of Electroluminescence in GaN and AlGaN QW Sub-300nm DUV LEDs

Shyam Bharadwaj (Cornell University, USA); Cheng Liu (Rochester Institute of Technology, USA); Craig Moe and James Grandusky (Crystal IS, Inc., USA); Akira Yoshikawa and Jumpei Kasai (Asahi Kasei Corporation, USA); SM Islam and Vladimir Protasenko (Cornell University, USA); Leo Schowalter (Crystal IS, Inc., USA); Jing Zhang (Rochester Institute of Technology, USA); Debdeep Jena and Huili Xing (Cornell University, USA)

Commonly, DUV LEDs with high-Al composition (>55%) c-plane AlGaN quantum wells (QWs) are utilized to produce <280 nm emission. However, as the Al mole fraction is increased beyond ~65% to reach shorter wavelengths (<250 nm), the crystal-field splitoff hole (CH) band moves to higher energies than the heavy-hole (HH) and light-hole (LH) bands. This switch is accompanied by a transition from transverse electric (TE) to transverse magnetic (TM) dominant emission, resulting in drastically reduced efficiencies and light intensities collected from the typical c-face surface. In this work, we present a comparative study on the emission polarization properties of GaN- and AlGaN-QW LEDs in a wavelength range of 230 - 300 nm through angle and polarization resolved electroluminescence (EL) measurements and simulations. Since the HH and LH bands stay above the CH band in GaN-QWs, these LEDs promise TE dominant emission at all wavelengths.

We3B3.5

02:45 PM

DR 3 & 4

Comprehensive Analysis of Surface Morphology and Growth Mode of AlInGaN Films

Matthew Laurent (UC Davis, USA); Stacia Keller and Umesh Mishra (UCSB, USA); Srabanti Chowdhury (UC Davis; ASU, USA)

This study presents a systematic characterization of AlInGaN films grown as a function of thickness, V-III ratio, temperature, growth rate, and composition. The AlInGaN films grown in this study exhibited characteristic features of the spiral growth mode as described by Burton, Cabrera, and Frank. This growth mode was first observed in the III-N material system for the growth of MBE-grown GaN and occurs under highly non-equilibrium growth conditions. The spiral hillock radius of curvature can be described by $\rho_c = A/\ln\left[\left(P/P_0\right)\right]$, in which A is material-dependent, P is the partial pressure of growth precursors in the vapor phase, and P_0 is the vapor pressure of the solid. Adjusting P or P_0 via growth parameters had effects consistent with BCF theory for spiral growth. Finally, for very high AlN crystal fraction or V/III ratio, the AlInGaN films exhibited a 2-D island nucleation growth mode.

We3C3: RF (Narrow Band Gap)

Time:	5/30/2018, 01:30 PM - 03:00 PM
Room:	Salon T (Samberg Conference Center, 7th floor)
Chair:	Lars-Erik Wernersson (Lund University, Sweden)

We3C3.1 **III-V CMOS: Quo Vadis?**

01:30 PM *J. A. del Alamo, X. Cai, W. Lu, A. Vardi and X. Zhao (Microsystems Technology Laboratories, Massachusetts Institute of Technology, Cambridge, MA, USA)*

INVITED

Salon T

In the last few years, there has been a great deal of interest in the potential of III-V compound semiconductors, notably InGaAs, to advance CMOS scaling in the future. Yet, in spite of impressive device demonstrations, this effort has recently fizzled out. The value proposition behind III-V CMOS stands on the ability of nanoscale III-V transistors to deliver high current at low voltage. This should enable operating voltage reduction, an enhancement in the energy efficiency of logic operations and increases in transistor density, the heart of Moore's law. At its core goal, III-V transistors have yet to deliver. The performance of the most advanced InGaAs FinFETs, the most relevant device structure, has yet to match Si. The reasons appear multiple: sidewall scattering, high interface state density, electrical instability, band-to-band tunneling, manufacturing robustness and others. This talk will review these and other problematic issues with III-V CMOS and discuss possible solutions.

We3C3.2 **Fabrication of InGaAs Nanosheet Transistors with Regrown Source**

02:00 PM *Toru Kanazawa, Kazuto Ohsawa, Tomohiro Amemiya, Nobukazu Kise, Ryosuke Aonuma and Yasuyuki Miyamoto (Tokyo Institute of Technology, Japan)*

Salon T

High mobility channel materials such as III-V compounds and Ge have been developing to realize high-speed and low-power logic transistors. Thin body or multi-gate structures have also been introduced to suppress the short channel effects. A stacked-nanosheet transistor is a novel device structure for an extremely scaled channel length. It is expected to afford flexible design of the channel width and improved thickness controllability. In this report, we demonstrated InGaAs nanosheet transistors with the heavily doped regrown source for low series resistance. Two-stacked InGaAs nanosheets suspended by the regrown InGaAs were observed by SEM and TEM. The suppressed short channel effects appeared with the channel length of 40 nm, and the drain current of fabricated devices tend to be proportional to the width of nanosheets.

We3C3.3 **First Demonstration of InGaAs FinFETs on Si for RF Applications**

02:15 PM *Cezar Zota, Clarissa Convertino and Marilyne Sousa (IBM Research Zurich, Switzerland); Daniele Caimi (Zurich IBM Research Center, Switzerland); Lukas Czornomaz (IBM Research Zurich, Switzerland)*

Salon T

III-V materials, in particular the InxGa1-xAs system, have received considerable research attention due to their high electron mobility and injection velocity which makes them suitable as a replacement for strained Si in CMOS N-type FinFETs. FinFETs are also used for CMOS-RF applications, where high-frequency functionalities can be tightly integrated e.g. with logic circuits handling signal processing. For these applications, III-V materials are expected to allow for operation at higher frequencies, or with lower noise, i.e. improve the cutoff frequency ft, and maximum oscillation frequency fmax. In this work, we demonstrate the first RF-compatible InGaAs FinFETs integrated on Si. Promising performance of ft and fmax = 123 and 56 GHz, respectively, is reported. Key design parameters, including fin density, are highlighted. Finally, we show that scaling of fin dimensions offers significant improvement of the voltage gain over traditional HEMT technology and 14 nm Si FinFET CMOS RF.

We3C3.4 **Low Capacitance InGaAs Nanowire MOSFETs for High-Frequency Applications**

02:30 PM *Fredrik Lindelöw, Lasse Södergren and Erik Lind (Lund University, Sweden)*

Salon T

III-V nanowire MOSFETs is a promising candidate for future RF applications due to the excellent transport properties and high electrostatic control offered by the nanowire geometry. In this work we present a novel processing scheme for lateral nanowire MOSFETs that offers a path to reduce parasitic capacitances, a key component for high frequency transistors.

We3C3.5 **Mobility Extraction in Thin-Channel InGaAs MOSFETs**

02:45 PM *Xiaowei Cai (Massachusetts Institute of Technology, USA); Jesus Grajal (Universidad Politécnica de Madrid, Spain); Jesus del Alamo (MIT, USA)*

Salon T

In this work, we study mobility in thin-channel planar InGaAs MOSFETs. We have prepared InGaAs planar MOSFETs with intrinsic In0.7Ga0.3As channel and channel thicknesses (tc) from 8 to 2 nm. We observe a large frequency dispersion of transconductance from DC to 10 GHz, extracted from parametric, lock-in and S-parameter measurements. This indicates severe electron trapping in the oxide that worsens with decreasing tc. This not only affects device performance, but also obscures the true mobility extraction in conventional CV method. Since there is still prominent oxide trapping around 1 MHz, standard CV measures not only conducting carriers, but also a fraction of trapped carriers and results in an underestimation of electron mobility. Through gated-Hall measurements where only free electrons are measured, we find much less degradation with scaling and promising device performance even at 2 nm channel thickness with a peak Hall mobility of ~2500 $cm^2/V{\cdot}s$.

We3D3: Power (GaN)

Time:	5/30/2018, 01:30 PM - 03:00 PM
Room:	DR 5 & 6 (Samberg Conference Center, 6th floor)
Chair:	Michael J Uren (University of Bristol, United Kingdom (Great Britain))

We3D3.1

01:30 PM

DR 5 & 6

Normally-off p-GaN/AlGaN/GaN HEMTs by Hydrogen Plasma Treatment

Kai Fu (Arizona State University, USA); Ronghui Hao and Baoshun Zhang (Suzhou Institute of Nano-Tech and Nano-Bionics, Chinese Academy of Sciences, P.R. China); Yuji Zhao (Arizona state University, USA)

GaN based high electron mobility transistors are promising candidates for high power switching applications. Among normally-off solutions, p-GaN gate HEMTs are considered as one of the most promising candidates with a critical process of etching p-GaN over AlGaN barrier. Compared with that, we have demonstrated the first normally-off p-GaN/AlGaN/GaN HEMTs using hydrogen plasma treatment. In this work, a normally-off p-GaN/AlGaN/GaN HEMT is demonstrated with high BV and low current collapse factor. Also, we systematically investigate the hydrogen plasma treatment window including radio frequency power, treatment time and rapid thermal annealing effect. The high performance is mainly due to the high-resistivity-cap-layer introduced by p-GaN deactivation which forms a quasi-in-situ passivation layer. Besides, after a thermal stress test at 150 ºC for 1000 h, no clear degradation of Vth or gate leakage can be observed.

We3D3.2

01:45 PM

DR 5 & 6

Normally-OFF GaN HEMT Fabrication Using Soft and Selective Etching of the Si3N4 Cap Layer

Meriem Bouchilaoun (University of Sherbrooke, Canada); Ali Soltani (IEMN - Université de Lille, France); Christophe Rodriguez and Abdelatif Jaouad (University of Sherbrooke, Canada); Hassan Maher (Université de Sherbrooke, Canada)

This work reports on a new approach for the fabrication of normally-off AlGaN/GaN Metal-Oxide-Semiconductor High Electron Mobility Transistors (MOS-HEMT) based on the etching of in-situ Si3N4 layer under the gate electrode avoiding any exposition of the AlGaN barrier layer to fluorine plasma. This technic consists on a local modification of the Si3N4 layer using a soft hydrogen based plasma followed by a wet chemical etching of the modified Si3N4. The fabricated normally-off AlGaN/GaN HEMTs deliver a threshold voltage of +0.5V, a maximum drain current of 250mA/mm at a gate bias of +6V, and a gate leakage current bellow 1nA/mm. In this approach, the positive shift of the threshold voltage (Vth) is mainly due to the impact of the Hydrogen plasma on the 2D gas of the transistor.

We3D3.3

02:00 PM

DR 5 & 6

Tungsten-based Ion Implanted Ohmic Contacts in GaN HEMTs for High Temperature Applications

Mengyang Yuan and Tomás Palacios (Massachusetts Institute of Technology, USA)

In this work, we propose to increase the temperature stability of the contact, by combining a refractory metal such as tungsten (W) with Si-ion implantation, which locally dopes the material n-type and reduces the contact resistance. Non-alloyed Ti/Al/Ni/Au metal stacks were first studied on an AlGaN/GaN sample where the contact region was Si-ion implanted and annealed, prior to the metallization, at 1200 ℃ to activate the implanted species. A low Rc was obtained and indicates the effectiveness of ion implantation. Under same ion implantation and annealing conditions, a low Rc of 0.8 Ω·mm, Imax of 700 mA/mm were obtained with the W ohmic contacts and Rc was stable up to 300 ℃ for at least 30 min, while Rc of conventional alloyed Ti/Al/Ni/Au increased from 0.47 Ω·mm (RT) to 2.15 Ω·mm (300 ℃) under same conditions.

We3D3.4

02:15 PM

DR 5 & 6

Normally-off p-GaN Gate HEMT with Hydrogen Implantation Passivation

Qifeng Lyu and Huaxing Jiang (Hong Kong University of Science and Technology, Hong Kong); Peng Xiang and Kai Cheng (Enkris Semiconductor, P.R. China); Kei May Lau (Hong Kong University of Science and Technology, Hong Kong)

In this work, we demonstrate a novel normally-off p-GaN gate HEMT on Si using hydrogen ion implantation to deactivate the p-GaN in the access region. The device exhibits a high on/off current ratio of 10^8, a small subthreshold slope of 70 mV/dec, a threshold voltage of 1.35 V at Id of 1uA/mm. Without removing the p-GaN in the access region, a breakdown voltage as high as 1000 V at Id of 1 uA/mm is still achieved in the device. Moreover, the hydrogen implantation passivated p-GaN gate HEMT also exhibits excellent thermal stability, as evidenced by the low off-state leakage current from room temperature to 200 °C.

We3D3.5

02:30 PM

DR 5 & 6

MOVPE Growth of AlN/GaN/AlN HFET Structures on 4H-SiC

Frank Brunner, Oliver Hilt, Anna Reis and Joachim Wuerfl (Ferdinand-Braun-Institut, Germany); Markus Weyers (Ferdinand-Braun-Institut Berlin, Germany)

The development of a GaN-channel/AlN-buffer HFET technology opens up the opportunity for efficient high power amplification or power switching due to a very strong confinement of the 2D electron gas. Subject of this contribution are critical aspects of epitaxial growth development in MOVPE and layer stack design on large area 4H-SiC substrates. AlN buffer properties benefit from the good lattice- and thermal-matching of AlN and 4H-SiC avoiding excessive strain incorporation during growth. The thickness of the GaN channel layer has been varied between 50 nm and 200 nm resulting in different degrees of relaxation. AlN barrier layers in the thickness range of 5 nm to 10 nm were studied. X-ray analysis allows for a quantification of Ga carry-over into the barrier layer. Hall effect measurements revealed a sheet electron concentration of about 1.8×10^{13} cm^{-2} in conjunction with a 2DEG mobility of 900 cm^2/Vs. First devices

show maximum drain-source current densities of 0.8 A/mm, a maximum transconductance of 320 mS/mm and leakage currents as low as 10-8 A/mm.

We3D3.6

02:45 PM

DR 5 & 6

Vertical GaN-on-Si MOSFET with Monolithically Integrated Freewheeling Schottky Barrier Diode

Chao Liu (Ecole Polytechnique Fédérale de Lausanne (EPFL), Switzerland); Riyaz Mohammed Abdul Khadar (École Polytechnique Federale de Lausanne, Switzerland); Elison Matioli (EPFL, Switzerland)

MOSFETs with freewheeling diodes are highly desirable in several power converter topologies. The increased losses from the large turn-on voltage of intrinsic MOSFETs body diodes can be addressed by integrated Schottky barrier diodes (SBD). In this work, we demonstrate the first vertical GaN MOSFET with monolithically integrated freewheeling SBD, which offers reduced footprint with smaller parasitic components, and simplified packaging. Vertical GaN MOSFETs with integrated freewheeling SBD were grown on 6-inch silicon substrates with 4-µm-thick drift layer. The integrated MOSFETs-SBD exhibited e-mode operation with threshold voltage of 4.2 V, on/off ratio over 108 and a dramatic improvement in reverse conduction, without degradation in on-state performance from the integration of the SBD. The integrated SBD exhibited excellent performance, with R_{on} of 1.6 mΩ·cm^2, turn-on voltage of 0.5 V, ideality factor of 1.5, along with state-of-the-art breakdown voltage. These results reveal great potential of GaN-on-Si vertical MOSFETs for power converters.

We3D3.7

03:00 PM

DR 5 & 6

A New Generation of GaN Devices on 8-Inch Diameter, Thermal-Expansion Matched Substrates

Vladimir Odnoblyudov, Ozgur Aktas and Shari Farrens (Qromis Inc., USA); Cem Basceri (Qromis Inc, USA); Travis Anderson, Lunet Luna, Marko Tadjer, Andrew Koehler, Karl Hobart and Fritz Kub (Naval Research Laboratory, USA)

The 8-inch diameter QST® substrates produced by using the proprietary technologies of Qromis, Inc. is a revolutionary solution for epitaxy of high-performance GaN power, RF and optoelectronic devices. QST® substrates enable high-yield, high-performance, and low-cost production of GaN devices in an 8-inch Si-CMOS fabs. The revolutionary properties of QST® stem from its construction, which incorporates a ceramic core designed for thermal coefficient of expansion (CTE) match to GaN, encapsulating layers which provide CMOS foundry compatibility, and a single-crystal Si (111) seed layer that provides a well-known and well-characterized surface for GaN epitaxy. In this work, we demonstrate the capabilities of QST® substrates to support both classical devices such as HEMT transistor and new, next generation devices such as free-standing vertical-diodes with substrate-transfer and lateral-JFET transistors.

We4A4: Lasers

Time:	5/30/2018, 03:30 PM - 04:45 PM
Room:	Salon M (Samberg Conference Center, 7th floor)
Chair:	Stephanie Law (University of Delaware, United States)

We4A4.1

03:30 PM

Salon M

Inhibited Hot-Carrier Cooling in Type-II InAs/AlAsSb Quantum Wells: Controlled Decoupling of Electron-Phonon Relaxation

Hamidreza Esmaielpour and Vincent Whiteside (University of Oklahoma, USA); Herath Piyathilaka (West Virginia University, USA); Sangeetha Vijeyaragunathan and Bin Wang (University of Oklahoma, USA); Echo Adcock-Smith and Kenneth Roberts (University of Tulsa, USA); Tetsuya Mishima and Michael Santos (University of Oklahoma, USA); Alan Bristow (West Virginia University, USA); Ian Sellers (University of Oklahoma, USA)

Semiconductor quantum wells have been shown to exhibit decreased hot-carrier thermalization relative to bulk systems. We demonstrate that type-II quantum wells have the potential to further inhibit hot-carrier relaxation via the decoupling of the phonon channels through the spatial separation of photogenerated carriers. The spatial separation increases the radiative lifetime for the hot electrons, and leads to the formation of a robust phonon bottleneck at elevated temperatures. A decoupling of the thermalization coefficient was observed when the system transitioned from efficient type-I radiative recombination at low temperature to less efficient type-II recombination at elevated temperatures.

We4A4.2

03:45 PM

Salon M

Thermionic Cooling Effect in AlGaAs/GaAs Heterostructures

Aymen Yangui (University of Tokyo, Japan); Tifei Yan and Marc Bescond (Institute of Industrial Science, University of Tokyo, Japan); Naomi Nagai and Kazuhiko Hirakawa (University of Tokyo, Japan)

We have fabricated a thermionic cooling structure based on an asymmetric AlGaAs/GaAs double barrier heterostructure. Under an appropriate bias voltage, cold electrons are first injected into the quantum well (QW) by resonant tunneling through a thin and tall injector barrier. Electrons are subsequently removed from the QW by thermionic emission over a lower and thicker collector barrier. This rather simple electronic transport process efficiently removes heat from the QW. To determine the electron temperature, Te, in the QW, we measured the photoluminescence spectra as a function of the bias voltage and, by assuming the Maxwell-Boltzmann distribution for electrons, we deduced Te from the high-energy tails of the PL peaks. Te in the QW decreases with increasing V and reaches 250 K when V = 1 V. In contrast, Te in the electrode is almost unchanged even when V is varied. The experimental result is in

reasonable agreement with theory and clearly demonstrates the thermionic refrigeration effect in semiconductor heterostructures.

We4A4.3 **High-Contrast Gratings in VCSELs**

04:00 PM *Connie Chang-Hasnain (UC Berkeley, USA)*

INVITED Abstract not available.

Salon M

We4A4.4 **Stabilizing Color Chromaticity of RGB Light-emitting Diodes Using Monolithically-Integrated Photodetectors**

04:30 PM *Hoi Wai Choi, Kwai Hei LI and Haitao Lu (The University of Hong Kong, Hong Kong)*

Salon M

RGB light-emitting diodes are useful are many applications including lighting and display due to the possibility of color tuning by varying the intensities of the respective LED devices. However, the color chromaticity of such LEDs drift over time even with constant current driving, due to the degradation of light output over time. Color quality and consistency is an important attribute of light sources for many applications and environments, such as museums, operating theatres and displays. The color chromaticity has been recognized as an LED's "end of life" indicator as recommended by the Next Generation Lighting Industry Alliance. In order to maintain the light output, a feedback control system can be implemented to detect the instantaneous light output intensity and adjust the injection currents to the RGB LEDs. This detection scheme would typically involve external photodetectors mounted over the devices. In this work a compact photodetector is monolithically-integrated onto the wafer for on-chip detection from the adjacent LEDs, The photodetector uses the same device structure as the LED- the quantum well- for light detection, since luminescence and absorption are complementary processes;

We4B4: Wide Band Gap

Time:	5/30/2018, 03:30 PM - 04:45 PM
Room:	DR 3 & 4 (Samberg Conference Center, 6th floor)
Chair:	Mary Crawford (Sandia National Laboratories, USA)

We4B4.1 **40-nm-Gate GaN-on-Si HEMT with fT of 250 GHz**

03:30 PM

DR 3 & 4

Weichuan Xing (Nangyang Technological University, Singapore); Zhihong Liu (Singapore-MIT Alliance for Research and Technology, Singapore); Kumud Ranjan (Nanyang Technological University, Singapore); Yu Gao (Singapore-MIT Alliance for Research and Technology Center, Singapore); Geok Ing Ng (NTU, Singapore); Tomás Palacios (Massachusetts Institute of Technology, USA)

During the past decade, the high-frequency performance of the GaN-on-Si HEMTs is continuously increasing but still lags behind their counterparts on SiC. In this work, we demonstrate deeply-scaled InAlN/GaN-on-Si HEMTs. A high cut-off frequency f_T of 250 GHz was obtained in a 40 nm gate device. To the best of our knowledge, this f_T value is the highest among the reported GaN-on-Si transistors. Delay analysis was carried out and the effective electron velocity is extracted to be 1.1e7 cm/s. DIBL results show that Short channel effect is obvious in the 40-nm gate device, but much smaller than that in an AlGaN (20 nm)/GaN HEMT. After surface passivation using a thin Al_2O_3, the f_T of 40 nm gate device decreased slightly by 6%, while the longer-gate device has less f_T droop. These excellent results show the great potential of InAlN/GaN HEMTs on Si for future mm-wave and sub-THz applications.

We4B4.2 **Field-Plate Related to Drain Current Degradation in GaN HEMTs**

03:45 PM

DR 3 & 4

Ferdinando Iucolano (STMicroelectronics, Italy); Alessandro Chini (University of Modena and Reggio Emilia, Italy)

One of the critical issues limiting the performances and reliability of GaN power devices is the degradation of their on-resistance (R_{ON}) when they are operated at high drain-source voltages. Being able to monitor R_{ON} variation during device operation thus becomes a necessary task in order to investigate the physical mechanisms leading to the observed drifts. Standard measurement equipment does not allow to perform easily this task, specifically when R_{ON} variation should be monitored when the device operates in switch-mode. Moreover, to better understand the physical mechanisms involved it is very important to monitor other device parameters such as its threshold-voltage V_{TH} which is typically not monitored during device switch-mode operation. Therefore, in this work is presented a novel testing methodology which allows the simultaneous monitoring of device R_{ON} and V_{TH} during switch-mode operation with the ability to capture the variation of said parameters starting from the very first switching cycles.

We4B4.3 **Using Nanopatterns to Reduce Thermal Resistance at Diamond-Silicon Interfaces**

04:00 PM *Zhe Cheng (Georgia Institute of Technology, USA); Tingyu Bai, Yekan Wang and Chao Li (UCLA, USA); Tatyana Feygelson, Marko Tadjer and Bradford Pate (Naval Research Laboratory, USA); Brian M. Foley and Baratunde Cola (Georgia Institute of Technology, USA); Mark Goorsky (University of California, Los Angeles, USA); Karl Hobart (Naval Research Laboratory, USA); Samuel Graham, Jr (Georgia Institute of Technology; Oak Ridge National Laboratory, USA)*

DR 3 & 4

The integration of chemical vapor deposited (CVD) diamond with electronic devices is under development to help mitigate the intense hotspots that arise from joule heating during operation. However, the benefits of this approach is limited by the thermal resistance between the semiconductor and diamond that exists because of the way the materials are integrated. By growing CVD diamond on nanopatterned silicon substrates with varying pattern sizes, for the first time, our work provides a general strategy to significantly reduce thermal resistance of both the diamond-silicon interface and diamond layer near the interface.

We4B4.4 **Molecular Beam Epitaxial Growth of Scandium Nitride and Heterostructures**

04:15 PM *Joseph Casamento, Debdeep Jena and Huili Xing (Cornell University, USA)*

DR 3 & 4

Scandium Nitride (ScN) has emerged as a promising compound semiconductor material, with applications ranging from dislocation reduction in the Gallium Nitride family of semiconductors, to a method to boost the piezoelectric properties of AlN by 4-5X for use in bulk-acoustic wave (BAW) resonator RF filters for mobile phones. If ScN can be epitaxially integrated with GaN semiconductors and heterostructures, it can open up several applications in transistors, LEDs and Lasers, and enable new applications. The promising optoelectronic properties of ScN stem from its ability to potentially adopt several crystal structures, from rocksalt cubic to wurtzite hexagonal and h-BN-like nonpolar hexagonal. In this work we report the MBE growth of ScN and its integration with III-V nitrides GaN, AlN, and their corresponding heterostructures. Recent results indicate that ScN prefers to form coherent twin boundaries in the (111) out-of plane orientation instead of a hexagonal crystal structure.[1] This leads to a polarity discontinuity at the semiconductor interfaces, leading to high charge densities and potential two-dimensional electron gas (2DEG) formation. This underpins potential new device architectures for epitaxial III-nitrides.

We4B4.5 **Enhanced Deep Ultraviolet Response of SiC APDs**

04:30 PM

DR 3 & 4

Anand Sampath, Stephen Kelley and Jeremy Smith (US Army Research Lab, USA); Ryan Enck (US Army Research Laboratory, USA); Brenda VanMil (US Army Research Lab, USA); Yaojia Chen and Joe C. Campbell (University of Virginia, USA); Michael Wraback and Gregory Garrett (US Army Research Lab, USA)

In this paper, we report on enhancing the performance of 4H- SiC APDs in the deep ultraviolet (DUV) spectrum between 200-250 nm through collection of carriers by drift and increased gain associated with the higher ionization rate of holes over electrons in this material. Through experiment and modeling we demonstrate that the spectral response of 4H-SiC APDs can be significantly improved by designing the device structure to deplete toward the illuminated n-type layer under large reverse bias. This lead to significant suppression of surface recombination and enhancement of the DUV photoresponse These results are promising for realizing a high sensitivity DUV single photon counting avalanche photodiodes.

We4C4: Organic Semiconductors

Time:	5/30/2018, 03:30 PM - 04:45 PM
Room:	Salon T (Samberg Conference Center, 7th floor)
Chair:	David Gundlach (National Institute of Standards and Technology, United States)

We4C4.1 **Microstructure and Morphology Measurements for Organic Electronics**

03:30 PM *Dean DeLongchamp (National Institute of Standards and Technology, USA)*

INVITED

Salon T

Since the invention of semiconducting polymers in the 70's, the relevance of their solid state structure to their electronic properties has been a topic of intense study. Surprisingly, little consensus has been reached on what aspects of polymer semiconductor film structure actually impact the electronic properties. Although order and orientation must matter, at what length scales are they relevant? I will discuss our development of methods to measure the structure of organic semiconductor materials including polarized absorption spectroscopies (IR, vis, and X ray), scanning probe techniques, scattering techniques, and transmission electron microscopy measure the packing structure of polymer semiconductors. Ultimately, a molecular-level picture may ultimately be more useful than microstructure-level one. To obtain such a picture, new methods such as polarized resonant soft X-ray scattering (P-RSoXS) may be used to probe structure in these heretofore unmeasurable regions.

We4C4.2 **The Role of Higher Order Effects in Rubrene/C60 OLEDs**

04:00 PM *Sebastian Engmann (National Institute of Standards and Technology, USA); Adam Barito, Emily Bittle and Lee Richter (National Institute of Standards and Technology); Chris Giebink (The Pennsylvania State University, USA); David Gundlach (National Institute of Standards and Technology, USA)*

Salon T

Quantum and coherent spin phenomena in organic semiconductors have gained recent interests, as some of these effects can be observed, manipulated, and studied at room temperature. Besides the potential for future developments towards quantum based sensors, computing, and information, established technologies like organic light emitting diodes and organic photovoltaics can benefit near term from harnessing higher order effects such as triplet-triplet annihilation (TTA) and singlet fission (SF). In OLEDs TTA enables device performance above the 25% emission efficiency limit of singlet emitters, as 75% of injected carriers form triplets. Recent reports have shown devices with electroluminescence (EL) turn-on at about half of the bandgap voltage for a series of heterojunctions. These devices commonly share a small molecule emitter (and hole transport layer) like rubrene and an electron transport layer such as C60. The reduced turn-on voltage was attributed to either 1) an Auger-assisted energy up-conversion process at the heterojunction interface or/and 2) Dexter transfer of triplet charge transfer (CT) states into triplet exciton states, followed by triplet-triplet annihilation (TTA). For rubrene based devices, TTA was assigned to be the origin of the reduced turn-

on voltage and the formation of an intermediate CT-state was assigned of crucial importance. We show that the CT-state is not a necessary requirement for a reduced turn-on voltage by systematically altering the CT-state density via introduction of a thin insulating bathocuproine (BCP) layer between the small molecule/C60 heterojunction interface, or a mixed rubrene: C60 interlayer, resulting in either a greatly depressed or enhanced formation of the CT-state and recombination rate. We find that suppressing the CT-formation by a 3nm thick BCP interlayer yields a 3-fold increase in device luminance compared to the rubrene/C60 device, while maintaining the same low turn-on voltage. The increased luminance of devices with BCP interlayer suggest a reduction in parasitic effects of the CT-state. Examining the current density-voltage-characteristics, J(V), of the OLEDs more closely, we observe diode ideality factors of about 1.5 in the heterojunction devices, whereas this value is around 2 in a rubrene only devices not exhibiting the low turn-on voltage. The effective value of 1.5 rules out a coherent triplet formation process and auger-recombination in the C60 based heterojunctions. The overserved luminescence-current density-characteristics, L(J), show a linear dependence in the small current limit, whereas a quadratic dependence is expected for coherent as well as incoherent triplet-triplet annihilation processes. Our electrical analysis suggests that the origin of the observed low-voltage turn-on is not due to an Auger or triplet-triplet annihilation process. Rather, it suggests that classical radiative band-to-band recombination is the most favourable recombination process.

We4C4.3 **Impact of Organic Dopants on Monolayer Transitional Metal Dichalcogenides**

04:15 PM *Siyuan Zhang, Heather Hill, Angela Hight Walker, Christina Hacker and Sujitra Pookpanratana (National Institute of Standards and Technology, USA)*

Salon T

Atomically thin two-dimensional (2D) transitional metal dichalcogenides (TMDs) are a promising class of materials for nanoelectronics with unique optical and electronic properties. The properties of mono- to few-layer TMDs are highly sensitive and reactive to their local environment (ambient conditions and adsorbates) and the interfaces within a fabricated device structure (gate dielectric, contacts), which can all impact their electronic properties and extrinsic device characteristics. Technological commercialization of TMDs requires that their electronic properties (e.g., charge carrier density) be well-controlled or engineered for specific device functionality. Integrating organic molecules to surfaces and interfaces of TMDs is a promising route to achieve these goals. Organic molecules provide a nearly limitless range of possibilities in tailoring the chemical composition and structure for a desired functionality with footprints in the nanometer-scale. Using novel molecular-based oxidants and reductants as chemical dopants, we show that they are effective at tuning the electrical properties of field-effect transistors (FET) based on four different TMDs (MX2: M is Mo or W, X is S or Se). Sub-hundred-micron size (ca. 50 μm to 100 μm) of MX2 were exfoliated from bulk crystals via a gold-mediated transfer technique, and the monolayer thickness was confirmed by Raman spectroscopy and confocal microscopy. MX2 devices were fabricated using CMOS-compatible photolithography processes with a bottom-gate, top-contact FET device configuration. Rhodium-based organometallic dimer

([RhC5(CH3)5(C5H5)]2) and "magic blue" ([(4-BrC6H4)3N]SbCl6) are the molecular reductant and oxidant, respectively. The MX2 is exposed to the dopants via solution. The transfer characteristics of an MX2 device can be modulated with the solution concentration and treatment time of the dopant solution. N-doping of all four MX2 devices is achieved, and the devices appear to be degenerately doped. Detailed characterization by X-ray photoelectron, Raman, and photoluminescence (PL) spectroscopies provides insight on the underlying physical mechanism of the molecular reductants and oxidants on the thin MX2 materials. The molecular p-doping (n-doping) treatments induced a consistent shift of the MX2 occupied energy levels closer to (farther from) the Fermi energy as measured by XPS. The PL of the n-doped MX2 is consistently decreased in intensity and redshifted when compared to the pristine or p-doped MX2. The impact of the p- and n- molecular dopants on the optical and electrical properties will be discussed.

We4C4.4

04:30 PM

Salon T

Growth of Molecularly Doped Organic Single Crystal by a Novel Method Using Electrospray and Low Vapor Pressure Solvent

Keita Takeuchi (Sophia University, Japan)

We have successfully demonstrated the growth of dye-doped plate-like single crystals of wide range doping concentration from 0.17 to 15.5 mol% with high controllability by use of newly developed a novel crystal growth method. In the growth method, a low vapor pressure liquid thin film is used as a crystal growth field and fine droplets of solute are supplied from the liquid surface by an electrospray system. The dye-doped single crystal plats exhibited photoluminescence emission from doped color-centers, and the PL intensity clearly depended on the doping concentration. We also found interesting nature that the incorporation and precipitation of dopant molecule has threshold in the solute supply rate and solute concentration.

We4D4: Novel Materials (2D Materials)

Time:	5/30/2018, 03:30 PM - 04:45 PM
Room:	DR 5 & 6 (Samberg Conference Center, 6th floor)
Chair:	John Heron (University of Michigan - Ann Arbor, USA)

We4D4.1

03:30 PM

INVITED

DR 5 & 6

High Hole Mobility, 3D Vertical Integration Compatible WSe2 FETs Grown by MBE on ALD Oxides

Christopher Hinkle (University of Texas at Dallas, USA)

WSe2 grown by molecular beam epitaxy (MBE) on atomic layer deposited (ALD) high-k oxides on a Si platform is demonstrated in field-effect transistors (FETs, Figure 1a and 1b) with 3D vertical integration compatible fabrication temperatures (< 550 °C). Using electric double layer (EDL) gating, devices exhibiting ambipolar behavior with drain currents exceeding 1 uA/um and ON-OFF ratios greater than 10^4 are shown in Figure 1c. Field effect hole mobilities greater than 40 cm^2/V-s are measured, Figure 1d, which is orders of magnitude higher than other MBE reported TMD mobilities. The achievement of relatively high-mobility transistor channels at vertical integration compatible processing temperatures shows the potential for integrating transition metal dichalcogenides (TMDs) into CMOS process flows.

We4D4.2

04:00 PM

DR 5 & 6

Van Der Waals Growth of h-BN/graphene Heterostructures Using Molecular Beam Epitaxy

Martin Heilmann, Siamak Nakhaie and Michael Hanke (Paul-Drude-Institut für Festkörperelektronik, Germany); Muhammad Bashouti (Ben-Gurion University of the Negev, Israel); Marcelo Lopes and Henning Riechert (Paul-Drude-Institut für Festkörperelektronik, Germany)

Led by the discovery of graphene, other two-dimensional (2D) materials with metallic, semiconducting or insulating behavior have emerged over the last couple of years. The vertical stacking of two or more of these materials allows the fabrication of novel 2D heterostructures, which could enable atomically thin and flexible devices. Such heterostructures are currently mostly fabricated using mechanical stacking of exfoliated 2D sheets, a time-consuming and inherently non-scalable process. To advance heterostructures comprising of different 2D materials with clean interfaces and for processing them on large-area, heteroepitaxial growth within a controlled environment will be crucial. Here we present two different promising approaches for a scalable growth of 2D heterostructures, comprising of graphene and hexagonal boron nitride (h-BN), by molecular beam epitaxy.

We4D4.3

04:15 PM

INVITED

DR 5 & 6

Electric Double Layer Dynamics in Graphene FETs: Using Ions to Control Transport in Two-Dimensional Materials

Susan Fullerton and Ke Xu (University of Pittsburgh, USA); Md Mahbubul Islam and David Guzman (Purdue University, USA); Alan Seabaugh (University of Notre Dame, USA); Alejandro Strachan (Purdue University, USA)

Electrostatic gating of two-dimensional (2D) materials with ions is an effective method to achieve high carrier density (10^{13} - 10^{14} cm^{-2}) and excellent gate control by creating an electric double layer (EDL) with large capacitance density (>2 $\mu F/cm^2$). I will review our use of EDL gating to investigate transport properties of 2D materials, and introduce new device concepts that employ EDL gating as an active device component. I will focus on our recent study of EDL dynamics in a polymer-based electrolyte on graphene FETs. Using both experiments and molecular dynamics simulations we show that the EDL dynamics can (1) occur over timescales relevant to electronics (pico- to nanoseconds), (2) be tuned by orders of magnitude by tuning the applied field strength, and (3) show a non-linear dependence with field-strength.

We5PP-L: Poster Session - Lasers

Time:	5/30/2018, 05:00 PM - 06:30 PM
Room:	Walker Memorial (Building 50-140)

We5PP-L.1 **1.3 Micron 8-Wavelength Laterally Coupled Distributed Feedback Laser Array**

Walker (50-140)

Ankang Li, Jian Wang, Changzheng Sun, Yaqiong Wang, Bing Xiong, Yi Luo, Zhibiao Hao, Yanjun Han, Lai Wang and Hongtao Li (Tsinghua University, P.R. China)

A 1.3 μm 8-wavelength laterally coupled distributed feedback (LC-DFB) laser array was realized by lateral gratings in one AlGaInAs-InP epi-wafer. The coupling coefficient was improved by adjusting the depth and duty ratio of grating, and highly selective CH4/H2/Ar reactive ion etching (RIE) between InP and AlInAs was adopted for precise control of the depth of the LC grating. The stable single-mode operation of 8 wavelengths was demonstrated with the wavelength spacing of ~3.4 nm and the average side mode suppression ratios (SMSR) ~ 41.3 dB.

We5PP-L.2 **Influence of Highly Stacked Layer Numbers in Quantum-Dot Lasers**

Walker (50-140)

Atsushi Matsumoto and Kouichi Akahane (National Institute of Information and Communications Technology, Japan); Toshimasa Umezawa (National Institute of Information and Communication Technology (NICT), Japan); Shinya Nakajima and Naokatsu Yamamoto (National Institute of Information and Communications Technology, Japan)

Quantum dots (QDs) are very promising materials. Further, many high performance QD photonic devices, such as laser diodes (LDs) and semiconductor optical amplifiers (SOAs), have been reported. One of the disadvantages of the QD structure is the relatively low gain coefficient compared to the multi-quantum well structure. Therefore, the characteristics of such devices have been improved primarily by increasing the density of QDs in a layer or stacking QD layers. In our group, we have developed the strain-compensation technique; by utilizing it, we can obtain highly stacked QD structures that have indicated high-temperature-stable QD-LDs and ultra-fast QD-SOAs. However, the influence of stacked layer numbers on the properties of QD-LDs have not been investigated, despite the need for the optimization of the device structure. In this paper, we investigated that by experiments and numerical calculations.

We5PP-L.3 **Continuously Tunable Colloidal Quantum Dot Distributed Feedback Lasers Integrated on Chirped Grating**

Walker (50-140)

Hyunho Jung, Changhyun Han and Hanbit Kim (Seoul National University, Korea); Yeonsang Park and Kyung-Sang Cho (Samsung Advanced Institute of Technology, Korea); Heonsu Jeon (Seoul National University, Korea)

We present colloidal quantum dots (CQDs) distributed feedback (DFB) laser integrated on a chirped grating, of which lasing wavelength changes continuously as a function of location. A period-chirped surface grating is fabricated using a modified Lloyd-type laser interference lithography (LIL) setup where a flat mirror is replaced with a concave one. A dense red-emitting CdSe/CdS/ZnS CQDs film is spin-casted on silicon substrate, which is subsequently released and transferred onto a period-chirped surface grating formed on a quartz plate. Upon optical excitation, the fabricated DFB laser structure exhibits a single-mode lasing action at laser threshold of ~0.4 mJ/cm^2. The lasing wavelength is observed to shift gradually from 613.4 nm to 623.2 nm as the pump spots is scanned over a distance of ~5.6 mm. These results demonstrate that the modified LIL setup can produce high quality chirped gratings at low cost, which should be useful for various sophisticated photonic devices.

We5PP-L.4 **Wet-transfer of Colloidal Quantum Dot Thin Films and Its Application**

Changhyun Han, Hyunho Jung, Jongho Lee and Myungjae Lee (Seoul National University, Korea); Yeonsang Park and Kyung-Sang Cho (Samsung Advanced Institute of Technology, Korea); Heonsu Jeon (Seoul National University, Korea)

Walker (50-140)

We report a method of wet-transferring a dense colloidal quantum dot (CQD) thin-film. Two chemically orthogonal polymer layers, poly(vinyl alcohol) as a sacrificial layer and poly(methyl methacrylate) for temporary mechanical support, are used during the transfer process and removed afterwards, resulting in a single CQD film transferred on an alien substrate. CQD films of various thicknesses are transferred successfully with neither mechanical damage nor optical degradation. We can repeat the wet-transfer process multiple times to form a CQD heterostructure consisting of different CQD layers. In addition, we fabricate a distributed feedback (DFB) laser structure by transferring a CQD film on a transparent substrate integrated with a surface grating. When excited optically, the CQD DFB laser structure exhibits a single sharp emission peak with low laser threshold, demonstrating the applicability of the wet-transfer process.

We5PP-L.5 **In-situ and Ex-Situ Metrology for VCSEL Epitaxy**

Volker Blank (LayTec AG, Germany); Martin Zorn (JENOPTIK Diode Lab GmbH, Germany); Christian Kaspari, Joachim Rest and Johannes K Zettler (LayTec AG, Germany); Kolja Haberland (LayTec GmbH, Germany); Thomas Zettler (LayTec AG, Germany)

Walker (50-140)

In the production process of VCSEL devices, the epitaxy of the layer stack is one of the most critical steps. This talk will focus on latest advances in in-situ process control for VCSEL epitaxy in Aixtron planetary MOCVD reactors and ex-situ characterization by two-dimensional wafer mapping. First, we will present data, how the thickness of key layers (in DBRs and cavity) can be determined routinely from in-situ reflectance data. This analysis is recipe based and can be applied automatically for every production run with the respective results forwarded to the fab's MES system for statistical process control

and feed-forward corrections of the related MOCVD run parameters. In the second part of the talk we will focus on spectral in-situ measurements of the VCSEL's cavity resonance positions and DBR stop-band positions. Utilizing an XRD-gauged database of high-temperature n k(T) optical properties and the accurate sensing of the wafer temperature during growth, from this high-temperature spectral signatures the wavelength position of the respective device-relevant room-temperature signatures can be directly deduced. Applying this methods to different wafer-zones at all wafers in the reactor allows for a real-time evaluation of process yield even for sophisticated VCSEL device structures. Ex-situ characterization via photoluminescence and white-light reflectance provides spatial information about the uniformity of the layers across the entire wafer area.

We5PP-L.6 **Reduction of Lasing Wavelength Variation Due to Injection Current into GaInAsP/InP Membrane Distributed-Reflector Laser Bonded on Si**

Walker (50-140) *Weicheng Fang, Tatsuya Uryu, Daisuke Inoue, Nagisa Nakamura, Takamasa Yoshida, Tomohiro Amemiya, Nobuhiko Nishiyama and Shigehisa Arai (Tokyo Institute of Technology, Japan)*

To improve temperature characteristics of GaInAsP/InP membrane distributed-reflector laser with BCB bonding on Si, we reduced its electric resistance by shortening the distance between p-electrode to the active region, and also reduced its thermal resistance by adopting a thin BCB. As the results, a threshold current of 0.3 mA at 20°C and a continuous-wave operation up to 100°C were obtained for the device with the active DFB section length of 40 μm and the stripe width of 0.8 μm. By shortening the distance of p-electrode to 0.5 μm, the electric resistance was reduced to 375 Ω which was approximately 1/3 of previously reported DR laser. From the lasing wavelength variation against an injection current, the thermal resistance was estimated to be around 1900 K/W which was 1/2.8 of previously reported device and is considered to be attributed to a reduction of the BCB thickness from 2 &μm to 0.5 &μm.

We5PP-L.7 **Introduction of Ridge-Waveguide Structure for Low-Power Operation of GaInAsP/InP Membrane Distributed-Reflector Laser**

Walker (50-140) *Nagisa Nakamura, Tatsuya Uryu, Zhichen Gu, Tomohiro Amemiya, Nobuhiko Nishiyama and Shigehisa Arai (Tokyo Institute of Technology, Japan)*

To solve problems of Large Scale Integrate circuits (LSIs) such as heat generation and delay arising in the global wiring layers, the replacement by on-chip optical interconnection is expected to be one of the solutions. We have proposed and realized membrane Distributed-Reflector (DR) laser as light source for on-chip optical wiring on LSI. By introducing ridge structure, we can shorten the distance between p-side electrode and active region by the enhanced lateral optical confinement and to reduce the power consumption by reducing the resistance of p-InP side cladding layer. In this

research, we investigated the ridge membrane waveguide structure for further reduction of power consumption of membrane laser and report the possibility of low power operation.

We5PP-L.8 **Temperature-insensitive InGaAs/InAlAs Quantum Cascade Lasers Using Metal-Organic Vapor Phase Epitaxy**

Walker (50-140) *Dong Hak Kim, Dong-Hwan Jun, Hae Yong Jeong, Young-Jin Jeon and Young-Su Choi (KANC, Korea); Jungho Kim (Kyung Hee University, Korea); JoonHyun Kang (Korea Institute of Science and Technology, Korea); Hyun-Duk Yang (KIST, Korea); Jindong Song (Korea Institute of Science; Technology, Korea); Il Ki Han (KIST, Korea)*

We studied to compare lattice matched and strain compensated quantum cascade lasers (QCLs) based on InGaAs/InAlAs multi-quantum well (MQW) grown by metal-organic vapor phase epitaxy (MOVPE). Using the control of In mole fraction in the InGaAs and InAlAs layers, we could achieve both strain compensation and preventing loss of thermal effect due to large band offset between the energy state of InGaAs and InAlAs layers. The bandgap and lattice constant of the both InGaAs and InAlAs epitaxial layers was calculated using Vegard's law. And then, the lattice matched and strained QCLs were designed and deposited on InP substrate using MOVPE.

We5PP-L.9 **Investigation of Thermo-Optic Wavelength Tuning Techniques of Hybrid III-V/SOI DFB Lasers for LiDAR Applications**

Walker (50-140) *Moataz Eissa and Junichi Suzuki (Tokyo Instittue of Technology, Japan); Nobuhiko Nishiyama and Shigehisa Arai (Tokyo Institute of Technology, Japan)*

LiDAR (Light Detection and Ranging) is extending its role in various applications such as autonomous cars and drones. Towards achieving an on-chip FMCW type LiDAR system based on Si photonics, possible wavelength tuning techniques of the hybrid III-V/SOI DFB laser are theoretically investigated. Both tuning efficiency and speed are calculated for top and side micro-heaters and compared with Si waveguide direct heating by lateral current injection. The Si waveguide in the latter approach should be shallow doped with an n-type concentration of 10^{16} cm^{-3} to conduct the tuning current with high resistance for heating. The induced electric field causes negligible electro-optical effects, moreover, the shallow doping causes negligible additional optical loss. Based on this calculation, Si waveguide direct heating yields the highest efficiency (~ 4 nm/W per 1 mm cavity length). In addition, FMCW triangular sweep with high modulation frequencies (up to MHz range) are possible. Such high performance is attributed to the close proximity of the tuning heat source to the laser core.

We5PP-ON: Poster Session - Organic and Novel Semiconductors

Time:	5/30/2018, 05:00 PM - 06:30 PM
Room:	Walker Memorial (Building 50-140)

We5PP-ON.1 **All Exciplex Structure of Highly Efficient Tandem WOLEDs**

Walker (50-140)

Wen-Yi Hung and Pin-Yi Pin-Yi Chiang (National Taiwan Ocean University, Taiwan); Ken-Tsung Wong (National Taiwan University, Taiwan); Chih-Hao Chang (Yuan Ze University, Taiwan)

We succeeded in fabricating an exciplex-based organic light-emitting diode (OLED) systematically tuned device structure to render a high blue exciplex OLED with EQE of 10.5%. We then constructed a device structure configured by two parallel blend layers of mCP/PO-T2T and TAPC/CN-T2T, generating blue and yellow exciplex emission, respectively. The resulting device demonstrates for all-exciplex-based WOLED with excellent efficiencies EQE: 19%, CE: 49.7 cd/A, and PE: 31.2 ml/W with CIE (0.31, 0.41) and CRI 61 that are nearly independent of EL intensity. The tandem architecture and blend-layer D/A (1:1) configuration are two key elements that fully utilize the exciplex delay fluorescence, providing a paragon for the use of low-cost, abundant organic compounds en route to commercial WOLEDs.

We5PP-ON.2 **GaZnO-based Anode with Low Refractive Index for Organic Light-Emitting Diodes**

Walker (50-140)

Chih-Hao Chang, Po-Chen Chiu, Hao-Hsuan Chiu and Yi-Ning Lai (Yuan Ze University, Taiwan); Wen-Yi Hung (National Taiwan Ocean University, Taiwan)

The efficiency of conventional OLEDs is unsatisfactory due to its inherent structure of the multiple stacking films, leading that the generated light is trapped or quenched in the thin films and the radiation mode of OLEDs generally makes up only about 20%~25% of the light generated. We developed a new flexible GZO-based TCO by doping a small amount of silicon into GZO (i.e. SGZO) to simultaneously decrease the refractive index and increase the conductivity. The low refractive index of TCO anode could reduce the total reflection and thus boost the ratio of the radiation mode. In addition, the high refractive index of Mo-doped GZO (MGZO) film is suitable to combine with SGZO film for constructing a composite flexible electrode, benefiting the enhancement of the out-coupling efficiency of OLEDs. As a result, the blue phosphorescent OLEDs with optimized SGZO/MGZO anode achieved peak efficiencies up to 31.5%.

We5PP-ON.3 **Efficient TADF-based Organic Light-Emitting Diodes Using Donor-Acceptor-Donor Borylated Compounds**

Walker (50-140)

Chih-Hao Chang (Yuan Ze University, Taiwan); Chin-Wei Lu and Chih-Chieh Tsai (Providence University, Taiwan); Yu-Chien Hsh, Chun-Han Lin and Chia-Wei Liao (Yuan Ze University, Taiwan)

Thermally activated delayed fluorescence (TADF) based on conventional aromatic compounds are continually proposed in recent years, which are seen as the third generation of OLED emitters. Recently, borane-based complexes have attracted much attention as TADF emitters due to the lower-lying vacant p-orbital and electron deficiency of boron atom. We report here a new series of donor-acceptor-donor borylated compounds using functional acridan derivatives as the donor moieties, which generates the facile intramolecular charge transfer upon excitation. Three types of donor adopted in these borylated compounds including phenothiazine, phenoxazine, and 9,9-dimethyl-9,10-dihydroacridine, which were respectively designed for constructing efficient TADF compounds. The transient PL decay curves of three compounds clearly present two-component decay including a nanosecond-scale prompt and microsecond-scale delayed components, confirming the typical TADF characteristics. In addition, green-emitting device achieved a maximum efficiency of 19.3% (56.8 cd/A) along with a saturated green emission color.

We5PP-ON.4 **Oxide/metal/oxide Based-Transparent Conductive Electrodes for Highly Flexible and Transparent ReRAM**

Walker (50-140)

Byeong Ryong Lee, Ju Hyun Park and Tae Geun Kim (Korea University, Korea)

we demonstrate wide bandgap oxide/Ag/wide-bandgap oxide electrodes as transparent electrodes for ReRAM. The transmittance and sheet resistance of transparent electrodes with ZnO, Ag and Al_2O_3 layers were measured as a function of the oxide layer thickness. We fabricated crossbar array ReRAMs with a 36 × 36 array on flexible substrates using optimized transparent electrodes. The oxide layer in oxide/Ag/oxide transparent electrodes also act as a resistive switching layer. The ReRAMs have the structure of ZnO/Ag/ZnO/Ag/ZnO and Al_2O_3/Ag/Al_2O_3/Ag/Al_2O_3. Both devices exhibited stable and repeatable unipolar ReRAM behavior on flexible substrates, and Al_2O_3/Ag/Al_2O_3/Ag/Al_2O_3 cells exhibited the best performance with a large on/off ratio. The transmittance of the device exhibited higher than 95% in the visible region (350-800 nm). Our proposed concept will contribute to the advancement in flexible and transparent (ReRAM) technology due to its structural simplicity and functional diversity using various wide bandgap materials. More details will be presented at the conference.

We5PP-ON.5 **Silicon Based Magnetoresistance and Non-Volatile Spin Logic-Memory Device**

Xiaozhong Zhang and Zhaochu Luo (Tsinghua University, P.R. China)

Walker (50-140) Magnetoresistance (MR) in Silicon has attracted a lot of attentions because of its fundamental interests and broad application potential. We achieved a large MR (>1000 % at 0.05 T) in silicon at room temperature, which is associated with the impurity onsite Coulomb interaction and the space charge limited current. Our findings will help to design silicon-based magnetic device of high performance and pave the way for magnetoelectronics in silicon. We also developed a magnetic logic-memory device by coupling anomalous Hall effect and negative differential resistance phenomena. All four basic Boolean logic operations （AND，OR，NAND，NOR） could be programmed by magnetic bit at room temperature with high output ratio (> 1000 %) . This work demonstrated non-volatile information reading, processing and writing could be realized in one step and one device. Hence, logic and non-volatile memory could be closely integrated in one chip.

We5PP-ON.6 **Effect of Schottky Interfaces in Yttria Based Memristive Devices**

Mangal Das, Amitesh Kumar, Rohit Singh, Md Arif Khan and Biswajit Mandal (Indian Institute of Technology Indore, India); Shaibal Mukherjee (Indian Institute of Technology, Indore, India)

Walker (50-140)

In this work, we have demonstrated the transformation from unipolar to bipolar switching via interface engineering method for the first time. Design of our experiment allows us to capture intermediate stages of change in resistive switching (RS) behavior as we move from single Schottky to dual Schottky contacts in our device. We have fabricated four types of devices by varying bottom electrode (BE) material (N(n-Si), P(p-Si), A(Al), and AH(Al)). Device AH has similar deposition conditions as A, however, the dimensions are half of A. Device N, shows unipolar analog switching behavior (first quadrant), which may originate due to Schottky behavior (Al/Y2O3) at one interface.Device A shows RS in both (third and first) quadrants whereas N3 shows RS in the only first quadrant. Devices N and A show the transformation from unipolar to bipolar RS by realizing from one schottky interface to dual Schottky interfaces.

We5PP-ON.7 **Dual Ion Beam Sputtered Novel Resistive Memory Device Exhibiting Memristive Behavior**

Walker (50-140) *Amitesh Kumar, Mangal Das, Md Arif Khan and Rohit Singh (Indian Institute of Technology Indore, India); Vivek Garg (Indian Institute of Technology, Indore, India); Abhinav Kranti (Indian Institute of Technology Indore, India); Shaibal Mukherjee (Indian Institute of Technology, Indore, India)*

Memristor suggested to be fourth fundamental element in 1971 has recently gained wide attention after HP scientists fabricated a real memristor. Resistive random access memory (RRAM) based on transition metal oxides has been widely investigated as a next-generation non-volatile memory to be an important application for memristor. RRAM is a two terminal device which reversibly switches between low resistance state (LRS) and high resistance state (HRS) upon applying electrical stimulus in a particular range at RESET/SET voltages respectively. In this work, we demonstrate a forming-free resistive memory with memristive characteristics using ZnO thin film. Oxygen vacancies/interstitials defects in ZnO thin film are engineered by a novel technology of Dual Ion Beam Sputtering (DIBS) to suit switching needs. In general, a forming process is necessary to activate the resistive memory devices before performing any resistive switching (RS). Abundant oxygen vacancies in film ensures forming- free behavior of device. Besides, sufficient non-lattice oxygen ions in ZnO thin film assist set/reset of device. Interfacial AlOx formation/dissolution at Al/ZnO interface ensures bipolar resistive switching with smooth transition between resistance states (HRS and LRS). To start with fabrication of device, 60 nm thick ZnO thin film is deposited over Al/SiO_2/Si substrate at a substrate temperature of 100 °C, with DIBS background pressure of 1 × 10-8 mBar and Ar:O_2 (2:3) (flow rate in sccm), respectively. Finally, circular Al electrodes of 500 µm is deposited on the surface of ZnO thin film. Further, I-V characteristics are measured by sweeping a DC voltage in sequence of 0-(+8 V)- 0-(-8 V)-0 in steps of 0.5 V for a compliance current of 1 mA. Set and reset voltages of device are evaluated to be at -6/6 V. Device shows excellent endurance measured at 0.1 V for 250 cycles Retention performance assessed at 0.1 V read voltage exhibits outstanding non-volatile behavior for 106s extrapolated to 10 years. Presence of oxygen vacancies (VO), interstitial oxygen ions (IO) and lattice oxygen ions are confirmed by X-ray photoelectron spectroscopy (XPS) Photoluminescence (PL) of ZnO thin film. HR-TEM image of Al/ZnO interface shows an amorphous AlOx interfacial layer (~4-5 nm) formed at interface for the device in high resistance state (HRS) state. Formation of this interfacial layer at RESET voltage transits the device from LRS to HRS and dissolution at SET voltage leads to change device state to LRS. Our memory device as fabricated by DIBS exhibits excellent performance parameters, retention and endurance to implement it for a practical RRAM. Our work could play a very significant role in realizing similar memristive devices with high performance parameters in future.

We5PP-ON.8 **Inverse Rashba-Edelstein Magnetoelectric Devices for Neuromorphic Computing**

Andrew Stephan, Jiaxi Hu and Steven Koester (University of Minnesota, USA)

Walker (50-140) Neuromorphic computing is useful for many data processing applications such as noise filtering and recognition. In this work a novel cellular neural network (CNN) design is proposed which uses nanomagnets (NM) as nonvolatile neurons. The NMs natively approximate the sigmoid function on inputs by switching when the critical field is applied. Control of the neurons is achieved via a magnetoelectric capacitor coupled to each NM which applies an effective magnetic field dependent on the applied charge. The synapses in this CNN consist of MOSFET repeaters gated by an inverse Rashba-Edelstein (IRE) interface voltage. This voltage is determined by the spin polarization of the current being driven through the NM into the IRE interface. Simulations show this network low-pass filtering on images with significant noise ratios in as little as 60 picoseconds at a cost of 5 femtojoules per device.

We5PP-ON.9 **The Optical Property Characterization of AgGaTe2 Prepared by the Two-Step Closed Space Sublimation**

Walker (50-140) *Aya Uruno (Waseda University, Japan); Masakazu Kobayashi (Waseda University, Japan)*

The bandgap of AgGaTe2 at room temperature (1.3 eV) is almost the optimum value for fabricating solar cells. In this study, optical properties of the AgGaTe2 layer were studied by means of low temperature photoluminescence and room temperature photo-response spectroscopy. Obtained data suggest the AgGaTe2 grown under the controlled condition would exhibit high optical properties, and applicable to photovoltaic devices.

We5PP-PD: Poster Session - Power Devices

Time:	5/30/2018, 05:00 PM - 06:30 PM
Room:	Walker Memorial (Building 50-140)

We5PP-PD.1 **3.3-mΩ·cm^2 GaN-based Vertical Trench MOSFET with Threshold Voltage Reaching 6.2 V**

Xing Lu (South China University of Technology, P.R. China)

Walker (50-140)

We present the fabrication and characterization of GaN-based Vertical Trench metal-oxide-semiconductor field-effect transistors (MOSFETs) grown on a bulk GaN substrate. The MOSFET exhibited enhancement-mode (E-mode) operation with a high threshold voltage (Vth) of 6.2 V and a specific on-resistance (Ron) of 3.3 mΩ·cm^2. With an off-state drain current below 10-5 A/cm^2 at a zero gate bias, the fabricated device showed a high on/off current ratio of 108. However, the compromised breakdown performance was limited by the gate dielectric of the device rather than the n/p/n structure itself. The n/p/n structure with a 5 µm thick drift layer yielded an excellent current blocking capacity up to 600 V.

We5PP-PD.2 **Temperature Dependent Performance of GaN HEMT on Silicon and Bulk GaN Substrates**

Walker (50-140)

Lars Heuken, Muhammad Alshahed, Alessandro Ottaviani and Mohammed Alomari (Institute for Microelectronics Stuttgart, Germany); Michael Heuken (AIXTRON SE, Germany); Clemens Waechter and Thomas Bergunde (AZUR SPACE Solar Power GmbH, Germany); Joachim Burghartz (Institut für Mikroelektronik Stuttgart, Germany)

The temperature dependent electrical behavior of GaN HEMT grown on Silicon (GaN/Si) and Bulk GaN (GaN/GaN) substrates was measured. Measurements presented include the vertical leakage current of the full stack in forward and reverse direction up to 600 V for temperatures up to 200 °C as well as transfer characteristics for the same temperature range. Measurements are supported by simulations based on established models. An increase of leakage currents with increasing chuck temperature is observed for both substrate types revealing a positive temperature coefficient. Comparing temperature dependent measurements, high vertical voltages (200 V) reveal similar temperature dependence of the leakage currents. For low voltages (10 V), however, the GaN/Si HEMT shows a diverging leakage current trend indicating a different carrier emission coefficient. The applied field and temperature dependency of the leakage current can be explained by leakage mechanisms such as trap-assisted conduction and space-charge limited current with a Poole-Frenkel component.

We5PP-PD.3 **Study of AlGaN/GaN Schottky Barrier Diodes Combined Anode Metal with p-GaN Layer and Ohmic Contact**

Walker (50-140)

Yi-Sheng Chang, Bo-Hong Li, Wang Hsiang-Chun and Hsien-Chin Chiu (Chang Gung University, Taiwan); Hsueh Kuang-Po (Vanung University, Taiwan)

In this work, a novel AlGaN/GaN-on-Si SBDs combined anode metal with p-GaN layer and ohmic contact was successfully fabricated. The proposed SBDs with LG of 3 μm exhibited excellent device characteristics of low VON was 0.1 V and reverse VBR was over 600V. The VON values of the SBDs in this study have a significant decrease by using dual anode metal of Schottky and ohmic contacts. In addition, the p-n junction is also beneficial for suppression reverse leakage current to enhance VBR by a p-GaN gate on top of an AlGaN barrier depletes 2DEG carriers in the channel, which demonstrates that the AlGaN/GaN-on-Si SBDs combined anode metal with p-GaN layer and ohmic contact structure has a great potential application to the high-speed switching device.

We5PP-PD.4 **Correlation Between Gate Leakage Current and Current Collapse in Oxygen Plasma Treated GaN/AlGaN/GaN-on-Si HEMTs**

Walker (50-140)

Young-Ki Kwon, Ji Hyun Hwang, Ha Jin Mun, Sungbae Lee, Sung-Min Hong and Jae-Hyung Jang (Gwangju Institute of Science and Technology, Korea)

Gallium nitride (GaN) based high-electron-mobility-transistors(HEMTs) have great advantages for high power and high speed applications due to the excellent material properties of GaN. However, there are several issues related to reliability of HEMTs such as gate leakage currents and current collapse. Large gate leakage currents cause inferior noise characteristics and unnecessary power consumption and the current collapse limits microwave output power. In this study, oxygen surface plasma treatment has been carried out in various manner to clarify the correlation between gate leakage current and current collapse in GaN/AlGaN/GaN HEMTs. As a result, we have found the trade-off relationship between the gate leakage current and current collapse.

We5PP-PD.5 **AlGaN/GaN HEMTs with Reduced Self-Heating**

Walker (50-140)

Maira Elksne, Abdullah Al-Khalidi and Edward Wasige (University of Glasgow, United Kingdom (Great Britain))

One of the main limitations of the current GaN HEMT technology is device self-heating.This paper presents a new method of obtaining distributed gate HEMT devices showing decreased self-heating effect. Selective oxygen plasma treatment at room temperature is used to obtain planar devices with isolated regions along the device width resulting in increase in the saturated drain currents and transfer characteristics due to efficiently distributed heat. This new technology shows improved device performance and provide a route to higher power density GaN devices for high power applications.

We5PP-PD.7 **High-Voltage Properties of Strained GaN Quantum Well HEMTs on AlN**

Austin Hickman, Samuel Bader, Reet Chaudhuri, Kazuki Nomoto, SM Islam, Huili Xing and Debdeep Jena (Cornell University, USA)

Walker (50-140)

The barriers in conventional GaN HEMTs are AlGaN, and the buffer is GaN (Eg=3.4 eV). Replacing both the barrier and the buffer with the much wider bandgap AlN (Eg~6 eV), has the potential to increase the breakdown voltage of nitride HEMTs. In this work, we demonstrate the first studies of the breakdown voltage for AlN/GaN/AlN quantum well HEMTs (GaN QW HEMTs). A QW HEMT with IDsat = 1.32 A/mm for Vg = 0 V, five orders of Ion/Ioff modulation was selected for BV measurement. For the selected device, Lgd = 3 µm, Lg = 1.5 µm, and Lds = 5.5 µm. A BV of 186 V was observed, corresponding to an effective breakdown field of 0.62 MV/cm. These initial numbers are not too different from field-plate engineered and passivated HEMTs, and show high promise for improvement.

We5PP-PD.9 **3D Simulation of Gallium Nitride FinFETs Optimized for High Linearity Applications**

Qingyun Xie (Massachusetts Institute of Technology, USA); Garrett Schlenvogt and Thomas Jokinen (Silvaco, Inc., USA); Tomás Palacios (Massachusetts Institute of Technology, USA)

Walker (50-140)

Novel structures in the drain access region are proposed for GaN FinFETs. In order to better understand the characteristics of these novel designs, 3D simulations were conducted. Firstly, the simulations verify the threshold voltage modulation effect which has been experimentally demonstrated. More importantly, the 3D simulations indicate that the novel designs allow the control of the Cgd vs. VG and Cgd vs. VD curves, while maintaining almost identical transfer and output curves. The different I-V and C-V profiles of various novel designs indicate the possibility of engineering these curves at the device-level, which could play an important role in the linearity of the HEMTs.

We5PP-PD.10 **Simulation of a Normally off GaN Vertical Fin Power Fet Transistor to Study Its Breakdown Mechanism**

Marie-Clara Pépin and Hassan Maher (Université de Sherbrooke, Canada); Christophe Rodriguez (University of Sherbrooke, Canada); Ali Soltani (IEMN - Université de Lille, France)

Walker (50-140)

By its physicochemical properties, GaN is an excellent material for high-power electronic applications. Indeed, lateral GaN-based transistors such as HEMT show great performance. However, this device is facing several difficulties that prevent the use of the total capability of this wide gap material (GaN). Among these difficulties , there is 1) the presence of a high electric field at the device surface, 2) the high electron density along the 2D narrow channel that generates a lot of heat and 3) being lateral, the device normalized performance per cm^2 will be degraded. To bypass most of these issues, devices with vertical architecture are a good alternative since they confine the current and the electric field in the GaN-bulk layer, which also improve the heat dissipation. In

the work presented in this paper we used Sentaurus TCAD tool to optimize the device architecture to improve the R_{on} and breakdown voltage of the device.

We5PP-PD.11 **Large Periphery GaN HEMTs Modeling Using Distributed Gate Resistance**

Walker (50-140)

Bilal Hassan and Adrien Cutivet (UniversitÌé de Sherbrooke, Canada); Ali Soltani (IEMN - Université de Lille, France); Christophe Rodriguez (University of Sherbrooke, Canada); François Boone and Hassan Maher (Université de Sherbrooke, Canada); Meriem Bouchilaoun (University of Sherbrooke, Canada)

This work presents a study on distributed gate resistance modeling for the large periphery of the GaN HEMTs. This new modeling technique permits a general procedure adaptable to any further modeling of the intrinsic region. The proposed method is experimentally conducted by using two fingers Normally-on common gate GaN HEMT devices with different development (0.25, 0.5, 1 and 2mm). We showed that the distributed gate resistance model gives a better representation of the transistor as compared to the classical model based on lumped elements. Furthermore, the distributed model reduces the error from 17% to 2.8% and 10% to 1.5% error for Ft and Fmax respectively as compared to the classical model. Thorough demonstration and extraction technique will be described during the oral presentation.

We5PP-PD.12 **Thermal Performance of Silicon Dioxide Conduction Blocking Layers in GaN VHEMT Devices**

Walker (50-140)

Izak Baranowski and Hong Chen (Arizona State University, USA); Houqiang Fu (Arizona state University; Arizona State University, USA); Jossue Montes, Kai Fu, Tsung-Han Yang and Xuanqi Huang (Arizona State University, USA); Yuji Zhao (Arizona state University, USA)

Typically, p-GaN is used for the CBL, however, growing the p-GaN layer via metal organic chemical vapor deposition (MOCVD) results in the Mg being passivated by H, and therefore the hypothetical >3eV blocking layer is not achieved. Therefore, there is impetus to explore other materials for CBL applications, such as SiO_2, however, previous work on SiO_2 CBL's neglected thermal considerations. This work simulated using Silvaco TCAD two GaN VHEMT devices, one with a conventional p-GaN CBL and one with a SiO_2 CBL under both isothermal and non-isothermal conditions. At Vd=20V and VG=0V, the SiO¬2 CBL devices saw more heating, possessing a hotspot of 396K, compared to 379K for the pGaN device. In spite of the increased heating, the on-resistance was still lower for the SiO_2¬ CBL device (0.266 Ω cm^2) than that of the conventional p-GaN CBL device (0.331 Ω cm^2).

We5PP-RF: Poster Session - RF Devices

Time:	5/30/2018, 05:00 PM - 06:30 PM
Room:	Walker Memorial (Building 50-140)

We5PP-RF.1 **On the Large Signal Modeling of MM-wave GaAs PIN Diodes**

Walker (50-140)

Iltcho Angelov (Chalmers University of Technology; GOTMIC AB, Sweden); Marcus Gavell (Chalmers, Sweden); Goran Granstrom (GOTMIC, Sweden); Mattias Ferndahl (Gotmic AB, Sweden)

With extension of foundries capabilities, became possible to arrange, combine different type of processes, different type of devices: Transistors, Diodes, PIN diodes etc. This way we can arrange new types of circuits, improve the performance of complex MMIC, simplify the control circuits. Their use will be quite important for developing the new generation of MM-wave MMIC circuits, including 5G MMIC. The paper is dealing with improving the PIN Diode Large Signal (LS) models, targeted for use in the MM region. The LS model is globally defined, no flags, converge well. The LS PIN diode model was experimentally evaluated with IV, Spar and LS, Power Spectrum measurements and will be used in MM wave MMIC designs.

We5PP-RF.2 **Ratchet Effect in AlGaAs/ InGaAs Multi-Finger High Electron Mobility Transistors**

Walker (50-140)

Sergey Rudin and Greg Rupper (United States Army Research Laboratory, USA); Michael Shur (Rensselaer Polytechnic Institute, USA)

The hydrodynamic simulations of the sub-THz and THz response in InGaAs ratchet field effect structure with multiple gate fingers reveal a significant responsivity enhancement compared to similar non-ratchet structures. In high mobility structures, the response exhibits a plasmonic peak broadened by impurity and phonon scattering and by the viscosity of the electronic fluid. The device with a feature size of 100 nm shows response up to 8 THz. At high frequencies, high mobilities, and short feature sizes the electron viscosity in the channel becomes a dominant attenuation mechanism. The finite ratchet structures also exhibit plasmonic peaks at lower plasmonic frequencies corresponding to the wavelengths determined by the overall length of the structures. These results are important for the modeling, design, and optimization of highly sensitive sub-THz and THz ratchet plasmonic devices.

We5PP-RF.3 **Development of 25 GHz InGaAs/InP P-I-N Photodetectors for High Speed Optical Communications**

Walker (50-140)

Debdas Pal (MACOM, USA)

The demand of high speed InGaAs/InP p-i-n photodetectors operating from 1 to 1.65 µm has increased significantly. This is primarily due to the applications in data centers and other optical network systems. Therefore, it is necessary to develop a manufacturing process of photodetectors for mass production. Hybrid mesa process with zinc diffusion was developed to manufacture 25G p-i-n photodiodes. The photodetectors showed very low dark current of about 0.32 nA at 5V and speed of about 24.5 GHz at 2.5V. The peak responsivity was about 0.8 A/W.

We5PP-RF.4 **High Power mmW Switch Technologies**

Timothy Boles (MACOM Technology Solutions, USA)

Walker (50-140)

As the state-of-the-art of RF monolithic switch development advanced, the design complexity increased from simple single pole-single throw, series configured, relatively narrow bandwidth structures to multiple pole-multiple throw, broadband, multiple series, multiple shunt, and multiple series-multiple shunt constructed switches. Over this same timeframe, the maximum incident RF power handling also increased into the range of 30 dBm to 33 dBm. Within the last few years, both GaAs pHEMT and SOI PIN diode technologies have developed approaches to address the fundamental thermal limitations associated with the underlying basic material properties and have produced high frequency switches capable of handling incident power levels that range between 20 watts to 100 watts of continuous wave RF energy. Recently, microwave and mmW control components based upon GaN HEMT technologies utilizing silicon carbide, sapphire, or high resistivity silicon substrates are being proposed as an alternative to more traditional silicon and GaAs approaches. This paper will discuss the advantages and limitations of these GaN HEMT technologies for high power switch functions.

We5PP-RF.5 **High Fmax AlGaN/GaN-on-Si HEMT with Thick Rectangular Gate**

Walker (50-140)

Kai-Chieh Hsu, Li-Cheng Chang, Yung-Ting Ho and Chao-Hsin Wu (National Taiwan University, Taiwan)

We demonstrate AlGaN/GaN-on-Si HEMT on Si substrate with the Lg of 160 nm rectangular gate. In order to reduce Rg, the thickness of rectangular gate is increased to 315 nm. The maximum drain current is over 1 A/mm and the peak gm is 291 mS/mm. Owing to the thick rectangular gate, Rg can be reduced effectively down to 0.21Ω-mm. The relatively high fmax of 126.46 GHz thus can be achieved. The fmax and the Rg are comparable to the devices with T-shaped gate.To the best of our knowledge, this fmax value is relatively high among the reported GaN-based transistors on Si substrates with rectangular gate and is comparable to the devices with T-shaped gate.

We5PP-RF.6 **High Speed GaN-based micro-LED Arrays for Visible Light Communication**

I-Chen Tseng (Graduate Institute of Photonics and Optoelectronics National Taiwan University, Taiwan); Chao-Hsin Wu (National Taiwan University, Taiwan)

Walker (50-140)

LEDs can achieve higher bandwidth through scaling a device, but the optical modulation amplitude (OMA) will degrade at the same time. By designing more array numbers, we can enhance light intensity and get better extinction ratio to improve the quality of data transmission, i.e, an open eye diagram.

We5PP-RF.7 **E-Mode InGaAs Quantum Well Fin-structured MOSHEMTs with (NH4)2S Passivation**

Shun-Cheng Yang and Chao-Hsin Wu (National Taiwan University, Taiwan)

Walker (50-140) InGaAs based high electron mobility device is a promising candidate for sub-10 nm technology node because of superior electron mobility and high frequency response. However, poor interface quality between III-V materials and oxide layer has been a challenge for people to replace silicon with III-V materials in CMOS technology. (NH4)2S passivation has been widely reported to improve the interface quality of III-V materials [1], [2]. In this work, we determine an optimal (NH4)2S passivation condition for MOSHETMs by extracting interface trap density (DIT) of MOSCAP structure. In addition, to comply with Moore's law, we need to reduce power consumption of HEMTs. In this paper, we utilize fin-shaped structure to generate additional sidewall gate control and realize enhancement mode Fin-structured MOSHEMTs (FinMOSHEMTs).

We5PP-RF.8 **Al Composition Dependence of Etching Selectivity of GaN/AlGaN for Threshold Voltage Control of AlGaN/GaN HEMTs**

Jumpei Sumino (Nagoya Institute of Technology, Japan); Yamato Osada and Ryuuichirou Kamimura (ULVAC Inc., Japan); Yuya Ikedo, Naoki Kato, Kazuyuki Fukumura and Akio Wakejima (Nagoya Institute of Technology, Japan)

Walker (50-140)

Normally-off characteristics with a high drain current in AlGaN/GaN HEMTs require both high Al-composition and thin layer of AlGaN. We confirmed high etching-selectivity (75) of a GaN cap over AlGaN with a high Al-composition of 0.25. This high selectivity results in only 0.2-nm-etching of AlGaN during 100% over etching of the 17-nm-thick GaN cap. In addition, using this selective dry-etching, the AlGaN/GaN HEMT is confirmed to be fabricated.

We5PP-RF.9 **Current Driven Dyakonov-Shur Instability in Ballistic Nanostructures with a Stub**

Gregory Aizin (Kingsborough Community College, USA); John Mikalopas (Kingsborough College, USA); Michael Shur (Rensselaer Polytechnic Institute, USA)

Walker (50-140)

The plasma wave instabilities in ballistic Field Effect Transistors (FETs) have a promise of developing sensitive THz detectors and efficient THz sources. One of the difficulties in achieving efficient resonant plasmonic detection and generation is assuring proper boundary conditions. We now propose to achieve the optimum boundary conditions by introducing a narrow region of an increased width in the plasmonic FET channel (a stub). The stub introduces an impedance Z_{st} that could vary from zero to infinity at the plasma frequency depending on the stub length The mathematics of the problem is similar to the mathematics of a transmission line with a stub). We derived and solved the dispersion equation for the device with a stub. The proposed design provides a way to achieve the optimum boundary conditions and could also be used for multi finger structures of a higher THz detectivity or yielding a larger generated THz power.

We5PP-RF.10 **X-band GaN HEMT Power Amplifier on 6H-SiC with 110 W Output Power**

Quan Wang (Shandong University; Institute of Semiconductors, Chinese Academy of Sciences, P.R. China); Xiaoliang Wang, Hongling Xiao, Lijuan Jiang, Chun Feng, Wei Li and Fengqi Liu (Institute of Semiconductors, Chinese Academy of Sciences, P.R. China); Xiangang Xu (Shandong University, P.R. China); Zhanguo Wang (Institute of Semiconductors, Chinese Academy of Sciences, P.R. China)

Walker (50-140)

By introducing both the high mobility GaN channel layer and AlN interlayer, high quality AlGaN/AlN/GaN HEMT structure with the highest 2DEG mobility to the best of our knowledge was grown on 3-inch diameter semi-insulating 6H-SiC substrates by MOCVD. The fabricated eight-cell internally-matched GaN HEMTs device using this structure exhibited state-of-the-art performances with a maximum continuous-wave output power of 110.9 W at 8 GHz.

We5PP-RF.11 **Large-Element Array of Resonant-Tunneling-Diode Terahertz Oscillator for High Output Power at 1 THz Region**

Walker (50-140) *Safumi Suzuki and Masahiro Asada (Tokyo Institute of Technology, Japan)*

Small-size and high-output power THz sources are highly desired for compact imaging system. In this work, we report a large element array of RTD THz oscillator integrated with dipole array antenna. In an array operation, the electrodes of single oscillators were connected in parallel and then oscillators were simultaneously driven. The output power increases linearly with the array number. A high output power of 0.73 mW was obtained at ~1 THz with 89-element oscillators array. Several peaks were observed in the oscillation spectrum because the elements were not coupled with each other for the mutual injection locking. This multi-peak property is convenient for the suppression of interference fringes in THz imaging.

We5PP-RF.12 **Improved DC and RF Performance of AlInN/AlN/GaN HEMTs with a Triethylgallium-Grown GaN Channel**

Walker (50-140) *En-Shuo Lin, Indraneel Sanyal, Yen-Chang Lee, Yu-Chuan Lin, Jen-Inn Chyi and Wei Jen Hsueh (National Central University, Taiwan)*

In this work, AlInN/AlN/GaN HEMTs with their GaN channel grown with triethylgallium (TEG) source and trimethylgallium (TMG) source on Si substrates are investigated. It is found that the AlInN/AlN/GaN HEMT with a TEG-grown channel performs better than that with TMG-grown channel in terms of both DC and RF characteristics. Hall-effect measurement shows that the electron mobility increases from 1,740 cm^2/V.s to 1,820 cm^2/V.s and the sheet resistance decreases from 312 Ω/□ to 271 Ω/□ as the GaN channel is grown by TEG. HEMTs with 0.4 μm gate-length exhibit an fT of 37.1 GHz and an fmax of 55.7 GHz.

We5PP-RF.13 **An RTD-based Frequency Tunable Oscillator Monolithically Integrated with an InP Schottky-Barrier Diode for Sub-THz Applications**

Walker (50-140) *Jaejin Lim and D. Ha (KAIST, Korea); Maengkyu Kim (Korea Advanced Institute of Science and Technology, Korea); Kyounghoon Yang (KAIST, Korea)*

In this work, we present the RTD-based THz frequency-tunable oscillators monolithically integrated with an InP Schottky-barrier varactor diode, which is reported for the first time to our knowledge as an RTD/SBD MMIC tunable oscillator. The oscillation frequency was found varied from 159 to 178 GHz by tuning the bias voltage of VSBD from 0.95 to 4.5 V. A maximum output power of 70 μW was measured from the RTD-based frequency-tunable oscillator at VSBD = 4.5 V.

We5PP-RF.14 **Electron Transport Properties of Novel Ga1-xInxSb Quantum Well Structures with Strained Al0.4In0.6Sb/Al0.3In0.7Sb Stepped Buffer**

Walker (50-140)

Koki Osawa, Mizuho Hiraoka, Tomoya Kishi and Yuki Endoh (Tokyo University of Science, Japan); Jun Takeuchi (Tokyo University of Sciense, Japan); Ryuto Machida and Hiroki Fujishiro (Tokyo University of Science, Japan)

We demonstrate the improved electron transport properties of the novel Ga0.20In0.80Sb QW structure with the strained Al0.40In0.60Sb/Al0.30In0.70Sb stepped buffer. The strained stepped buffer makes the lateral lattice constant of the barrier/buffer larger, and then the GaInSb QW channel of larger In content can be employed, which results in the smaller electron effective mass m* in the channel and the deeper QW. The Ga0.20In0.80Sb QW channel with the strained Al0.40In0.60Sb/Al0.30In0.70Sb stepped buffer (with the superlattice structure) exhibits the electron mobility μ of 16,187 cm^2/Vs, the sheet electron density NS of 2.04×10^{12} cm^{-2}, and the sheet resistance RS of 189 ohm/square). As compared with the InSb HEMT, μ is decreased to 91 %, NS is increased to 186 %, and RS is decreased to 57 %. These indicate the potential of the Ga1-xInxSb QW structures with the strained stepped buffer for the ultra-low power and Terahertz applications.

We5PP-RF.15 **DC and RF Performances of InAs FinFET and GAA MOSFET on Silicon**

Walker (50-140)

Qi Cheng (University of Delaware, USA); Sourabh Khandelwal (Macquarie University, Australia); Yuping Zeng (University of Delaware, USA)

Owing to its excellent material properties, InAs is an attractive channel material for post-Si high-speed application.In this work, a benchmarking computational study about InAs FinFET and GAA MOSFET is demonstrated.

We5PP-RF.16 **Modeling the Parasitic Bipolar Effect in InGaAs FinFETs**

Xin Zhao, Alon Vardi and Jesus del Alamo (MIT, USA)

Walker (50-140) We present a first-order model of the parasitic bipolar effect in InGaAs FinFETs that captures the gate length and fin width dependences observed experimentally. An equivalent circuit model is shown for the excess off-state current. In long channel devices, the current gain drops exponentially due to base recombination, confirmed by the experimental data. This has allowed us to extract the diffusion length of electrons in transistor channel that depends linearly on the fin width. In short channel transistors, the source recombination is expected to dominate and the current gain scales with inverse of the gate length. A linear dependence on the fin width is predicted. Both are confirmed by experiments.

We5PP-RF.17 **Characterization and Modeling of GaAsSb/InAs Nanowire Backward Diodes on the Basis of Quantum Transport Theory and S-parameter Measurement Up to 110 GHz**

Walker (50-140)

Shinpei Yamashita and Michihiko Suhara (Tokyo Metropolitan University, Japan); Kiyoto Asakawa (Tokyo Metropolitan College of Industrial Technology, Japan); Kenichi Kawaguchi (Fujitsu Limited; Fujitsu Laboratories Ltd., Japan); Tsuyoshi Takahashi and Masaru Sato (Fujitsu Laboratories Ltd., Japan); Naoya Okamoto (Fujitsu Limited; Fujitsu Laboratories Ltd., Japan)

Semiconductor heterostructure backward diodes (BWDs) have potential to reveal high sensitive detection of electromagnetic field under the zero bias condition utilizing their strong nonlinearity of I-V characteristic and small junction capacitance. Moreover, fabrication and estimation of GaAsSb-based heterostructure nanowires (NWs) has recently been reported. In this paper p-GaAsSb/n-InAs nanowire backward diodes (NW-BWDs), which have been fabricated in our group, were investigated with respect to their S-parameter measurement up to 110 GHz. Besides measurements, the RF characteristics of the NW-BWD is modeled on the basis of our particular quantum transport theory for the first time. The equivalent circuit model that is clarified in this paper, include quantum transport-oriented circuit topology to express broadband range of admittance unlike conventional equivalent circuits of BWDs ever reported.

We5PP-RF.18 **Analysis of Terahertz Radiation Characteristics in a Bow-Tie Antenna-Integrated Resonant Tunneling Diode Transmitter Modulated by Photocurrent Toward RoF Technology**

Walker (50-140)

Masataka Nakanishi, Michihiko Suhara and Naoto Okumura (Tokyo Metropolitan University, Japan); Kiyoto Asakawa (Tokyo Metropolitan College of Industrial Technology, Japan)

Resonant tunneling diodes (RTDs) have been widely investigated for such as its terahertz oscillation characteristic. The highest frequency record of 1.98 THz was experimentally reported in the InP based-RTD with an integrated slot antenna. Focusing on its potential of several hundred GHz oscillations, we have been proposed and studied a bow-tie antenna integrated resonant tunneling diode transmitter. In this paper modulation characteristics of the propose transmitter is numerically analyzed referring experimental reports for InP based triple-barrier resonant tunneling diodes (TBRTDs) towards radio over fiber (RoF) applications. Possibilities of modulation of several hundred GHz radiation due to several tens Gbps of OOK photocurrent are suggested, Further improvement toward high speed and large output power can be investigated by optimization of individual device performance and integrated structural parameters.

We5PP-RF.19 **Comprehensive Study on $Ga_xIn_{1-x}Sb$ High Electron Mobility Transistors Considering Interface**

Walker (50-140) *Takahiro Suzuki, Yui Fujisawa, Shougo Kawamura, Konosuke Kumasaka, Ryuto Machida and Hiroki Fujishiro (Tokyo University of Science, Japan)*

The challenges for achieving the higher f_T in the InSb HEMT include (1) control of the channel strain that comes from the large lattice constant of channel (2) conquest of the small electron density of state that comes from the small m* in channel, and (3) suppression of the enhanced interface roughness scattering that also comes from the small m* in channel. Our idea of solving the challenges is engineering of m* by using the $Ga_xIn_{1-x}Sb$ channel as an alternative to the InSb. DC and RF performances of the $Ga_xIn_{1-x}Sb$ HEMTs are analyzed comprehensively by using the quantum-corrected Monte Carlo simulation. Under the roughness scattering, the $Ga_xIn_{1-x}Sb$ HEMTs (x = 0, 0.2, 0.4, Lg = 30 nm) still exhibit the peak fT around 1.3 THz, showing the potential for the THz operation. In the real device, the $Ga_{0.2}In_{0.8}Sb$ and $Ga_{0.4}In_{0.6}Sb$ HEMTs will surely gain an advantage because of the larger $\mu \times Ns$.

We5PP-WBG: Poster Session - Wide Band Gap

Time:	5/30/2018, 05:00 PM - 06:30 PM
Room:	Walker Memorial (Building 50-140)

We5PP-WBG.1 **Influence of the AlN/GaN-based Superlattice Buffer on the Breakdown Voltage of the GaN HEMTs Grown on Si**

Walker (50-140)

Christian Manz (Fraunhofer IAF, Germany); Fouad Benkhelifa (IAF Fraunhofer, Germany); Lutz Kirste (Fraunhofer Institute for Applied Solid State Physics, Germany); Oliver Ambacher (Fraunhofer IAF; IMTEK, University Freiburg, Germany)

We have grown, characterized and simulated AlN/GaN superlattice structures in detail. Our SL structure consists of 120 periods of AlN/GaN with a total thickness of 2,7µm. A series of different samples with the same period length, but different AlN/GaN ratio was grown and investigated. Standard characterization of AlN/GaN SL structures were performed. Furthermore the vertical breakdown voltage was measured. Capacitance-voltage (CV) measurements were performed and used as basis for simulations. There is a strong relationship between breakdown-voltage, electron density in the SL and relative AlN thickness.

We5PP-WBG.2 **Si-doped GaN Films Grown by Reactive Co-Sputtering of GaAs and Si in Argon-Nitrogen Mixture**

Walker (50-140)

Shyam Mohan and Syed Major (Indian Institute of Technology Bombay, India)

The continuously increasing demand of high quality GaN films for a wide range of applications has been driving the exploration of alternative deposition processes. Earlier work from our group has demonstrated that epitaxial GaN films can be deposited by reactive magnetron sputtering of a GaAs wafer with 100 % nitrogen as the sputtering-cum-reactive gas [1]. This approach has now been extended towards the growth of n-type, Si doped GaN films by reactive magnetron co-sputtering of Si and GaAs in argon-nitrogen sputtering atmosphere. These films have been grown on sapphire at a substrate temperature of 700 °C, over GaN buffer layers of thickness ~ 100 nm, grown at 300 °C. The target was a GaAs wafer, covered partially (~ 5 % of the area of erosion track) with Si. The incorporation of Si in the films was controlled by increasing the argon percentage in the sputtering atmosphere from 0 - 85 % (with concurrent decrease of nitrogen from 100 - 15 %). The growth rate of the films increases from ~ 1µm/h to ~ 2 µm/h, with increase in argon percentage in the sputtering atmosphere. The thickness of all the films was about 800 nm. X-ray powder diffraction studies show that all the films display a single phase consisting of the wurtzite GaN, with nearly complete c-axis orientation. The films deposited with 100 % nitrogen show a slightly larger value of lattice parameter 'c', which decreases monotonously with increase of argon percentage in the sputtering atmosphere. SIMS studies confirm the incorporation of Si in the films, which increases with increase of argon percentage in the sputtering atmosphere. Traces

of arsenic are found in all the Si-doped GaN films, which also increases slightly with argon percentage. Atomic force microscopy studies show particle like surface morphology of all the films with lateral size features of (80 ± 20) nm. With increase in argon percentage to 50%, the surface roughness decreases from ~ 8 nm to ~ 1 nm, but increases at higher argon percentage. UV-VIS spectra show that all the films exhibit high transparency in the visible and NIR region, with sharp interference fringes, suggesting the high optical quality of the films. The band gaps of the films were determined from the plots of α2 against photon energy. The values of band gap were found to be in the range of 3.3 eV to 3.4 eV, exhibit a small increase with increase of argon percentage in the sputtering atmosphere. The measurement of electrical transport parameters of Si-doped GaN shows that the argon percentage in sputtering atmosphere strongly influences the electrical properties of Si-doped GaN films. With increase in the argon percentage, the resistivity decreases by four order of magnitude to a value of ~ 10-2 Ω-cm for the film deposited with 85 % argon. Correspondingly, the carrier concentration increases monotonically from ~ 1 x 10^{18} cm^{-3} to ~ 6 x 10^{19} cm^{-3}, along with an increase in mobility from ~ 0.1 cm^2/V-s to ~ 12 cm^2/V-s. These results provide the evidence for effective and controlled doping of Si in sputtered GaN films over a wide range.

We5PP-WBG.3 **Carrier Trapping Properties of Defects in Mg-implanted GaN Probed by Monoenergetic Positron Beams**

Walker (50-140)

Akira Uedono (University of Tsukuba, Japan); Shinya Takashima, Masaharu Edo and Katsunori Ueno (Fuji Electric Co., Japan); Hideaki Matsuyama (Euji Electric Co., Japan); Werner Egger and Toenjes Koschine (UniBwM, Germany); Christoph Hugenschmidt and Marcel Dickmann (TUM, Germany); Kazunobu Kojima and Shigefusa Chichibu (Tohoku University, Japan); Shoji Ishibashi (AIST, Japan)

Vacancy-type defects in Mg-implanted GaN were probed using monoenergetic positron beams. Mg ions were implanted to provide a 500-nm-deep box profile with Mg concentrations ([Mg]) of 1E17 - 1E19 /cm^3 at room temperature. In the as-implanted samples, the major defect species was a complex of a Ga vacancy and a nitrogen vacancy. After annealing above 1000C, the major defect species was changed to vacancy clusters due to vacancy agglomeration. This agglomeration was suppressed, and the agglomeration onset temperature was decreased with a decreasing [Mg]. For samples with [Mg] >= 1E18 /cm^3, the trapping rate of positrons by vacancy-type defects decreased after annealing above 1100-1200°C. This decrease was attributed to the change in the defect charge states from neutral to positive due to a downward shift of the Fermi level. The carrier trapping/detrapping properties of the vacancy-type defects and their time dependences were also revealed.

We5PP-WBG.4 **Thermal Behavior of Defects Generated in GaN by Low-Dose Mg-ion Implantation**

Masamichi Akazawa, Naoshige Yokota and Kei Uetake (Hokkaido University, Japan)

Walker (50-140)

We investigated the thermal behavior of defects generated in GaN by low-dose Mg-ion implantation at relatively low temperatures (< 800°C) compared with that needed for the activation of Mg atoms as acceptors, typically higher than 1200°C. To investigate the near-surface region, MOS diodes on Mg-implanted GaN were fabricated. The obtained C-V characteristics and computer simulation showed that defect states were generated at EC-E = 0.76 eV in the implanted region and that the carrier concentration in the near-surface region was reduced. We found the detected defect states disappeared with the partial recovery of the carrier concentration by annealing at 500°C subsequent to the ion implantation. Considering the low dosage of the Mg ions and the recovery temperature of the defects, the origin of the detected deep-level states seems to be related to a simple point defect.

We5PP-WBG.5 **Correlation of Photo-Response with Bulk Defect States in DIBS Grown ZnO Based Thin Films**

Walker (50-140)

Md Arif Khan, Rohit Singh, Ritesh Bhardwaj, Amitesh Kumar, Mangal Das and Abhinav Kranti (Indian Institute of Technology Indore, India); Shaibal Mukherjee (Indian Institute of Technology, Indore, India)

In this work, we demonstrate repeatable defect energy states in ZnO and its alloy CdZnO grown by dual ion beam sputtering (DIBS). The defects density distribution (Nd) around the mean defect energy states proportional to the spread of responsivity curve at secondary peaks has been graphically depicted. ZnO has a very significant defect chemistry and a process with repeatable defect states could be utilized for multiple applications as it gives access to multiple energy states in the same energy band gap of the material

We5PP-WBG.6 **Nitrogen-face AlN-based Field-Effect Transistors**

Walker (50-140)

Hironori Okumura (University of Tsukuba; MIT, Japan); Jori Lemettinen and Sami Suihkonen (Aalto University, Finland); Tomás Palacios (Massachusetts Institute of Technology, USA)

We achieved the high-quality nitrogen-face AlN growth on SiC by MOCVD. Using the AlN layers, we demonstrated the first nitrogen-face AlN-channel MESFETs and graded AlGaN/AlN polarization FETs. The both devices had a normally-on operation and pinch-off characteristics under an applied gate bias. In AlN-channel MESFETs, the subthreshold swing was 1.2 V/decade. Id is effectively modulated by Vgs and shows good saturation. The maximum Id was 10 uA/mm for Vgs = +5 V. The off-state Id was 90 pA/mm at room temperature. The Id on/off ratio was 1.1×10^5. In graded AlGaN/AlN PolFETs, the subthreshold swing was 1.8 V/decade. The maximum Id was 3.3 uA/mm for Vgs = +5 V. The Id on/off ratio was 3.5×10^4.

We5PP-WBG.7 **Growth of Gallium Nitride Thin Film on Amorphous Glass Substrate Through Pulsed Direct Current Sputtering Deposition**

Walker (50-140)

Wei-Sheng Liu (Department of Photonics Engineering, Yuan Ze University, Taiwan); Yu-Lin Chang and Hui-Yu Chen (University of Yuan Ze, Taiwan)

In this paper, we present the growth of high-quality GaN films on amorphous glass substrate through pulsed direct current (DC) sputtering deposition technique. The addition of ZnO buffer layers in this work improved the crystalline quality of the GaN films on the amorphous substrate. The GaN films were deposited at a substrate temperature of 300 °C and the thickness of the deposited GaN films were maintained at 300 nm. The experimental results indicated that the GaN films with a low sputtering power of 75 W and low growth temperature of 300 °C exhibited improved columnar crystal growth and enhanced XRD intensity with a narrow FWHM value. The results indicate the high potential of sputtering-deposited GaN films on glass substrates for the fabrication of large-scale and low-cost optoelectronic devices.

We5PP-WBG.8 **Low-temperature Electrical Transport Properties of MgZnO/ZnO Heterostructures**

Walker (50-140)

Rohit Singh, Md Arif Khan, Amitesh Kumar and Abhinav Kranti (Indian Institute of Technology Indore, India); Shaibal Mukherjee (Indian Institute of Technology, Indore, India)

In this work, we investigated the low-temperature electrical transport properties of MgZnO/ZnO heterostructures grown by dual ion beam sputtering (DIBS), which is crucial for the fabrication of ZnO-based heterostructure transistor by sputtering. Temperature-dependent magnetoresistance (MR) measurements were performed in longitudinal geometry up to 8 T and 1.5 K to 300 K for two heterostructures of different Mg compositions (20 at. % and 30 at. %). The temperature dependent sheet resistance shows almost metallic behavior. This may be due to the formation of two-dimensional electron gas (2DEG) at the MgZnO/ZnO heterointerface. To further understand the low-temperature electrical transport properties of these heterostructures, the sheet resistance is also measured for variation of the magnetic field at a fixed temperature.

We5PP-WBG.10 **The Growth of a Discrete GaN Array with Micro Size on Thin Al_2O_3 Membrane**

Walker (50-140)

Seungmin Lee, Daeyoung Moon, Daehan Choi and Hyejin Lim (Seoul National University, Korea); Yongjo Park (Advanced Institutes of Convergence Technology, Korea); Euijoon Yoon (Seoun National University, Korea)

In this study, a discrete GaN array with micro size was grown on sapphire nano-membrane structure by MOCVD. A discrete GaN array was formed by using different growth rate for each crystal plane of GaN and controlling the spacing of nano-membrane. So, micro-sized GaN array with 14x14 μm^2 and 50x50 μm^2 was fabricated by controlling the length and the number of stripe-patterned sapphire nano-membrane. Since the stress of the GaN thin film caused by lattice mismatch divides into nano-membrane and GaN film, threading dislocation density of GaN on sapphire nano-

membrane was reduced by about 40%, compared to that of GaN on planar substrate. In addition, through transfer of GaN film on Si substrate using wafer bonder, we confirmed that thin nano-membrane can be easily broken by mechanical force, which is advantageous in transfer process.

We5PP-WBG.11 **Electronic Structure of (ZnO)1-x(InN)x Alloys Calculated Using IQB Theory**

Ryota Furuki, Masato Oda and Yuzo Shinozuka (Wakayama University, Japan)

Walker (50-140) We theoretically elucidate the electronic structure of a novel semiconductor alloy, (ZnO)1-x(InN)x, whose electronic structure can be modified by altering the alloy composition (x), and it is expected to be applied to excitonic light-emitting devices, solar cells. The IQB theory, which has been proposed for calculating various random alloys, is applied to evaluate electronic band structure of (ZnO)1-x(InN)x by focusing on the randomness of its alloy and the charge mismatch among II-VI and III-V. It is shown that around x = 0.5, the bottom of the conduction band is strongly modulated by the anion p states, resulting large bowing of the band gap, which is consistent with the experimental results.

We5PP-WBG.12 **Repeatability of InAlN HEMT Growth by High-Speed-Rotation Single- Wafer MOCVD Tool**

Walker (50-140) *Yasushi Iyechika, Hajime Nago, Masayuki Tsukui and Hideshi Takahashi (NuFlare Technology, Inc., Japan)*

InAlN as a barrier layer in high electron mobility transistor (HEMT) structure is advantageous over AlGaN in lattice-matched growth to GaN and larger spontaneous polarization. On the other hand, metal organic chemical vapor deposition (MOCVD) grown InAlN is known to have unintentional Ga inclusion depending on the chamber condition. We developed a high-speed-rotation single-wafer MOCVD tool which is favorable for suppression of deposition on the reactor wall and is expected to suppress Ga inclusion in InAlN. Using the tool we confirmed InAlN growth of very low Ga inclusion, good in-wafer uniformity and good repeatability on 6-inch Si-wafers. Also fairly low and uniform sheet resistance of HEMT structure on an 8-inch wafer was confirmed.

We5PP-WBG.13 **In-situ Surface Treatment of GaN Substrates for Homoepitaxial Growth by MOCVD**

Walker (50-140)

Fen Guo and Yanbin Qin (Institute of Semiconductors, Chinese Academy of Sciences, P.R. China); Quan Wang (Shandong University; Institute of Semiconductors, Chinese Academy of Sciences, P.R. China); Lijuan Jiang, Wei Li, Chun Feng, Xiaoliang Wang and Fengqi Liu (Institute of Semiconductors, Chinese Academy of Sciences, P.R. China); Xiangang Xu (Shandong University, P.R. China); Zhanguo Wang (Institute of Semiconductors, Chinese Academy of Sciences, P.R. China)

In this work, we used a novel in-situ surface treatment, i.e., periodic deposition and desorption (PDD) of the GaN substrate in MOCVD chamber, to prepare the GaN substrate before epitaxy. The experimental results show that the Si impurity between GaN epilayer and GaN substrate can be effectively reduced and GaN epilayer with high quality can be obtained.

We5PP-WBG.14 **MOCVD-grown BAlN-contained Heterojunctions**

Walker (50-140)

Haiding Sun and Kuang-Hui Li (KAUST, Saudi Arabia); Young Jea Park, Theeradetch Detchprohm and Russell Dupuis (School of Electrical and Computer Engineering, Georgia Institute of Technology, USA); Xiaohang Li (King Abdullah University of Science and Technology, Saudi Arabia)

Boron-aluminum-nitride (BAlN) is an emerging III-nitride alloy with large bandgap. We demonstrated a significant increase in the thickness (i.e., 100 nm) and B content to 14.4% for single-phase wurtzite BAlN layer. Furthermore, we found that the bandgap of BAlN transitioned from direct to indirect as the B content increased to 12%. This result indicates that it is unlikely for BAlN to be the sole material for the active layer. Therefore, BAlN would probably have to be integrated with Al-rich AlGaN to form heterostructures for application. Here we grew BAlN/AlGaN heterostructures using MOCVD. We conducted detailed characterizations related to the microstructure, defect formation, and strain within the BAlN and AlGaN layers. Furthermore, we measured the conduction and valence band offset in such heterojunction. Our theoretical study and experimental analysis provides insights for future research and development of the BAlN/AlGaN heterostructures for optical and power electronics.

We5PP-WBG.15 **Electrical and Optical Studies of Ga-doped ZnO Films Grown by Reactive Co-Sputtering of Zn and GaAs**

Walker (50-140)

Appani Shravan Kumar (Indian Institute of Technology - Bombay; IIT-Bombay, India); Samanth Vinil Rayapati (IIT-Bombay, India); Syed Major (Indian Institute of Technology Bombay, India)

GZO films were obtained by reactive co-sputtering of Zn and GaAs. Typically, the GZO film deposited at 375°C with 5% O_2 in sputtering atmosphere exhibits ~ 80% transmittance in visible and resistivity of 7.3 x 10-4 Ω-cm, with corresponding carrier concentration of 1.1 x 10^{21} cm^{-3} and Hall mobility of 7.5 $cm^2V^{-1}cm^{-1}$. The oxygen (%) in sputtering atmosphere is found to be critical so that within a small window of O_2

percentage (5 - 6%), a drastic increase in resistivity is observed. These conducting films exhibit plasma resonance in NIR and followed by high reflectance in infrared region and substantial increase in band gap by ~ 0.5 eV. The increase in band gap is attributed a combination of Moss-Burstein effect Band gap narrowing effect. A strong dependence of effective mass on carrier concentration observed and approaching a value of 0.7me at carrier concentration of ~ 10^{21} cm^{-3}.

We5PP-WBG.16 **Mg Recoil Implantation into GaN with Incident Nitrogen Ion**

Toshikazu Yamada (National Institute of Advanced Industrial Science and Technology, Japan)

Walker (50-140)

GaN is a fascinating material for applications due to its high breakdown field, high switching speed, and low switching losses. But a fundamental technique for a device fabrication of GaN has not been established yet. It is quite difficult to prepare p-type GaN by ion implantation of Mg. During the implantation process, the incident Mg ions gives severe damage to the bulk. Furthermore, the damage of GaN bulk is difficult to recover by thermal annealing. A reduction of the damage by the incident Mg beam on implantation process is still essential. Therefore, we have demonstrated the lowering of the damage by using a so-called recoil implantation method. However, in this case, the incident beam is not Mg ions but Nitrogen ions. We found that the recoiled Mg atoms in the GaN penetrated into the bulk GaN without a heavy bombardment damage

We5PP-WBG.17 **Time-resolved Optical Studies of the Annealing-Induced Conductivity Increase in P-Type GaNSb**

Walker (50-140)

Antonio Llopis (Army Research Laboratory, USA); Wendy Sarney and Stefan Svensson (US Army Research Laboratory, USA); Natalie Segercrantz (Aalto University, Finland); Yannick Baumgartner (Lawrence Berkeley National Laboratory, USA); Min Ting (University of California, Berkeley; Lawrence Berkeley National Laboratory, USA); Kin Man Yu (Lawrence Berkeley National Lab, USA); Samuel Mao (University of California, Berkeley, USA); Wladek Walukiewicz (Lawrence Berkeley National Lab, USA); Michael Wraback (US Army Research Lab, USA)

This work demonstrates a correlation between increased p-type behavior and drop in resistivity in annealed GaNSb with a reduction in bandtail states. This reduction of bandtail states is observed via pump-probe differential transmission spectroscopy as a change from photoinduced absorption to photoinduced bleaching of the states. This change suggests a change from more amorphous behavior to more crystalline-like behavior. We also demonstrate that the absorption and conductivity must be primarily determined by the properties of the amorphous GaNSb material present between GaN crystallites.

We5PP-WBG.18 **Growth of High Quality AlInN/GaN HEMTs on 150 mm Si Substrates Using an Step-graded AlGaN and AlN/GaN Superlattice Composite Buffer**

Walker (50-140)

Chuan-Yue Yu, Shiou-Ming Wu, Indraneel Sanyal and Jen-Inn Chyi (National Central University, Taiwan)

We demonstrate a 6 nm barrier AlInN/AlN/GaN HEMT grown on 150 mm Si (111) substrate by employing a composite buffer layer, which consists of an AlN/GaN superlattice and a step-graded AlGaN layer. A record electron mobility of 1,940 cm^2/V.s has been achieved with this buffer design. To our knowledge, this is one of the best electron mobility obtained on 6 nm AlInN HEMTs grown on Si. Schottky HEMTs fabricated on these two samples reveal that sample B has a lower on-resistance, higher three terminal breakdown voltage (490 V vs 460 V), as well as a higher two terminal horizontal breakdown voltage (710 V vs 660 V).

We5PP-WBG.19 **Mapping Nanoscale Optical Properties of V-pit Defects in GaN-on-Si LEDs via Cathodoluminescence in Scanning Transmission Electron Microscopy**

Walker (50-140)

Zhibo Zhao (Massachusetts Institute of Technology`, USA); Silvija Gradecak and Akshay Singh (Massachusetts Institute of Technology, USA); Sarah Goodman (MIT, USA); Govindo Syaranamual and Saurabh Srivastava (Singapore-MIT Alliance in Research and Technology, Singapore); Jing Yang Chung and Abdul Kadir (National University of Singapore, Singapore); Li Zhang (Singapore-MIT Alliance in Research and Technology, Singapore); Soo-Jin Chua (National University of Singapore, Singapore); Eugene A. Fitzgerald (Massachusetts Institute of Technology, USA); Stephen Pennycook (National University of Singapore, Singapore)

In this work, we use cathodoluminescence in scanning transmission electron microscopy (CL-STEM) to map nanoscale optical properties around V-pit defects found in InGaN/GaN QW heterostructures grown on Si substrates. Near certain V-pit defects, we observe the emergence of additional emission peaks (centered at 380 nm) blue-shifted with respected to the targeted QW emission wavelength (480 nm). Further, we find that these emission peaks shift as a function of position across certain V-pit defects. Hyperspectral mapping of selected V-pit defects reveals shorter wavelength emissions near the side-walls exhibiting a continuous red-shift of ~20-30 nm approaching the dislocation core. Finally, we couple cathodoluminescence spectroscopy with structural imaging in S/TEM and investigate correlations between the observed spectral inhomogeneities and structural defects including well-width fluctuations, dislocation character, and compositional variations.

We5PP-WBG.20 **Gamma-ray and Proton Radiation Effects in AlN Schottky Barrier Diodes**

Walker (50-140)

Jossue Montes (Arizona State University, USA); Houqiang Fu (Arizona state University; Arizona State University, USA); Tsung-Han Yang, Xuanqi Huang, Hong Chen, Izak Baranowski and Kai Fu (Arizona State University, USA); Yuji Zhao (Arizona state University, USA)

Aluminum nitride schottky barrier diodes were fabricated by metal organic chemical vapor deposition and subjected to a wide range of temperature and radiation doses. This study used gamma-ray irradiation from 0 to 90 MRads and protons at an energy of 3 MeV at various fluxes, from 10^9 /cm^2 up to 10^{15} /cm^2. The temperature ranges considered were 20 °C to 120 °C. Current-voltage tests, capacitance-voltage tests, and high-resolution x-ray diffraction (HR-XRD) measurements were used. It was found that gamma-ray irradiation did not appreciably impact forward currents or the sample crystallinity (as determined by HR-XRD). Proton bombardment did not appreciably impact currents until the very highest dose (10^{15} /cm^2), but did have an impact on sample crystallinity. Carrier concentrations as determined from capacitance measurements did not appreciably change with increasing proton dose until the very highest dose.

We5PP-WBG.21 **MOCVD Growth of AlGaN on SiC Substrates for High Efficiency Deep UV LED**

Walker (50-140)

Abdullah Almogbel, Burhan Saifaddin, Christian J Zollner and Michael Iza (University of California, Santa Barbara, USA); Hamad Albraithen, Ahmed Y. Alyamani and Abdulrahman M. Albadri (King Abdulaziz City for Science and Technology, Saudi Arabia); Steven DenBaars (University of California, Santa Barbara, USA); Shuji Nakamura (University of California Santa Barbara, USA); James Speck (University of California, Santa Barbara, USA)

We report on the use of pre-growth high temperature nitridation as a mechanism to prevent the formation of cracks and voids on AlGaN thinfilms grown on Silicon Carbide substrate. Direct growth of AlN and AlGaN on SiC resulted in heavily cracked films. Cracking of AlN and AlGaN grown on SiC is generally attributed to the difference in the thermal expansion coefficient between the SiC and the AlGaN/AlN epitaxial layers. However, it was discovered that in-situ, pre-growth treatment of the SiC substrate at high temperature of 1250°C, in an ambient gas mixture of Ammonia (NH3) and Hydrogen (H2) can effectively prevent the formation of cracks and voids on the episurface, without affecting the crystal quality. Similar treatment at a "cold" temperature of 1000°C did not prevent the cracking. Also, a high temperature treatment without ammonia did not yield the same effect as well. Which emphasizes the importance of the high temperature treatment and ammonia gas in this mechanism of cracking prevention.

We5PP-WBG.22 **High Al-AlxGa1-xN Channel Field Effect Transistors over Thick AlN/Sapphire Templates**

Walker (50-140) *Sakib Muhtadi, Abu Shahab, Xuhong Hu, Kamal Hussein, Seongmo Hwang, Antwon Coleman, Fatima Asif, Richard Floyd, Mvs Chandrashekhar, Grigory Simin and Asif Khan (University of South Carolina, USA)*

We report high-Al AlGaN/AlGaN HEMTs with various Al fraction. The developed technology results in linear contacts with 7 - 9 Ohm*mm resistance and devices with peak drain currents up to 450 mA/mm. AlxGa1-xN channel HEMTs were grown over the AlN/sapphire templates where the barrier layer composition was fixed at x=0.65 while the channel composition was varied from x=0.40 to x=0.5

We5PP-WBG.23 **Optical Characterization of Undoped and Si Doped GaN Grown on C-Plane GaN Free Standing Substrate by Spectroscopic Ellipsometry Above the Fundamental Gap**

Walker (50-140) *Naoto Kumagai, Hisashi Yamada, Toshikazu Yamada and Xue-Lun Wang (National Institute of Advanced Industrial Science and Technology, Japan); Mitsuaki Shimizu (National Institute of Advanced Industrial Science and Technology (AIST), Japan)*

Dielectric properties of undoped and Si doped GaN grown on c-plane GaN free standing substrate has been characterized by spectroscopic ellipsometry above the fundamental band gap. The measurement from 1.1 to 9 eV covers critical points of E1 (B) and E1(C) from ~7 to ~8 eV of wurtzite GaN. All samples in this study were grown by MOCVD with the same condition except for doping concentration. Si doping concentrations were 4E15 and 3E16 per cubic centimeter. The general oscillator model was employed to fit to measured pseudo dielectric functions. The mean squared error of fitting results were less than 1. Dielectric functions of undoped and Si doped GaN were evaluated by optical model considering surface roughness from AFM. Compared to undoped GaN, Si doped GaN shows the broadening and red shifting at E1(B) as doping concentration increases, while the feature at E1(C) doesn't show remarkable change.

We5PP-WBG.24 **Defect Control in GaN-on-Si Wafers for Power Electronics Applications**

Hongjing Huo, Peng Xiang, Liyang Zhang, Ni Yin and Kai Cheng (Enkris Semiconductor, P.R. China)

Walker (50-140)

In the past decade, GaN-on-Si based power devices have become one of the most promising candidates used in the next generation power electronics systems because it well leverages the performance and cost. Thanks to stress engineering, detrimental defects in GaN-on-Si materials including cracks, pits and etc. have been minimized. In addition to cracks and pits, particles and crescents have been little studied systematically. In this work, defects in 150 mm GaN-on-Si wafers including cracks, pits, particles and crescent have been investigated by Candela. The influence of varied growth parameters and buffer structures on defect level have been thoroughly studied. By choosing the proper buffer structures, defects can be minimized on 150 mm GaN-on-Si wafers which is suitable for 600 V applications. However, with increased buffer thickness, the defect level is significantly increased, which leads to a potential barrier for future 1200 V device fabrications.

Rump Session	
Time:	5/30/2018, 7:00 PM - 8:30 PM
Room:	Wong Auditorium (Building E-51)
Moderator:	Eugene Fitzgerald (Massachusetts Institute of Technology, United States)

Industrial III-V's: *Continuing the Single Life or More Fulfillment Through Marriage with Silicon?*

Panelists:

- *Timothy Boles (MACOM)*
- *Michael Heuken (Aixtron)*
- *Jose Jimenez (Qorvo)*
- *Wayne Johnson (IQE)*
- *Tom Kazior (Raytheon)*
- *Matsumoto Koh (Taiyo Nipon Sanso)*
- *Steve Ringel (4Power LLC)*

THURSDAY

5/31/2018

TECHNICAL PROGRAM

IPRM
Est. 1989

Cambridge / Boston, Massachusetts

CSW2018

2018
iSCS

Th1A5: Lasers

Time:	5/31/2018, 08:30 AM - 10:00 AM
Room:	Salon M (Samberg Conference Center, 7th floor)
Chair:	Nelson Tansu (Lehigh University, United States)

Th1A5.1 **Mid-Infrared Quantum Cascade Lasers and Applications**

08:30 AM *Claire Gmachl (Princeton University, USA)*

INVITED Abstract not available.

Th1A5.2 **Evolution of Material Systems for THz Quantum Cascade Lasers**

09:00 AM *Hermann Detz (TU Wien; Austrian Academy of Sciences, Austria); Martin Kainz, Sebastian Schönhuber, Tobias Zederbauer, Donald MacFarland, Michael Krall, Christoph Deutsch, Martin Brandstetter, Aaron M Andrews, Werner Schrenk, Karl Unterrainer and Gottfried Strasser (TU Wien, Austria)*

Salon M

THz Quantum cascade lasers (QCLs) are compact coherent sources with designable emission wavelengths between 30 µm and 3 mm. Their main hurdle for the integration into optical systems is the limited operating temperature < 200 K. This work focuses on low-effective mass material systems based on InGaAs and InAs quantum wells, which provide higher optical gain compared to the commonly used GaAs/AlGaAs heterostructures. With InAlAs and GaAsSb, we compare two prospective barrier materials for InGaAs-based active regions, which allow to identify the optimum balance between effective mass, barrier height and thickness. Currently, InGaAs/InAlAs and InGaAs/GaAsSb THz QCLs reach operating temperatures of 155 K and 142 K. We furthermore report on the first operational InAs-based THz QCLs, which still require in-plane confinement by a magnetic field due to the early stage of development. We will benchmark the different material systems for THz QCLs, present state-of-the-art results and outline potential future directions.

Th1A5.3

09:15 AM

Salon M

III-V Superlattices on InP/Si Metamorphic Buffer Layers for Λ~4.8Mm Quantum Cascade Lasers

Ayushi Rajeev (University of Wisconsin-Madison, USA); Bei Shi (The Hong Kong University of Science and Technology, Hong Kong); Qiang Li (Hong Kong University of Science and Technology, Hong Kong); Jeremy Kirch, Micah Cheng and Aaron Tan (University of Wisconsin-Madison, USA); Kei May Lau (Hong Kong University of Science and Technology, Hong Kong); Luke Mawst and Thomas Kuech (University of Wisconsin-Madison, USA)

Monolithic integration of InP-based quantum cascade lasers (QCLs) with Si combines the optoelectronics advantage of the direct bandgap of III-Vs with the cost effective CMOS technology leading to a multitude of applications such as photonic integrated sensor circuits. To that extent, a metamorphic InP substrate utilizing InAs/ InAlGaAs quantum dots as dislocation filters in the InP buffer on a Si (001) substrate is used for regrowth of a mid-IR quantum cascade laser. Test strain-compensated In0.39Al0.61As (11.48nm)/ In0.635Ga0.365As (11.9nm) superlattice (SL) structure is grown atop this substrate using MOCVD, to compare the planarity of the constituent layers and interfaces to those grown on InP. 5-stages of the QCL active region were regrown to assess the quality of the SL through HRXRD, HRTEM and PL. Efforts are underway to optimize the surface polishing procedure and perform the regrowth of 30-40 stages of the active region in order to obtain a QCL with an emission wavelength of 4.8 μm.

Th1A5.4

09:30 AM

Salon M

Interband Cascade Light Emitting Devices for the Mid-IR Spectral Region

Chadwick Canedy and Chul-Soo Kim (Naval Research Laboratory, USA); Mijin Kim (KeyW Corporation, USA); William Bewley and Charles Merritt (Naval Research Laboratory, USA); Michael V Warren (ASEE Fellow at Naval Research Laboratory, USA); Stephanie Tomásulo, Igor Vurgaftman and Jerry Meyer (Naval Research Laboratory, USA)

Light emitting devices (LEDs) operating in the midwave-infrared (mid-IR) region of the electromagnetic spectrum are drawing increasing attention for applications requiring a broadband, incoherent source with continuous wave (cw) output. Such applications include dynamic scene projection and spectroscopic techniques for chemical sensing and noninvasive disease analysis. While mid-IR LEDs and LED arrays have been under development for several decades, until recently their performance has generally been quite poor, with maximum cw output powers for packaged commercial devices operating at room temperature no greater than 300 μW. In 2014, NRL demonstrated interband cascade light-emitting devices (ICLEDs) that emitted up to 1.6 mW in cw mode at 25 ºC. In this work, we report on NRL's recent development of ICLEDs with improved performance over the recently demonstrated cw mode devices. We will discuss the extension of this result using a split-stage architecture that further enhances the output power and efficiency.

Th1A5.5

09:45 AM

Salon M

High-index-contrast 1.55 Um AlInGaAs/InP Laser Heterostructure Waveguides Through Selective Core Oxidation

Yuan Tian and Douglas Hall (University of Notre Dame, USA)

An InP-based high-index-contrast deep-etched ridge waveguide structure suitable for low bend loss routing and the fabrication of compact on-chip ring or loop geometry lasers is realized through the controlled selective lateral oxidation of the strained AlInGaAs multi-quantum well waveguide core sandwiched between InP cladding layers in a 1.55 µm telecom wavelength diode laser heterostructure. The process is enabled by first depositing a thin protective layer to fully suppress the thermal dissociation of exposed InP surfaces during a subsequent 525 °C oxygen-enhanced wet thermal oxidation process. Both the selective epitaxial regrowth of ~30-100 nm InGaAs via MOCVD and the atomic layer deposition of ~6 Å of HfO_2 are found to provide effective protection. Lateral core oxidation of 0.5-1.1 µm is achieved with oxidation times of 2.5-3 hr, yielding a regrowth-free high optical confinement, reduced capacitance, and contact resistance structure for the integration of high-speed, low-bend loss laser and modulator devices.

Th1B5: Wide Band Gap

Time:	5/31/2018, 08:30 AM - 10:00 AM
Room:	Wong Auditorium (Building E-51)
Chair:	Zetian Mi (University of Michigan, USA)

Th1B5.1

08:30 AM

Wong (E-51)

Phase-transition Cubic GaN with ~29 % Internal Quantum Efficiency

Richard Liu (University of Illinois at Urbana Champaign, Micro and Nanotechnology Laboratory); Richard Schaller (Argonne National Laboratory, USA); Chang Qiang Chen (University of Illinois at Urbana Champaign, Material Research Laboratory); Can Bayram (University of Illinois at Urbana Champaign, Micro and Nanotechnology Laboratory)

We present structural and optical characterizations of the phase-transition c-GaN. Under optimized Si nano-patterning condition, transmission electron microscopy reveals no threading dislocations and electron backscatter diffraction shows no phase mixing. Temperature-dependent CL study reveals a record c-GaN room-temperature internal quantum efficiency (IQE) of ~ 29%, which is 2.4 times greater than that of h-GaN. A relatively shallow acceptor with an activation energy of 126 meV is identified. Using the IQE value and carrier decay lifetime of 11 ps obtained from time-resolved PL in, the radiative lifetime of c-GaN is determined to be 38 ps, which is ~12.4 times faster than the radiative lifetime of bulk h-GaN. The polarizability of c-GaN is calculated to be 8.3×10^{-11}, which is seven orders smaller than that of h-GaN. These inherent properties of c-GaN are promising for the next generation high-efficiency III-nitride-based LEDs and photonic devices.

Th1B5.2

08:45 AM

Wong (E-51)

Impact of Indium Distribution in Quantum Wells on Efficiency Droop of InGaN Light Emitting Diodes

Sarah Goodman (MIT, USA); Akshay Singh (Massachusetts Institute of Technology, USA); Zhibo Zhao (Massachusetts Institute of Technology`, USA); Dong Su and Kim Kisslinger (Brookhaven National Laboratory, USA); Rob Armitage, Isaac Wildeson and Parijat Deb (Lumileds LLC, USA); Silvija Gradecak (Massachusetts Institute of Technology, USA)

Indium gallium nitride/ gallium nitride (InGaN/GaN) quantum well (QW) LEDs have high quantum efficiencies and are the cornerstone of modern lighting solutions. However, InGaN LEDs suffer from efficiency droop - the quantum efficiency peaks at low injection currents and subsequently decreases monotonically with increasing current. We employ high-resolution structural characterization techniques to study a range of droop minimizing device designs with variations in the active region structural parameters and composition. Non-uniformity of indium composition within the QWs is one factor that has been suggested to contribute to efficiency droop. We use electron energy-loss spectroscopy in a scanning transmission electron microscope to characterize the

composition and spatial extent of indium in LED designs with varying performance characteristics. We demonstrate that the choice of imaging parameters is critical in conducting an artifact-free investigation of indium fluctuations, and we investigate the correlation between the efficiency of the devices and the presence of indium fluctuations.

Th1B5.3

09:00 AM

INVITED

Wong (E-51)

A Decade of Nonpolar and Semipolar III-Nitrides: A Review of Successes and Challenges

Daniel Feezell (Center for High Technology Materials, University of New Mexico, USA)

More than a decade ago, nonpolar and semipolar III-nitrides were proposed as a solution to many inherent materials issues in III-nitrides. This talk will review the successes and challenges of nonpolar and semipolar III-nitrides after more than a decade of development. I will discuss where nonpolar and semipolar III-nitrides have shown clear promise (e.g., polarization pinning in VCSELs, higher gain in lasers, faster modulation speed in LEDs) and where have they failed to deliver (e.g., LED efficiency droop, LED green gap). The relevant background and important developments over the last decade will be covered and I will give some perspectives on the successes, failures, and future outlook for these materials and related devices.

Th1B5.4

09:30 AM

Wong (E-51)

Investigation of Mg δ-Doping for Low Resistance N-polar p-GaN Films Grown at Reduced Temperatures by MOCVD

Cory C Lund (UCSB, USA); Anchal Agarwal and Brian Romanczyk (University of California Santa Barbara, USA); Thomas Mates (University of California, USA); Shuji Nakamura (University of California Santa Barbara, USA); Steven DenBaars (Advisor, USA); Umesh Mishra and Stacia Keller (UCSB, USA)

P-type Mg δ-doping was explored for the deposition of N-polar p-GaN films at a reduced temperature of 900 C to minimize the thermal degradation of high In composition active regions in devices such as long wavelength LEDs and tunnel transistors. Various δ-doping process parameters were investigated and the results compared to those obtained for layers grown using standard continuous doping. As the δ-doping period was reduced from 25 to 5 nm, the p-GaN bulk resistivity decreased from 6.8 to 2.8 Ωcm. The p-layer resistivity rose with increasing Mg concentration independent of the doping scheme. For a similar average Mg concentration, however, continuous doping resulted in a lower resistivity compared to δ-doping. After optimization of the p-layer structure and contact fabrication process, a minimum specific contact resistance of 2.8 $m\Omega cm^2$ and a minimum resistivity of 1.57 Ωcm were achieved, surpassing previously reported N-polar p-GaN results.

Th1B5.5

09:45 AM

Wong (E-51)

Demonstration of the Highly Radiative Nature of Semi-Polar (20-21) High Al-content AlGaN Quantum Wells by Time-Resolved Photoluminescence

Chelsea Haughn and Greg Rupper (United States Army Research Laboratory, USA); Thomas Wunderer, Zhihong Yang and Noble Johnson (Palo Alto Research Center, USA); Michael Wraback and Gregory Garrett (US Army Research Lab, USA)

We used time-resolved photoluminescence to study high aluminum composition AlGaN multi-quantum wells grown on (20-21) AlN for deep UV emitters. Radiative recombination lifetimes of 80 ps were observed at low temperatures and are faster than the 3.5 ns lifetimes reported in similar semi-polar heterostructures in literature. Lifetimes are explained by an increase in wave function overlap due to a decrease in polarization field and is supported by modelling using non-equilibrium Green's function theory calculations. We compare our lifetimes in semi-polar AlGaN QWs to ultra-narrow QWs grown on c-plane AlN that were designed to reduce polarization fields and find improved lifetime and radiative efficiency and reduced localization at monolayer interfaces, suggesting moving to semi-polar growth would be advantageous for deep UV emitters.

Th1C5: Novel Materials & Devices

Time:	5/31/2018, 08:30 AM - 10:00 AM
Room:	Salon T (Samberg Conference Center, 7th floor)
Chair:	Susan Fullerton (University of Pittsburgh, United States)

Th1C5.1 **Transition Metal Dichalcogenide Memristors and Memtransistors**

08:30 AM *Mark Hersam (Northwestern University, USA)*

INVITED

Salon T

Layered two-dimensional (2D) transition metal dichalcogenides (TMDs) have emerged as leading candidates for next-generation semiconductor technologies. While most studies have exploited their traditional semiconductor characteristics, monolayer TMDs also possess defect structures that are potentially useful for emerging neuromorphic computing applications. In particular, previous studies have shown that the barrier to vacancy motion in monolayer TMDs is substantially lowered at grain boundaries. Since vacancies act as n-type dopants in TMDs, low barriers to vacancy motion suggest the possibility of reconfiguring the doping profile under modest nonequilibrium conditions. Indeed, early studies have revealed defect motion in polycrystalline monolayer MoS2 following the application of lateral electrical fields, resulting in memristive charge transport characteristics. The memristive response in polycrystalline monolayer MoS2 can also be modulated with a gate terminal, enabling the realization of hybrid memristor/transistor devices (i.e., memtransistors) that show promise as foundational circuit elements for neuromorphic computing.

Th1C5.2 **Efficient Learning with Ultra-low Power Compound Synaptic Devices**

09:00 AM *Huan Zhao (University of Southern California, USA); Ivan Sanchez Esqueda (University of Southern California; Information Sciences Institute, USA); Jing Guo and Zhipeng Dong (University of Florida, USA); Han Wang (University of Southern California, USA)*

Salon T

we designed compound synaptic devices based on ultrathin oxidized boron nitride (BNOx) binary synapses and demonstrated their efficiency programming through simulations. The BNOx compound synapse derives its advantages from the ultralow power consumption of individual BNOx synaptic device due to its ultimately thin geometry giving rise to pA level operating current. It can offer clear benefits over conventional synapses in terms of accuracy and power efficiency. The compound synapses could be promising for applications in synaptic learning network, low-power memory-centric computing, and neuromorphic computation in general.

Th1C5.3

09:15 AM

Salon T

A Gate Tunable Memristive Device Based on 2D Materials for Emulating Hetero-Synaptic Plasticity

Xiaodong Yan (University of Southern California, USA); Matthew Chin and Madan Dubey (Army Research Laboratory, USA); Han Wang (USC, USA)

Modulatory input-dependent plasticity is a common type of hetero-synaptic response where the efficacy of neuro-transmission in a nearby chemical synapse is modulated by the releasing of neuro-modulators. Solid-state devices that can mimic such plasticity are highly desirable for improving the functionality and reconfigurability of neuromorphic electronics. However, conventional Si based CMOS technology requires complex circuitry to mimic modulatory synaptic plasticity while most existing memristive synaptic devices does not offer such functionalities. In this work, we demonstrated a tunable artificial synaptic device concept based on the unique properties of graphene and tin oxide that can mimic the modulatory input-dependent plasticity.

Th1C5.4

09:30 AM

INVITED

Salon T

TBD

Andrea Ferrari (University of Cambridge, United Kingdom (Great Britain))

Abstract not available.

Th1D5: RF (Power)

Time:	5/31/2018, 08:30 AM - 10:00 AM
Room:	DR 5 & 6 (Samberg Conference Center, 6th floor)
Chair:	Srabanti Chowdhury (UC Davis, United States)

Th1D5.1

08:30 AM

DR 5 & 6

Impact of Traps on RF HEMT Linearity

Wenyuan Sun (the Ohio State University, USA); Jose Jimenez (Qorvo, USA); Aaron Arehart (The Ohio State University, USA)

In this work, the linearity of RF GaN HEMTs grown at two conditions are compared in terms of adjacent channel power ratio (ACPR) for both frequency and time division duplexing (FDD/TDD) and the traps responsible for the nonlinearities in each scheme is identified. Using constant drain current deep level transient spectroscopy (CID-DLTS), the trap energies and concentrations are characterized directly in HEMTs to determine their specific impact on threshold voltage instability and dynamic on-resistance. It is demonstrated that the EC-0.57 eV trap limits linearity in FDD applications where microsecond scale instabilities are most problematic while the EC-0.72 eV trap, with its millisecond range time constant, is most responsible for non-linearities in the TDD scheme. These results indicate that controlling specific trap concentrations for specific applications can result in better device linearity, so identifying the conditions that impact specific traps is important to further improve GaN HEMT linearity.

Th1D5.2

08:45 AM

DR 5 & 6

Influence of Fe- And C-doped Buffers on Microwave Output Power and Dynamic Effects in AlGaN/GaN HEMTs

Johan Bergsten, Sebastian Gustafsson, Mattias Thorsell and Niklas Rorsman (Chalmers University of Technology, Sweden)

In this paper the performance of Fe- and C-doped buffers in AlGaN/GaN HEMTs are evaluated with respect to DC-characteristics and dynamic effects. The dynamic behavior is evaluated using pulsed-IV, continuous wave load-pull (at 10 GHz) and pulsed-RF measurements (at 2 GHz). The devices behave similarly from a DC-perspective. However, under dynamic operation severe trapping in the C-doped buffer causes degraded performance compared to the Fe-doped devices. In load-pull measurements the output power was 2.0 and 4.8 W/mm for the C- and F-doped devices respectively. In pulsed-RF measurements these numbers were 2.7 and 7.9 W/mm. Even though the Fe-doped devices could supply a larger output power, both devices suffered from buffer trapping induced time dependent gain collapse after a large input power pulse. The results show that both technologies require further optimization before fully utilizing the potential of the AlGaN/GaN HEMT structure.

Th1D5.3 **AlxGa1-xN/AlN/GaN and DH- AlxGa1-xN/GaN HEMTs Threshold Voltage Model**

09:00 AM

DR 5 & 6

Wondwosen Muhea (Universitat Rovira i Virgili, Spain); Nawel Kermas (Universitat Rovira i Virgili, Algeria); Fetene Yigletu (Addis Ababa Institute of Technology, Ethiopia); Roger Cabré and Benjamín Iñiguez (Universitat Rovira i Virgili, Spain)

Physics-based models for the threshold voltage and Schottky barrier height of AlGaN/AlN/GaN HEMTs are presented. Assuming the condition of charge neutrality across the barrier (AlGAN) layer, analytical expression is derived for the Schottky barrier height and this further applied to develop threshold voltage model for the AlGAN/AlN/GaN device. The calculated threshold voltage is validated with the parameter value extracted from the static I-V transfer curve experimental data. In addition to this, we have incorporated the model in the DC-current model previously developed by our group and simulation of a AlGAN/AlN/GaN device I-V and gm-V characteristics is carried out and excellent agreement is obtained between model generated and experimental data. We have also adapted our previously developed current and threshold voltage models to double channel AlGaN/GaN HEMTs for the first time and the model is in good agreement with measurement data.

Th1D5.4 **N-polar GaN HEMTs Grown on Bulk GaN Using PAMBE for Highly Efficient Mm-Wave Power Amplifiers**

09:15 AM

DR 5 & 6

Shubhra S Pasayat (University of California Santa Barbara, USA); Elaheh Ahmadi (UC-Santa Barbara, USA); Brian Romanczyk, Onur Koksaldi and Anchal Agarwal (University of California Santa Barbara, USA); Matthew Guidry (University of California, Santa Barbara, USA); Chirag Gupta (University of California Santa Barbara, USA); Christian Wurm (University of California, Santa Barbara, USA); Stacia Keller and Umesh Mishra (UCSB, USA)

N-polar GaN-HEMTs grown on mis-cut foreign substrates by MOCVD have demonstrated outstanding performance for mm-wave power amplifiers. For high efficiency, the device is biased near the pinch off in class AB mode. For N-polar GaN HEMTs, a decrease in electron mobility is observed with a decrease in gate bias due to dislocation scattering and/or penetration of 2-DEG wave-function into the back barrier (due to thin AlN interlayer). In this work, using PAMBE, N-Polar GaN HEMTs were grown with thick AlN interlayer on on-axis bulk GaN substrates. Dispersion free, high current density over 1 A/mm and good small signal performance (fmax/fT = 14.6/8.9 GHz) was obtained for a device with 0.75µm gate length and 5µm source-drain spacing. A lower mobility decline rate (near pinch off compared to zero gate bias) was observed for these devices compared to conventional MOCVD grown N-Polar GaN-on-sapphire HEMTs. These results demonstrate potential for GaN-on-GaN N-Polar HEMTs.

Th1D5.5

09:30 AM

INVITED

DR 5 & 6

The Superlattice Castellated Field Effect Transistor (SLCFET): A Novel Low Loss, Broadband RF Switch Technology with an Fco Figure of Merit > 2THz

Robert Howell, Justin Parke, Ron Freitag, Ishan Wathuthanthri, Ken Nagamatsu, Josephine Chang, Eric Stewart and Shalini Gupta (Northrop Grumman, USA)

The unique device architecture of the SLCFET was engineered to solve the long standing limitation of FET RF switch performance, based on the insight that fringing capacitance fundamentally limits improvement in FET RF switch performance when applying traditional device scaling. However, this limitation can be overcome by using a superlattice to stack multiple 2DEG channel layers, providing a way to lower ON resistance without adversely impacting OFF capacitance. In order to control the charge in each of the 2DEG channels simultaneously, a three dimensional, castellated gate structure is used, resulting in a device structure that can be successfully scaled for improved Fco and RF switch performance.

Th2A6: Lasers

Time:	5/31/2018, 10:30 AM - 12:30 PM
Room:	Salon M (Samberg Conference Center, 7th floor)
Chair:	Claire Gmachl (Princeton University, United States); Javad Shabani (NYU, United States)

Th2A6.1 **Quantum Cascade Lasers on Metamorphic Buffer Layer**

10:30 AM *Arkadiy Lyakh (University of Central Florida, USA)*

INVITED

Salon M

Lasing for ridge-waveguide devices processed from a 40-stage quantum cascade laser structure grown on a 6-inch GaAs and Ge-coated Si substrates with a metamorphic buffer is reported. The 4.6μm structure used in the proof-of-concept experiment had a typical design, including an Al0.78In0.22As/In0.73Ga0.27As strain-balanced composition, with a high strain both in quantum wells and barriers, and an all-InP waveguide design with a total thickness of 8 μm. Surface morphology analysis suggests that laser performance can be significantly improved in both cases by reducing strain for the active region layers relative to InP bulk waveguide layers.

Th2A6.2 **Ultra-broadband Tunable InAs/InP Quantum Dot External Cavity Laser**

11:00 AM *Hui-Hong Yuan (Institute of Semiconductors, Chinese Academy of Sciences, P.R. China); Feng Gao (Institute of Semiconductors, Chinese Academy of Sciences, P.R. China); Tao Yang (Institute of Semiconductors, Chinese Academy of Sciences, P.R. China)*

Salon M

External cavity (EC) lasers based on quantum dot (QD) broad gain medium have shown its potentiality in various scientific fields including spectroscopic analysis, biomedical treatments and environmental monitoring. In particular, InAs/InP EC-QD lasers emitting around 1.55um are of great interest for fiber-optic data communication based on dense wavelength division multiplexing technology and coherent optical communication systems. In this work, we demonstrate an ultra-broadband tunable external cavity InAs/InP quantum dot laser, by applying chirped multiple quantum dot layers as the active region and optimizing the facet reflectivity. An ultra-broad tuning range of 221nm encompassing S-C-L bands is achieved under a relatively low pulsed current of 0.5A. Furthermore, the maximum tuning range under different currents reaches up to 239nm.

Th2A6.3 **Modal Shaping of Photonic Band-Tail States in Photonic Crystal Alloys**

11:15 AM *Myungjae Lee (Seoul National University, Korea); Ségolène Callard and Christian Seassal (Institut des Nanotechnologies de Lyon, France); Heonsu Jeon (Seoul National University, Korea)*

Salon M

It has been suggested theoretically that photons can be strongly localized in a disordered superlattice as a result of random but coherent multiple scatterings. These localized photon states are expected to exhibit spectro-spatial modal properties that are very similar to those of electronic band-tail states in a semiconductors system. Lately, we experimentally proved the existence of the so-called photonic band-tail states and also characterized their modal properties using a photonic crystal alloy system. In this study, we demonstrate that properties of the photonic band-tail states can be actively controlled, which include the number of lasing modes, lasing wavelength, spatial extent, and even shaping of modal profile. We expect that our band-tail lasers can lead to the semiconductor random lasers with novel properties and sophisticated functionalities required for the future photonic devices and systems.

Th2A6.4 **High Temperature Continuous-Wave Operation of Quantum-Dot Lasers on On-Axis Si (001) Substrate**

11:30 AM *Jinkwan Kwoen (The University of Tokyo, Japan); Bongyong Jang (University of Tokyo, Japan); Takeo Kageyama and Katsuyuki Watanabe (The University of Tokyo, Japan); Yasuhiko Arakawa (University of Tokyo, Japan)*

Salon M

Laser devices for silicon photonics are expected to be used in an integrated environment near CMOS devices. For this reason, quantum dot (QD) laser with excellent thermal properties has been considered a strong candidate for Si photonics light source. In the meantime, direct growth of QD lasers on Si (001) on-axis substrates is attracting attention due to the possibility of monolithic integration on a CMOS compatible wafer. In previous reports, 5 to 7 layer-stacked dot-in-well (DWELL) structure was used as the active layer and Be doping at QD capping layer was adopted for the high temperature operation. In this work, we report CW operation of an InAs/GaAs QD laser at the world's highest temperature of 101°C among any III-V lasers grown on Si (001) on-axis substrates. This highest temperature operation was attained by growing of 8 layer-stacked structure without the use Be-doping in the QD capping layers.

Th2A6.5 **Development of Si-based GeSn Laser**

11:45 AM *Shui-Qing Yu (University of Arkansas, USA)*

INVITED

Salon M

We demonstrated optically pumped GeSn lasers on Si with broad wavelength coverage from 2 to 3 μm. The growth mechanism of GeSn alloys using an industry standard chemical vapor deposition reactor was discussed. The maximum Sn composition of 17.5% was achieved. The highest lasing temperature was measured as 180 K.

Th2A6.6 **Ultrawide Strain-Tunable Light Emission from InGaAs Nanomembranes**

12:15 PM

Salon M

Xiaowei Wang (Boston University, USA); Xiaorui Cui (University of Wisconsin – Madison, USA); John Reno (Sandia National Laboratories, USA); Max Lagally (University of Wisconsin – Madison, USA); Roberto Paiella (Boston University, USA)

Wavelength-tunable semiconductor lasers are a key technology for several important application areas, including ultrahigh-bandwidth optical networks, data storage, spectroscopy and sensing. Currently, the operation of these devices typically relies on shifting the reflectivity spectrum of a grating mirror or external cavity, so that the resulting tuning range is necessarily limited to a fraction of the gain spectrum (e.g., several ten nm for near-infrared devices). Here we consider an alternative approach that could provide greatly enhanced tunability, based on the controlled introduction of strain in semiconductor nanomembranes (NMs) to shift the entire gain spectrum. By virtue of their nanoscale thicknesses, crystalline NMs can feature the flexibility of soft polymeric materials and thus sustain very large strain levels under external mechanical stress. Here we investigate light emission from mechanically stressed NMs based on In0.53Ga0.47As, and demonstrate a record-wide tuning range of over 200 nm.

Th2B6: Wide Band Gap (Nanostructures)

Time:	5/31/2018, 10:30 AM - 12:30 PM
Room:	Wong Auditorium (Building E-51)
Chair:	Jean-Christophe Harmand (Centre de Nanosciences et de Nanotechnologies, CNRS, France)

Th2B6.1

10:30 AM

Wong (E-51)

High Quality Single-Mode GaN Nanowire Laser Arrays for Nanophotonics and Nanometrology

Mahmoud Behzadirad (Center for High Technology Materials (CHTM), University of New Mexico (UNM), Albuquerque, NM, USA); Neal Wostbrock and Mohsen Nami (Center for High Technology Materials (CHTM), University of New Mexico (UNM), USA); Daniel Feezell (Center for High Technology Materials, University of New Mexico, USA); Steven Brueck (University of New Mexico, USA); Tito Busani (Center for High Technology Materials (CHTM), University of New Mexico (UNM), USA)

We present high optical quality GaN NW arrays fabricated using a cost-effective and scalable top-down approach tailored by interferometric lithography (IL). GaN NW arrays from 35 to 300 nm diameters and aspect-ratios from 10 to 50 have been fabricated with atomic-scale sidewall roughness (<1 nm). Using FDTD modeling, modal properties of different diameter NWs were studied and propagation of HE11 mode in a single-mode vertical-cavity NW was also studied. Theoretical modeling results reveal a strong relation between NW diameter and reflection of the mode during the round trip in the cavity. Single-mode lasing at ~366 nm with FWHM of 0.15 nm was observed in the experimental photoluminescence (PL) measurement of fabricated GaN NW arrays. We also present the first study and fabrication of GaN NW emitter as a tip for nanoscale atomic force microscopy (AFM) suitable for near-field scanning optical microscopy (NSOM) application.

Th2B6.2

10:45 AM

Wong (E-51)

Europium Doped GaN Nanocolumn Light-Emitting Diodes Exhibiting High Emission-Wavelength Stability

Hiroto Sekiguchi (Toyohashi University of Technology, Japan)

Europium-doped GaN has an advantage in sharp red luminescence and a stable emission wavelength. However, any increase in the Eu concentration would lead to degrade the crystal quality and a decrease in the emission efficiency. A GaN nanocolumn would be one of solution for improving its optical property. The optical properties of GaN:Eu nanocolumns and the fabrication of GaN:Eu nanocolumn LEDs are reported. GaN:Eu nanocolumns were grown on Si substrate by rf-MBE. Emission efficiency of nanocolumns showed high values in high Eu concentration range compared with that of thin film. Next, GaN:Eu nanocolumn LEDs were fabricated. A clear rectification characteristic and a sharp luminescence with a peak wavelength of 620 nm were observed. The peak wavelength shift was less than 0.2 nm with increasing the current from 1 to 20 mA. These result suggests that GaN:Eu nanocolumn LEDs have great potential for stable-wavelength optical devices.

Th2B6.3

11:00 AM

INVITED

Wong (E-51)

III-Nitride Nanostructures Grown by MBE: Basics and Applications

Enrique Calleja Pardo (Polytechnical University of Madrid, Spain)

Selective Area Growth (SAG) by Molecular Beam Epitaxy (MBE) is one of the best approaches to develop a variety of nanostructures on different substrates. Some basic aspects of SAG will be first addressed, referring to the initial stages of nano/microrod nucleation within the mask nano/microholes leading to a final stable hexagonal structure, the factors controlling the nano/microrod diameter in axial heterostructures, and the dislocation filtering efficiency as a function of the nano/microrod geometry. Applications such as nano-LEDs, Single Photon Emitters, nano-FETs and pseudo-substrates will be discussed.

Th2B6.4

11:30 AM

Wong (E-51)

STEM Study of Polarity and Inversion Domains in GaN Nanowires and AlN Buffer Layers

Alexana Roshko, Matthew Brubaker, Paul Blanchard, Todd Harvey and Kris Bertness (National Institute of Standards and Technology, USA)

We have used ABF imaging to investigate the influence of growth conditions on polarity of GaN nanowires and underlying AlN buffer layers deposited on Si(111) substrates by plasma assisted molecular beam epitaxy. Growths were initiated with AlN layers followed by AlN and/or GaN buffer layers. N-polar AlN buffers were found to have uniform polarity with some Al-polar IDs near the surface of thicker layers. GaN nanowires grown spontaneously on these buffers were also N-polar and some contained IDs, which propagated from the underlying AlN. In contrast, the Al-polar buffers were found to have mixed polarity. In these samples, the AlN layer at the Si substrate interface

was not Al-polar, but rather was uniformly N-polar. As the film thickness increased above 20 to 30 nm the polarity inverted.

Th2B6.5

11:45 AM

Wong (E-51)

GHz Bandwidth GaN/InGaN Core-Shell Nanowire-Based Micro-LEDs for High-Speed Visible Light-Communication

Mohsen Nami (Yale University, USA); Arman Rashidi (Center for High Technology Materials, University of New Mexico, USA); Morteza Monavarian (Center for High Technology Materials, The University of New Mexico, USA); Mostafa Peysokhan (University of New Mexico, USA); Ashwin Rishinaramangalam (Center for High Technology Materials, University of New Mexico, USA); Isaac Stricklin (University of New Mexico, USA); Igal Brener (Sandia National Laboratories, USA); Steven Brueck (University of New Mexico, USA); Daniel Feezell (Center for High Technology Materials, University of New Mexico, USA)

In this work, we present the first study of 3-dB modulation bandwidth and RF characteristics in GaN/InGaN core-shell nanowire-based LEDs. A micro-LED comprised of a 60 µm x 60 µm area of nanowires was fabricated. The LEDs were grown on c-plane GaN on sapphire using pulsed-mode selective-area MOCVD and consist of GaN cores with a diameter of 600 nm and a height of 1 µm. The GaN cores were surrounded by 4 pairs of m-plane InGaN quantum wells grown on the sidewalls of the nanowires, followed by ~200 nm of p-GaN, grown in continuous mode. The internal quantum efficiency (IQE) of the LED was measured using the conventional method of temperature-dependent integrated photoluminescence. An IQE of 62% was achieved, which is higher than previously reported nanowire-based LEDs. A 3-dB modulation bandwidth of 1.2 GHz was measured at a current density of 1 kA/cm^2, which is higher than all previously published planar c-plane LEDs. An equivalent small-signal electrical circuit for the LEDs was proposed and the related transfer function of the circuit was derived. Using this function, expressions for the input impedance and modulation response were obtained and a minimum differential carrier lifetime of 330 ps was determined.

Th2B6.6 **Optical Absorption and Passivation of Surface States in III-nitride Photonics**

12:00 PM

Wong (E-51)

Ian Rousseau and Gordon Callsen (Ecole Polytechnique Fédérale de Lausanne (EPFL), Switzerland); Jean-François Carlin (EPFL-LASPE, Switzerland); Raphaël Butté (Ecole Polytechnique Fédérale de Lausanne, Switzerland); Nicolas Grandjean (EPFL, Switzerland)

III-nitride surface states play an important role when device size is reduced due to increased surface-to-volume ratio. In our work, we show that optical losses of more than 100 cm^{-1} at 450 nm are induced by reversible photoinduced oxygen desorption from III-nitride microdisk resonators. Studies of whispering gallery modes in nominally identical doped and undoped microdisks suggest that the spectral changes originate at the III-nitride material surface rather than the space charge region. Finally, we show that oxygen passivation of the microdisk surface improves Q to state-of-the-art values exceeding 10,000 at 475 nm. These results indicate the relative strength of optical absorption by surface states in III-nitride devices and are of paramount importance for facet passivation in laser diodes and micro/nano-wire light-emitting diodes.

Th2B6.7 **Band Engineering of InGaN/GaN Multiple-Quantum-Well (MQW) Solar Cells**

12:15 PM

Wong (E-51)

Xuanqi Huang (Arizona State University, USA); Houqiang Fu (Arizona state University; Arizona State University, USA); Hong Chen, Izak Baranowski and Jossue Montes (Arizona State University, USA); Brendan Gunning and Dan Koleske (Sandia National Laboratories, USA); Yuji Zhao (Arizona state University, USA)

We have demonstrated high-performance InGaN multi-quantum-well (MQW) solar cells through the engineering of energy band structures with AlGaN layers. High Resolution X-Ray Diffraction measurement showed that high structural integrity was well maintained with AlGaN layers in solar cell structures. Time-resolved photoluminescence results illustrated that carrier lifetime increased by more than 40% in the structures with AlGaN layers compared with the reference, indicating improved carrier collection. The illuminated current-density (J-V) measurements further confirmed that the short-circuit current (Jsc) benefited most from this design and increased at least 46%. Furthermore, the power conversion efficiency (PCE) of the best device almost doubled over the reference structure and a more than 68% enhancement in PCE was demonstrated on average. Our results here therefore introduce a new design approach towards the goal of high-performance InGaN solar cells aiming for the integration with multijunction cells and specific applications beyond conventional materials.

Th2C6: Novel Materials & Devices

Time:	5/31/2018, 10:30 AM - 12:30 PM
Room:	Salon T (Samberg Conference Center, 7th floor)
Chair:	Christopher Hinkle (University of Texas at Dallas, United States)

Th2C6.1 **Growth and Electronic Properties of Heusler Epitaxial Thin Films**

10:30 AM *Chris Palmstrom (University of California Santa Barbara, USA)*

INVITED

Salon T

Heusler compounds are an exciting family of ternary intermetallics that can be composed of elements from a large fraction of the periodic table. Their electronic properties are predicted to depend on the number of valence electrons per formula unit. In general, Heusler compounds form two main variants: half-Heuslers (XYZ) with the C1b crystal structure and full-Heuslers (X2YZ) with the L21 crystal structure. They have been predicted and experimentally shown to exhibit novel electronic and magnetic properties, such as half-metallic ferromagnetism, semiconducting and superconducting. A number of half-Heusler compounds are predicted to be topological non-trivial insulators or semimetals and should display topological surface states, which would be useful for spintronic applications. In this presentation, I will emphasize the molecular beam epitaxial growth and properties of Heusler compounds grown on III-V semiconductors. Their application in spintronic devices will also be discussed.

Th2C6.2 **Optical Tuning of the Charge Carrier Type in InAs/GaSb Quantum Wells**

11:00 AM *Fabian Hartmann (University of Wuerzburg, Germany); Lukas Worschech (Universität Würzburg, Germany); Martin Kamp (Universität Wurzburg, Germany); Pierre Pfeffer (University of Wuerzburg, Germany); Sven Höfling (Universität Würzburg, Germany); Georg Knebl (University of Würzburg, Germany)*

Salon T

Here, we present a study on the optical tunability in InAs/GaSb double quantum wells with its typical type-II broken band alignment and inverted band structure. Under constant optical excitation, the majority charge carrier type switches from electron to hole. Within the majority charge carrier type transition, the coexisting minority charge carrier contribution indicates electron-hole hybridization with a non-trivial topological phase. The optical tuning is attributed to the negative photoconductivity of antimonide materials in combination with a persistent charge carrier build-up of photo generated charges at the surface and substrate side of the device, respectively. Our findings pave the way towards electro-optical applications utilizing InAs/GaSb double quantum wells.

Th2C6.3

11:15 AM

Salon T

Giant Enhancement in Sensitivity of GaAs MEMS Terahertz Bolometers by Coherent Internal Mode Coupling

Ya Zhang, Boqi Qiu, Naomi Nagai and Kazuhiko Hirakawa (University of Tokyo, Japan)

MEMS resonators are very attractive for sensing applications owing to their ultrahigh sensitivities. In this work, we report a giant enhancement in thermal responsivity (i.e., resonance frequency shift induced by heating) of the GaAs MEMS bolometer by internal mode coupling effect. We fabricated a GaAs doubly clamped MEMS beam resonator, using a modulation-doped AlGaAs/GaAs heterojunction. When the first bending mode is driven into the nonlinear Duffing oscillation regime and its resonance frequency is equal to 1/3 of the resonance frequency of a higher resonance mode, we observed an internal mode coupling due to the cubic-term nonlinearity. When a heat modulated at 550 Hz is applied to the resonator in the internal mode resonance condition, we have observed a giant enhancement in the thermal responsivity by ~60 times. We attribute this enhancement to the coherent energy transfer between the two strongly coupled MEMS oscillation modes. The observed effect can widely be applied to high-sensitivity sensing applications, particularly, to very high-sensitivity THz detection at room temperature.

Th2C6.4

11:30 AM

INVITED

Salon T

Pathways to Low Energy Control of Magnetism Using Multiferroics

John Heron (University of Michigan - Ann Arbor, USA)

In this talk, I will discuss two approaches toward the non-volatile, low-energy dissipation, switching of the magnetization with an applied electric field using fundamentally different magnetoelectric coupling in multiferroic heterostructures.

Th2C6.5

12:00 PM

Salon T

Room-Temperature Spin-Orbit Torque Switching Induced by a Topological Insulator

Jiahao Han (Massachusetts Institute of Technology, USA); Anthony Richardella (The Pennsylvania State University, USA); Saima Siddiqui and Joseph Finley (Massachusetts Institute of Technology, USA); Nitin Samarth (The Pennsylvania State University, USA); Luqiao Liu (Massachusetts Institute of Technology, USA)

The strongly spin-momentum coupled electronic states in topological insulators (TI) have been extensively pursued to realize efficient magnetic switching. However, previous studies show a large discrepancy of the charge-spin conversion efficiency. Moreover, current-induced magnetic switching with TI can only be observed at cryogenic temperatures. We report spin-orbit torque switching in a TI-ferrimagnet heterostructure with perpendicular magnetic anisotropy at room temperature. The obtained effective spin Hall angle of TI is substantially larger than the previously studied heavy metals. Our results demonstrate robust charge-spin conversion in TI and provide a direct avenue towards applicable TI-based spintronic devices.

Th2C6.6

12:15 PM

Salon T

Electronic Structure of Two-Dimensional Group-IV Chalcogenides Vertical Heterostructures

Hussain Alsalman (KACST; University of Minnesota Twin Cities, USA); Javad Azadani and Roberto Grassi (University of Minnesota Twin Cities, USA); Steven Koester and Tony Low (University of Minnesota, USA)

2D group-IV chalcogenides with formula MX (M= Sn, Ge, Si & X= S, Se, Te) have recently been a topic of great interest for their potential applications in the field of nanomechanics, catalysis, photovoltaics and energy storage. In this work, we will present a comprehensive density functional theory (DFT) calculation for vertical heterostructures of group-IV chalcogenides. The thirty six heterostructure combinations of this type of polymorph will be detailed along with emphasis on cases with significant findings. Our primarily results show that the two layers hybridize strongly, leading to drastic modification of the electronic bandstructure of the heterostructure. The electronic wavefunctions in the low energy lying bands are strongly mixed between the layers, suggesting that the new structure should be viewed as a new material instead of conventional heterostructure which retains distinct properties of its parent constituent.

Th2D6: Wide Band Gap (Ga_2O_3)

Time:	5/31/2018, 10:30 AM - 12:30 PM
Room:	DR 5 & 6 (Samberg Conference Center, 6th floor)
Chair:	Marko Tadjer (Naval Research Laboratory, United States)

Th2D6.1

10:30 AM

DR 5 & 6

A First Principles Approach on the Possibility of P-Type Ga_2O_3

Alexandros Kyrtsos, Masahiko Matsubara and Enrico Bellotti (Boston University, USA)

Ga_2O_3 has attracted much attention as a new wide bandgap semiconductor with various applications. However, the task to realize p-type material has proven challenging. In this work, various substitutional dopants are investigated for the possibility of p-type conductivity using density functional theory (DFT). Both standard DFT and hybrid functional calculations are performed in order to identify the positions of the (0/-) transition levels which are relevant for the p-type conductivity of the material. All the investigated dopants result in deep acceptor levels. In light of these results, we compare our findings with other wide bandgap oxides and examine the feasibility of p-type Ga_2O_3.

Th2D6.2

10:45 AM

DR 5 & 6

Analysis of Thermal Conductivity in Bulk and Thin-Film β-Ga_2O_3 Using Time-Domain Thermoreflectance (TDTR)

Jie Zhu, Sandhaya Koirala, Xuewang Wu and Yingying Zhang (University of Minnesota, Twin Cities, USA); Steven Koester (University of Minnesota, USA); Xiaojia Wang (University of Minnesota, Twin Cities, USA)

Over the past decade, monoclinic gallium oxide (β-Ga_2O_3) has emerged as an ultra-wide bandgap semiconductor of particular interest, due to its large bandgap which leads to a breakdown field much higher than conventional materials. However, β-Ga_2O_3 -based devices still have considerable challenges, particularly regarding thermal effects. Compared to other wide-bandgap materials, the thermal conductivity of β-Ga_2O_3 is nearly one order of magnitude lower than that of Si, GaN, and SiC. One possible approach to mitigate such thermal issues is to transfer thin-film β-Ga_2O_3 onto different substrates to improve heat dissipation. In this work, we use an ultrafast laser-based time-domain thermoreflectance technique to study the thermal conductivity of β-Ga_2O_3 single crystals, and thin films of β-Ga_2O_3 exfoliated from bulk single crystals and transferred onto different substrates. For bulk single crystals, we use a beam-offset method to map the anisotropic thermal conductivities of β-Ga_2O_3 along [102, [010] and ⊥(-201) crystalline orientations.

Th2D6.3

11:00 AM

DR 5 & 6

Novel p-Type Oxides of Corundum-Structured α-$(Rh,Ga)_2O_3$ and α-Ir_2O_3

Kentaro Kaneko, Shu Takemoto and Shin-ichi Kan (Kyoto University, Japan); Takashi Shinohe (FLOSFIA INC., Japan); Shizuo Fujita (Kyoto University, Japan)

Corundum-structured α-(Rh,Ga)2O3 and α-Ir_2O_3 thin films were fabricated on c-plane sapphire (α-Al_2O_3) substrates by mist CVD technique. Obtained thin films were single-phased and corundum-structured α-$(Rh,Ga)_2O_3$ and α-Ir_2O_3,respectively, which were determined from X-ray diffraction (XRD) profiles and electrical diffraction spots of cross-sectional transmission electron microscope (TEM) images. All the diffraction spots from the thin film are situated slightly inside of the sapphire substrate due to the difference of lattice constants, as well as the evidences of having a corundum structure for the thin film. The thin films showed p-type conductivities by Hall effect measurements. Besides the lattice mismatch between α-Ir2O3 and α-Ga_2O_3 was calculated as 0.3 % along a-axis. α-(Rh,Ga)2O3 and α-Ir2O3 are strong candidates for a p-type layer of α-Ga_2O_3 based bipolar devices.

Th2D6.4

11:15 AM

DR 5 & 6

Anisotropic Electrical Properties of Vertical β-Ga_2O_3 Schottky Barrier Diodes on Single-Crystal Substrates

Houqiang Fu (Arizona state University; Arizona State University, USA); Hong Chen, Xuanqi Huang, Izak Baranowski, Jossue Montes and Tsung-Han Yang (Arizona State University, USA); Yuji Zhao (Arizona state University, USA)

This work investigates the effect of crystalline anisotropy on the electrical properties of β-Ga_2O_3 electronics. Vertical (010) and (-201) β-Ga_2O_3 Schottky barrier diodes (SBDs) were fabricated on single-crystal substrates grown by the edge-defined film-fed growth (EFG) method, and their electrical properties such as temperature-dependent I-V and C-V characteristics were comprehensively measured and compared. At forward bias, the (010) SBD had a larger turn-on voltage and Schottky barrier height (SBH) than the (-201) SBD due to different surface properties such as Fermi level pinning and band bending. The difference in the electron mobilities results from the anisotropic electronic transport properties of β-Ga_2O_3 . At reverse bias, the (010) SBD showed a smaller leakage current and larger breakdown voltage due to its higher SBH. These results indicate the crystal orientation can significantly affect the electrical properties of β-Ga_2O_3 electronics.

Th2D6.5

11:30 AM

DR 5 & 6

β-Ga_2O_3 Nano-Membrane FETs on a Diamond Substrate

Jinhyun Noh, Sami Alajlouni, Mengwei Si and Hong Zhou (Purdue University, USA); Marko Tadjer (Naval Research Laboratory, USA); Ali Shakouri and Peide Ye (Purdue University, USA)

We have demonstrated top-gate nano-membrane β-Ga_2O_3 FETs on a high thermal conductivity diamond substrate. The devices exhibit enhanced performances with record high maximum ID of 980 mA/mm and 60% lower ΔT, compared to sapphire ones at the same consumed DC power conditions.

Th2D6.6

11:45 AM

DR 5 & 6

Enhancement-mode β-Ga_2O_3 Vertical Power Transistors with an Output Current of 750 a/cm^2 and Breakdown Voltage of 560 V

Zongyang Hu, Kazuki Nomoto, Wenshen Li and Nicholas Tanen (Cornell University, USA); Kohei Sasaki and Akito Kuramata (Novel Crystal Technology, Inc., Japan); Tohru Nakamura (Hosei University, Japan); Debdeep Jena and Huili Xing (Cornell University, USA)

Gallium Oxide is one of the most important new semiconductor materials for high-power applications. With an experimentally reported critical electric field up to 5.2 MV/cm, an electron mobility of 100-150 cm^2/Vs and low-cost high-quality substrates and epitaxial layers, β-Ga_2O_3 promises high-voltage and high-power devices with performance at least comparable to those of SiC and GaN. Various lateral channel Ga_2O_3 transistors have been reported in the past 5 years, however, development of vertical Ga_2O_3 transistors has just started since last year with limited successes. Wong et al. reported vertical MOSFETs with a buried current blacking layer (CBL) by ion implantation but with a weak gate modulation [1], We reported vertical FinFETs or MISFETs fabricated using bare Ga_2O_3 substrates with n~1×10^{17}cm^{-3}, achieving an Ion/Ioff of >109 and an output current >7 kA/cm^2; but, the high doping concentration led to normally-on operation and a breakdown voltage (BV) ~185 V in these transistors [2]. Sasaki et al. reported vertical trench MISFETs with an Ion/Ioff ~103 and an output current ~300 A/cm^2 but also with normally-on operation and a BV ~20 V [3]. In this work, we show the first high-performance vertical Ga_2O_3 power transistors. Enhancement mode (E-mode) with a threshold voltage (Vth) > 1.5 V, an output current >750 A/cm^2 and a breakdown voltage of >560 V are simultaneously achieved.

Th2D6.7 **'Electronics on Anything' Using Wide Bandgap Amorphous Oxide Semiconductors**

12:00 PM *Rebecca L Peterson, Christopher Allemang and Youngbae Son (University of Michigan, USA)*

INVITED

DR 5 & 6

Amorphous oxide semiconductors (AOS) such as indium gallium zinc oxide and zinc tin oxide are wide bandgap semiconductors with bandgaps of approximately 3eV. The spherical shape of the metal s-orbitals which form the conduction band causes crystalline and amorphous films to exhibit similar electron mobility of 10-20 $cm^2/V/s$. Recently, AOS thin film transistors have been widely commercialized for high resolution and large area display backplanes. Here, we describe our recent work to expand the range of applications for wide bandgap AOS. By realizing thin film power transistors and diodes, as well as memristors using wide bandgap amorphous zinc tin oxide, we are enabling future BEOL heterogeneous additive integration of thin film electronics or roll-to-roll manufacturing of large area electronics, to realize our future vision of "Electronics on Anything."

FRIDAY

6/1/2018

TECHNICAL PROGRAM

IPRM
Est. 1989

Cambridge / Boston, Massachusetts

CSW2018

2018
iSCS

Fr15PP-ND: Poster Session - Novel metarials and device physics

Time:	6/1/2018, 08:30 AM - 10:00 AM
Room:	Walker Memorial (Building 50-140)

Fr15PP-ND.1 **Development and Characterization of a MOVPE Technology for 2D Transition Metal Dichalcogenides**

Walker (50-140)

Annika Grundmann (RWTH Aachen, Germany); Matthias Marx (AIXTRON SE, Germany); Holger Kalisch and Andrei Vescan (RWTH Aachen, Germany); Dominik Andrzejewski (University Duisburg Essen, Germany); Tilmar Kümmell (University Duisburg-Essen, Germany); Gerd Bacher (Univerität Duisburg Essen, Germany); Michael Heuken (AIXTRON SE, Germany)

Metalorganic vapor phase epitaxy (MOVPE) is expected to be ideally suited for the deposition of MoS2 monolayers and heterostructures. Only little is known about the nucleation and film formation process, and dedicated MOCVD reactor technology is still lacking. Therefore, we developed MOVPE processes and technology, systematically investigating the impact of the epitaxial parameters on the nucleation process and lateral growth of 2D MoS2 on c-sapphire (0001) substrates. For MOVPE, an AIXTRON planetary hot-wall reactor in 10 × 2" configuration is employed. In order to investigate the temperature dependence of lateral growth, a 2-step process is introduced, with MoS2 nucleation occurring in step I and lateral growth of existing crystals in step II. In step II, the surface temperature is varied while the reactor pressure remains at 30 hPa. Investigations of the lateral growth in the 2-step process show the typical 3 MOVPE temperature-dependent growth regimes with a transport-limited regime between 785 °C and 905 °C.

Fr15PP-ND.2 **Properties of InP on Si Grown by Corrugated Epitaxial Lateral Overgrowth**

Walker (50-140)

Giriprasanth Omanakuttan (Royal Institute of Technology-KTH, Sweden); Oscar Martínez (University of Valladolid, Spain); Saulius Marcinkevicius and Tomás Uzdavinys (KTH Royal Institute of Technology, Sweden); Juan Jiménez (Unversity Valladolid, Spain); Sebastian Lourdudoss (Royal Institute of Technology, Sweden); Yan-Ting Sun (Royal Institute of Technology-KTH, Sweden)

High crystalline quality InP/Si with direct heterojunction is promising for photonic integration and high efficiency photovoltaics. Corrugated epitaxial lateral overgrowth (CELOG) has been developed to fabricate InP/Si with low dislocation density by hydride vapor phase epitaxy technology. In this work, the crystalline quality of CELOG InP/Si is investigated by low temperature cathodoluminescence. The impact of CELOG InP/Si crystalline quality on minority carrier lifetime is studied by time resolved photoluminescence. In the cross-section of CELOG InP/Si, a long carrier lifetime of 0.7 ns was observed near the InP/Si heterojunction with high crystalline quality, which is higher than 0.15 ns of conventional InP/Si direct heteroepitaxial layers and approaching

the value of 1.75 ns measured on InP layers homoepitaxially grown on a native InP substrate. Such high-crystalline quality CELOG InP/Si heterojunctions can be expected to facilitate the realization of high efficiency Si based multi-junction solar cell and photonic integrated circuits in near future.

Fr15PP-ND.3 **FastHall™: A Method to Measure Low Mobility Materials for Multi-Carrier Analysis**

Jeffrey Lindemuth (Lake Shore Cryotronics, USA)

Walker (50-140) The Hall effect is the primary method to measure carrier density, mobility and carrier type in materials. The most common method for measuring the Hall effect in semiconductors uses a DC magnetic field. The community has developed a well-defined protocol for removing spurious voltages in the measurement. Reversing the magnetic field and subtracting the measured voltages will remove any voltage that does not depend on the magnetic field. As research interest in studies of the transport mechanisms expands beyond semiconductors, with moderate to high mobility, the standard DC field method reaches its limit of applicability, of approximately 10 $cm^2/(V\ s)$. We present a new measurement protocol based on the reverse-field reciprocity theorem. This method is suited to measure low mobility material. It is a DC field method and generates data for multi-carrier analysis of low mobility material.

Fr15PP-ND.4 **Significant Conductivity Enhancement of Conductive PEDOT:PSS Films Through a Treatment with Formic Acid Method**

Walker (50-140)

Wen-Ray Chen (National Formosa University, Taiwan); Po-Hsun Hsu (National University of Kaohsiung, Taiwan); Pao-Hsun Huang (National Cheng-Kung University, Taiwan); Chien-Jung Huang (National University of Kaohsiung, Taiwan)

In this article, significant conductivity enhancement was observed on transparent and conductive PEDOT:PSS films after a treatment with formic acids. The PEDOT:PSS films showed excellent performance with a low sheet resistance of 35ohm/sq and 80.1% transparence without sacrificing its transparency and other electronic properties when PEDOTPSS films was treated with formic acid twice, immersion acid and dripping acid on surface. And we used the method of heating and stirring, which decrease the procedure time and instability of multilayer films, before spin-coating process to enhance the quality of monolayer film.

Fr15PP-ND.5 **In-situ ALD Annealing in Germanium-doped Contact Black Phosphorus Field-Effect Transistors**

Walker (50-140)

Kai-Lin Fan (National Taiwan University; Integrated Optical Electronic Device, Taiwan)

High performance BP FET is demonstrated by the annealing in ALD process to the Germanium doped BP S/D contact. The Ge-BP alloy Ohmic contact is formed and confirmed by the low temperuture mesurement. Ti-BP FET is fabricated and compared. ALD Al_2O_3 passivation in Ge-BP FET shows its facility and necessary for next generation MOSFETs.

Fr15PP-ND.6 **InSe Metal Contact Optimization for Enhanced InSe FET Performance**

Walker (50-140)

Badreyya AlShehhi (Masdar Institute, United Arab Emirates); Srinivasa Tamalampudi (Masdar Institute, USA); Irfan Saadat (Faculty - Masdar Institute of Science and Technology, United Arab Emirates); Ibraheem Almansouri (Masdar Institute of Science and Technology, United Arab Emirates)

It is important to investigate the properties of various metal contacts with InSe before integrate it into chemical sensor. In this work, we are investigating InSe's physical, optical and electrical properties. This includes tuning of the band gap by changing the flakes thickness. Also, exploring the metal/InSe contact space where the interaction of different metals with different thickness InSe films is studied to come up with optimum contact for the targeted application. This also includes integration and characterization of this material system as field-effect transistor (FET) device and as an optical sensor. Further, we are investigating the band gap varies with thickness and thickness dependent electrical characteristics of InSe FET device by choosing the different flake thickness ranges from 10 nm to 60 nm.

Fr15PP-ND.7 **3D Self-Consistent Quantum Transport Modeling for GaAs Gate-All-Around Nanowire Field-Effect Transistor with Scattering Effects**

Walker (50-140)

Han-Wei Hsiao and Yuh-Renn Wu (National Taiwan University, Taiwan)

As the gate length of metal-oxide-semiconductor field-effect transistors (MOSFETs) has been scaled down into the sub-10 nm regime, semi-classical Boltzmann transport theory can no longer accurately describe the behavior of electronic transport because of the dominant quantum mechanical effects. The non-equilibrium Green's function (NEGF) is a powerful and versatile theoretical framework, which has a wide range of applications for modeling nanostructure transport. We developed a three-dimensional quantum transport simulator based on solving the Schrodinger equation under NEGF method and Poisson equation self-consistently to study the characteristics of GaAs gate-all-around (GAA) nanowire FET in the presence of electron-phonon scattering, ionized impurity scattering, and surface roughness scattering effects. The phenomena of current spectrum broadening due to inelastic transition processes and the electrical properties including threshold voltage, ohmic, and saturation region can be captured by our

simulation. In addition, we also compare the results of NEGF-Poisson solver with the traditional drift-diffusion model.

Fr15PP-ND.8 **Ultrasonic Vibration Processing as Promising Methodology for Compound Semiconductor Defect Engineering: ZnCdTe Application**

Walker (50-140)

Valentina Korchnoy (Technion - Israel Institute of Technology, Israel); Michael Lisiansky (Tower Semiconductor Ltd, Israel); Alex Berner (Technion-Israel Institute of Technology, Israel)

Intrinsic defects and contaminations removal from the undoped p-type Cd0.96Zn0.04Te (CZT) single crystals has been achieved by the ultrasound vibration processing (UVP) at the room temperature. Surface analysis based on Auger Electron Spectroscopy, Energy Dispersive Spectroscopy, and Scanning Electron Spectroscopy shows a significant reconstruction of the crystal surface after processing, namely, the appearance of numerous "volcano craters" and triangle-shaped defects with a typical size of 0.2-5.0 µm. Elemental analysis of these defects shows that they are Te inclusions emerged on the surface. Distinct presence of copper is found in both the thin surface layer and in the defects emerged on the surface. The surface reconstruction is associated with a remarkable change in the bulk material properties, electrical (an increase in the resistivity by a factor of ~6) and optical (an IR transmittance increase). Ultrasonic processing purifies the whole CZT material from the small Te agglomerates (precipitates, associated defects) together with the contaminant (copper). UVP also extracts a part of inclusions mainly located in the layer adjacent to the surface (approximately, 30-50 µm thickness). Thereby, the starting material is released from the most harmful intrinsic defects that deteriorate the performance and reliability of the electronic devices. The proposed method, being low temperature and non-equilibrium, has significant benefits compare to the traditional high temperature annealing techniques used in nowadays practice.

Fr15PP-ND.9 **Reduction of Bismuth Segregation in GaAsBi/GaAs QWs Grown by MBE Using a Two-Substrate-Temperature Technique**

Walker (50-140)

Pallavi Patil, Fumitaro Ishikawa and Satoshi Shimomura (Ehime University, Japan); Esperanza Luna (Paul-Drude-Institut für Festkörperelektronik, Leibniz-Institut im Forschungsverbund Berlin, Germany)

In this work, we critically investigated the growth interruption time and manually/ automatic shutters control effect on the interfaces in GaAsBi QW structure growth using the two-substrate-temperature technique. For this study, high-resolution X-ray diffraction (HRXRD) and TEM techniques were used, with specific attention directed towards interface chemical diffusion caused by Bi segregation. We observed lateral irregularities in the QWs for the sample grown with manual shutter control operation with 5-10 min growth interruption. However, no extended defects were observed within the QWs for the sample grown with automatic shutter control and 5 min growth

interruption. Measurement of local Bi compositional profiles across the QW for samples using 002 dark-field imaging confirmed symmetric Bi distribution, with a significant decrease in Bi segregation due to the use of the two-substrate-temperature technique. These improvements positively reflect in the optical properties.

Fr15PP-ND.10 **Optical Polarization Switching in (20-21) InGaN Quantum Wells and Estimation of Deformation Potentials D5 and D6**

Walker (50-140)

Roy Chung and Gregory Garrett (US Army Research Lab, USA); Ryan Enck (US Army Research Laboratory, USA); Michael Wraback and Anand Sampath (US Army Research Lab, USA)

In this work, we discuss the optical polarization switching of InGaN (In content < 0.05) multiple quantum wells (MQWs) coherently grown on a partially relaxed AlGaN layer (Al content < 0.4) on a (20-21) GaN substrate. The strain state in the MQWs is controlled by the underlying AlGaN, allowing the strain components to change without changing In composition. The compositional inhomogeneity is also expected to be negligible at In content < 0.05. These conditions allow us to simplify the parameter space. Given the low In composition and weak shear strain, our k·p calculations suggest that the partial relaxation in AlGaN leads to the enhancement of strain along [10-1-4] relative to [11-20] in compressively strained InGaN QWs, raising the |Y>-like valence band faster than |X>-like valence band. The strain induced optical polarization switching could provide another experimental method to explore the deformation potentials, D5 and D6, in InGaN layer.

Fr15PP-ND.11 **Investigation of the Dynamic Characteristics of High Power p-GaN Gate AlGaN/GaN HEMTs**

Walker (50-140)

Shiou-Ming Wu, Indraneel Sanyal, Geng-Yen Lee and Jen-Inn Chyi (National Central University, Taiwan)

We investigate the dynamic I-V and C-V characteristics of commercial 650 V E-mode p-GaN Gate AlGaN/GaN HEMTs after the application of off-state drain bias stress or on-state gate bias stress. The device exhibits dynamic R_{on} being larger than unity after low off-state drain bias stress while less than unity after high off-state drain bias stress. It is found that the de-trapping process leads to a dynamic R_{on} ratio less than unity. A significant change in ΔVth due to different on-state gate stresses is observed. On-state stress below 7 V causes positive ΔVth, indicating negative charge trapping under the gate whereas, 7 V on-state stress results in a negative shift in threshold voltage, indicating a positive charge accumulation/trapping under the gate at the valence band of the p-GaN/AlGaN interface. This in-depth and systematic investigation of the dynamic behavior of p-GaN gate AlGaN/GaN pave the road to a broad understanding of device stability and reliability issues.

Fr15PP-ND.12 **Interplay Between Fabry-Pérot Resonance and Disorder Effect in Middle Mobility Quantum Point Contacts**

Walker (50-140)

Motoi Takahashi (Tohoku University, Japan)

The middle-mobility triple-gate quantum point contacts (QPCs) is a suitable system to study interplay between FP resonance and disorder effect. Disorder in the device results in conductance fluctuation without clear quantized characteristics at zero center gate bias (Vcg). However, FP resonance increases with increasing Vcg, whereas the disorder effect decreases with Vcg. The FP-like oscillations make dot-like structures in transconductance (dG/dVsg) plots. On the other hand, stripe-like structures are dominant in the disorder dominated regions. These studies suggest a possibility to separate FP oscillation from the disorder induced dot-like structures by using nonlinear dc transport characteristics in addition to the conventional transport measurements.

Fr15PP-ND.13 **Hall Effect and Magnetization Measurements of Cobalt (Co) Doped Zinc Oxide (ZnO) Polycrystalline Samples**

Walker (50-140)

Nelly Bautista (Fundación Universitaria Unipanamericana, Colombia); Elkin Giovanni Pineda Rojas and Álvaro Mariño Camargo (Universidad Nacional de Colombia, Colombia)

We reported on polycrystalline samples of cobalt (Co) doped Zinc Oxide (ZnO), $(ZnO)_{1-x}Co_x$ with different Co content $0.01 \leq x \leq 0.1$ prepared by solid state reaction method. The samples were annealed at 1100°C during two hours in order to reduce the resistivity of the samples (10^6 orders). X Ray Difraction (XRD) measurements indicates that the sample are free of secondary phases. No Co clusters were observed. Resistance and Hall effect measurements were carried out using Van Der Pauw geometry with a magnetic field of about 5000 Oe perpendicular to the surface of the samples. The carrier concentration increases by the Co concentration while the mobility of the carrier decreases. The magnetization measurements indicated that the carrier concentration would seem to be only one of the causes of ferromagnetism.

Fr15PP-ND.14 **Graphene-Metal Contact Optimization for Ballistic RF Transistor Application**

Nazir Hossain, Poorna Marthi, Jean Francois Millithaler and Martin Margala (University of Massachusetts Lowell, USA)

Walker (50-140)

Semiconductor researchers are attracted by Graphene for its extraordinary high carrier mobility exceeding 2×10^6 $cm^2/V\,s$, high saturation velocity= 5.5×10^7 cm/s, high current density ~1.6×10^9 $A\cdot cm^{-2}$, and higher mechanical strength with thickness of sub-nanometer regime. Graphene-based field effect devices are excellent candidates for the high frequency applications. The key factor to improve the graphene device performance for the high frequency electronics is reducing the contact resistance of the source and the drain which is responsible for the current saturation. TLM structure has been fabricated on SiO_2-based Graphene and measurements have provided as result a low contact resistance ~600 Ωμm and a resistivity ~$1.8x10^{-6}$ cm^{-2} for the single layer graphene on 100 x 200 μm contact pad and Transfer Length LT = 5.6 μm. It would be possible to reduce this contact resistance by accumulating the layer thickness of graphene.

Fr15PP-NS: Poster Session - Nanostructures

Time:	6/1/2018, 08:30 AM - 10:00 AM
Room:	Walker Memorial (Building 50-140)

Fr15PP-NS.1 **Low-to-mid Al Content AlInN Layers Deposited on Si(100) and Si(111) by RF Sputtering**

Walker (50-140)

Rodrigo Blasco and Arantzazu Nuñez-Cascajero (Univesidad de Alcala, Spain); Akhil Ajay and Eva Monroy (CEA-Grenoble, France); Sirona Valdueza (University of Alcala, Spain); Fernando Naranjo (Univesidad de Alcala, Spain)

Development of III-nitrides on silicon substrates has raised a lot interest, driven by the promise of merging the well-established low-cost Si technology with the exceptional properties of III-nitrides. Research on this field has mostly focused on (111)-oriented Si substrates, as this crystallographic plane shows hexagonal symmetry, which is compatible with the wurtzite structure of III-nitrides. However, the development of a nitride-on-Si(100) technology would be even more appealing since (100) is the conventional orientation in silicon electronic devices and solar cells. In this work we study the structural, morphological and optical properties of low-to-medium Al content AlInN thin films deposited on Si(100) and Si (111) by Radio frequency magnetron sputtering at low substrate temperature (300ºC) changing the RF power applied to the Al target. The layers present similar structural properties, with their morphology (compacity, surface roughness) improving for increasing Al composition, crystalline quality can be achieved on both substrates.

Fr15PP-NS.2 **Structural Characteristics of GaAs/GaAsBi Nanowires**

Walker (50-140)

Kosuke Yano and Kyohei Takada (Graduate Schoolof Science and Engineering, Ehime University, Japan); Pallavi Patil and Satoshi Shimomura (Ehime University, Japan); Yumiko Shimizu (Toray Research Center, Japan); Fumitaro Ishikawa (Ehime University, Japan)

We report the structural characteristics of GaAs/GaAsBi core-multi shell nanowires. Bi-containing GaAs nanowires showed specific morphological deformation compared to standard GaAs nanowires. The nanowires show corrugated surface morphologies in contrast to standard GaAs nanowire which should show sharp facets. From the cross-sectional observation, we can see clear formation of three-multi-layered core-shell structure. The longitudinal section showed characteristic contrast modulation. We observe a dark lines aligned parallel to the surface. The width of the line largely modulated, showing the width 1.8 nm and 9.2 nm at the thinnest and largest positions, respectively. The modulation should related to the accumulation of Bi elements, suggesting the formation of disc or dot like low-dimensional quantum structure. The modulation of Bi element presumably induced by large miscibility gap or large strain between GaAs and GaBi. That also induces the inter-diffusion of Bi elements to the inner core or outer shell.

Fr15PP-NS.3 **Growth and Photoluminescence Properties of InSb/GaSb Nano-Stripes Grown by Molecular Beam Epitaxy**

Walker (50-140)

Supeeranat Posri and Supachok Thainoi (Chulalongkorn University, Thailand); Suwit Kiravittaya (Naresuan University, Thailand); Aniwat Tandaechanurat (International School of Engineering (ISE), Chulalongkorn University, Thailand); Noppadon Nuntawong (NECTEC, Thailand); Suwat Sopitpan (Thai Microelectronics Center (TMEC), Thailand); Visittapong Yordsri (National Metal and Materials Technology Center, Thailand); Chanchana Thanachayanont (National Metal and Material Technology Center, Thailand); Songphol Kanjanachuchai, Somchai Ratanathammaphan and Somsak Panyakeow (Chulalongkorn University, Thailand)

InSb/GaSb nano-structures have continuously gained research interests because of their potential applications in infrared wavelength. Here, we report a successful realization of InSb/GaSb nano-stripe ensemble and its photoluminescence (PL) properties. Atomic force microscopy (AFM) of an uncapped InSb/GaSb sample shows that deposited InSb is formed into nano-stripes. Typical nano-stripe dimensions are 200-260 nm in length, 120-160 nm in width and 18-30 nm in height. Power-dependent and temperature-dependent PL spectroscopies of capped InSb/GaSb nano-stripes are conducted. Low-temperature PL peaks are observed at 1600 nm (0.78 eV), 1675-1700 nm (0.73-0.74 eV) and 1850 nm (0.67 eV) and they are attributed to the emission from GaSb substrate, InSb wetting layer (WL) and InSb nano-stripe ensemble, respectively. Intense PL signal without any signatures of crystal defects is observed. This work will enhance the utilization of InSb/GaSb in nano-photonic and opto-electronic applications.

Fr15PP-NS.4 **Grazing Incidence Small Angle X-Ray Scattering on a Laboratory Diffractometer for Measurement of Critical Dimensions in Periodic Nanostructure Arrays**

Walker (50-140)

Mike Hawkridge (Malvern Panalytical, USA); Lars Grieger (Malvern Panalytical, The Netherlands)

In recent years, there has been an increasing use of quantum confinement and coupling in arrayed nanostructures to produce new and improved performance in devices such as LED TV's and laser diodes. Engineering the behavior and characteristics of such devices requires careful control and therefore measurement of the critical dimensions. Techniques such as scanning probe microscopy provide sufficient precision at the surface, but dimensionality of buried structures can only be readily measured by electron microscopy techniques. While these methods are accurate and easy to interpret, they are also destructive, time consuming in terms of sample preparation and not necessarily representative of the entire sample. One method of measuring buried nanostructures that requires little sample preparation, is non-destructive and is more representative of the whole sample is grazing incidence small angle x-ray scattering (GI-SAXS). Here, we present GI-SAXS results obtained with a multipurpose laboratory diffractometer equipped with a sealed x-ray source from III-V semiconductor multi-layer quantum well and wire samples grown by molecular beam epitaxy techniques. The results are found to compare favorably to direct microscopy methods and demonstrate the applicability of laboratory based GI-SAXS to measurement of dimensions in periodic nanostructures.

Fr15PP-NS.5 **Native Oxide AlGaOx Outermost Shell for a Passivation Structure of GaAs-related Multi-Layered Nanowires**

Walker (50-140)

Naoki Tsuda (Graduate School of Science and Engineering, Ehime University, Japan); Fumitaro Ishikawa (Ehime University, Japan)

We report the growth and synthesis of passivated GaAs-related structure with outermost AlGaO layer formed by the atmospheric native oxidation.The growth of the GaAs-related nanowires were carried out with molecular beam epitaxy on the Si (111) substrate using vapor liquid solid growth mode with Ga self-catalyst. We grow GaAs/Al0.2Ga0.8As/GaAs/Al0.9Ga0.1As layers to form core-multishell structure, having the entire wire diameter about 180 nm. The Al0.2Ga0.8As layer was introduced as a passivation layer of the GaAs core. The outermost Al0.9 Ga0.1As layer was grown to form native oxide film. To form the native oxide, the wire was investigated after leaving the sample in the atmosphere for a certain time. We can see the formation of passivation layer of multi-layered Al0.2Ga0.8As shell. The outermost AlGaOx shell was transformed to amorphous from Al0.9Ga0.1As by the native oxidation. In contrast, the inside wires preserves single-crystalline structure.

Fr15PP-NS.6 **Molecular Beam Epitaxial Growth of GaInNAs Nanowires**

Walker (50-140)

Mitsuki Yukimune and Hiroya Ikeda (Graduate School of Science and Engineering, Ehime Univercsty, Japan); Ryo Fujiwara (Graduate School of Science and Engineering, Ehime University, Japan); Mattias Jansson, Weimin Chen and Irina Buyanova (Physics, Chemistry and Biology, Linköping University, Sweden); Fumitaro Ishikawa (Ehime University, Japan)

Quaternary GaInNAs is a material of interest due to its band gap tunability and a large conduction band offset with respect to GaAs. Here we report on the growth of GaAs/GaInNAs/GaAs core-multishell nanowires (NWs) by plasma-assisted molecular beam epitaxy using constituent Ga-induced vapor-liquid-solid growth on Si(111) substrates. The GaInNAs shell nominally contains 30% of In and 2% of N. The grown NWs are typically 3-5 µm long and have a diameter of about 400 nm on average. Cross sectional BF and HAADF-STEM images confirm existence of multi-layered shell structure. The nanowires preserve single crystalline structure without showing recognizable defects. EDX elemental mapping certificates the formation of GaAs/GaInNAs/GaAs core-multishell structure. The NWs exhibit a broad room temperature photoluminescence band at around 1.0 eV, which seems to be defect-related. The further optimizations of the NW structure and growth conditions will improve their optical quality, promising for future applications in nanoscale optoelectronics.

Fr15PP-NS.7 **Growth of GaNAs Nanowires with Nitrogen Concentration over 2Percent**

Walker (50-140)

Ryo Fujiwara (Graduate School of Science and Engineering, Ehime University, Japan); Hiroya Ikeda and Mitsuki Yukimune (Graduate School of Science and Engineering, Ehime Univercsty, Japan); Mattias Jansson, Weimin Chen and Irina Buyanova (Physics, Chemistry and Biology, Linköping University, Sweden); Fumitaro Ishikawa (Ehime University, Japan)

We report the growth of GaNAs nanowires having N concentration over 2%. We grew GaAs/GaNAs/GaAs core-multishell nanowires by plasma-assisted molecular beam epitaxy using constituent Ga-induced vapor-liquid-solid growth on Si(111) substrates. The GaNAs shell nominally contains 0%, 2%, and 3% of nitrogen. A cross sectional bright-field STEM image confirms the existence of core-multishell layers by the dark contrast in the middle of the wire shell. EDX investigations reveal the existence of nitrogen in the middle shell. This indicates the formation of the GaAs core, GaNAs shell, and GaAs outermost shell. From the performed room temperature µ-photoluminescence (PL) measurements, the sample without nitrogen shows a PL peak at 1.41 eV, at the bandgap of GaAs. On the other hand, the PL emission in N-containing structures is shifted to 1.14 eV and 0.95 eV, for the samples nominally containing 2 and 3%, respectively, as expected because of the bandgap bowing effect.

Fr15PP-NS.8 **Morphological Evolution in CdS Thin Films from Flowers to Reef like Structures**

Nupur Saxena and Tania Kallsi (Central University of Jammu, India); Pragati Kumar (Central University of Jammu (CUJ), Jammu, India)

Walker (50-140)

Surface morphological evolution is observed in thermally activated nanocrystalline CdS (nc-CdS) thin films. The chemical bath deposited nc-CdS thin films show flower like structures on micro-crack background. Thermal annealing of nc-CdS thin films at different temperatures viz. 300, 350, 400 and 450 C for 3 hours in Ar ambient developed surface morphology towards reef like structures with clear particle boundaries at higher temperatures. Besides, structural phase transition from zinc blende (cubic) to wurtzite (hexagonal) is observed, at 350 C in nc-CdS thin films. It is observed that on increasing the annealing temperature longitudinal optical phonon Raman mode shifts toward higher frequency side in either of the crystal structure and bandgap reduces. Photoluminescence study illustrates thermally activated enhancement in green emission and disappearance of yellow and red emission in both the structures. The enhancement in green emission is very high in hexagonal phase as compared to cubic phase.

Fr15PP-NS.9 **Investigations of Light Polarization of GaAs/AlGaOx Nanowire**

Jun Natsui (Graduate School of Science and Engineering, Ehime University, Japan); Naoki Yamamoto (Tokyo Institute of Technology, Japan); Fumitaro Ishikawa (Ehime University, Japan)

Walker (50-140)

We investigate the further detailed optical properties of individual GaAs/AlGaOx nanowire focusing on its characteristic light polarization. We fabricate oxide heterostructure nanowire by selective wet oxidation of GaAs/AlGaAs core-shell type nanowire grown on Si substrate. Applying adequate oxidation condition, we obtain GaAs/AlGaOx nanowire. The optical characteristics of the nanowires were investigated by cathodoluminescence using a scanning transmission electron microscopy combined with a light detection system, allowing selective detection of light emitted in a specific direction with desired polarization. Cathodoluminescence photon mapping images show strong light polarization for the polarizations parallel to the nanowire axis at wavelengths between 330 nm and 750 nm. The wire show polarization degrees about 40-50% over the entire visible wavelengths. Hence, the wire may have applications to polarized light sources.

Fr15PP-NS.10 **Theoretical Study of Nucleation and Growth of in Nanostructures During Droplet Epitaxy on Patterned GaAs Substrates**

Walker (50-140)

Sergey Balakirev, Maxim Solodovnik, Mikhail Eremenko, Ilya Mikhaylin and Oleg Ageev (Southern Federal University, Russia)

In this work, kinetic Monte Carlo model based on the analytical nucleation theory is used to describe the processes of droplet epitaxy of In on the patterned GaAs substrates. The simulation results demonstrate that the formation of nanostructures on the As-stabilized surface is accompanied by the initial formation of the wetting layer whereas it is almost completely prevented on the Ga-stabilized surface. Due to the large diffusion length of In adatoms, holes on the substrate are filled completely over a wide range of growth rates and temperatures. However, as the growth rate increases and/or the substrate temperature decreases on the As-stabilized surface, the probability of formation of nanostructures outside the holes and at their boundaries increases. On the substrates with triangular-shaped holes, formation of the wetting layer is observed on the walls whereas on the side walls of rectangular holes the wetting layer does not form.

Fr15PP-NS.11 **Droplet Epitaxy of in/algaas Nanostructures**

Walker (50-140)

Maxim Solodovnik, Sergey Balakirev, Mikhail Eremenko, Ilya Mikhaylin and Oleg Ageev (Southern Federal University, Russia)

The influence of the composition of the epitaxial layer and the main control parameters of the droplet epitaxy process on the morphological and structural characteristics of self-organized In/AlGaAs droplet arrays was studied. The results of experimental studies of the In/AlGaAs system showed a significant difference from the results for Ga/AlGaAs. An increase in the Al content in the epitaxial layer significantly changes the kinetics of the growth processes. At growth temperatures below 200°C, an increase in the Al content leads to an increase in the droplet density, with an approximate unchanging of their sizes. An increase in the growth temperature up to 300°C leads to an increase in the size of the droplets with an increase in the Al content. The range of variation in the density of arrays also tends to expand as the Al content in the surface epitaxial layer increases.

Fr15PP-NS.12 **Self-Formation of InAs Quantum Dots on Oxide/Semiconductor Substrates by Molecular Beam Deposition**

Walker (50-140)

Koichi Yamaguchi, Akinori Makaino, Katsuyoshi Sakamoto and Tomah Sogabe (The University of Electro-Communications, Japan)

Self-assembled quantum dots (QDs) on oxide/semiconductor substrates have much attractive potential for applications of optoelectronic QD devices. We demonstrate the fabrication of InAs QDs on SiO_2/Si and SiOx/GaAs substrates by molecular beam deposition (MBD). Individual InAs dots with a single crystal grain were deposited separately on the oxide film by precisely adjusting the growth condition. InAs dots were spontaneously formed by a Volmer-Weber mode growth. The dot density was

$1.5\sim3.0\times10^{11}$ cm^{-2}, and the dot size was smaller than a de Broglie wavelength. From the theoretical calculation of QD quantum levels in vacuum/InAs QD/SiO_2 structure, observed photoluminescence peaks could be assigned by QD transitions based on the ground state (GS) of heavy hole (hh), the GS of light hole and the first excited state (ES) of hh. The MBD of semiconductor QDs on oxide/semiconductor substrates is a promising method to further extend QD device applications.

Fr15PP-NS.13 **Study of Strain and Energy Profile in InAs Quantum Dot-In-A-Well Heterostructure with InGaAs, InAlGaAs and GaAsN Matrix**

Walker (50-140) *Jhuma Saha, Debi Panda, Mahitosh Biswas and Debabrata Das (Indian Institute of Technology Bombay, India); Subhananda Chakrabarti (Center for Excellence in Nanoelectronics, IIT Bombay, India)*

The optical properties of InAs quantum dot-in-well structures with three different well matrix have been investigated. The matrix elements are InGaAs, InAlGaAs, and GaAsN. The photoluminescence emission peak has been validated from the simulated structures with their corresponding experimental values. The hydrostatic and biaxial strain along with the electron and whole eigen states have been computed and compared for the three heterostructures. The DWELL heterostructure with GaAsN matrix offers the longest PL peak of 1.4 μm, as it acts as a strain compensating layer. It also has a better strain minimization inside the dots, compared to other matrix elements. Hence, the optimum structure can be useful for LASER fabrication which will be applicable for optical communication.

Fr15PP-NS.14 **Impact of Nitrogen Content on Strain and Photoluminescence of GaAs1-xNx Capped InAs Quantum Dots**

Walker (50-140) *Debi Panda, Jhuma Saha, Mahitosh Biswas and Debabrata Das (Indian Institute of Technology Bombay, India); Subhananda Chakrabarti (Center for Excellence in Nanoelectronics, IIT Bombay, India)*

Effect of nitrogen content on the strain and photoluminescence emission wavelength of InAs quantum dots (QDs) has been investigated. The InAs QD has been capped with 4 nm GaAsN followed by 50 nm GaAs layer, where nitrogen composition was varied from 0% to 2.5%. The simulated results have been verified by the reported experimental record, with an error of less than 2%. The PL peak has been red-shifted with higher nitrogen content, as it minimizes the lattice disparity and modulates the strain inside the QD heterostructure. Capping of GaAsN with 2.2% and 2.5% nitrogen provides room temperature PL peak near to the optical communication wavelength (i. e. 1.5 μm). This may be attributed to significant strain relaxation throughout the QD heterostructure. Thus, the enhanced properties of GaAsN capped InAs QDs with 2.2 or 2.5 % nitrogen content can make them suitable for infrared photodetection and lasing applications.

Fr15PP-NS.15 **Hybrid InAs Stranski-Krastanov and Submonolayer Quantum Dot Solar Cell: Towards Enhanced IR Harvesting**

Walker (50-140)

Debabrata Das, Debi Panda, Jhuma Saha and Vinayak Chavan (Indian Institute of Technology Bombay, India); Subhananda Chakrabarti (Center for Excellence in Nanoelectronics, IIT Bombay, India)

Here, we are introducing heterogeneously coupled SK on SML QD heterostructure. This hybrid heterostructure has a potential to provide inter dot electronic coupling with reduced amount of cumulative strain. Additionally, it may provide better photon absorption efficiency, higher carrier lifetime with optimized dot density and size distribution. All of these features are profitable for the application of photovoltaic energy conversion. Till now none of the research groups have reported this hybrid quantum dot solar cell (QDSC). Very few reports are there, which investigate this new configuration thoroughly. Here we compare a conventional QDSC with this hybrid QDSC. Photoluminescence and photoluminescence excitation spectroscopy shows the signature of inter dot carrier transition. The improvement in NIR energy conversion efficiency is validated through external quantum efficiency measurement.

Fr15PP-NS.16 **Vertical Arrangement of InGaAs / GaAs (Sb) Quantum Dots with AlGaAsSb Insertion Layer in Solar Cell Device**

Walker (50-140)

Wei-Sheng Liu (Department of Photonics Engineering, Yuan Ze University, Taiwan); Shao-Yang Lin, Ren-Yo Liu and Hsiao-Chien Lin (University of Yuan Ze, Taiwan)

In order to enhance the short-circuit current density of GaAs-based solar cells, vertically aligned InGaAs quantum dots have been investigated to form intermediate bands (IBs) that can absorb photons with energies lowered than the GaAs energy band gap. To develop a high performance QD-IBSC, the formation of an IB through vertically coupled QD layers is necessary. Three QD-IBSCs were grown by using a Riber 32P solid-source molecular beam epitaxy system. This study manifested a highly stacked vertically aligned InGaAs/GaAs(Sb) quantum dot (QD) structure without finding crystal dislocation in the cross-sectional TEM images. In addition, the improved dot-size uniformity with reduced dot size deviation by capping GaAsSb layer on InGaAs QDs was observed. The results of this study clarify the material quality of columnar QD structures and performances of QD-IBSC devices. These improvements make the proposed InGaAs/GaAs(Sb)/AlGaAsSb QD structure the promising candidate for improving the performances of IBSC devices.

Fr15PP-NS.17 **Alternative Approached to Extend the Emission Spectrum in Coupled Multilayer QDs Structure by Using GaAs Capping Layer**

Walker (50-140)

Binita Tongbram (Indian Institute of Technology Bombay, India); Subhananda Chakrabarti (Center for Excellence in Nanoelectronics, IIT Bombay, India)

We investigate the effect of GaAs capping layer thickness on coupled InAs/GaAs QD structures through the insertion of an additional 2.5-ML QD seed layer with a fixed GaAs spacer of 8.5 nm in ten-period-stacked coupled multilayer heterostructures with a 2.1-

ML InAs active layer. The GaAs capping layer was 10-nm thick in Sample A and 12-nm thick in Sample B. The proposed structures are characterised by temperature-dependent PL measurements and in-plane high-resolution X-ray diffraction (HRXRD). Low-temperature (19 K) PL measurements for the GaAs-capped sample were conducted. A large (110 nm) redshift was observed on extending the capping layer thickness from 10 nm (Sample A) to 12 nm (Sample B). The ground state PL peak was at 1092 and 1202 nm for Samples A and B, respectively. We found that the use of a 12-nm GaAs capping layer in coupled multistacked structures yields substantial advantages such as strong quantum confinement, narrow FWHM, and high crystalline quality.

Fr15PP-NS.18 **Multiple Stacking of Capping Temperature-Controlled InAs/GaAs Quantum Dots with AlGaAs Barrier Layers for Broadband Emission**

Toshiyuki Kaizu, Takaaki Koike and Takashi Kita (Kobe University, Japan)

Walker (50-140)

We fabricated five-layer stacked InAs quantum dots (QDs) with different capping temperatures for broadband emission, in which each QD layer was sandwiched by AlGaAs barrier layers. The photoluminescence (PL) spectrum exhibited multiple peaks originating from the capping temperature-controlled QDs, and the broadband emission with a linewidth of ~166 nm was achieved at room temperature owing to a suppression of the thermal carrier escape from small QDs with high capping temperatures. Moreover, the axial resolution in air when using the five-layer stacked QDs with the barrier layers as a light source in an OCT system was estimated to be ~6.0 μm from the Fourier transformed spectrum of the PL spectrum.

Fr15PP-NS.19 **HSQ Etching Resistance Dependence on Substrate**

Jie Zhang, Kazy Shariar and Yuping Zeng (University of Delaware, USA)

Walker (50-140) This work demonstrates the substrate effects on the etching resistance of HSQ. Bulk GaSb substrate and Si substrate with 260 nm thermally grown oxide layer are utilized. Three samples are characterized (respectively labelled with A, B, C). Square patterns of 100 μm× 100 μm are respectively formed on GaSb substrate (Sample A) and Si/SiO_2 substrate (Sample B). Sample C is bare Si/SiO_2 substrate with no HSQ pattern.All the three samples undergo inductively coupled plasma (ICP) dry etching process for 20 s. Sample A is then dipped into diluted HF solution for 2 mins to strip the remaining HSQ resist. Sample C is measured by ellipsometer before and after dry etching.The thicknesses of HSQ resist for each square on sample A and B at each step are examined by surface profilometer. It can be concluded almost no HSQ are etched away on Si/SiO_2 substrate and etching depth of HSQ is ~70nm on GaSb substrate.

Fr15PP-NS.20 **Effect of Bis(trifluoromethane) Sulfonimide (Super Acid) Treatment on Electrical Properties of InAs Nano Ribbons**

Walker (50-140) *Kazy Shariar, Jie Zhang, Zijian Wang, Robert Opila and Yuping Zeng (University of Delaware, USA)*

In this work, we report the first ever surface treatment of InAs using Bis(trifluoromethane) sulfonimide (Super Acid) and its effect on the electrical properties of InAs. The electrical properties were measured using TLM structures. TLM structures were made on MBE grown InAs epitaxially transferred to Si/SiO_2 surface. E-beam lithography was used to make uniform 4-micron width ribbon and open the contact pad area. E-beam evaporation was used for metal deposition. Kelvin measurements were done using HP4156 parameter analyzer and Kelvin probes. TLM measurements were done before any treatment of the sample, after Bis(trifluoromethane) sulfonimide (Super Acid) treatment and removal of SA using IPA. The results show that linearity of resistance changes after SA treatment. XPS study was done to identify the reason for changing the linearity of the resistance.

Fr15PP-NS.21 **Theoretical Investigations for Surface Reconstructions of Submonolayer InAs Grown on GaAs(001)**

Walker (50-140) *Tomonori Ito, Toru Akiyama, Kohji Nakamura and Abdul-Muizz Pradipto (Mie University, Japan)*

Surface reconstructions of submonolayer InAs grown on GaAs(001) crucial for quantum dot formation are systematically investigated using ab initio calculations. The calculated surface formation energies suggest that the surface reconstructions change from the (4×3) to the (2×4) surfaces via a newly found c(4×4) with two In-As and one As dimers. Despite the lattice mismatch favouring the (4×3), the (4×3) with two In-As and one As dimers is less stable than the c(4×4) with the same dimer constituents. This gives one possible interpretation for the complexity not only of the reconstructions but also of the growth processes at submonolayer InAs where the (2×4) domain with InAs coverage θ =1.33 monolayer (ML) coexists with the (4×3) even at θ = 0.76 ML and the InAs growth dose not proceed on the (4×3) beyond θ = 0.96.

Fr15PP-NS.22 **A Hydrogen-free ICP Etch of Indium Phosphide Using Chlorine/Argon Chemistry**

Walker (50-140) *Katie Hore and Zhanxiang Zhao (Oxford Instruments Plasma Technology, United Kingdom (Great Britain)); Ligang Deng (Oxford Instruments & Plasma Technology, United Kingdom (Great Britain)); Mark McNie (Oxford Instruments Plasma Technology, United Kingdom (Great Britain))*

A hydrogen-free ICP etch of InP and InP-related materials using argon-diluted chlorine has been developed. The process has a good selectivity to a SiO_2 mask and produces high-quality etched surfaces. Good control of substrate temperature is important for surface quality and profile control. The process can also be used to etch InGaAs and aluminum-containing materials. Marathon runs have proved the process gives a repeatable etch rate and exceeds the target of 425 μm etching of InP between cleans. Endpointing further enables variations in nominal layer thickness and/or run-run etch rate to be eliminated.

Fr15PP-Opt: Poster Session - Optoelectronics

Time:	6/1/2018, 08:30 AM - 10:00 AM
Room:	Walker Memorial (Building 50-140)

Fr15PP-Opt.1 **Metamorphic InGaAs Avalanche Photodiodes Towards mid-IR on InP**

Walker (50-140)

Yingjie Ma (Shanghai Institute of Microsystem and Information Technology, P.R. China); Yi Gu (Shanghai Institute of Microsystem and Information Technology, Chinese Academy of Sciences, P.R. China); Xingyou Chen (Shanghai Institute of Microsystem and Information Technology, P.R. China); Yanhui Shi (Shanghai Institute of Microsystem and Information Technology, USA); Wanyan Ji, Ben Du and Yonggang Zhang (Shanghai Institute of Microsystem and Information Technology, P.R. China)

Enhanced performances for metamorphic InGaAs separated absorber and multiplication (SAM) avalanche photodiodes towards mid-IR on InP are realized by conducting extensive exploration on the electric field and energy band engineering. Inverted doping of n-4×10^{15} cm^{-3} in a thicker multiplier are utilized to lower the peak electric field, leading to two orders of magnitude lower dark current density down to 4.8×10-5 A/cm^{-2} in comparison to that for our previous device. A thicker linearly-graded InxGa1-xAs layer up to 1 µm is introduced to lower the residual dislocation defects. Further reduced dark currents as well as increased gain factors are achieved simultaneously. Based on such optimized metamorphic APD structure, longer cutoff wavelengths up to 2.6 µm with an In0.83Ga0.27As absorber is also demonstrated. In addition, a versatile digitally-graded metamorphic buffer structure consisting of alternated multilayers of In0.52Al0.48As and In0.82Al0.18As on InP is also proposed to mitigate the dislocation deficiencies.

Fr15PP-Opt.2 **Doping Engineering of Extended Wavelength InGaAs Photodetectors**

Walker (50-140)

Xingyou Chen (Shanghai Institute of Microsystem and Information Technology, P.R. China); Yi Gu (Shanghai Institute of Microsystem and Information Technology, Chinese Academy of Sciences, P.R. China); Yingjie Ma and Ben Du (Shanghai Institute of Microsystem and Information Technology, P.R. China); Yanhui Shi (Shanghai Institute of Microsystem and Information Technology, USA); Yonggang Zhang (Shanghai Institute of Microsystem and Information Technology, P.R. China)

Wavelength-extended In0.83Ga0.17As PIN photodetectors with 8×10^{15} and 4×10^{16} cm^{-3} doped absorption layers were grown by gas source molecular beam epitaxy and demonstrated. Dark current mechanisms were analyzed according to current-voltage curves at different temperatures and bias voltages. Results displayed that they showed comparable device performance around room temperature and low bias voltage, but relatively large difference at lower temperatures and higher bias voltages. The 4×10^{16} cm^{-3} doped In0.83Ga0.17As photodetector showed comparable performance near room temperatures but inferior performance at lower temperatures with respect to the 8×10^{15} cm^{-3} doped one. With a higher doped absorber in the photodetector, though the

generation-recombination dark current was suppressed by the narrower depletion region, but the trap-assisted tunneling dark current increased more quickly at low temperatures and relatively high reverse bias voltages due to a higher trap density.

Fr15PP-Opt.3 **Towards the Monolithic Integration of GaSb Solar Cells on Si**

Julie Tournet and Yves Rouillard (University of Montpellier, CNRS, France); Eric Tournié (Université de Montpellier, France)

Walker (50-140)

We report on the first growth and processing of a GaSb single junction solar cell on a Si subtrate. A GaSb-on-GaSb homoepitaxial cell was first developed to serve as a reference. This cell overcomed the state-of-the-art for GaSb solar cells with a record efficiency of 5.9 % under AM1.5g. The manufacturing procedure had to be adapted for the GaSb-on-Si heteroepitaxial cell in order to circumvent the high defect density at the GaSb/Si interface. The direct growth and new fabrication procedures will be presented. Preliminary measurements show an efficiency of 0.6 % for the GaSb-on-Si heteroepitaxial cell. Although significantly reduced, this result compares favorably to the most recent advancements on GaSb-on-GaAs heteroepitaxial cells. Updated progress will be discussed at the conference.

Fr15PP-Opt.4 **Growth and Material Characterizations of Type-II InAs/GaSb Superlattice**

Marie Delmas and Yaksh Rawal (Cardiff University, United Kingdom (Great Britain)); Baolai Liang (University of California, Los Angeles, USA); Diana Huffaker (Cardiff University, United Kingdom (Great Britain))

Walker (50-140)

The growth by molecular beam epitaxy of Type-II InAs/GaSb superlattice will be presented. In particular, we studied the shutter sequences at the GaSb-on-InAs and InAs-on-GaSb interfaces in order to compensate the tensile strain of InAs with GaSb. Both Sb-soak and migration enhanced epitaxy method have been investigated and their influence on structural and optical properties analyzed. Device structures (pin photodiodes) have then been grown using the optimized shutter sequence and their electrical performances evaluated.

Fr15PP-Opt.5 **InP-based Solar Cells Integrated on Si for High Efficiency Low Cost PV**

Walker (50-140)

Stefano Soresi, Claire Besançon and Nicolas Vaissiere (III-V Lab, France); Gwénaëlle Hamon (Total S.A. Renewables, France); Alexandre Larrue (III-V Lab, France); José Alvarez (GeePs CentraleSupélec, France); Mickael Martin and Thierry Barron (LTM CNRS, CEA, France); Jean Decobert (Alcatel-Thales III-V Lab, France)

Most of the current photovoltaic efficiency world records are obtained with III-V single- and multi-junction devices. Direct heteroepitaxy of such devices onto Si substrates is a promising way to reduce their high cost, keeping their manufacturing process sustainable for industry. We present all the building blocks of a dual junction cell lattice matched on InP and integrated on a Si substrate via MOVPE. The top cell has a 1.34 eV bandgap InP absorber layer and presents a conversion efficiency of 11.7% under 1 sun concentration. By combining it with a In0.53Ga0.47As bottom cell, it is possible to obtain a high efficiency tandem device. The tunneling of the photogenerated carriers is guaranteed by a high efficiency (JPeak of 1000 A/cm^2) Al0.48In0.52As/InP tunnel junction. The integration on Si can be performed by using a GaAs/InP buffer layer. AFM, XRD and SEM characterizations demonstrate that template's quality is compatible with an MOVPE regrowth.

Fr15PP-Opt.6 **Piezoelectric 2DEG "Metal" Electrodes for High Responsivity, Low Dark Current AlGaN/GaN Photodetectors**

Walker (50-140)

Ananth Saran Yalamarthy, Ruth Miller, Karen Dowling and Debbie Senesky (Stanford University, USA)

Owing to its wide and direct-tunable band gap, GaN is an excellent material platform to make UV photodetectors. These devices find use in radiation-rich and high-temperature environments thereby supporting space exploration and in-situ harsh environment process monitoring. Here, we demonstrate a MSM photodetector by replacing the Schottky metal electrodes with underlying 2DEG mesa regions as the "metal" electrodes. We note that our devices offer excellent responsivity (up to 578 AW^{-1}) and NPDR values (up to 7e10 W^{-1}) as well as fast response times (10%-90%) of about 0.3 ms. We also demonstrate successful operation of these devices from room temperature up to 200 degrees Celsius. These results suggest the use of 2DEG electrodes in high responsivity, low dark current UV photodetectors.

Fr15PP-Opt.7 **Light Extraction Enhancement of AlGaInP LED by Etching Process**

Walker (50-140)

Ray-Hua Horng, You-Cheng Lin and Fu-Gow Tarntair (National Chiao Tung University, Taiwan); Dong Wuu (NCHU, Taiwan)

High-power red light AlGaInP based LED in the current applications of the market has been very common and mature. However, the driving current of LED should be at last 2.5 A/mm2 in the projector applications. Due to the high operation temperature, the LEDs application in the project system should be the bare die. It means that it does not be allowed to package for this kind application. In this case, the light extraction will be

very low due to the high refractive index of AlGaInP epilayer. In this study, the light extraction of the LED was enhanced by surface texture process, which can be used to reduce the total reflection between light emitting p-GaP interface (refraction coefficient, n~3.5) and air (n=1). The texture structures were achieved by nano-imprinting technique and the nano-columns array of p-GaP were formed by wet, dry and wet & dry etching. By the initial result of dry etching, the luminous flux curve with different ICP dry etching condition, it showed that the light extraction was enhanced about 151% under driving current 400 mA with the ICP dry etching parameters: source/bias power = 250/100 W; Cl2= 15 sccm; Ar=30 sccm; BCl3= 60 sccm, etching time= 40 s.

Fr15PP-Opt.8 **High-efficiency AlGaN-based Deep Ultraviolet Flip-Chip Light Emitting Diodes**

Tae Hoon Park, Tae Ho Lee and Tae Geun Kim (Korea University, Korea)

Walker (50-140) We report AlGaN-based deep UV LEDs fabricated using AlN/Al reflectors with reasonably good ohmic contact properties for both n- and p-AlGaN layers. Here, AlN layer prevents UV absorption and reflection loss of a single metal (Al) layer. Compared to the reference LEDs with typical metal contacts, our deep-UV LEDs exhibit much improved device performances.

Fr15PP-Opt.9 **SOA-integrated High Power 128 Gb/s Coherent Optical Modulator Fabricated on Semi-Insulating InP Substrate**

Walker (50-140) *Satoshi Nishikawa (Mitsubishi Electric Corporation, Japan); Yuichiro Horiguchi (Mitsubishi Electric Corporartion, Japan); Yohei Hokama, Masakazu Takabayashi, Syusaku Hayashi, Koichi Akiyama, Fukiko Hirose, Hayato Sano, Keita Mochizuki, Keigo Fukunaga and Keisuke Matsumoto (Mitsubishi Electric Corporation, Japan); Eitaro Ishimura (Mitsubishi electric corporation, Japan)*

We report Mach-Zehnder Modulator (MZM) devices for coherent modulation with monolithically integrated semiconductor optical amplifiers (SOAs) on semi-insulating InP substrate. MZMs have high-mesa structure buried with benzocyclobutene to make electrode flat and to reduce device capacitance. MZMs are driven with differential drive with characteristic impedance of 100 Ω with 128 Gb/s DP-QPSK modulation to reduce driver power consumption. SOAs are designed to have buried heterostructure to improve temperature characteristics. High output power of 2.5 dBm for single polarization and low insertion loss of 0 dB were demonstrated, owing to low loss transfer between high mesa and buried structure and SOA with high heat dissipation.

Fr15PP-Opt.10 **High Efficiency Optical Mode Coupling Between Si Waveguide and III-V/Si Hybrid Sections by Double Taper-Type Coupler Structure**

Walker (50-140)

Takehiko Kikuchi (Sumitomo Electric Industries, LTD, Japan); Junichi Suzuki and Fumihito Tachibana (Tokyo Instittue of Technology, Japan); Naoko Inoue and Hideki Yagi (Sumitomo Electric Industries, LTD., Japan); Moataz Eissa and Takuya Mitarai (Tokyo Instittue of Technology, Japan); Tomohiro Amemiya, Nobuhiko Nishiyama and Shigehisa Arai (Tokyo Institute of Technology, Japan)

Applying the III-V/Si hybrid integration technology to a large-scale photonic integrated circuit (PIC) is very attractive to realize new-generation PIC with high speed response, compactness, and low power consumption. In this presentation, we proposed the double taper-type coupler structure for high-efficiency optical mode coupling between Si waveguide and III-V/Si hybrid sections. SOI with Si waveguide patterns and III-V epitaxial wafers were directly bonded by the N2 plasma-activated bonding. After InP substrate removal, 1st and 2nd taper structures were formed by i-line stepper lithography and RIE techniques, respectively. The optical coupling loss for one double taper-type coupler was approximately 0.2 dB, i.e., optical coupling efficiency of 95% was achieved. This high coupling efficiency originates from small misalignment in the center of tapers (< 0.1 μm) ensured by i-line stepper lithography, and this result had good agreement with theoretical analysis. This result demonstrated that this structure is very useful for the realization of a large scale III-V/SOI hybrid PIC.

Fr15PP-Opt.11 **Device Performance Improvement of Thin Film Transistor with Ti-Doped GaZnO / InGaZnO / Ti-Doped GaZnO Sandwich Composite Channel**

Walker (50-140)

Wei-Sheng Liu (Department of Photonics Engineering, Yuan Ze University, Taiwan); Yi-Hung Lin, Chien-Lung Huang, Chih-Wei Wang, Yi-Ming Chu and Chih-Hao Hsu (University of Yuan Ze, Taiwan)

Thin-film transistors (TFTs) with indium-gallium-zinc-oxide (IGZO) channel layers have significant development for display applications. However, this oxide-based TFT device still present challenges of device performances with declined operational stability because of the adsorption of moisture and oxygen when the devices are exposed to the ambient atmosphere without passivation layers. In this study, two TFTs with different channels were made. The first TFT is designed with a typical single 50 nm-thick amorphous IGZO channel layer as IGZO SC-TFT and the other designs a sandwich composite channel TFT (CC-TFT) with 10-nm thick Ti-doped GaZnO (GTZO) / 30-nm thick a-IGZO / 10-nm thick GTZO layers. As a result, the CC-TFT exhibits a field-effect mobility of 14.1 cm^2/V-s, a SS of 0.33 V/decade, a cut-off current of 2.92 × 10-12 A, a threshold voltage of 1.7 V and a switching current ratio of 3.95 × 107, which are better than those of the SC-TFT.

Fr15PP-Opt.12 **Photoluminescence Properties of GaInAs/InP Layers by Ar Fast Atom Beam for Room Temperature Surface Activated Bonding Toward Hybrid PIC**

Walker (50-140)

Yuning Wang and Kumi Nagasaka (Tokyo Institute of Technology, Japan); Junichi Suzuki (Tokyo Instittue of Technology, Japan); Liu Bai (Tokyo Institute of Technology, Japan); Takuya Mitarai (Tokyo Instittue of Technology, Japan); Tomohiro Amemiya, Nobuhiko Nishiyama and Shigehisa Arai (Tokyo Institute of Technology, Japan)

Toward the realization of photonic integrated circuits (PICs) consisting of active devices such as lasers and amplifiers, surface activated direct wafer bonding (SAB) technology based on fast atom beam (FAB) is considered one of attractive solutions. Different with other bonding technologies such as hydrophilic bonding and plasma activated bonding (PAB), SAB can provide high bonding strength even by room temperature bonding. In this paper, the influence of Ar-FAB irradiation on GaInAsP/InP wafers has been investigated by comparing their Photoluminescence (PL) properties with different irradiation conditions, including the irradiation time and irradiation current. The results revealed strong dependence of irradiation current to PL degradation. Also, fabrication of an InP/SOI hybrid wafer was carried out using the investigated condition and high bonding area was successfully achieved even at room temperature. Results of mentioned investigations proved the feasibility of room temperature SAB technology in the fabrication of III-V/Si hybrid PICs.

Fr15PP-Opt.13 **AlInN-on-silicon Solar Cells Deposited by RF Sputtering Thickness Effect**

Walker (50-140)

Rodrigo Blasco and Arantzazu Nuñez-Cascajero (Univesidad de Alcala, Spain); Louis Grenet (CEA Grenoble, France); Javier Olea (Universidad Complutense de Madrid, Spain); Fernando Naranjo (Univesidad de Alcala, Spain); Sirona Valdueza (University of Alcala, Spain)

Applications in photovoltaics and in high-electron-mobility transistors have impelled a research effort on AlInN thin films. However, there is a difficulty to synthesize In-rich AlInN alloys by molecular beam epitaxy or metalorganic vapor phase epitaxy due to phase separation effects. In contrast, radio-frequency (RF) sputtering allows the synthesis of low-cost, large-area and single phase nanocrystalline AlInN layers, which deposition can be performed at low temperature on both crystalline and amorphous substrates. It is hence an easy technology to be scaled up to industry. In this work we study the effect of the thickness (65, 90, 100 and 145 nm) on the structural of In-rich n-AlInN deposited on p-Si(111) and photovoltaic properties of the heterojunctions. Samples were deposited at 550ºC in a nitrogen environment with an In and Al RF power of 40 W and 150 W, respectively.

Fr15PP-Opt.14 **InP-based Electro-Absorption Modulator Operating at 25Gbps from 25 to 65°C in C Band**

Walker (50-140)

Hua Yang (Tyndall National Institute, UCC, Ireland); Niall Kelly and Moises Jezzini (Tyndall National Institute, UCC, Cork, Ireland); Agnieszka Gocalinska (Tyndall National Institute, UCC, Ireland); Kevin Thomas (Tyndall National Institute, Ireland); Emanuele Pelucchi (Tyndall National Institute, UCC, Ireland); Frank H Peters (University College Cork, Ireland)

Multiple Quantum Well (MQW) electro-absorption modulators (EAMs) based on the quantum confined stark effect (QCSE) are a key component in Photonics Integrated Circuits (PICs). They offer high speed operation, a large extinction ratio, low driving voltage, a small footprint and also can be used with monolithic and hybrid integration. EAMs operating in the C band at 25Gbps at a high temperature and with a wide temperature tolerance are crucial for the new generation of 100G (25x4) or 400G (25x16) fiber communication systems by eliminating the temperature controller, and thus reducing the power consumption at significantly lower cost.InP based EAMs with AlInGaAs/AlInGaAs MQWs are found superior to those with InGaAsP/InGaAsP MQWs in operating with lower drive voltages due to a larger conduction bandgap offset (ΔEc) than the InGaAsP system. This results in better carrier (electrons) confinement in the wells, producing a sharp exciton absorption spectrum over a wide bias range , also reduce the excitonic broadening effect due to temperature, thus enabling the EAM to operate over a wide range of temperatures. We demonstrate a lumped element InP-based EAM with AlInGaAs/AlInGaAs MQWs and isolated pedestal contacts operating at 25Gbps over a temperature range from 25 to 65 °C in the C band.

Fr15PP-Opt.15 **Sidewall Roughness Atomic Force Microscopy Characterization of Deep Etched InP/$Al_xG_{1-x}I_yAs_{1-y}$ Structures**

Walker (50-140)

Reasat Fahim (University of Glasgow, United Kingdom (Great Britain))

In this study the sidewall roughness of deep dry etched structures is measured with an Icon atomic force microscopy (AFM) high resolution imaging. The measurements are performed directly on the vertical sidewall of a standard InP-based laser structure, consist of InP and its lattice matched quaternary alloy $Al_xG_{1-x}I_yAs_{1-y}$. The waveguide-like structures are created with a standard lithography process, using an inductively coupled plasma-reactive ion etching (ICP-RIE) with a Chlorine Cl2-based chemistry to achieve a target etch depth larger than 6 µm. Several optimization experiments were performed varying the ICP coil and platen powers and the relative gas concentrations and flows in Cl2 plasma gas chemistry. Smooth vertical sidewall dry etched profile with optimized ICP coil power as well as with increasing etch depth is observed.

Fr15PP-Opt.16 **Characterization of Pseudomorphic AlGaN LEDs on AlN Substrates Emitting Below 240 nm**

Walker (50-140) *Leo Schowalter, James Grandusky and Craig Moe (Crystal IS, Inc., USA); Jumpei Kasai, Tomohiro Morishita and Akira Yoshikawa (Asahi Kasei, Japan)*

In this work, LEDs targeting a wavelength of 235nm were pseudomorphically grown by MOCVD on free-standing, single crystal aluminum nitride substrates. A Si-doped, Al.85Ga.15N was used for the n-contact and the active region consisted of five quantum well structures consisting of 3nm thick Al.75Ga.25N wells sandwiched between AlGaN barriers with 85% or higher Al concentration. In our study, the thickness of the quantum wells was varied between 2 and 4nm in thickness. As predicted in prior work, light extraction is hindered at wavelengths shorter than 240nm as the emission mode on c-face AlN substrates switches from TE to TM mode at these high Al concentrations. In spite of the photon extraction issue, UVC LEDs at 240 nm have been demonstrated with 2.4 mW of power at 200 mA. At 230nm and at 227nm, and at a current of 100mA, 0.25mW and 50μW have been demonstrated, respectively.

Fr1PP-Ga: Poster Session - Ga_2O_3

Time:	6/1/2018, 08:30 AM - 10:00 AM
Room:	Walker Memorial (Building 50-140)

Fr1PP-Ga.1 **Temperature-dependent Ga_2O_3 Growth on Sapphire by MOCVD**

Kuang-Hui Li, Haiding Sun, Carlos Torres-Castanedo, Che-Hao Liao and Hsin-Hung Yao (KAUST, Saudi Arabia); Serdal Okur, Tom Salagaj, Aaron Feldman and Gary Tompa (SMI, USA); Xiaohang Li (KAUST, Saudi Arabia)

Walker (50-140)

We present Ga_2O_3 epitaxial growth on the c-plane sapphire substrates under different growth temperature, ranging from 600 to 1100 °C in a MOVPE reactor. The MOVPE reactor and gas flow simulation for the growth conditions are shown in Fig. 1. The MOVPE reactor is made of quartz tube, and the reactor has two gas inlets flowing tri-ethyl-gallium (TEG) and O_2 together with Ar carrier gas. During 30 minutes epitaxial growth, the TEG/O_2 partial pressure ratio was kept at 0.0104 (0.03 Torr/2.874 Torr) and the temperature was varied between 600 and 1100 °C at chamber pressure of 100 Torr. The samples grew from 600 to 1100 °C is defined as S600 to S1100. The surface roughness and morphology, crystal structure and quality, growth rate, and transmission spectrum of the epilayers are characterized by various experimental techniques.

Fr1PP-Ga.2 **Demonstration of Solar-Blind Avalanche Photodetectors Based on Exfoliated β-Ga_2O_3**

Sooyeoun Oh and Jihyun Kim (Korea University, Korea)

Walker (50-140)

β-Ga_2O_3 is an emerging wide band-gap material for application in high power devices and solar-blind photodetectors due to its optical and electrical properties. High-performed solar-blind photodetectors require high response to UV-C because few photons with short wavelength reach from the sun due to absorption in ozone layer. Avalanche photodetectors can be a solution to this problem. Herein, we fabricated the exfoliated β-Ga_2O_3 micro-flake based solar-blind avalanche photodetectors and characterized their photoresponse properties. The crystal structure and quality of exfoliated β-Ga_2O_3 micro-flakes were analyzed. The fabricated solar-blind photodetectors with Schottky diode exhibited low dark current, high photo-to-dark ratio, high sensitivity to UV-C light, fast and stable on/off characteristics. The enhancement of their responsivity that was attributed to multiplication gain, was obtained.

Fr1PP-Ga.3 **X-ray Detection Based on Vertical Ga_2O_3 Schottky Barrier Diodes**

Leidang Zhou (Xi'an Jiaotong University, P.R. China); Xing Lu (South China University of Technology, P.R. China)

Walker (50-140)

In this study, vertical Ga_2O_3 SBDs have been fabricated on a β-Ga_2O_3 bulk substrate and demonstrated as X-ray detectors for the first time. The response of the reverse biased Ga_2O_3 SBD to X-ray illumination was characterized. The detectivity and responsivity of the X-ray detector increased with the increase of revers bias voltage, and then reached 220k cmHz1/2/Gy and 900 nC/Gy at -25 V, respectively. The detector also exhibited a good transient response to the switching of X-ray illumination.

Fr1PP-Ga.4 **Thicknesses Effects and Defects-related Study on ZnGa2O4 Epilayer with High-Voltage Measurement**

Li-Chung Cheng, Chiung-Yi Huang and Ray-Hua Horng (National Chiao Tung University, Taiwan)

Walker (50-140)

Recently, oxide-based materials have attracted much attention due to its wide band gap properties therefore they are excellent candidates for high-power switching and photodetector applications. In our previous study, ZnGa2O4 thin-film grown by MOCVD could sustain high breakdown voltage over 378V. In this study, we investigated the physical characteristics ZnGa2O4 thin-film with different thin-film thicknesses 70, 50, 40, and 25 nm. Also, the defects caused from either oxygen vacancies or interface dislocation would have some effect on the ZnGa2O4 epilayer and had also been demonstrated.

Fr1PP-Ga.5 **Miscibility and Phase Separation in (InxGa1-x)2O3**

Charlotte Wouters (Leibniz Institute of Crystal Growth, Germany)

Walker (50-140)

In this work, preliminary results on the miscibility and phase formation in the (In,Ga)2O3 system are presented. Thin epitaxial (InxGa1-x)2O3 films with a laterally varying In content are grown on c-sapphire substrates using the PLD continuous composition spread method[2] and studied on nanometer scale by high resolution transmission electron microscopy (TEM). Our experimental results show that in good agreement with ab initio calculations in the compositional range between 0.5>xIn>0.9, phase separation into an indium rich bixbyite phase (x(In)>90%) and a hexagonal InGaO3 (II) or a monoclinic InGaO3 phase with an In content of approximately 50-70% is consistently observed. For lower In contents xIn<0.5, we observe a variety of phases (β,ε,c,h) dependant on growth conditions. The thermodynamically stable monoclinic β-phase can be destabilised by changing the partial pressure or introducing Sn during growth. This proves the flexibility of the Ga atom to adopt various coordination numbers.

Fr1PP-Ga.6 **Phase Transition Temperatures of α-Ga_2O_3 on Sapphire**

Riena Jinno, Kentaro Kaneko and Shizuo Fujita (Kyoto University, Japan)

Walker (50-140) α-Ga_2O_3 , which is one of the ultra wide-bandgap (UWBG) semiconductors, has attracted attentions as a next-generation material of a power device. The phase transition temperature of 650°C was considered to be a sever problem for α-Ga_2O_3 -based device processes and reliability. In this paper, we report the growth of α-Ga_2O_3 above 650oC and the renewed phase transition temperature.

Fr1PP-Ga.7 **β-Ga_2O_3 Hollow Nanospheres Based Ultraviolet Photodetector**

Prachi Sharma, Stefan Turan, Gabriel Gedler, Chulsung Bae and Shayla Sawyer (Rensselaer Polytechnic Institute, USA)

Walker (50-140)

In this work we present β-Ga_2O_3 hollow nanospheres based UV photodetector. Hollow nanospheres offer attractive features for high performance photodetectors like high surface to volume ratio, high efficiency of harvesting light and unique electron transport properties for fast transient response. The β-Ga_2O_3 hollow nanospheres are fabricated using a template based method. The advantage of using a template based approach is that the size of the hollow spheres can be easily tuned by changing the size of the template. Monodispersed polystyrene (PS) spheres prepared using dispersion polymerization are used as templates. Solvothermal synthesis is used to synthesize PS/gallium oxide hydroxide (GaO(OH)) core shell spheres. Calcination of the core shell spheres at 900°C for one hour results in the formation of uniform β-Ga_2O_3 hollow nanospheres. This study will also present the steps for synthesis of the PS templates and β-Ga_2O_3 hollow nanospheres and material characterization of the hollow spheres.

Fr1PP-Ga.8 **Characterization of Corundum-structured α-Ga_2O_3 Layer Grown by Hydride Vapor Phase Epitaxy Methods**

Hoki Son (University of Korea, Korea); Daewoo Jeon (Korea Institute of Ceramic Engineer; Technology, Korea)

Walker (50-140)

We fabricated crack-free α-Ga_2O_3 on c-plane sapphire substrate by HVPE. The HVPE system that set up consists of a resister heater in a horizontal hot wall was a suitable method for α-Ga_2O_3 template. Oxygen and gallium chloride synthesized Ga metal and HCl were used as the precursors, and N2 was used as the carrier gas. The growth temperature was changed in the range of 410 - 700°C. The growth rate of α-Ga_2O_3 epilayer can be controlled in the range of 3 - 15μm/h by the growth conditions. The full width at half maximum (FWHM) values of ω-scan X-ray rocking curve was indicated to 17 arcsec for (0006) and 1853 arcsec for (10-14) on α-Ga_2O_3 grown at 450℃. The optical band gap was able to get transmittance and its value is 5.0 eV. The growth temperature and HCl flow sensitively changed the growth rate that affected the crystalline.

Fr1PP-Ga.9 **Ga_2O_3 : Transparent Conductive Oxide with Plasma Adjusted Properties**

Walker (50-140)

Alban Maertens (CentraleSupelec; LMOPS, France); Samuel Margueron (Université de Lorraine, France); Frédéric Genty (CentraleSupelec, France); Adulfas Abrutis (University of Vilnius, Lithuania); Thierry Belmonte, Pascal Boulet and Jaafar Ghanbaja (Université de Lorraine, France); Abdelkrim Talbi (IEMN, France); Ausrine Bartasyte (FEMTO-ST Institute, France)

Ga_2O_3 thin films grown on C-sapphire by hot wire CVD, were alloyed with SnO_2, with a concentration from 0 to 15 at% of Sn composition. No conductivity has been measured on as-grown or annealed samples at 1000 °C. High transparency in visible range was measured with bandgap estimated between 4.9 and 5 eV. X-ray diffraction patterns depicted new space group and phase while increasing Sn content. Hydrogen and argon radio-frequency-plasma treatment were used to modify material properties. It resulted in an increase of the conductivity and a decrease of transparency. The conductivity change is related to Sn concentration, but also to the hydrogen presence brought by the plasma. Those treatments are not stable with temperature which decreases the conductivity.

Fr1PP-Ga.10 **Origin of Deep Pits Formed on (001) β-Ga_2O_3 Homoepitaxial Layers Grown by Halide Vapor Phase Epitaxy**

Walker (50-140)

Keita Konishi (Tokyo University of Agriculture and Technology, Japan); Ken Goto (Tamura Corporation, Japan); Hisashi Murakami (Tokyo University of Agriculture and Technology, Japan); Akito Kuramata and Shigenobu Yamakoshi (Tamura Corporation, Japan); Yoshinao Kumagai (Tokyo University of Agriculture and Technology, Japan)

The origin of deep pits formed in the halide vapor phase epitaxy (HVPE) layer grown on (001) β-Ga_2O_3 substrates is investigated. Ga_2O_3 was grown by HVPE on (001) β-Ga_2O_3 substrate with an off-cut-angle of 0.5° toward [010]. The density of deep pits in the HVPE grown layer after CMP was counted to be 10^3 - 10^4 cm^{-2}, which was almost equal to the density of dislocations in the substrate used. Dislocation was found at the bottom of the pit, and the dislocation appeared on the substrate surface was found to be the origin of the pit by using transmission electron microscopy. The dislocation was running at an angle of 60° from the substrate surface, i.e., parallel to (011). Therefore, the deep pits were completely disappeared when Ga_2O_3 was grown on (011) β-Ga_2O_3 substrate prepared from the same EFG-bulk crystal for preparation of (001) β-Ga_2O_3 substrates.

Fr1PP-Ga.11 **Ga_2O_3 Current Aperture Vertical Electron Transistors with N-Ion-Implanted Current Blocking Layer**

Walker (50-140)

Man Hoi Wong (National Institute of Information and Communications Technology, Japan); Ken Goto, Akito Kuramata and Shigenobu Yamakoshi (Tamura Corporation, Japan); Hisashi Murakami and Yoshinao Kumagai (Tokyo University of Agriculture and Technology, Japan); Masataka Higashiwaki (National Institute of Information and Communications Technology, Japan)

β-Ga_2O_3 is being actively pursued for power devices owing to its wide bandgap of 4.5 eV and the availability of melt-grown native substrates for high quality epitaxy. Vertical β-Ga_2O_3 power transistors, which are preferred over lateral topologies for high voltage and high power ratings, have shown promising performance. In our previous demonstration of a current aperture vertical Ga_2O_3 metal-oxide-semiconductor field-effect transistor, a current blocking layer (CBL) formed by Mg-ion implantation was employed for electrical isolation between source and drain, but its effect was compromised by thermal diffusion of Mg. In this work, an N-doped CBL was adopted in light of its higher thermal stability and larger blocking voltage than with Mg doping. A substantially lower leakage current with N-ion implantation than with Mg-ion implantation suggested that the former resulted in a larger barrier. The effective CBL thickness obtained by capacitance-voltage measurements was consistent with the absence of N diffusion.

Fr1PP-Ga.12 **Epitaxial Growth Mechanism of Inserted Rotation Domain for Orthorhombic ε-Ga_2O_3 Film on (100) TiO_2 Substrate by Mist Chemical Vapor Deposition**

Walker (50-140)

Daisuke Tahara, Hiroyuki Nishinaka and Masahiro Yoshimoto (Kyoto Institute of Technology, Japan)

We demonstrated the epitaxial growth of ε-Ga_2O_3 thin film on tetragonal (100) TiO_2 substrate by mist CVD. For the orthorhombic {122} reflex which reflexes cannot be found in the hexagonal structure, twelve peaks were observed, and we identified ε-Ga_2O_3 as the orthorhombic crystal structure. To investigate the in-plane relationship between (0001) ε-Ga_2O_3 and (100) TiO_2, we evaluated the XRD ϕ scanning of the ε-Ga_2O_3 {135} and TiO_2 {110}. The six symmetric peaks were observed at the ε-Ga_2O_3 {135}. Thus, orthorhombic ε-Ga_2O_3 grown on (100) TiO_2 has three rotation domains, contributing to two diffractions. Two diffraction peaks of TiO_2{110} reflex were observed at the same angle positions as peaks of ε-Ga_2O_3 {135} reflex. Therefore, we determined that the epitaxial orientation relationship was (001) ε-Ga_2O_3 // (100) TiO_2, and in-plane epitaxial relationships were ε-Ga_2O_3 [130] // TiO_2 [010], [01(_)1(_)] and [01(_)1].

Fr1PP-Ga.13 **Characterization of Halide Vapor Phase Homoepitaxial β-Ga_2O_3 Films Co-doped by Silicon and Nitrogen**

Walker (50-140) *Marko Tadjer, Andrew Koehler and Jaime Freitas Jr (Naval Research Laboratory, USA); Matty Specht (American Society for Engineering Education, USA); Karl Hobart, Evan Glaser, Travis Anderson and Fritz Kub (Naval Research Laboratory, USA); Akito Kuramata (Tamura Corporation, Japan)*

Unlocking the full potential of β-Ga_2O_3 as an ultra-high breakdown power electronics material will require thick, low defect density films with controlled total free carrier concentration (ND-NA). Doping with nitrogen, a known acceptor in β-Ga_2O_3 , has not lead to the demonstration of room temperature p-type conductivity in β-Ga_2O_3 despite several recent attempts. In this work, we demonstrate record low free carrier concentration (1.85e14 cm^{-3}) and high breakdown voltage (2.38 kV) in β-Ga_2O_3 where both Si and N dopants were present. The HVPE epitaxial films were grown on (001) Fe-doped semi-insulating β-Ga_2O_3 substrates by Novel Crystal Technology. Epilayer thickness was verified by secondary ion-mass spectroscopy (SIMS) to be 9.2 µm. The SIMS measurements also indicated Si and N concentrations of 5e15 cm^{-3} and 2e17 cm^{-3}, respectively, suggesting N acted as a compensating defect but was not fully ionized at room temperature.

Fr1PP-Ga.14 **Crystallographically-dependent Thermal Boundary Conductance Across metal/Ga_2O_3 Interfaces**

Walker (50-140) *Brian M. Foley, Samuel Kim, Luke Yates and Zhe Cheng (Georgia Institute of Technology, USA); Samuel Graham, Jr (Georgia Institute of Technology; Oak Ridge National Laboratory, USA)*

Power electronic devices are critical components for the conversion and control of electrical power. While wide band gap materials (GaN, SiC) have had a major impact by enabling the development of smaller and faster devices, researchers continue to seek disruptive improvements in power device performance. As a result, the so-called ultra-wide band gap (UWBG) semiconductors have entered the discussion with β-Ga_2O_3 emerging as an exciting candidate. With a band gap of ~4.9 eV and easier to synthesize than AlN and Diamond, the figure of merit for β-Ga_2O_3 based devices exceeds that of commercially available 4H-SiC and GaN. Given these potential benefits of using β-Ga_2O_3 for power devices, the thermal conductivity of pure β-Ga_2O_3 is about an order of magnitude lower than both 4H-SiC and GaN, indicating that device self-heating may be the limiting factor when it comes to the power handling capabilities of these devices. Additionally, many characteristics of real devices (doping, defects, etc) will further impede phonon transport within the material. This presentation will focus on thermal transport in doped β-Ga_2O_3 single crystals along various crystallographic directions, as well as transport across metal/β-Ga_2O_3 heterointerfaces. The goal of this work is to provide researchers with new perspectives that promote a "thermal-first" approach to device design.

Fr1PP-Ga.15 **Temperature-dependent Electrical Properties of β-Ga_2O_3 Schottky Barrier Diodes on Highly Doped Single-Crystal Substrates and Their Reverse Current Leakage Mechanisms**

Walker (50-140)

Tsung-Han Yang (Arizona State University, USA); Houqiang Fu (Arizona state University; Arizona State University, USA); Xuanqi Huang, Hong Chen, Jossue Montes, Izak Baranowski and Kai Fu (Arizona State University, USA); Yuji Zhao (Arizona state University, USA)

In this paper, lateral (-201) β-Ga_2O_3 SBDs with various geometries were fabricated on a highly doped single-crystal substrate grown by edge-defined film-fed growth (EFG) method. A high on/off ratio∼10E8 was obtained and the turn-on voltage of the devices was about 1.1 V at room temperature. A specific contact resistance of 1.0E-5 Ω·cm^2 and a sheet resistance of 3.7E2 Ω/sq indicate a good behavior for the ohmic contact. The ideality factor decreased from 1.65 to 1.29 while the Schottky barrier height increased from 0.95 eV to 1.12 eV from 20 °C to 200 °C. Larger contact distance results in higher resistivity of the surface leakage path and thus lower the surface leakage current. At higher reverse bias, the leakage current increased because of the hopping conduction driven by the electric field. The reverse surface leakage currents increasing with increased temperature is possibly due to stronger hopping conduction at higher temperature.

Fr1PP-Ga.16 **Growth of Mg Doped (010) β-Ga_2O_3 by Plasma Assisted Molecular Beam Epitaxy**

Walker (50-140)

Akhil Mauze (University of California, Santa Barbara, USA); James Speck (UCSB, USA); Elaheh Ahmadi (UC-Santa Barbara, USA); Thomas Mates (University of California, USA)

Mg shows promise for compensation of n-type dopants in β-Ga_2O_3 . In this study we investigate Mg-doped (010) β-Ga_2O_3 layers grown by plasma assisted molecular beam epitaxy grown on (010) β-Ga_2O_3 substrates. Atomic Force Microscopy was used to characterize the surfaces of these layers and found that higher growth temperatures yield poorer surfaces with more pitting for substrate temperatures from 600 °C to 700 °C. We also demonstrate that Mg concentration has little to no dependence on growth temperature in the same range with a constant cell temperature of 400 °C. By changing the Mg cell temperature from 345 °C to 450 °C, Mg concentrations could be controlled from 1 x 10^{17} cm^{-3} to 6 x 10^{20} cm^{-3} as measured by Secondary Ion Mass Spectroscopy. Mg concentration demonstrates a weak dependence on Ga flux in both the O-rich and Ga-rich growth regimes.

Fr1PP-Ga.17 **Electrical Properties of alpha-Ga_2O_3 Films on M-Plane Sapphire Substrates**

Walker (50-140)

Kazuaki Akaiwa, Katsuya Ohta, Takahito Sekiyama and Tomoki Abe (Tottori University, Japan); Takashi Shinohe (FLOSFIA INC., Japan); Kunio Ichino (Tottori University, Japan)

We previously reported the successful fabrication of conductive corundum-structured alpha-Ga_2O_3 films on c-plane sapphire substrates by Sn-doping. However, because of relatively lower electron mobility and the severe carrier compensation, improvement of

electrical property is necessary for the actual device application of alpha-Ga_2O_3 films. Recently, we successfully fabricated conductive Sn-doped alhpa-Ga_2O_3 films on m-plane sapphire substrates. Fabricated films on m-plane sapphire showed remarkably higher electron mobilities compared with those on c-plane sapphire substrates. This result suggests the reduction of crystal defects critically influencing on the electrical properties of films. In this paper, we show the fabrication of conductive Sn-doped alpha-Ga_2O_3 films grown on m-plane sapphire substrate and the evaluation of their electrical properties.

Fr1PP-Ga.18 **Metal-Assisted Chemical Etch of β-Ga_2O_3 : Towards the Formation of Smooth Vertical Damage-Free and High Aspect Ratio Fin Array**

Walker (50-140)

Munho Kim and Hsien-Chih Huang (University of Illinois, USA); Kelson Chabak (Air Force Research Laboratory, USA); Xiuling Li (University of Illinois, USA)

We demonstrate the formation of various 3D Ga_2O_3 structures including vertical nanofin array with 10:1 aspect ratio and smooth sidewalls, using the metal-assisted chemical etching (MacEtch) method.

Fr1PP-Ga.19 **Optimization of Dynamic Switch Loss Metrics for Lateral β-Ga_2O_3 Devices**

Walker (50-140)

Andrew Green (United States Air Force; KBRwyle, USA); Kelson Chabak and Michael Schuette (Air Force Research Laboratory, USA); Günter Wagner (Leibniz Institute for Crystal Growth - IKZ, Germany); Dennis Walker, Kevin Leedy and Antonio Crespo (Air Force Research Laboratory, USA); Miles Lindquist (Air Force Research Laboratory, KBRwyle, USA); Gregg Jessen (Air Force Research Laboratory, USA)

β-Ga_2O_3 has simultaneously shown to have high breakdown field, a wide range of doping, and melt based bulk growth. Over the past few years, many epitaxial and transistor developments have occurred. Promising device results have been demonstrated such as high breakdown field, high voltage enhancement mode operation, and RF operation. With the current improvements in the device performance, it will be important to benchmark the current progress and create a roadmap for future β-Ga_2O_3 based power electronics. Hwang's material Figure of Merit scales with the critical field and mobility, which naturally applies to β-Ga_2O_3 due to its large expected breakdown field. Total power loss is a combination of DC conduction and dynamic switching losses incurred during switching operation. This talk will characterize and optimize state-of-the-art β-Ga_2O_3 devices fabricated by the Air Force Research Laboratory with respect to dynamic switching losses. We will review device geometries and epitaxial growth variations that directly influence dynamic switch loss.

Fr2A7: Photonics

Time:	6/1/2018, 10:30 AM - 12:30 PM
Room:	Salon M (Samberg Conference Center, 7th floor)
Chair:	Shui-Qing Yu(University of Arkansas, USA)

Fr2A7.1

10:30 AM

INVITED

Salon M

THz Difference-Frequency Generation in Quantum Cascade Lasers on Silicon

Mikhail Belkin (The University of Texas at Austin, USA)

Abstract not available.

Fr2A7.2

11:00 AM

Salon M

Orientation-dependent Modulation Response of High-Speed InGaN/GaN Blue Light-Emitting Diodes for Visible-Light Communication

Morteza Monavarian (Center for High Technology Materials, The University of New Mexico, USA); Arman Rashidi, Andrew Aragon and Ashwin Rishinaramangalam (Center for High Technology Materials, University of New Mexico, USA); Sang Ho Oh (University of California, Santa Barbara, USA); Steven DenBaars (University of California, Santa Barbara); Daniel Feezell (Center for High Technology Materials, University of New Mexico, USA)

In this work, for the first time, we experimentally compare the modulation bandwidth vs. current density for InGaN/GaN LEDs on nonpolar (10-10), semipolar (20-2-1), and polar (0001) orientations. The results indicate that nonpolar and semipolar LEDs exhibit larger modulation bandwidths at the relatively low current densities needed for LED operation (<500 A/cm^2) where efficiency remains higher and power dissipation is lower. At 500 A/cm^2, the nonpolar LED achieves a 3dB bandwidth of ~1 GHz, while the semipolar and polar LEDs exhibit bandwidths of 260 MHz and 75 MHz, respectively. The nonpolar and semipolar LEDs also show a lower carrier density for a given current density. We have also separately demonstrated another nonpolar m-plane µLED with a record 3dB modulation bandwidth of 1.5 GHz at 1 kA/cm^2 and 1.35 GHz at only 250 A/cm^2. The results support using nonpolar and semipolar orientations to achieve high-speed LEDs operating at low current densities.

Fr2A7.3 **Gan/AlGaN Nanowire Heterostructures for Mid-Infrared Intersubband Technology**

11:15 AM

Salon M

Akhil Ajay (CEA-Grenoble, France); Rodrigo Blasco (Univesidad de Alcala, Spain); Jakub Polaczynski, Maria Spies and Martien den-Hertog (CNRS-Insititute Neel, France); Eva Monroy (CEA-Grenoble, France)

In this work, we report the longest wavelengths observed using Intersubband (ISB) transitions in III-nitride nanowires and the first measurement of ISB absorption in GaN/AlGaN multi-quantum wells in GaN nanowires (NWs). As a first approach to red shift the ISB transition energy upto ~6 µm, we focused on a GaN/AlN active region, varying the width of the GaN wells in the range of 4-6 nm. Alternatively, we synthesized GaN NWs containing a GaN/AlGaN (4 nm / 3 nm) active region. The use of AlGaN reduces the internal electric field in the wells, red shifting the ISB transition compared to samples with same quantum well dimension with AlN barriers. Structural characterization shows well-defined and homogeneous AlGaN barriers. We successfully observe red shifted ISB absorption at ~6 µm at room temperature.

Fr2A7.4 **Thermal Reliability Analysis of InGaN Solar Cells**

11:30 AM

Salon M

Xuanqi Huang (Arizona State University, USA); Houqiang Fu (Arizona state University; Arizona State University, USA); Hong Chen, Izak Baranowski, Jossue Montes and Tsung-Han Yang (Arizona State University, USA); Brendan Gunning and Dan Koleske (Sandia National Laboratories, USA); Yuji Zhao (Arizona state University, USA)

We investigate the thermal stability of InGaN solar cells under thermal stress at elevated temperatures from 400°C to 500°C. High Resolution X-Ray Diffraction (HRXRD) analysis reveals that material quality of InGaN/GaN did not degrade after thermal stress. The external quantum efficiency (EQE) characteristics of solar cells were well-maintained at all temperatures, which demonstrates thermally robust nature of InGaN materials. Analysis of current density-voltage (J-V) curves indicates that the degradation of conversion efficiency of the solar cell is mainly caused by the decrease in open-circuit voltage (Voc), while short-circuit current (Jsc) and fill factor (FF) remain almost constant. The decrease of Voc after thermal stress is attributed to the compromised metal contacts. Transmission line method (TLM) results further confirmed that p-type contacts became Schottky-like after thermal stress. The Arrhenius model was employed to estimate the failure lifetime of InGaN solar cells under different temperatures. These results suggest that while InGaN solar cells have high thermal stability, the degradation in metal contact could be the major limiting factor for these devices under high temperature operation.

Fr2A7.5

11:45 AM

Salon M

Evidence for Recombination-Induced Degradation Processes in InGaN-based Optoelectronic Devices

Carlo De Santi, Matteo Meneghini, Alessandro Caria and Nicola Renso (University of Padova, Italy); Ezgi Dogmus (IEMN-CNRS Lille, Italy); Malek Zegaoui (IEMN-CNRS, France); Farid Medjdoub (Institute of Electronics, Microelectronics and Nanotechnology, France); Enrico Zanoni (DEI, Italy); Gaudenzio Meneghesso (University of Padova, Italy)

For the first time, we demonstrate recombination-induced defect generation in InGaN/GaN-based optoelectronic devices, by stressing InGaN/GaN high periodicity MQW structures: the results will significantly improve the understanding of the degradation of optoelectronic devices, since - so far - only current-driven or temperature-induced degradation processes were investigated. The analysis was carried out on high periodicity InGaN/GaN MQWs: during stress in short-circuit condition under illumination with a 405 nm, 361 W/cm^2 laser diode, the short circuit current was found to decrease significantly. This degradation process is gradual, and ascribed to an increase in the defect concentration. By means of photocurrent spectroscopy experiments, the generation of gallium vacancies and/or their complexes is the most likely cause for the degradation of the device. Stress tests in open circuit condition, i.e. without any current flow, show a clear degradation in the device after stress, not caused by a variation in reflectivity, providing evidence for recombination-induced degradation process.

Fr2A7.6

12:00 PM

INVITED

Salon M

III-nitride Microlasers on Silicon Integrated on a 2D Photonic Platform

Philippe Boucaud (CNRS-CRHEA, France); Farsane Tabataba-Vakili (C2N, France); Laetitia Doyennette (L2C, France); Christelle Brimont and Thierry Guillet (Laboratoire Charles Coulomb (L2C), CNRS-University Montpellier 2, France); Stephanie Rennesson (Université Côte d'Azur, CRHEA-CNRS, France); Eric Frayssinet, Benjamin Damilano, Jean-Yves Duboz and Fabrice Semond (CRHEA-CNRS, France); Moustafa El Kurdi (C2N-Univ Paris Sud, France); Sébastien Sauvage (C2N-CNRS, France); Xavier Checoury (CNRS Univ Paris Sud 11, France); Bruno Gayral (CEA-CNRS, INAC-SP2M, CEA Grenoble, France)

The III-nitride semiconductors like AlN and GaN epitaxially grown on silicon represent a promising platform for photonic in the ultra-violet and visible range. Many applications of this platform can be envisioned from quantum technologies, bio-applications, microdisplays, visible light communications to novel types of optical sources. A full photonic platform combines passive and active elements, including laser sources. So far, III-nitride on silicon photonic platforms were reported either with passive elements and out-coupling gratings for light injection or extraction or with LEDs coupled to waveguides and detectors. In parallel, many demonstrations of microlasers have been reported but with single devices operating under optical and electrical injection. In this presentation, we will report on the combined integration of III-nitride microlasers with a III-nitride photonic circuitry. The investigated structures were grown on silicon and consist of a combination of AlN, GaN and InGaN layers. The micro-emitters are mushroom-type

microdisks that are side-coupled with bus waveguides. Efficient light coupling in the visible range around 400 nm imposes gap distances from microdisks to bus waveguides lower than 100 nm. Loaded quality factors larger than 2000 have been obtained. The emission from the microdisk whispering gallery modes is coupled to the waveguides and out-coupled to free space with grating couplers. All passive elements are suspended in air. In order to avoid reabsorption of the emission in the waveguide, a specific etching step procedure was introduced to remove the quantum wells from the waveguides and the gratings. Lasing from InGaN quantum wells is demonstrated at room temperature under pulsed optical pumping with this platform. This demonstration illustrates the potential of III-nitrides on silicon to achieve active photonic circuits operating in the blue spectral range. We will discuss the future opportunities offered by this platform.

Fr2B7: Nanostructures

Time:	6/1/2018, 10:30 AM - 12:30 PM
Room:	DR 3 & 4 (Samberg Conference Center, 6th floor)
Chair:	Cezar Zota (IBM Research Zurich, Switzerland)

Fr2B7.1 **Scaling Effect on Vertical FETs Using III-V Nanowire-Channels**

10:30 AM

DR 3 & 4

Katsuhiro Tomioka (Hokkaido University; GS-IST and RCIQE, Japan); Hironori Gamou (Hokkaido University, Japan); Akinobu Yoshida (Hokkaido Univerisy, Japan); Junichi Motohisa (Hokkaido University, Japan)

III-V nanowire (NW)-channel MOSFETs on Si are exceedingly investigated because they are promising alternative channels for fast n-channel FETs. We have reported InGaAs nanowire-channel and modulation doping technique by using core-shell structure for the vertical surrounding-gate transistor (VSGT) on Si. However, device scalability of the NWs for the VSGT on Si have been less investigated. Here, we report on several scaling effects on the III-V NW-channel vertical surrounding-gate transistor (VSGTs) on Si.

Fr2B7.2 **Multi-nanowire In-Plane-Gate Field Effect Transistors**

10:45 AM

DR 3 & 4

Giovanni Santoruvo (Ecole Polytechnique Federale de Lausanne, Switzerland); Elison Matioli (EPFL, Switzerland)

In this work, we introduce the Multi-nanowire In-Plane-Gate Field-Effect-Transistors (Multi-NW IPGFETs), which are formed by an array of AlGaN/GaN HEMT nanowires, where the current is controlled by two co-planar gates. This device structure does not require gate oxides which, together with the planar arrangement of the gate and channel, lead to an extremely small gate capacitance, down to the aF range. Multi-NW IPGFETs differ from single-wire IPGFETs by their excellent scaling up capabilities. In this work, we demonstrate Multi-NW IPGFETs with large ON-state current of 800 mA/mm, gm of 340 mS/mm, small on-resistance of 1.41 Ω.mm, excellent gate control with ON-OFF ratio of 108 and sub-threshold slope of 80 mV/dec, which is remarkable considering that only two planar side gates control all the NWs. The large current and transconductance together with the extremely small gate capacitance make these devices very promising for future high-frequency applications.

Fr2B7.3

11:00 AM

DR 3 & 4

Bandgap Engineering of GaAsSb/InGaAs P-channel Hetero-junction Tunnel Field-Effect Transistors with a GaSb Pocket Layer

Wei Jen Hsueh, Jin-Yang Chen, Cheng Yu Chen, Andrey Katkov and Jen-Inn Chyi (National Central University, Taiwan)

P-channel hetero-junction tunneling field-effect transistors (HTFETs) of p^+-$GaAs_{0.51}Sb_{0.49}$/i-$GaAs_{0.51}Sb_{0.49}$/i-$GaAs_xSb_{(1-x)}$/n^+-$In_{0.53}Ga_{0.47}As$ have been designed and simulated by using Synopsys Sentaurus TCAD. A GaSb pocket layer is proposed to reduce the effective tunneling barrier (E_{beff}) from 0.63 eV to 0.38 eV at the $GaAs_{0.51}Sb_{0.49}$/$In_{0.53}Ga_{0.47}As$ junction, which leads to an I_{ON} current equals to 50 uA/um at V_{DS}= -0.3 V and V_{GS}= -0.6 V, while I_{OFF} remains at $4x10^{-11}$ uA/um at V_{GS} = 0 V, simultaneously. Inserting a pocket layer with type-II junction InAs/$GaAs_{0.1}Sb_{0.9}$ insertion layer results in an off-current as low as 10^{-11} uA/um, a high on-current of 200 uA/um at V_{DS} = -0.3 V and V_{GS} = -0.6 V, and a subthreshold swing (S.S.) of 20 mV/dec simultaneously.

Fr2B7.4

11:15 AM

INVITED

DR 3 & 4

III-V Nanowire MOSFETs: A Path Towards 10 nm High-Performance Transistors

Lars-Erik Wernersson (Lund University, Sweden)

III-V nanowires transistors have the potential to extend the scaling roadmap by offering a higher drive current, or more importantly a higher transconductance, at a given geometry. The promise has triggered a wide range of research efforts both related to materials questions like nanowire growth and to device processing and characterization. In this talk, we will present InAs/GaInAs MOSFETs and GaAsSb/InAs TunnelFETs with high-performance demonstrating that III-V nanostructures indeed may compete with other technologies.

Fr2B7.5 **GaAsSb/InAs Nanowire Backward Diodes for Ambient RF Energy Harvesting**

11:45 AM

DR 3 & 4

Tsuyoshi Takahashi (Fujitsu Laboratories Ltd., Japan); Kenichi Kawaguchi (Fujitsu Limited; Fujitsu Laboratories Ltd., Japan); Masaru Sato (Fujitsu Laboratories Ltd., Japan); Naoya Okamoto (Fujitsu Limited; Fujitsu Laboratories Ltd., Japan); Michihiko Suhara (Tokyo Metropolitan University, Japan)

Ambient RF energy harvesting is an attractive method of supplying alternative power to drive sensors for the internet of things (IoT). Backward diodes have potential to provide more efficient RF-to-DC conversion in comparison to Schottky diodes. Nanowire (NW) structures have been considered to improve the characteristics of the backward diodes, which require high nonlinearity and low junction capacitance (Cj). In this work, for the first time, we report the microwave sensitivity (which is related to conversion efficiency) of GaAsSb/InAs NW backward diodes. Sensitivity of 25 kV/W was obtained for the 96-NW-array diode at 2.4 GHz, whereas a value of 4 kV/W was obtained for the 730-NW-array diode. The observed sensitivities are comparable to those of a conventional Schottky diode. Therefore, further improvement in sensitivity can be achieved by optimizing the numbers of NWs and heterojunction structures in NW backward diodes.

Fr2B7.6 **Magnetic Influence on Cryogenic InP HEMT DC Characteristics**

12:00 PM

DR 3 & 4

Isabel Harrysson Rodrigues (Chalmers University of Technology, Sweden); Arsalan Pourkabirian, Giuseppe Moschetti and Joel Schleeh (Low Noise Factory AB, Sweden); Per-Åke Nilsson (Chalmers University of Technology, Sweden); Jan Grahn (Chalmers University of Thechnology, Sweden)

InP HEMTs are used in many ultra-low-noise and high-speed applications, such as cryogenic LNAs, where some are exposed to high magnetic fields, such as MRI scanners. It is therefore of high interest to study how the performance of these transistors are affected by a magnetic field. In a previous study, cryogenic AlGaAs/GaAs HEMT LNAs operating below 1 GHz in high static magnetic fields was reported. It was found that the noise temperature of the LNA increased with magnetic field. We present the results of cryogenic DC measurements for a 1x100um InP HEMT, and how the DC characteristics are affected under applied static magnetic fields. We found that the influence on the cryogenic HEMT DC current-voltage, when increasing the in-plane parallel magnetic field, was negligible. In contrast, when the transistor was oriented perpendicular to the magnetic field, the DC behavior of the HEMT was strongly affected.

Fr2B7.7

12:15 PM

DR 3 & 4

Towards Horizontal Heterojunctions for Tunnel Field Effect Transistors with Template Assisted Selective Epitaxy via MOCVD

Simone Tommaso Šuran Brunelli (University of California Santa Barbara, USA); Brian Markman, Jun Wu, Hsing Ying Tseng and Aranya Goswami (UCSB, USA); Chris Palmstrom (University of California Santa Barbara, USA); Mark J W Rodwell (University of California, Santa Barbara, USA); Jonathan Klamkin (University of California Santa Barbara, USA)

We report results on the area selective and template assisted epitaxial growth of InP, utilizing dielectric based confined structures on InP substrates, which, thanks to their geometry, could enable horizontal heterojunctions, that can find application in the next generation of tunnel-FET devices. The templates are fabricated so that only a small area of the InP substrate, dubbed seed, is visible to the growth atmosphere. Growth is initiated selectively only at the seed and then proceeds in the hollow channel towards the source hole. As a result, growth resembles epitaxial lateral overgrowth from a single nucleation point and allows orientation in an arbitrary, template defined direction. Scanning electron microscopy (SEM) is used to confirm growth, and transmission electron microscopy (TEM) to verify growth quality.

Fr2F1: Ga_2O_3 Keynotes

Time:	6/1/2018, 10:30 AM - 12:30 PM
Room:	DR 5 & 6 (Samberg Conference Center, 6th floor)
Chair:	Shizuo Fujita (Kyoto University, Japan)

Fr2F1.1 **Introduction of Gallium Oxide Technologies**

10:30 AM *Masataka Higashiwaki (National Institute of Information and Communications Technology, Japan)*

DR 5 & 6

It is my great pleasure to organize a focused session on gallium oxide (Ga_2O_3) materials and devices in CSW 2018. This special session will cover the structural, electrical, and optical properties of Ga_2O_3 and showcase state-of-the-art key technologies of epitaxial growth and devices. I believe that we can provide the best opportunity for participants to learn the current status and future prospects of Ga_2O_3 electronics and optoelectronics. At the beginning of the session, I will give a short introductory talk covering fundamental information about synthesis, material properties, and devices of Ga_2O_3 . Invited and contributed presentations on each specific topic will follow.

Fr2F1.2 **Development of (AlxGa1-x)2O3/Ga_2O_3 Heterostructures and Devices**

10:45 AM *James Speck (University of California, Santa Barbara, USA)*

INVITED

DR 5 & 6

β-Ga_2O_3 is a promising wide bandgap semiconductor for power electronics due to its ~4.8 eV bandgap, reasonable electron mobility, the availability of large area melt grown substrates, and the ability to form heterostructures by alloying on the group III site. In this presentation, we provide an overview of UCSB work on the development of plasma-assisted MBE growth of β-Ga_2O_3 , systetmatic doping studies with Sn and Ge [1], etching and contact studies [2], and the development of the heterostructure system β-(AlxGa1-x)2O3/β-Ga_2O_3 [3,4]. Recently we realized modulation doping of β-(AlxGa1-x)2O3/β-Ga_2O_3 and demonstrated basic MODFET transistors with sheet charge densities as high as $1.2x10^{13}$ cm^{-2} [5]. We summarize the many opportunities and challenges in materials growth and development of a viable device technology.

Fr2F1.3 **Development of Halide Vapor Phase Epitaxy of Ga_2O_3 for Power Device Applications**

11:20 AM *Yoshinao Kumagai (Tokyo University of Agriculture and Technology, Japan)*

INVITED

DR 5 & 6

High-speed growth of thick and high-purity β-Ga_2O_3 layer by atmospheric-pressure halide vapor phase epitaxy (HVPE) is described. GaCl generated by the reaction between Ga metal and Cl2 at 850°C and an oxygen source gas were transported by N_2 carrier gas to the growth zone. It was found that the use of O_2 or H_2O as an oxygen source gives a high growth rate more than 10 μm/h at the growth temperature of 1000°C on (001) β-Ga_2O_3 substrates. However, the layer grown using H2O revealed increased Si impurity and effective donor concentrations (N_D-N_A) of 2×10^{16} cm^{-3}, while the layer grown using O_2 revealed Si impurity concentration below 2×10^{15} cm^{-3} and N_D-N_A of below 10^{13} cm^{-3}. Thus, the non-hydrogenous GaCl-O_2-N_2 system is effective to achieve growth of high-purity layer, which enabled control of n-type carrier concentration within the range of 10^{15} to 10+ cm^{-3} by intentional Si doping using $SiCl_4$ gas

Fr2F1.4 **Material and Device Engineering for Gallium Oxide Field Effect Transistors**

11:55 PM *Siddharth Rajan (The Ohio State University, USA)*

INVITED

DR 5 & 6

Recent development of β-Ga_2O_3 based field effect transistors will be discussed, including delta-doped and modulation-doped β-(AlxGa1-x)2O3/Ga_2O_3 field effect transistors. β-phase Ga_2O_3 has emerged as a promising candidate for a wide range of device applications. The wide bandgap energy and the predicted high breakdown field, together with the availability of low-cost native substrates, make β-Ga_2O_3 a promising material compared to other conventional wide bandgap materials, such as GaN and SiC. We will discuss recent advances in development of lateral transistors, and the demonstration delta-doped β-Ga_2O_3 MESFETs and β-(AlxGa1-x)2O3/Ga_2O_3 MODFETs as promising candidates for electronic device applications. The 2-dimensional electron gas channels formed in both the MESFET and the MODFET structures can enable aggressive vertical scaling, which is beneficial for the applications of β-Ga_2O_3 in both power and high-frequency devices.

Fr3A8: Photonics

Time:	6/1/2018, 01:30 PM - 03:00 PM
Room:	Salon M (Samberg Conference Center, 7th floor)
Chair:	Mikhail Belkin (The University of Texas at Austin, United States)

Fr3A8.1

01:30 PM

INVITED

Salon M

Heterointegration of Photonics and IR Materials on Large-mismatched Substrates via Direct MBE Growth

Amy W. K. Liu (IQE Inc., USA); Dmitri Loubychev and Joel Fastenau (IQE Inc, USA); Aled Morgan and Stuart Edwards (IQE Silicon, United Kingdom (Great Britain)); Matthew Fetters, Hubert Krysiak, Joe Zeng, Michael Kattner, Phil Frey and Scott Nelson (IQE Inc., USA); Rowel Go, Pedro Figueiredo, Matthew Suttinger and Arkadiy Lyakh (University of Central Florida, USA)

Heterogeneous integration of III-V semiconductor devices with Si CMOS circuitry has attracted significant interest for its potential in next generation monolithic hybrid integrated circuits and silicon photonics applications. Such integration provides the combined advantages of high level integration and volume production of Si-based electronic circuitry with superior high speed and optical performance of III-V components. Various technologies have been implemented to achieve this, from pick-and-place die transfer to full wafer bonding to direct growth of III-V's on Si, but all require the implementation of high-quality III-V epilayers on Si CMOS host substrates. Several direct heteroepitaxial growth approaches to monolithic integration of III-V optical and IR device on Si substrates will be presented. Focus will be on comparing InP- and GaSb-based device structures grown on GaAs and Ge-coated Si substrates.

Fr3A8.2

02:00 PM

Salon M

High Responsivity InP Nano Photo-Detector Monolithic Integrated on (001) Silicon Substrates by Heteroepitaxy

Zhao Yan (The Hong Kong University of Science and Technology, Hong Kong); Yu Han and Kei May Lau (Hong Kong University of Science and Technology, Hong Kong)

With strong confinement of the optical modes inside nanowires, nanowire photodetectors have been demonstrated with higher responsivity when compared to conventional planar devices. However, practical devices applications is limited by the transfer onto another host substrate and random wire orientations. Here we report on high responsivity InP nano-ridge photodetectors monolithic integrated on industry standard (001) Si substrates by direct heteroepitaxy. Highly ordered in-plane InP nano-ridges were grown on patterned Si substrates using the aspect ratio trapping technique. From X-Ray diffraction and transmission electron microscope characterization, the InP nano-ridges show good crystalline quality. InP nano photodetectors were fabricated with a two-step process, and demonstrated with record high responsivity on CMOS compatible (001) Si substrates. These results suggests their potential applications in Si based photonic integrated circuits.

Fr3A8.3

02:15 PM

Salon M

GaSb Based Materials and Devices Epitaxially Grown onto Silicon

Evangelia Delli, Peter Hodgson, Eva Repiso, Jonathan Hayton and Adam Craig (Lancaster University, United Kingdom (Great Britain)); Richard Beanland (University of Warwick, United Kingdom (Great Britain)); Andrew R J Marshall, Anthony Krier and Peter Carrington (Lancaster University, United Kingdom (Great Britain))

III-V semiconductor heterostructures grown on GaSb and InAs substrates are widely used to produce high performance optoelectronic devices operating in the technologically important mid-infrared spectral (MIR) range. However, these substrates are expensive, have poor thermal conductivity and only available in small sizes. Integration onto Si substrates offers the opportunity to overcome these shortcomings and opens the possibility of new applications in lab-on-chip MIR photonic integrated circuits. However, there are several fundamental problems in the growth on silicon, such as the large lattice and thermal coefficients mismatch and the polar/non-polar character of the III-V/Si interface which lead to antiphase domains (APDs). In this work, we report on novel growth techniques using molecular beam epitaxy to produce high quality APD-free GaSb epilayers onto Si. InAsSb based light emitting diodes grown on top of the GaSb/Si buffer layers are also reported which show bright electroluminescence peaking at 4.5 μm at room temperature.

Fr3A8.4

02:30 PM

Salon M

Defect Filtering in InP-on-Si via Strain-Compensated InGaAsP Superlattices in MOCVD

Ludovico Megalini (UCSB, USA); Simone Tommaso Šuran Brunelli (University of California Santa Barbara, USA); Aidan Taylor (UCSB, USA); William Charles (SUNY Polytechnic Institute, USA); Brandon Isaac (University of California, Santa Barbara, USA); John E Bowers (University of California, USA); Jonathan Klamkin (University of California Santa Barbara, USA)

The use of InGaAsP strain compensated super lattices (SCSLs) is reported as means to reduce threading dislocation density in the InP-on-GaAs-on-Si heteroepitaxy via metal organic chemical vapor deposition (MOCVD). Compared to the strain uncompensated structure, strain compensation has been suggested to be beneficial in reducing the generation of misfit dislocation. Each layer was individually calibrated with conventional homo-epitaxy and its strain estimated with X-ray diffraction (XRD) measurements. Substrates used are 300 mm in diameter, (001) exact oriented silicon wafers which were nano-patterned with silicon dioxide stripes to produce aspect ratio trapping mechanisms, then v-grooves were etched to expose the [111] facets in the formed trenches to reduce anti phase boundary formation while over-etching to produce an undercut beneath the oxide mask to exploit defect necking mechanisms. Grown samples were then characterized utilizing electron channeling contrast imaging (ECCI), transmission electron microscopy (TEM), XRD and atomic force microscopy (AFM).

Fr3A8.5

02:45 PM

Salon M

High-efficient InP-based Waveguide Photodiodes Monolithically Integrated with 90° Hybrid Towards Next-Generation Coherent Transmission Systems

Takuya Okimoto (Sumitomo Electric Device Innovations, Inc., Japan); Hideki Yagi (Sumitomo Electric Industries, LTD., Japan); Satoru Okamoto, Kenji Sakurai, Koji Ebihara, Kouichiro Yamazaki, Yoshifumi Nishimoto, Kazuhiko Horino, Tatsuya Takeuchi and Yasuo Yamasaki (Sumitomo Electric Device Innovations, Inc., Japan); Mitsuru Ekawa (Sumitomo Electric Industries, Ltd., Japan); Yoshihiro Yoneda (Sumitomo Electric Device Innovations, Inc., Japan)

Toward the next generation coherent transmission system over 1 Tb/s, further wide 3-dB bandwidth of InP-based photodiodes monolithically integrated with the 90° hybrid through the butt-joint regrowth process is expected to realize 100 Gbaud coherent receivers. However, tradeoff between the wide 3-dB bandwidth and high responsivity occurs because a thinner absorption layer of photodiodes brings about the decrease of optical coupling efficiency due to mismatch of mode fields at the butt-joint interface. In this paper, we report an investigation of new waveguide photodiodes which enables us to overcome this tradeoff. By inserting n^--GaInAsP layer under the absorption layer, our new photodetector exhibited high responsivity as high as 0.150 A/W at a wavelength of 1.55 μm which was 10% higher than that of the previous one and wide 3 dB bandwidth of 50 GHz under high optical input power condition.

Fr3B8: Nanostructures

Time:	6/1/2018, 01:30 PM - 03:00 PM
Room:	DR 3 & 4 (Samberg Conference Center, 6th floor)
Chair:	Katsuhiro Tomioka (Hokkaido University, Japan)

Fr3B8.1

01:30 PM

DR 3 & 4

Single Nanowire Laser with GaAsSb-based Multiple-Superlatticed Gain Structure

Dingding Ren (Norwegian University of Science and Technology, Norway); Lyubomir Ahtapodov and Julie Nilsen (NTNU, Norway); Jianfeng Yang (University of New South Wales, Australia); Anders Gustafsson (Lund University, Sweden); Junghwan Huh (NTNU, Norway); Gavin Conibeer (UNSW Australia, Australia); Antonius van Helvoort (NTNU, Norway); Bjørn-Ove Fimland and Helge Weman (Norwegian University of Science and Technology, Norway)

In this contribution, we report on the realization of high quality-factor, single-mode, room-temperature lasing from single nanowires containing multiple (up to six) GaAsSb/GaAs superlattices by pulsed laser excitation. Nanowire superlattices were grown by molecular beam epitaxy on an electron beam patterned Si(111) substrate with SiO_2 mask into dense arrays with high-yield. By changing the Sb composition in the GaAsSb superlattices, the lasing wavelength can be tuned from 890 nm to 990 nm. The radiative recombination takes place in the GaAsSb potential wells of the superlattices, resulting in a reduced lasing threshold ~ 75 uJ/cm^2 per pulse and a high characteristic temperature of ~ 129 K. Polarization measurements show that the lasing emission is strongly polarized perpendicular to the nanowire axis, which correlates well to the TE01 mode from finite-difference time-domain simulations.

Fr3B8.2

01:45 PM

DR 3 & 4

Fully-Strained InGaAs/InP Quantum Well Nanopillar Lasers on Silicon with Dimensions Far Exceeding the Critical Thickness

Kar Wei Ng (University of Macau, Macao); Jonas Kapraun, Fabian Schuster and Connie J. Chang-Hasnain (University of California Berkeley, USA)

The integration of III-V-based optoelectronics with silicon is promising in enabling unprecedented functionalities while reducing power consumption in personal electronics. Here, we demonstrate a potential pathway via the growth of In0.28Ga0.72As/InP quantum well (QW) nanopillar lasers on silicon using metalorganic chemical vapor deposition. High-resolution transmission electron microscopy shows that the wurtzite crystal lattice continues seamlessly across the 20-nm InGaAs well and InP barrier without any observable misfit dislocations. Diffraction patterns taken at the QWs reveal that the 5-period QWs are fully bi-axially strained in the {1$\bar{1}$20} planes. Such fully-strained growth is extraordinary considering that the total QW thickness is 15 times over the theoretical critical value under >1.7% lattice mismatch. Upon optical pump, we observed prominent emission near 1300-nm. Lasing action can be achieved under higher

pump power, attesting to the high-quality strained QWs and excellent optical confinement provided by the pillar cavity.

Fr3B8.3 **Self-assembled InGaAs Quantum Dots for Quantum Nanophotonics**

02:00 PM *Allan Bracker (Naval Research Lab, USA)*

INVITED

DR 3 & 4

Semiconductor quantum dots are promising components for single or entangled photon sources, sensors, and as nonlinear nodes in photonic neural networks. Unfortunately, their stochastic growth process makes it difficult to integrate them into complex photonic devices using standard fabrication techniques. To address the random growth positions of quantum dots, we have developed a patterned-substrate technique to control nucleation position, while still maintaining excellent optical properties. The natural inhomogeneity in quantum dot emission energies can be overcome with a laser-induced heating and crystallization of a hafnium oxide coating that locally strains individual quantum dots in a GaAs membrane. This talk will describe these techniques as well as recent work on an energy-tunable Raman single photon source and spin-sensitive motion sensing in a membrane resonator.

Fr3B8.4 **High-density InAs Quantum Dots for High-Efficiency Photodetection in Telecom and THz Band**

02:30 PM

DR 3 & 4

Toshimasa Umezawa (National Institute of Information and Communication Technology (NICT), Japan); Kouichi Akahane, Atsushi Matsumoto, Atsushi Kanno and Naokatsu Yamamoto (National Institute of Information and Communications Technology, Japan)

III-V quantum dots are very attractive for high-sensitivity photodetection devices in telecommunication and THz-wave communications, as well as solar-cell applications. Because of the high efficiency related to discrete quantum energy levels, and sufficient low dark current caused by the carrier confinement effect can be expected, quantum dot based infrared photodetectors (QD-PD) in the 5-20 μm wavelength range were reported. However, low temperature operation at 77 K was required for infrared photodetection. The operational temperature strongly depends on the QD conditions, including the density and uniformity. Moreover, very few reports on highly efficient QD-PD, related to 1.5 μm optical fiber communication (telecom) applications have been presented. In this work, we report a 1.5-10 μm QD-PD, which is applicable for telecom and THz-wave detection applications.

Fr3B8.5

02:45 PM

DR 3 & 4

Unique Polarization-Dependent Photoluminescence Property of GaSb/GaAs Quantum Dots on (001) Ge Substrate Grown by Molecular Beam Epitaxy

Zon Zon, Pakawat Phienlumlert and Supachok Thainoi (Chulalongkorn University, Thailand); Suwit Kiravittaya (Naresuan University, Thailand); Aniwat Tandaechanurat (International School of Engineering (ISE), Chulalongkorn University, Thailand); Noppadon Nuntawong (NECTEC, Thailand); Suwat Sopitpan (Thai Microelectronics Center (TMEC), Thailand); Visittapong Yordsri (National Metal and Materials Technology Center, Thailand); Chanchana Thanachayanont (National Metal and Material Technology Center, Thailand); Songphol Kanjanachuchai, Somchai Ratanathammaphan and Somsak Panyakeow (Chulalongkorn University, Thailand); Yasutomo Ota (The University of Tokyo, Japan); Satoshi Iwamoto and Yasuhiko Arakawa (University of Tokyo, Japan)

Complex nanostructures can provide unique electronic/optical characteristics. Here, we report a combined growth of elongated self-assembled GaSb/GaAs quantum dots (QDs) and growth of GaAs on (001) Ge substrate. This combination leads to a QD ensemble with unique polarization properties. The photoluminescence (PL) peak emitted from GaSb QDs is observed at around 0.9 eV. The intensity is varied periodically as the polarizer angle is rotated. We observe the unique 90° periodicity of the PL intensity and it relates to the QD elongation direction. The intensity maxima are along local <110> directions of each GaAs anti-phase domain and they correspond to [110] and [1-10] directions of Ge substrate. This finding is in contrast to the 180° rotational symmetry of the polarization-dependent PL of typical elongated QDs.

Fr3C7: Novel Materials & Characterization

Time:	6/1/2018, 01:30 PM - 03:00 PM
Room:	Salon T (Samberg Conference Center, 7th floor)
Chair:	Asif Khan (Georgia Institute of Technology, USA)

Fr3C7.1

01:30 PM

INVITED

Salon T

Liquid-Solid Interface as Crystal Growth Front

Masamitu Takahasi (National Institutes for Quantum and Radiological Science and Technology, Japan)

It has been known that ordered structures are induced in liquid when it comes into contact with a crystalline substrate. Such atomic-scale orderings are relevant to various kinds of physical and chemical phenomena including crystal growth. Owing to its penetrating feature, X-ray diffraction is suitable for probing the atomic-scale ordering at the interface buried in liquid. Through in situ X-ray diffraction under MBE conditions, it has recently been confirmed that the atomic orderings formed in catalyst droplets for vapor-liquid-solid growth of semiconductor nanowires and in liquid Ga layers during RF-MBE growth of GaN. This work has presented a unique technique peering into the deeply-buried growth front that is inaccessible by conventional RHEED or optical monitors.

Fr3C7.2

02:00 PM

Salon T

Atomically-resolved Operando Surface Studies of III-V Nanowire Devices by Scanning Tunneling Microscopy and Spectroscopy

Sarah McKibbin, Johan Knutsson, James Webb, Olof Persson, Martin Hjort, Sebastian Lehmann, Kimberly A. Dick, Anders Mikkelsen and Rainer Timm (Lund University, Sweden)

Scanning tunneling microscopy and spectroscopy (STM/S) is often restricted to flat, isotropic surfaces. Here we show how STM/S can be used to also study surfaces of nanostructures with a high aspect ratio, such as nanowires, across heterostructure interfaces or even during device operation. We show atomically resolved STM images of InAs nanowires with interfaces between zincblende and wurtzite crystal phase and correlate these with STS data of the local density of states, demonstrating that the atomically abrupt structural interface is accompanied by an almost equally abrupt electronic transition. Furthermore, we present two approaches to perform STM/S studies on semiconductor nanowire devices during electrical operation, with the aim to directly investigate the influence of atomic-scale surface properties on nanostructure device performance.

Fr3C7.3 **Characterization of Epilayer Transfer by Colored Picosecond Acoustics**

02:15 PM *Arnaud Devos (IEMN CNRS, France); Patrick Emery (MENAPiC, France)*

Salon T

Numerous devices are based on semiconductor hetero-structures first grown on a specific wafer and then transferred to another. That's the case of LED, mirrors, lasers, high power transistors. The bonding quality is a critical issue for example to ensure efficient heat evacuation. The non-destructive control of a epi-layer/substrate interface is challenging. It's first buried under several microns of non transparent matter. A high sensitivity to bonding is required: strong delamination detection is not enough for the final application. Here we show how the Colored Picosecond Acoustic (APiC) technique offers a unique way to analyze the adhesion quality in complex stacks by combining light and sound at the nanoscale. APiC is a femtosecond laser technique that realizes a sonar with hypersonic waves(10-100GHz). We will present the application of the APiC technique to a non destructive mapping of adhesion in a vertical laser structure bonded to another substrate for thermal reasons.

Fr3C7.4 **Total Tomography of Nonplanar InGaAs Quantum Wells on GaAs Nanowires**

02:30 PM *Lincoln Lauhon (Northwestern University, USA)*

INVITED

Salon T

Nanoscale III-As semiconductor heterostructures, particularly nanowires with non-planar quantum wells, show great potential for next generation compact light sources and novel computing schemes. We have used atom probe tomography (APT) to map atomic distributions in three dimensions with nanoscale resolution, providing new insights into the growth mechanisms of InGaAs quantum wells on nanowire "substrates" and the non-uniform alloy and dopant distribution that result from facet-dependent kinetics. In concert, we have conducted x-ray Bragg projection ptychography to map the 3-D strain distribution both locally at heterointerfaces and globally along the length of the nanostructures; nanodiffraction also reveals the spatial distribution of stacking faults and transitions between zincblende and wurtzite phases. Knowledge of the nanoscale distribution of strain, structure, and composition is used to explain the emission characteristics of unconventional InGaAs quantum wells and provide insights into the factors that drive variations in composition.

Fr3F2: Ga_2O_3 Growth and Characterization

Time:	6/1/2018, 01:30 PM - 03:00 PM
Room:	DR 5 & 6 (Samberg Conference Center, 6th floor)
Chair:	Siddharth Rajan (The Ohio State University, United States)

Fr3F2.1

01:30 PM

DR 5 & 6

Faceting and Catalysis During Molecular Beam Epitaxy of Ga_2O_3 Homoepitaxial Thin Film

Piero Mazzolini, Patrick Vogt, Zongzhe Cheng and Michael Hanke (Paul-Drude-Institut für Festkörperelektronik, Germany); Robert Schewski (Leibniz Institute for Crystal Growth - IKZ, Germany); Charlotte Wouters (Leibniz Institute of Crystal Growth, Germany); Martin Albrecht (Leibniz Institute for Crystal Growth - IKZ, Germany); Oliver Bierwagen (Paul-Drude-Institut für Festkörperelektronik, Germany)

Gallium oxide is recently attracting large interest in the field of power electronic devices. A deep understanding of the physical mechanisms ruling its functional properties requires fine control of the material growth. We present a study on β-Ga_2O_3 thin films deposited via molecular beam epitaxy on β-Ga_2O_3 (010) substrates. By RHEED, AFM, XRD, CV, TEM we investigate the role of substrate temperature and metal-to-oxygen flux ratio on the growth rate, layer structure, and surface morphology. We identify facets commonly formed under Ga-etching and a wide range of growth conditions, and demonstrate a significant enhancement of the growth rate by the catalyzing effect of an additional In flux[1]. These growth features will be discussed in comparison to Ga_2O_3 grown on β-Ga_2O_3 (100) substrates. This work was performed in the framework of GraFOx, a Leibniz-ScienceCampus partially funded by the Leibniz association. [1] P. Vogt et al., Phys. Rev. Lett. 119, 196001 (2017).

Fr3F2.2

01:45 PM

DR 5 & 6

Phase Change of Ga_2O_3 Films Grown by HCl-Enhanced MOCVD

Haiding Sun, Kuang-Hui Li and Carlos Torres-Castanedo (KAUST, Saudi Arabia); Serdal Okur, Gary Tompa and Tom Salagaj (SMI, USA); Xiaohang Li (KAUST, Saudi Arabia)

We demonstrated, for the first time, the successful growth tuning of three different phases of Ga_2O_3 in a MOCVD reactor by changing one growth parameter. Specifically, we introduced different flow rates of HCl gas along with constant Triethylgallium and O_2 precursors to precisely control the growth rate of Ga_2O_3 in α-, β- and ε-phases. This is the first time to introduce HCl during oxides growth in a MOCVD reactor. We revealed the impact of HCl flow on the growth rate, phase transition, microstructures and optical bandgap of the investigated Ga_2O_3 samples. In this HCl-enhanced MOCVD mode, the Cl impurity concentration was almost identical among the investigated samples. It is plausible that HCl may act as a catalyst, with the increase of HCl flow, the difference in free energy between the β-, ε and α become smaller, thus forming a thermally meta-stable phase which is confirmed by our DFT calculation.

Fr3F2.3

02:00 PM

INVITED

DR 5 & 6

Growth, Doping and Defects of Homoepitaxial β-Ga203 Grown by Metal Organic Vapor Phase Epitaxy

Martin Albrecht (Leibniz Institute for Crystal Growth - IKZ, Germany)

Monoclinic Ga_2O_3 (β-Ga_2O_3) is a semiconductor with a bandgap of 4.7eV and an estimated break down field of 8 M/Vcm. While p-type conduction is hampered due to intrinsic obstacles such as self-trapping of holes and a large effective hole mass, n-type conduction is achievable by doping with group-IV elements (Si, Sn, Ge). In this presentation we will review our results on n-type doping of MOVPE grown β-Ga_2O_3 layers grown on (100), (010) and (001) oriented β-Ga_2O_3 . Based on local vibrational mode spectroscopy and electro paramagnetic resonance measurements, we show that gallium vacancies and hydrogen are involved in compensation. Silicon and tin, the n-type dopants of practical importance, are effective-mass like shallow donors without any peculiarity. Furthermore, we show that structural defects (twin lamella) contribute to compensation and reduced carrier mobility in n-type doped homoepitaxially grown layers on (100) substrates by MOVPE.

Fr3F2.4

02:30 PM

DR 5 & 6

Electronic Raman Scattering in β-Ga_2O_3

Andreas Fiedler (Leibniz Institute for Crystal Growth - IKZ, Germany); Manfred Ramsteiner (Paul-Drude-Institut für Festkörperelektronik, Germany); Zbigniew Galazka and Klaus Irmscher (Leibniz Institute for Crystal Growth - IKZ, Germany)

Here we report on Raman spectroscopy investigations of highly n-type doped β-Ga_2O_3 single crystals. For degenerate material (n > 3 × 10^{18} cm^{-3}), we observe Raman lines at about 282 cm^{-1} (with a shoulder at 255 cm−1), which coincides with the ionization energy of effective-mass like donors (≈ 36 meV), and at about 564 cm^{-1}, which cannot be assigned to first-order scattering by phonons. These lines exhibit only a weak temperature dependence and are essentially independent of the shallow donor species (Sn or Si). Based on these observations, we attribute the doping induced Raman features to electronic Raman scattering caused by excitation of electrons from an effective-mass like donor impurity band into the conduction band. Consequently, the high-frequency Raman line at 564 cm^{-1} (= 2 × 282 cm^{-1}) is explained by second-order electronic Raman scattering.

Fr3F2.5

02:45 PM

DR 5 & 6

Blue Luminescence Quenching in beta-Ga_2O_3 Epitaxial Films by Nitrogen Doping

Takeyoshi Onuma (Kogakuin University, Japan); Yoshiaki Nakata (National Institute of Information and Communications Technology, Japan); Kohei Sasaki (Novel Crystal Technology, Inc., Japan); Tatekazu Masui (Tamura Corporation, Japan); Tomohiro Yamaguchi (Kogakuin University); Tohru Honda (Kogakuin University, Japan); Akito Kuramata and Shigenobu Yamakoshi (Tamura Corporation, Japan); Masataka Higashiwaki (National Institute of Information and Communications Technology, Japan)

N-doped beta-Ga_2O_3 films generally exhibit high resistivity, and N-implanted layer works well as a current blocking layer in vertical MOSFETs. In this study, temperature-dependent cathodoluminescence (CL) spectra of N-doped epitaxial films grown by RF-MBE are measured to investigate their electronic structure and defect states. Nitrogen concentrations are varied in a range of 7E16-1E18 cm^{-3}. CL spectra at low temperature for the lightly N-doped films exhibited UV luminescence band, which has been attributed to recombination of self-trapped excitons, and blue luminescence (BL) band is alternatively observed at 300 K. On the contrary, BL band is suppressed for the heavily N-doped films at all measured temperatures. In our previous study, BL band has been found to correlate with the oxygen vacancy (V_O). The results indicate decrease in V_O concentration by N-doping. It has been proposed that V_O compensates gallium vacancy (V_{Ga}) or related complexes, contributing to activate n-type Si impurities. Accordingly, decrease in V_O concentration by N-doping contributes the compensation of Si donors by V_{Ga}.

Fr3A9: Photonics

Time:	6/1/2018, 03:30 PM - 05:45 PM
Room:	Salon M (Samberg Conference Center, 7th floor)
Chair:	Arkadiy Lyakh (University of Central Florida, USA)

Fr3A9.1

03:30 PM

INVITED

Salon M

Silicon Photonics, Optical Phased Arrays, and LiDAR

Michael Watts (MIT, USA)

We review the development of silicon photonics and its impact on communications, nonlinear optics, and optical phased arrays. From on-chip lasers to <1fJ/bit modulators, highly efficient nonlinear frequency conversion and large-scale optical phased arrays, silicon photonics impact is only just beginning to be felt. Here, we present on a decade of work in the field of silicon photonics which led to the creation of AIM Photonics. We then consider optical phased arrays in general, future application to displays, and the potential impact of silicon photonics on the emerging solid-state LiDAR market. Starting from the LiDAR equation, we review the noise performance of phased array LiDAR with direct versus coherent detection in light of automotive requirements. In view of these considerations, we discuss the current challenges, opportunities, and advantages of chip-scale optical phased array based LiDAR. The limits of current silicon photonic device performance and considerations of electrical drive, III-V laser sources, and control of large-scale optical phased arrays will be presented. Finally, recent results on coherent silicon optical phased array based LiDAR chips will be discussed.

Fr3A9.2

04:00 PM

Salon M

Demonstration of 10Gbps Fundamental Optical Logic Gate Operation Using MQW-SOA

Yota Akashi, Shin'e Matsui and Shohei Isawa (Waseda University, Japan); Atsushi Matsumoto (National Institute of Information and Communications Technology, Japan); Yuichi Matsushima (Waseda University, Japan); Hiroshi Ishikawa (Waseda University); Katsuyuki Utaka (Waseda University, Japan)

In ultrafast photonic systems, all-optical signal processing seems effective for high-speed and efficient signal routing, and for this purpose we proposed an all-optical logic gate device that integrates a semiconductor optical amplifier (SOA) and micro ring resonators (MMRs), which can operate in NOT, AND and XNOR functions using nonlinear effects of cross gain modulation (XGM) and four wave mixing (FWM) of an SOA. We have investigated the precise operation conditions for efficient nonlinearities in a multi-quantum well (MQW)-SOA, and demonstrated high-speed XNOR operation at 10Gbps, which should be suitable as a bit-matching device for signal label recognition in routers.

Fr3A9.3 **Optical NAND Logic Gates Using Light Emitting Transistor (LET)**

04:15 PM *Chi-Wei Wang (National Taiwan University, Taiwan)*

Salon M We demonstrated a optical NAND gate with light-emitting transistors serving as light-emitting devices and photo-receivers. The optical signal switch controls the HPT switch, and the voltage input controls whether the current injects into the LET or not. The optical output is complementary to the AND gate.

Fr3A9.4 **Heterogeneous Integration for On-Chip Quantum Photonics with Single InAs Quantum Dots**

04:30 PM *Marcelo Davanco (NIST, USA)*

INVITED

Salon M Single quantum emitters are an important resource for quantum photonics, constituting building blocks for single-photon sources, qubits, and deterministic quantum gates. Robust implementation of such functions, however, can only be achieved through systems that provide both strong light-matter interactions and a low-loss interface between emitter and probing optical fields. We developed a heterogeneous photonic integration platform that provides such features in a scalable on-chip implementation, allowing direct integration of GaAs nanophotonic devices containing self-assembled InAs/GaAs quantum dots within passive photonic circuits composed of low-loss Si3N4 waveguides. We demonstrate a highly efficient optical interface between Si3N4 waveguides and single-quantum dots in various types of GaAs geometries, with photonic performance approaching that of devices optimized for each material individually. We demonstrate efficient single-photon emission into passive, on-chip Si3N4 waveguides, quantum dot radiative rate enhancement in hybrid microcavities, and outline a path for reaching the non-perturbative strong-coupling regime within our platform.

Fr3A9.5 **Incorporation of InGaAlAs Electroabsorption Modulated Lasers in a Generic InP Photonic Integrated Circuits Platform**

05:00 PM

Salon M *Norbert Grote (Fraunhofer Institute for Telecommunications, Heinrich-Hertz-Institut, Germany)*

Monolithic photonic integration using a generic platform that enables designing and fabricating complex InP based photonic integrated circuits (PIC) from a defined set of building blocks represents a viable way to offer low-cost access to this demanding technology. Over the past years Fraunhofer HHI has successfully been developing such a PIC platform providing full transmit (Tx) and receive (Rx) functionalities. To enhance the Tx speed capability to > 50 Gb/s incorporation of electro-absorption modulated DFB lasers (EML), preferably comprising an Al based active region (MQW), is highly attractive. We report on the technology process to implement such EML devices on the existing generic PIC platform. Early devices in an integrated configuration exhibited fiber coupled optical power up to 2.5 mW (EAM electrically open) and a static extinction ratio of about

20 dB, with an operating bias voltage in the 0.75-1.0 V range. The bandwidth of the EML was still limited to some 20 GHz due to parasitic effects.

Fr3A9.6

05:15 PM

Salon M

Highly Reliable Grown-junction InP/InGaAs Avalanche Photodiodes for High-speed Integrated Optical Receivers

Takumi Endo, Shin-ichi Domoto, Toru Uchida, Masami Ishiura, Ikuo Hanawa, Daisei Shoji, Yoshihiro Yoneda and Atsushi Yasaki (Sumitomo Electric Device Innovations, Inc., Japan)

High-speed and high-sensitivity optical receivers for the 20-40 km transmission distance applications are expected. Avalanche photodiodes (APDs) are promising to provide the receivers which are expanded the transmission distance while suppressing the increase of electric power consumption because they have higher responsivity than p-i-n photodiodes due to their internal gain. In order to realize the high-speed APD, the thickness controllability of its thin-film multiplication layer is essential. Grown-junction APD is effective in achieving the precise thickness-controllability because of using epitaxial growth. However, there were several concerns such as the abnormal edge-breakdown and the degradation of device reliability because the multiplication layer applied with a high electric field exposes from the sidewall of mesa structure. We report the grown-junction InP/InGaAs APD which achieves both high-speed response and high reliability toward over 25 Gbaud receiver operation.

Fr3A9.7

05:30 PM

Salon M

Crosstalk Elimination in Infrared Geiger-mode Avalanche Photodiode Arrays

Mohamed Diagne, Richard Younger, Joseph Donnelly, Robert Bailey, William Goodhue, Michael Myszka, K. McIntosh and Erik Duerr (MIT Lincoln Laboratory, USA)

Intra focal plane array (FPA) crosstalk due to avalanche-emitted photons is a primary performance limiter of large 2-dimensional Geiger-mode avalanche photodiode (GmAPD) arrays. Analysis methods and experimental results from reduced-crosstalk InP-based detector arrays developed at MIT Lincoln Laboratory will be presented.

Fr3B9: Nanostructures

Time:	6/1/2018, 03:30 PM - 05:45 PM
Room:	DR 3 & 4 (Samberg Conference Center, 6th floor)
Chair:	Allan Bracker (Naval Research Lab, USA)

Fr3B9.1
03:30 PM
DR 3 & 4

Nanoscale Cathodoluminescence Investigation of GaN / AlN Quantum Dot Formation

Frank Bertram and Jürgen Christen (Otto von Guericke University Magdeburg, Germany); Gordon Schmidt (Otto-von-Guericke-University Magdeburg, Germany); Armin Dadgar (Universität Magdeburg, Germany); André Strittmatter (OvGU, Germany); Christoph Berger (University of Magdeburg, Germany); Jürgen Bläsing (OvGU, Germany); Peter Veit (Otto von Guericke University Magdeburg, Germany); Hannes Schürmann (University of Magdeburg, Germany); Sebastian Metzner (Otto von Guericke University Magdeburg, Germany)

With the objective to gain insight in the formation of MOVPE-grown GaN quantum dots a systematic series of GaN/AlN quantum dot samples with varying growth interruption time after GaN deposition have been grown. A direct nano-scale correlation of structural and optical properties of the sample set has been achieved using highly spatially resolved scanning transmission electron microscopy (STEM) as well as cathodoluminescence spectroscopy at low temperatures (LHe) directly performed in a STEM.

Fr3B9.2
03:45 PM
DR 3 & 4

Monitoring the Formation of GaN Nanowires in Molecular Beam Epitaxy by Polarization-Resolved Optical Reflectometry

Gabriele Calabrese (Paul-Drude-Institut für Festkörperelektronik, Germany); Pierre Corfdir (Paul-Drude-Institut, Germany); Apurba Laha (Indian Institute of Technology Bombay, India); Thomas Auzelle, Lutz Geelhaar, Oliver Brandt and Sergio Fernández-Garrido (Paul-Drude-Institut für Festkörperelektronik, Germany)

We explore the use of polarization-resolved laser reflectometry for monitoring the self-assembled formation of GaN nanowires on Si(111) in plasma-assisted molecular beam epitaxy. The growth of two nanowire ensembles is monitored using either transverse electric or magnetic polarized light. For both samples the reflectance exhibits an oscillatory behavior and the intensity maxima of the oscillations decrease during growth. For a quantitative understanding of the evolution of the reflected signal, the reflectance is computed using an effective medium approach. An attenuation factor is introduced in our simulations to reproduce the damping in the oscillations, attributed to increasing inhomogeneities in the thickness of the effective medium. Our simulations allow us to obtain in situ the temporal variation of the root mean square of the surface roughness, due to variations on a µm scale in the nanowire length and fill factor. Such information can not be obtained in situ using other characterization techniques.

Fr3B9.3

04:00 PM

INVITED

DR 3 & 4

MBE Growth of GaAs Nanowires Observed in Situ by TEM

Jean-Christophe Harmand (Centre de Nanosciences et de Nanotechnologies, CNRS; Université Paris-Saclay, France)

We will present original experiments of GaAs nanowire growth by molecular beam epitaxy (MBE) performed in an aberration-corrected transmission electron microscope (TEM). Growth proceeds by vapour-liquid-solid mechanism with a liquid (Au,Ga) catalyst droplet on top of the nanowires. The formation of each GaAs monolayer can be observed in real-time with the atomic resolution and the average growth rate can be easily adjusted within a large range. Relevant time scales and key parameters governing the morphological and structural characteristics of the nanowires are extracted.

Fr3B9.4

04:30 PM

DR 3 & 4

Intervalley Scattering and Interband Carrier Dynamics of the Γ3 and Γ1 Energy Bands of InN Using Ultrafast Spectroscopic Techniques

Blair C Connelly, Chad S Gallinat and Michael Wraback (US Army Research Laboratory, USA)

The band structure, and intervalley scattering and intraband carrier dynamics of the Γ1 and Γ3 valleys of InN are studied using ultrafast differential reflection (ΔR/R) and time-domain THz spectroscopy to monitor the evolution of carriers throughout the band structure. A 400-nm (800-nm) pump beam is used to excite electrons into the Γ3 (Γ1) valley, while a probe/second-pump beam - tuned both above (400 nm) and below (600 nm and 800 nm) the Γ3 valley, and above (800 nm) and below (2 μm and 2.2 μm) the Γ1 valley - monitors both ΔR/R and the THz signal as a function of time after the initial pump pulse. The combined measurements reveal a faster-than-previously-observed ~280-fs time associated with all intervalley scattering events (Γ3 to Γ1, or Γ1 to Γ3 to Γ1), followed by relaxation to the Γ1 valley minimum within ~600 fs, density-dependent carrier cooling in 10-20 ps, and a 350-ps recombination lifetime.

Fr3B9.5

04:45 PM

DR 3 & 4

THz Radiation Excited by Ultrafast Pulses from the Surface of Indium Nitride Nanomaterials

Chan-Shan Yang (National Taiwan Normal University, Taiwan); Tzu-Yuan Huang (National Tsing Hua University, Taiwan); Lung-Hsing Hsu, Tsung-Sheng Kao, Chien-Chung Lin and Hao-Chung Kuo (National Chiao Tung University, Taiwan); Osamu Wada (Kobe University, Japan); Ming-Chang Chou and Wai-Keung Lau (National Synchrotron Radiation Research Center, Taiwan); C. L. Pan (National Tsing Hua University, Taiwan)

Terahertz (THz) emission properties of InN have been investigated under femtosecond optical pulse excitation. THz intensity dependences on the incident angles and polarization angles of optical excitation have been systematically analyzed and compared with simulation based on optical rectification and Fresnel reflection from the surface. Agreement between the experiment and simulation has led to an unambiguous determination of THz emission mechanism as well as an optimization of films or pyramids structure and optical excitation conditions.

Fr3B9.6

05:00 PM

DR 3 & 4

Towards Nanowire HBT: Minority Charge Carrier Transition Through Npn Core-Multishell Nanowires

Lisa M Liborius, Khaled Arzi, Claudia Speich, Werner Prost, Franz-Josef Tegude, Artur Poloczek and Nils Weimann (University of Duisburg-Essen, Germany)

The I-V characteristics of radial heterostructure n-GaAs/InGaP/p-GaAs nanowire diodes have been investigated in this report. The reverse current of diodes with an InGaP spacer thickness <20 nm are dominated by tunneling processes with poor rectification properties. By increasing the spacer thickness from 20 nm to 100 nm a dominant enhancement has been achieved with respect to reverse currents and rectification ratios up to $2x10^6$. Dark saturation current densities as low as 20 pA/cm^2 and ideality factors of 1.3 are extracted from forward I-V characteristics. The improved reverse current behavior of the diodes allows the application as base-collector diode in a nanowire npn structure with an additional n-doped InGaP shell as emitter. Common emitter output characteristics with a current gain $\beta<1$ were measured, indicating a voltage controlled minority transport through the p-GaAs base shell in nanowires for the first time. The results will guide the development towards a nanowire bipolar transistor.

Fr3B9.7 **Reverse Bias Annealing Effects in N-polar GaN/AlGaN/GaN MIS-HEMTs**

05:15 PM

DR 3 & 4

Tetsuya Suemitsu (Tohoku University, Japan); Kiattiwut Prasertsuk (Institute for Materials Research, Tohoku University; Thai Microelectronics Center (TMEC), Japan); Tomoyuki Tanikawa (Institute for Materials Research, Tohoku University, Japan); Takeshi Kimura and Shigeyuki Kuboya (Tohoku University, Japan); Takashi Matsuoka (Institute for Materials Research, Tohoku University, Japan)

A reverse bias annealing (RBA) is performed on N-polar MIS HEMTs for the first time, and the results are compared with those for Ga-polar MIS HEMTs. In both N- and Ga-polar HEMTs, a hysteresis in double-sweep transfer characteristics was minimized by RBA with the condition of a negative gate bias of -10 V with the source and drain electrodes grounded. However, only the N-polar HEMT exhibited about 20% decrease in the maximum drain current density while no degradation in the drain current was observed in the Ga-polar HEMT. Such a different behavior between the N- and Ga-polar HEMTs might be ascribed to the difference in the current path during RBA. The degradation in the drain current in N-polar HEMTs has been successfully minimized by the two-terminal RBA, in which the reverse bias was applied to the gate with only the drain electrode grounded while the source electrode was open.

Fr3B9.8 **200 mm GaN-on-Silicon X-Band Microstrip MMIC with Cu Damascene**

05:30 PM

DR 3 & 4

Jeffrey LaRoche, Kelly Ip and Theodore Kennedy (Raytheon, USA); Lovelace Soirez (Skorpios, USA); Charles Wang, Azin Zarrasvand, Emily O'neill, William Davis, Clay Long, Eduardo Chumbes, Matthew Walsh, John Bettencourt and Kyle Richard (Raytheon, USA); Tina Trimble (Skorpios, USA); Thomas Kazior (Raytheon, USA)

Raytheon is developing a submicron (≤ 250 nm gate) GaN-on-Si, microstrip (50 µm thick), MMIC process on 200mm <111> Si with a copper (Cu) Damascene back end of line (BEOL) in a silicon foundry. This process is a fully subtractive (no liftoff), Au-free process that is optimized for low breakage on high-resistance (≥ 1,000 ohm-cm) Si wafers. Recently, this process development has demonstrated a full 250nm gate length, X-Band (9-10 GHz) GaN-on-MBE-Si microstrip MMIC peaking at 9.6 GHz with 1.1 W (1.3 W) output power and 38.9% (28.8%) PAE at 12 Vd (18Vd) as shown in Fig. 7. To the best of our knowledge this is the first demonstration of a GaN MMIC fully processed in a Si foundry.

Fr3C8: Novel Materials & Devices

Time:	6/1/2018, 03:30 PM - 05:45 PM
Room:	Salon T (Samberg Conference Center, 7th floor)
Chair:	Lincoln Lauhon (Northwestern University, United States)

Fr3C8.1 **Negative Capacitance Transistors: Physics, Materials and the State-of-Art**

03:30 PM *Asif Khan (Georgia Institute of Technology, USA)*

INVITED

Salon T

Negative capacitance transistors owing to the sub-60 mV/decade switching characteristics can enable the reduction of power supply voltage and the power dissipation in future nodes. This talk will give an overview of the exciting developments in the field of negative capacitance over the past nine years starting from the theoretical prediction in 2008 to the clean experimental demonstration of this phenomenon in ferroelectric materials and transistors recently. All three aspects of this technology: physics, materials and devices will be discussed.

Fr3C8.2 **Negative Capacitance MoS2 FET with Doped HfO_2 Ferroelectric/dielectric Gate Stack**

04:00 PM *Ahmad Zubair, Amirhasan Nourbakhsh, Mark Theng and Tomás Palacios (Massachusetts Institute of Technology, USA)*

Salon T

Obtaining a subthreshold swing (SS) below the thermionic limit of 60 mV/dec by exploiting the negative-capacitance (NC) effect in ferroelectric (FE) materials is a novel effective technique to allow the reduction of the supply voltage and power consumption in field effect transistors (FETs). At the same time, two-dimensional layered semiconductors, such as molybdenum disulfide (MoS_2), have been shown to be promising candidates to replace silicon MOSFETs in sub-5 nm-channel technology nodes. We demonstrate NC MoS_2 FETs by incorporating an atomic layer deposited ferroelectric Al (or Si)-doped HfO_2 , a technologically compatible material, in the FET gate stack.The minimum SS (SSmin) of the NC-MoS_2 FET built on the FE bilayer improved to 57 mV/dec at room temperature, compared with SSmin = 67 mV/dec for the MoS2 FET with only HfO_2 as a gate dielectric.

Fr3C8.3 **Band Gap Tuning Across the Visible Spectrum Without Alloying**

04:15 PM *Robert Makin, III and Krystal York (Western Michigan University, USA); Nancy Senabulya, James Mathis and Roy Clarke (University of Michigan, USA); Nathaniel Feldberg and Patrice Miska (Universite de Lorraine, France); Christina Jones, Logan Williams and Emmanouil Kioupakis (University of Michigan, USA); Roger Reeves (University of Canterbury, New Zealand); Steve Durbin (Western Michigan University, USA)*

Salon T

We introduce a revolutionary alloy-free approach to tuning band gap energy across the entire visible spectrum by systematic modification of cation sublattice ordering in two novel heterovalent semiconductors. Using this methodology, we present both theoretical and experimental support for an unprecedented degree of band gap variation (over 1 eV) and submit that in the case of ZnSnN2 and MgSnN2, we now have a viable alternative to the commercially dominant InGaN family of alloys. As part of the study, we report the first ever synthesis of MgSnN2 and confirm theoretical predictions for the structure and band gap of MgSnN2.

Fr3C8.4 **Topological Spintronic Devices**

04:30 PM *Nitin Samarth (The Pennsylvania State University, USA)*

INVITED

Salon T

Tetradymite narrow bandgap semiconductors (Bi2Te3, Bi2Se3, Sb2Te3, and their alloys) are known to support topologically protected, two dimensional (2D) helical Dirac fermion surface states characterized by a spin-texture in momentum space. The 'spin-momentum locking' of the 2D surface states in these three dimensional (3D) 'topological insulators' lends itself naturally to 'topological spintronics,' device applications that might exploit efficient spin-charge interconversion. We present an introductory overview of the emergence of 'topological spintronics' and then focus on recent experiments that probe spin-charge interconversion at the interface between a 3D topological insulator and an insulating ferrimagnet, with a view toward understanding how the spin Hall conductivity in topological insulators varies with chemical potential. An important issue examined in this context is the relative contribution to spin-charge conversion of the surface and bulk states, both of which have large spin-orbit coupling in the tetradymites. Finally, we address emerging demonstrations of spin-orbit torque switching using topological insulator/ferromagnetic metal heterostructures.

Fr3C8.5 **Silicene-on-silicide Platform**

05:00 PM *Cameron Volders, Anna Costine and Petra Reinke (University of Virginia, USA)*

Salon T

Silicene is a 2D material and close relative to graphene, and has been predicted to feature complex quantum phases. Silicene layers, which are synthesized on h-MoSi2(0001) nanocrystals present a low-buckled conformation, which is desirable to conserve the Dirac cone. We demonstrated the synthesis of silicene on MoSi2 with an STM study. Silicene is a high-T reconstruction and in epitaxial registry with the Si(001) substrate and the silicide crystallites. Scanning tunneling spectroscopy maps give insight in the coupling between silicide and silicene, and the LDOS across the silicene layer. The LDOS of h-MoSi2(0001) shows a bandgap as expected from the bandstructure and the LDOS of silicene is in agreement with the literature. Silicene is resilient to oxidation in comparison to other silicide surfaces, and presents characteristic defect motifs/perimeter states. The silicene-on-silicide platform provides a unique opportunity for device integration, and can potentially serve as a starting surface for atomic scale printing.

Fr3F3: Ga_2O_3 Characterization & Devices

Time:	6/1/2018, 03:30 PM - 05:45 PM
Room:	DR 5 & 6 (Samberg Conference Center, 6th floor)
Chair:	Gregg Jessen (Air Force Research Laboratory, United States)

Fr3F3.1 **Ultrafast Dynamics of Carrier and Exciton Recombination in beta-Ga_2O_3**

03:30 PM

DR 5 & 6

Okan Koksal and Farhan Rana (Cornell University, USA); Jared Strait (NIST, USA); Nicholas Tanen, Debdeep Jena and Huili Xing (Cornell University, USA)

In this work, we investigate ultrafast dynamics associated with the radiative and non-radiative recombination of photo-excited electrons-holes and excitons in beta-Ga_2O_3 by ultrafast photoluminescence (PL) and optical pump-probe spectroscopies. Our results can be explained by considering different pathways for carrier and exciton recombination in beta-Ga_2O_3 . In this paper, we will present physical models that explain our data and shed light on the ultrafast carrier and exciton dynamics in beta-Ga_2O_3 .

Fr3F3.2 **Electronic Transport of Donors and Acceptors in β-Ga_2O_3**

03:45 PM

DR 5 & 6

Shin Mou and Adam Neal (Air Force Research Laboratory, USA); Subrina Rafique (Case Western Reserve University, USA); Hongping Zhao (Ohio State University, USA); Elaheh Ahmadi (UC-Santa Barbara, USA); James Speck (UCSB, USA); Darren Thomson, Neil Moser, John Blevins, Kelson Chabak and Gregg Jessen (Air Force Research Laboratory, USA)

We have undertaken a study of Si, Ge shallow donors and Fe, Mg compensating acceptors in Ga_2O_3 through temperature dependent van der Pauw and Hall effect measurements of samples grown by a variety of methods, including edge-defined film-fed (EFG), Czochralski (CZ), molecular beam epitaxy (MBE), and low pressure chemical vapor deposition (LPCVD). Through fitting of the temperature dependent carrier density and mobility, we accurately determine the donor energies of both Si and Ge to be 30 meV in β-Ga_2O_3, enabled by accurate estimation of the compensating acceptor concentrations through mobility fitting. We also show that our Hall effect data are consistent with Si and Ge acting as typical shallow donors, rather than DX centers, about which there is some debate. High temperature Hall effect measurements of Fe doped β-Ga_2O_3 indicate that it remains weakly n-type, with an acceptor energy of 860 meV relative to the conduction band for the Fe deep acceptor. Van der Pauw measurements of Mg doped Ga_2O_3 indicate an activation energy of 1.1 eV, as determined from the temperature dependent conductivity.

Fr3F3.3

04:00 PM

DR 5 & 6

Trapping Effects in Si delta-Doped beta-Ga_2O_3 MESFETs

Joe McGlone, Zhanbo Xia, Chandan Joishi and Siddharth Rajan (The Ohio State University, USA); Steven Ringel (the Ohio State University, USA); Aaron Arehart (The Ohio State University, USA)

The impact of traps in β-Ga_2O_3 metal-semiconductor field effect transistors are discussed, focusing on the strong impact of buffer traps and buffer design on the terminal characteristics. Trap-induced threshold voltage (VT) instabilities upwards of 1.2 V are reported, along with their connection between intrinsic defects, impurities, and the role of the Fe-doped substrate. The MESFETs VT instabilities are due to two traps, Ec-0.70 and Ec-0.77 eV, where the Ec-0.77 eV trap is absent in the sample with a thick buffer layer. It is suggested the Ec-0.70 eV and Ec-0.77 eV traps are due to gallium vacancies and Fe impurities, respectively, which is consistent with previous studies. It is also shown that the measured gate leakage is dependent on the sample's atmosphere (i.e. air or vacuum) during the measurement, potentially caused by a surface leakage mechanism or a change in the gate-drain field profile. Therefore, both buffer design and surface passivation will be important areas of study for optimal transistor performance.

Fr3F3.4

04:15 PM

DR 5 & 6

Evaluation of Electrical and Thermal Performance of β-Ga_2O_3 MOSFETs for RF Operation

Manikant Singh, James Pomeroy, Callum Middleton and Michael J Uren (University of Bristol, United Kingdom (Great Britain)); Michael Casbon and Paul J Tasker (Cardiff University, United Kingdom (Great Britain)); Man Hoi Wong (National Institute of Information and Communications Technology, Japan); Kohei Sasaki (Novel Crystal Technology, Inc., Japan); Akito Kuramata and Shigenobu Yamakoshi (Tamura Corporation, Japan); Masataka Higashiwaki (National Institute of Information and Communications Technology, Japan); Martin Kuball (University of Bristol, United Kingdom (Great Britain))

β-Ga_2O_3 is a wide bandgap (4.9eV) semiconductor with an electric breakdown strength of 8 $MVcm^{-1}$. The Baliga figure of merit (BFOM) is 4× that of GaN which combined with the availability of large single crystal substrates, grown using relatively low cost melt grown methods has generated interest in β-Ga_2O_3 switch devices. We show an RF device with good CW large signal PAE of 9.1%, drain efficiency of 19.5% with Pout of 0.11W/mm at 1GHz even in a long gate length device. These values further improve to 12.2% PAE, 22.4% drain efficiency and Pout of 0.13W/mm for pulse operation. Using Gate and drain lag Pulse IV measurements we show minimal dispersions indicating minimal trapping and good epitaxy. Further using pulse study and elevated temperature measurements we show that thermal limitations seem to be a bigger hurdle limiting device performance than electronic traps. We assess the thermal resistance using Raman thermography and simulation. We measure a maximum temperature of 575°C close to the gate contact at a power dissipation of 5W/mm. Considering that the Raman measurement is spatial averaging over a depth, the measured value is a lower limit for

the channel temperature, resulting in a peak channel thermal resistance of 128 K·mm/W.

Fr3F3.5 **Threshold Voltage Engineering in E-mode Ga_2O_3 Fin-channel Transistors**

04:30 PM

DR 5 & 6

Wenshen Li, Zongyang Hu, Zexuan Zhang, Kazuki Nomoto and Nicholas Tanen (Cornell University, USA); Kohei Sasaki and Akito Kuramata (Novel Crystal Technology, Inc., Japan); Tohru Nakamura (Hosei University, Japan); Debdeep Jena and Huili Xing (Cornell University, USA)

Ga_2O_3 has emerged as an attracting material for high-power high-temperature electronics. The fin-shaped channel is a highly desired device topology to realize enhancement-mode operation, which can be employed in lateral or vertical transistors. In this work, we report the first demonstration of Vth engineering in E-mode Ga_2O_3 vertical fin-channel transistors. An increase of Vth from ~1.6 V to ~2.4 V is observed when the fin width (Wfin) is reduced from 0.4 μm to 0.1 μm. The Dit profile is extracted using the conductance method from the frequency-dependent C-V measurements. An analytical express for Vth is presented and an excellent match with the experimental data is achieved based on the extracted Qit (ϕs) and Dit profile. This work demonstrated a simple method to engineer Vth in Ga_2O_3 fin-channel transistors by varying the fin width and important understandings of the interface between Al_2O_3 and processed Ga_2O_3 .

Fr3F3.6 **P-type Cuprous Iodide Heterojunction with N-type Gallium Oxide**

04:45 PM

DR 5 & 6

Andrew Koehler and Marko Tadjer (Naval Research Laboratory, USA); James Gallagher (ASEE Postdoctoral Fellow Residing at Naval Research Laboratory, USA); Glenn Jernigan, Karl Hobart and Fritz Kub (Naval Research Laboratory, USA)

β-Ga_2O_3 is a front-runner in the competition for an ultrawide bandgap power semiconductor technology to supersede traditional wide bandgap materials, such as SiC and GaN. However, the difficulty in realizing p-type doping of β-Ga_2O_3 limits device architectures, as essentially every power device requires p-type doping, whether in an active region or for electrostatic control. In this work, we demonstrate p-n heterojunctions formed by p-type CuI synthesized on n-type β-Ga_2O_3 and show the potential for use in power devices. X-ray photoelectron spectroscopy (XPS) confirms the presence of CuI, where the copper is in the +1 oxidation state (Cu 2p) and iodine is in the -1 oxidation state (I 3d) based on the binding energies. Results from Hall effect measurements on the CuI films show p-type conductivity, with hole mobility of ~6.5 $cm^2/V·s$. Heterojunctions to β-Ga_2O_3 demonstrate rectifying characteristics with high forward current and low reverse leakage.

Fr3F3.7 **Ga_2O_3 Vertical Trench SBDs and FETs**

05:00 PM *Kohei Sasaki, Quang Tu Thieu, Daiki Wakimoto, Yuki Koishikawa, Akio Takatsuka and Akito Kuramata (Novel Crystal Technology, Inc., Japan); Shigenobu Yamakoshi (Novel Crystal Technology, Inc.)*

INVITED

DR 5 & 6

Gallium oxide (β-Ga_2O_3) is a suitable material for next generation high power devices because of its huge critical electric field strength. However, most current device structures are not enough to take advantage of the full potential of Ga_2O_3 because these structures are optimized for material properties of silicon. To bring out the potential of Ga_2O_3 , we propose a trench structure. We will share our recent progress with trench-type Ga_2O_3 devices.

EXHIBITORS

CSW 2018 - EXHIBITORS

The industrial exhibition at CSW 2018 plays a key role in the conference and helps to significantly reduce the registration fees to all attendees. Please show your appreciation to our exhibitors by visiting the exhibition. Thank you.

Booth Number	Company
1	EverBeing International Corp.
2	Hi-Solar Co., Ltd.
3	JX Nippon Mining & Metals
4	NTT Advanced Technology Corp.
5	Lake Shore Cryotronics, Inc.
6	Matheson Tri-Gas, Inc.
7	Plasma-Therm, LLC
8	WaferTech, LLC
9	Novel Crystal Technology, Inc.
10	DOWA Electronics Materials Co., Ltd.

DOWA ELECTRONICS MATERIALS CO.,LTD.

DOWA has been a leading supplier of GaAs wafers and GaAs based IR LEDs for 30 years. And we have been offering wide-bandgap materials such as high quality AlN template and AlGaN based UV LEDs for the last 10 years. We are looking for the opportunity for joint R&D projects in the area of wide-bandgap materials/wafers as well as Mid-wavelength IR LED & PDs.

EVERBEING INT'L CORP.

Everbeing is a world leading manufacturer of probe stations and micropositioners based in Taiwan. A probe station is an interface machine between testers and sample devices. With 25 years of history, we strive in producing reliable, precise, user-friendly products with affordable prices. Our inventory includes a broad range of probing accessories such as tips and tip holders. Our solutions cater to vast range of measurement applications which can be tailored to your specific needs.

Fraunhofer Heinrich Hertz Institute

Innovations for the digital society of the future are the focus of research and development work at the Berlin, Germany, based Fraunhofer Heinrich Hertz Institute (HHI). In this area, Fraunhofer HHI is a world leader in the development of mobile and optical communication networks and systems, fiber optical sensor systems as well as the processing and coding of video signals. Together with international partners from research and industry, Fraunhofer HHI works in the whole spectrum of digital infrastructure – from fundamental research to the development of prototypes and solutions. The institute develops standards for information and communication technologies and creates new applications as an industry partner. The Photonic Components department develops optoelectronic semiconductor components and integrated optical circuits for data transmission. Another focus is on infrared sensor systems, terahertz spectroscopy and high-performance semiconductor lasers for industrial and medical applications.

Hi Solar Optoelectronic Materials

Hi-Solar has been experienced for the past 16 years in sapphire substrate manufacturing. We are specialized in 2"-6" high-standard quality double side polished wafers for vertical LED substrates and 4"-8" quartz wafers for optoelectronic industry. We produce not only epi-ready wafers, but also offers repolishing(reclaim) service by removing GaN on sapphire surface while reducing costs by using our own patented technology.

JX Nippon Mining & Metals

ACROTEC

SEMICONDUCTOR MATERIALS

ACROTEC is the brand name for JX Nippon Mining & Metals Compound Semiconductor Materials (CSM) division.

We produce single crystal substrates InP, CdZnTe, CdTe, and ZnTe which are used in various

industries including Telecom, Imaging, Solar, Satellite, Etc. We also have a broad lineup of high purity metals.
JX continues to pursue the highest quality materials.

Supporting advanced research since 1968, Lake Shore Cryotronics is a leading innovator in measurement and control solutions for low temperature and magnetic field conditions. High-performance solutions from Lake Shore include Hall effect measurement systems for a broad range of material research applications, particularly those requiring temperature-dependent (15 K to 1273 K) and low-mobility material measurements; cryogenic probes stations for on-wafer probing of material samples at variable temperatures and in fields to more than 2 T; and award-winning, electromagnet-based VSMs. Also available: industry-leading cryogenic temperature sensors, controllers, and monitors, and instruments for measuring and controlling magnetic fields in research applications.

MATHESON is a single source for industrial, medical, specialty and electronic gases, MOCVD equipment, height performance purification systems, engineering and gas management services. Our mission is to deliver innovative solutions for global customer requirements.

NTT Advanced Technology has been providing extensive products and services, such as Nano technology, Network, Security, based on leading edge technologies to all types of Technology Companies, Universities, Laboratories, Government Entities and so on. Our GaN HEMT epi-wafer which is applicable for RF and Power device applications has been used by customers all over the world for both Production and R&D purposes for more than ten years. We are able to customize the layer structure and the 2DEG characteristics (the Sheet Resistivity, the Mobility and the Carrier Density) by tuning Al content of the barrier. Additionally, our GaN HEMT could be grown on Si, SiC, Sapphire, and GaN substrates so customers can choose the best substrates based on their preferences. We also provide a data of Surfscan, XRD-FWHM, bowing based on requests from customers.

Novel Crystal Technology Inc., established in June 2015, is a ‘carve-out’ venture from the TAMURA CORPORATION and technology transfer venture from the National Institute of Information and Communications Technology (NICT) in Japan.
We produce and sell gallium oxide substrates and epitaxial wafers for power device applications.
We also conduct R&D activities on gallium-oxide-based power devices. Regarding this new material ‘gallium oxide’ which has been rapidly attracting attention all over the world, our company is leading the world in both research and business areas.

Plasma-Therm is a U.S. manufacturer of advanced plasma-processing equipment, providing etch, deposition, and plasma dicing technologies used in semiconductor packaging, solid-state lighting, power, data storage, renewable energy, MEMS, nano-technology, photonics, and wireless communication markets. Plasma-Therm's global sales and service network supports over 600 commercial, academic, and governmental customers.

Wafer Technology, a member of the IQE plc group of companies, manufactures the world's broadest range of III-V substrates (GaAs, InP, GaSb, InSb and InAs) using both VGF and LEC growth techniques. Material is supplied as epi-ready substrates in 2”, 3” and 4'' diameter. All products are manufactured at the company’s Milton Keynes (U.K.) headquarters according to ISO 9001/14001 certified processes.

Note: The profiles above were provided by the Companies/Exhibitors

EVERBEING INT'L CORP.

Your Partner in Probing Solutions

Everbeing (EB) is a world leading manufacturer of probe stations and micropositioners based in Taiwan. With 25 years of history, we strive in producing reliable, precise, user-friendly products with affordable prices. Our inventory includes a broad range of probing accessories such as tips and tip holders. Our solutions cater to vast range of measurement applications which can be tailored to your specific needs.

Probe Stations

We offer stations capable of DC, RF, HVHC from 2" to 12" chucks. All are equipped with high resolution X-Y stages and stainless steel vacuum chucks. Microscope X-Y travel and chuck z-motion are among several options that can be included on our stations.

Above image is our smallest station yet. Please visit our booth to view the demo.

RF Probing

Our solutions cover a broad range of frequencies. For sub-90 GHz, our probe holders can be fix your RF probe heads for accurate and reliable probing. For higher frequencies, we manufacuture custom positioners that best fit your signal extenders.

Image above is our positioner holding an Anritsu extender and GGB probe

Micropositioners

From resolution as large as 5 µm to as small as 0.2 µm, EB micropositioners cover your needs. All offerings feature linear X-Y-Z motion with a 12mm travel range in all 3 axes. Included is a magnet switch for swift setup on and between stations.

Image references EB-050E, our most popular micropositioner.

No. 1 Jinshan 2nd St.
Hsinchu, 30080 Taiwan, R.O.C

www.everbeingprober.com
(647) 787-8816

Fraunhofer
Heinrich Hertz Institute

PHOTONIC COMPONENTS AT HHI

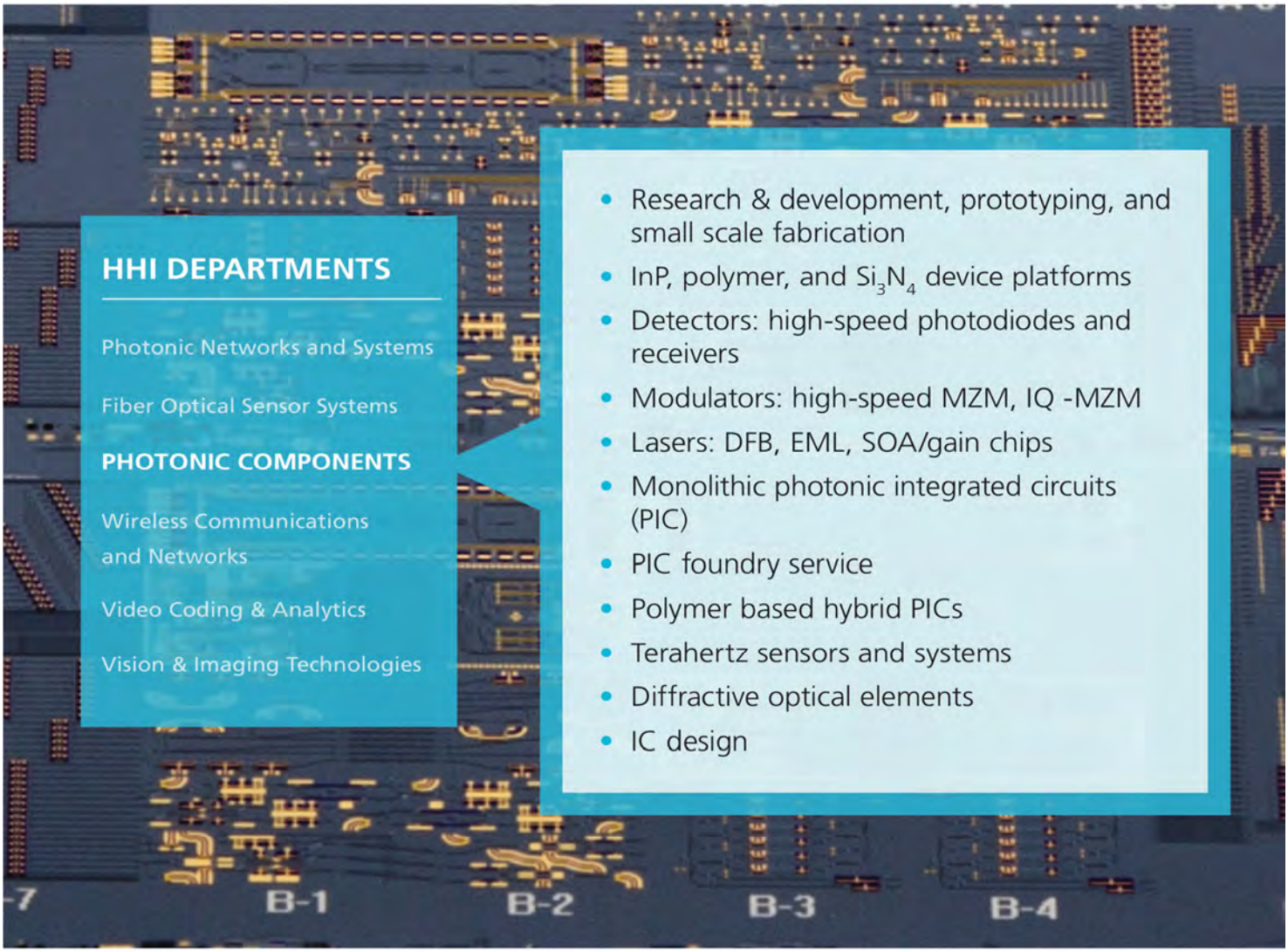

Contact

Fraunhofer Institute for Telecommunications,
Heinrich Hertz Institute, HHI
Einsteinufer 37
10587 Berlin

phone +49 30 31002-0
www.hhi.fraunhofer.de/en/departments/pc

Hi Solar
Optoelectronic Materials

What we do?

Reclaim Service
Sapphire
SiC
InP

Special Spec. Wafer for R&D
Sapphire
Si
SiC
GaN
Quartz
Glass

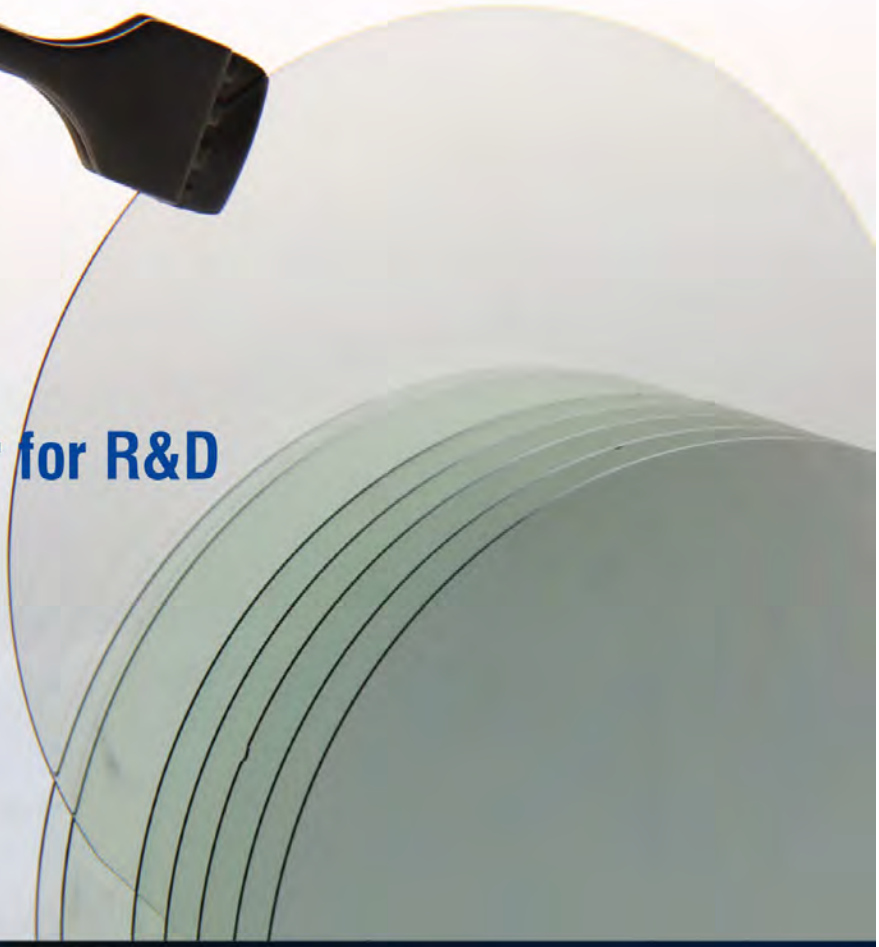

313, Cheomdangwagi-ro, Buk-gu, Gwangju, South Korea 61008
T +82 (62) 973-0490 F +82 (62) 973-0489 W www.hisolarled.co.kr
E david@hisolarled.com or chonhh@hanmail.net

ACROTEC

SEMICONDUCTOR MATERIALS

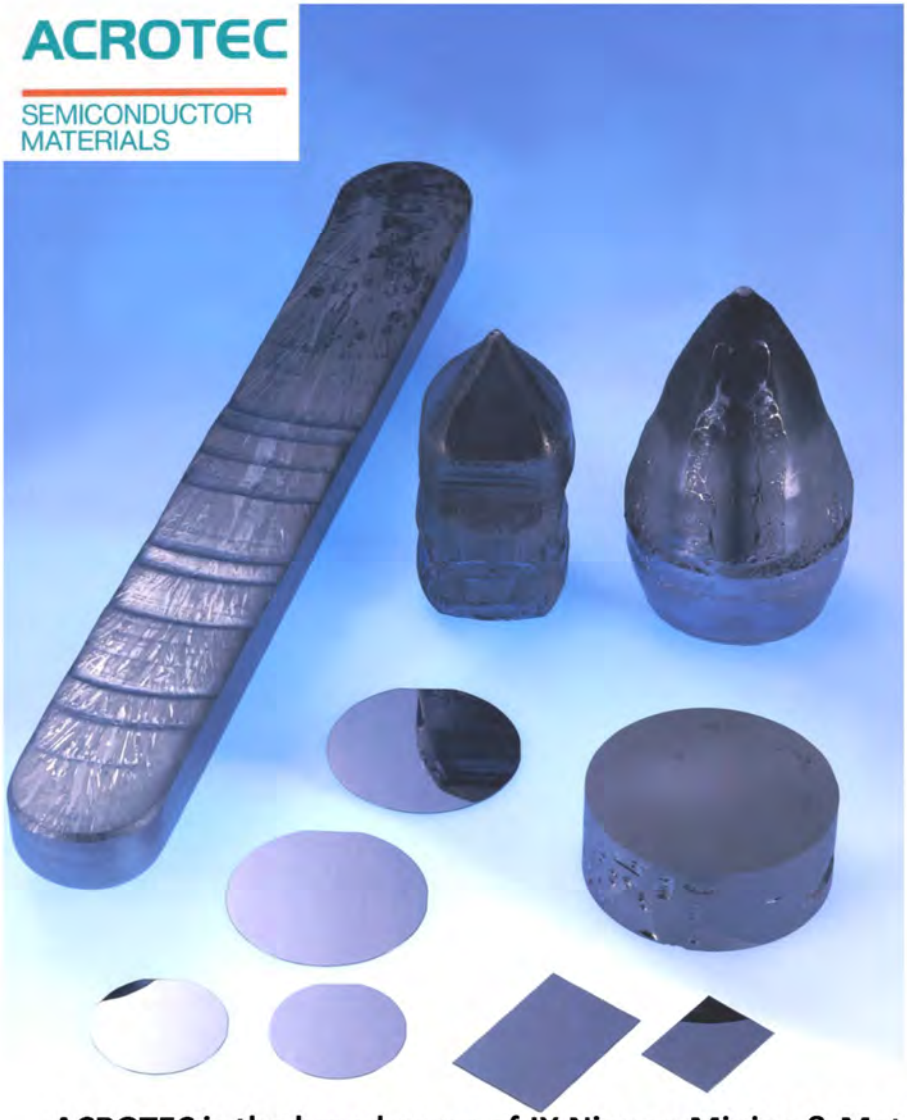

SINGLE CRYSTALS

InP (Dopants: S, Sn, Zn, Fe, None
Size:2inch , 3inch and 4inch)
CdTe, CdZnTe (Size:1x1~8x8cm2)

SOURCE MATERIALS

InP polycrystalline

HIGH PURITY METALS

In:7N, 6N
Cd:7N, 6N
Te:7N, 6N
Cu:9N, 6N
Ni:6N, 5N
Zn:6N, 5N
Ag:6N
etc.

ACROTEC is the brand name of JX Nippon Mining & Metals high quality Compound Semiconductor Materials. Our product line includes single crystal substrates InP, CdZnTe, ZnTe and high purity metals including 7N Indium, 6N Copper, 6N Silver, and many others.

JAPAN
JX Nippon Mining & Metals Corporation
Compound Semiconductor Department
1-2, Otemachi 1-chome, Chiyoda-ku, Tokyo 100-8164, Japan
TEL:+81-3-6257-7417 FAX:+81-3-6213-3609

NORTH AMERICA
JX Nippon Mining & Metals USA, Inc.
125 North Price Road, Chandler Arizona 85224 U.S.A.
TEL:+1-480-732-9857 FAX:+1-480-899-0779
sales@nmm-jx-group.com

EUROPE
JX Nippon Mining & Metals Europe GmbH
Neue Mainzer Str.20 60311 Frankfurt am Main, Germany
TEL:+49-(0)-69-2193653-0 FAX:+49-(0)-69-2193653-20
saleseurope@nmm-jx-group.com

TAIWAN
Nikko Metals Taiwan Co., Ltd / Longtan Works
No. 88, Longyuan 1 St Rd., Longtan Dist.,
Taoyuan City 32542, Taiwan R.O.C.
TEL:+886-3-499-1699 FAX:+886-3-499-1320

SINGAPORE
JX Nippon Mining & Metals Singapore Pte. Ltd.
16 Raffles Quay, #33-04 Hong Leong Building Singapore 048581
TEL:+65-6225-5413 FAX:+65-6227-0373

Advancing
Materials Characterization

Lake Shore offers precision platforms for materials research

Hall Effect Measurement Systems

Robust systems with advanced software for measuring Hall voltage, Hall coefficient, Hall mobility, resistivity, and more in a broad range of research applications.

- Ideal for variable temperature measurement and mobilities from 1 to 10^6 $cm^2/V\,s$
- Optional AC field extends mobility measurement range down to 10^{-3} $cm^2/V\,s$
- High and low resistance options
- Multi-carrier analysis option

Ideal for characterizing:
elemental semiconductors • transparent conducting oxides • compound semiconductors

Cryogenic Probe Stations

Micro-manipulated, precisely controlled platforms for better semiconductor measurements as a function of temperature and magnetic field.

- Fully tested on-wafer probing solutions for DC, RF, microwave, and THz-frequency measurements
- Optimized for C-V, I-V, pulsed I-V, and Hall effect measurements over a range of temperatures
- Ensure stable operation and reliable, repeatable measurements
- Cryogen and cryogen-free cooled configurations

Ideal for characterizing:
GaN and other wide-band gap devices • HEMTs • TMD and 2D materials

Stop by the Lake Shore table at Compound Semiconductor Week

Lake Shore CRYOTRONICS

50 YEARS

1968 — 2018

575 McCorkle Blvd, Westerville, OH
614.891.2243 | **www.lakeshore.com**

MATHESON MOCVD Solutions

MATHESON, as part of the TNSC Group, is uniquely qualified to provide end-to-end solutions for the MOCVD and compound semiconductor industry.

TNSC's world class MOCVD and compound semiconductor equipment technology combined with MATHESON's specialty gas, site service, purification and exhaust gas abatement solutions provide comprehensive and customized offerings for customers.

MATHESON offers Total Solutions Management for MOCVD Applications

- TNSC MOCVD Tools
- ULTIMA™ Ammonia, Arsine, and Phosphine
- Bulk and On-site Gas Production Solutions
- Process and Gas Handling Equipment
- NANOCHEM® Purification Systems
- Site Services, OEM Configurations and Turnkey Installations
- Specialized Cl_2 Dry Cleaning Systems
- Exhaust Gas Abatement Solutions

Product Line Up

GaAs, InP

Model	Type	Wafer Face	Wafer Size	Application
VR-3000	Vertical	Face up	3"x 1 wafer	Research
HR-3000	Horizontal	Face up	3"x 1 wafer	Research, Development
HR-4000	Horizontal	Face up	2"x 3 wafers	Development, Production
HR-6000	Horizontal	Face down	2"x 6 / 3"x 3 wafers	Development, Production
HR-8000	Horizontal	Face down	3"x 6 / 2"x 18 / 4"x 4 wafers	Development, Production
HR-10000	Horizontal	Face down	4"x 5 / 3"x 10 wafers	Production
BMC	Rotation & Revolution	Face down	2"x 42 ~ 6"x 6 wafers	Production

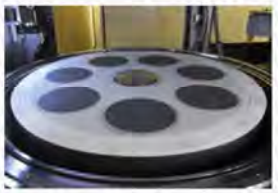

GaN

Model	Type	Wafer Face	Wafer Size	Application
SR-2000	Horizontal	Face up	2"x 1 wafer	Research
SR-4000	Horizontal	Face up	2"x 3 / 4"x1 wafers	Development, Production
SR-6000	Horizontal	Face up	2"x 6 / 3"x 3 / 6"x 1 wafers	Development, Production
UR25K	Rotation & Revolution	Face up	4"x 11 / 6"x 7 wafers	Production
UR26K	Rotation & Revolution	Face up	6"x 10 / 8"x 6 wafers	Production

*Customized MOCVD design/manufacturing to customer specification available upon request.

MATHESON
ask. . .The Gas Professionals™
A Taiyo Nippon Sanso Group Company

USA Office
150 Allen Road, Suite 302 Basking Ridge, NJ 07920
908-403-3304
www.mathesongas.com / www.mocvd.jp
email: infoMOCVD@mathesongas.com

https://www.linkedin.com/in/mathesonmocvd https://twitter.com/MTG_MOCVD https://www.facebook.com/MOCVD/

Gallium Oxide (Ga_2O_3) Substrates and Epitaxial Wafers

Novel Crystal Technology, Inc.
2-3-1 Hirosedai Sayama-shi Saitama 350-1328
TEL.+81-4-2900-0072 FAX.+81-4-2900-0059
http://www.novelcrystal.co.jp/ mail:sales@novelcrystal.co.jp

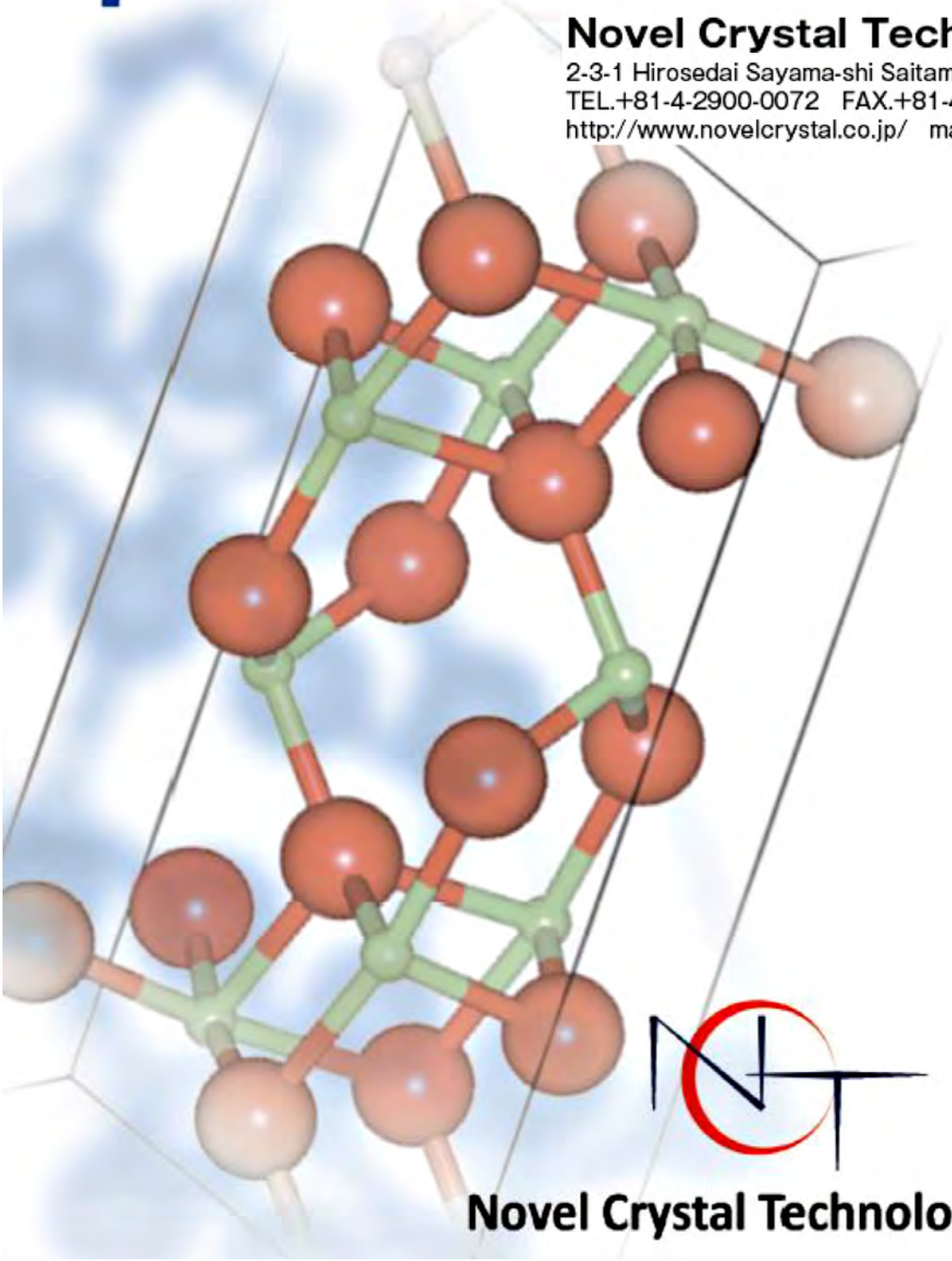

Novel Crystal Technology, Inc.

NTT-AT specializes in GaN epitaxial growth for Various Applications

GaN HEMT structure on Si sub.

Various Substrates with different wafer sizes are available

Substrate	Si	Sapphire	SiC	GaN
Wafer size	2"* – 8"	2" – 3"*	2" – 6 "	2" – 4 "

*Please check with NTT-AT when the 4 inch sapphire is compulsory for the growth.
*2inch Si can be used for the growth when customers can provide their own Si sub.

Typical Example of RF performances/Large signal for RF applications (on SiC)

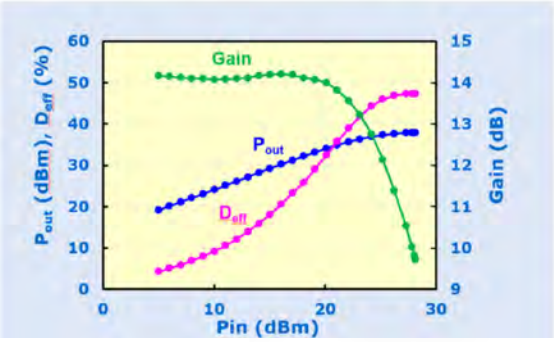

Typical Example of Leak current density for power application (on Si)

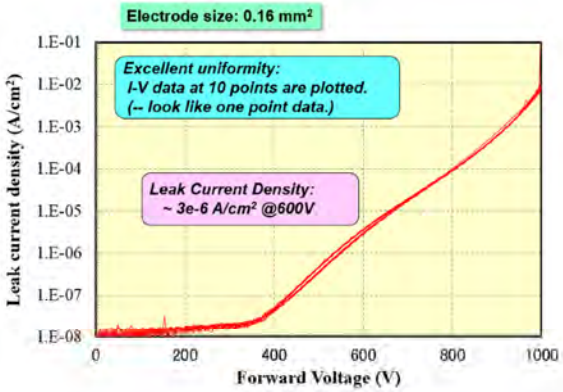

For more information and inquiry, please check NTT-AT's web site:
http://www.ntt-at.com/product/epitaxial/

NTT Advanced Technology Corporation

Where do CS Researchers find the best solutions?

- IC Manufacturing & Packaging
- Wireless
- Photonics
- Solid-State Lighting
- MEMS/NEMS
- Nanotechnology
- Renewable Energy
- Data Storage
- Photomask
- Research & Development

Plasma-Therm.

When you need help overcoming technical hurdles to bring your latest ideas to fruition, come to Plasma-Therm. You'll get solutions custom-tailored to your specific needs, backed by our breadth of experience, leading-edge technology, and innovative thinking. For more than 40 years we've been enabling Compound Semiconductor researchers to exceed the limits of what is possible. Bring us your challenges and together we'll redefine the boundaries.

Plasma-Therm

plasmatherm.com
sales@plasmatherm.com
+1.727.577.4999

Wafer Technology

- the universal choice

Wafer Technology's unrivalled range of materials, crystal growth techniques and product forms, provides high quality material solutions, whatever the application.

- Epitaxy Ready Wafers
- Polycrystalline Materials
- As-Cut Wafers
- MBE Source Materials
- Speciality Materials

GaAs InP InAs InSb GaSb *for all your III-V needs*

WAFER TECHNOLOGY LTD

Head Office and Manufacturing Plant
34 Maryland Road Tongwell Milton Keynes Bucks MK15 8HJ England United Kingdom
Telephone: +44(0)1908 210444 www.wafertech.co.uk sales@wafertech.co.uk

WAFER TECHNOLOGY LTD

SPONSORS

Cambridge / Boston, Massachusetts

CSW2018

CSW 2018 - SPONSORS

CSW 2018 would not have been possible without the strong support of our Sponsors. The CSW Organizing Committee sincerely appreciates their contribution to the conference and their commitment to the success of the Compound Semiconductor community.

Sponsorship Level	**Sponsors**
Platinum	Analog Devices Inc (ADI)
	MACOM
	The National Science Foundation
	Office of Naval Research
Gold	IQE
	Qorvo
Silver	Agnitron Technology Inc
	AIXTRON SE
Others	Massachusetts Institute of Technology
	Microsystems Technology Laboratories
	MIT.nano
	Institute of Electrical and Electronics Engineers (IEEE)

Microsystems Technology Laboratories and MIT.nano:
>35 years of micro-and nanoscale research at MIT

Engineering and science of the very small continues to surprise and delight us. It has been doing so at MIT for well over 35 years. MTL, the **Microsystems Technology Laboratories**, was created in the early 80s to bring faculty and students together to share experimental resources to advance the then emerging field of silicon integrated circuit technology. What happened in the following 35 years has been nothing but astounding. The microelectronics revolution has transformed human society like no other technology before. In fact, no other human endeavor has enjoyed sustained exponential progress over such a long time to such great benefit to us all.

What was perhaps unexpected 35 years ago was that the increasing ability to precisely engineer small and very complex structures would extend to materials well beyond silicon and far passed the initial set of applications in electronics. We have marveled at the explosion of creativity in fields as diverse as chemical engineering, mechanical engineering, material science, aeronautics and astronautics, biology and many others. MIT, through the facilities and services of MTL, has played a leading role in this exhilarating quest.

A key design principle of MTL has been the broad sharing of lab resources. This has made it possible for MIT to afford complex and costly equipment requiring extensive facilities, as well as expensive and sophisticated design software. A commitment to sharing also contributes to creating a large and diverse community of engineers and scientists that learn together, help each other, and collaborate on serendipitous projects that happen because they hang out together in the lab, in all manner of gatherings, or in social events.

35 years later, MIT is about to double down on its interest in the very small by opening a new center for exploration and innovation of nanoscience and nanotechnology right at the heart of campus. This is

MIT.nano. Founded on the principles that made MTL successful, MIT.nano will continue to explore the potential of the nanoworld to solve some of the world's most urgent problems in areas of transportation, communications, energy, health, computation, water and the environment.

MIT.nano is based on a new state-of-the-art 214,000 square foot (20,000 m^2) building that includes more than 47,000 sq ft (4,400 m^2) of clean room process space plus additional spaces for imaging/characterization, teaching and system prototyping. This new advanced facility will support the research, education, and entrepreneurship activities of the entire MIT community and partners.

MIT.nano is more than a facility; it extends well beyond its physical structure and research capabilities. It is defined by a diverse community of explorers, innovators, and pioneers with a thirst for all things nano, … researchers who tinker with atoms, one by one, and from these fantastically small building blocks, they construct a future of infinite possibility. Their shared journey of discovery, aided by the tools of MIT.nano, will lead to solutions to define our era.

The Nano Age is upon us, and MIT is ready.

-Jesús A. del Alamo,
Director,
Microsystems Technology Laboratories

-Vladimir Bulović,
Founding Director,
MIT.nano

Analog Devices, Inc. is a leading global high-performance analog technology company. Our products and technologies intelligently bridge the physical and digital domains through sensing, measuring, powering, connecting and interpreting. We design, manufacture and market a broad portfolio of solutions that leverage high-performance analog, mixed-signal and digital signal processing technology, including integrated circuits (ICs), algorithms, software, and subsystems. Since our inception in 1965, we have focused on solving our customers' toughest signal processing engineering challenges and playing a fundamental role in converting, conditioning, and processing real-world phenomena such as temperature, pressure, sound, light, speed, and motion into electrical signals to be used in a wide array of electronic devices.

MACOM is driving the industry's broadest portfolio of MMICs, diodes and transistors for the entire RF signal chain, enabling customers' most critical applications including SATCOM, T&M, ISM and current 4G-LTE to 5G connectivity. With our broad portfolio of technologies and products, we're helping customers achieve leading bandwidth, power, and reliability.

The National Science Foundation (NSF) is an independent federal agency created by US Congress in 1950 "to promote the progress of science; to advance the national health, prosperity, and welfare; to secure the national defense..." NSF support basic research and people to create knowledge that transforms the future.

The Office of Naval Research (ONR) coordinates, executes, and promotes the science and technology programs of the United States Navy and Marine Corps.

IQE is the leading global supplier of advanced semiconductor wafers with products that cover a diverse range of applications, supported by an innovative outsourced foundry services portfolio that allows the Group to provide a 'one stop shop' for the wafer needs of the world's leading semiconductor manufacturers.

Qorvo is the leading GaN RF supplier for the defense and cable industries. Since 1999, the company has been driving GaN research and innovation, offering proven GaN circuit reliability and compact, highly efficient products. Qorvo is a

Defense Manufacturing Electronics Agency accredited 1A Trusted Source, having completed the Defense Production Act Title III GaN on SiC program in 2014. The Company remains the only GaN supplier to achieve Manufacturing Readiness Level (MRL) 9. Qorvo drives the innovation of GaN products for next-generation systems – from DC through Ka-band – that offer robust performance, low maintenance and long operational lifetimes.

Agnitron Technology, Inc. is a compound semiconductor technology company and supports MOCVD equipment-related needs of R&D and production users. Agnitron's Agilis Series MOCVD Equipment Line offers a menu of options for reactor designs (single or dual), source configurations, metrology and many other performance items for advanced and flexible capabilities. Agilis offers configurations which support material growth capabilities for III-V, oxide, 2-D/TMD and many other related materials. Agnitron's Imperium Control Software and matched PLC package solutions offer sophisticated and reliable capabilities for production users as well as flexibility for users requiring updated control capabilities for legacy, modified or custom equipment. Visit www.agnitron.com or contact sales@agnitron.com for more information about our products and services.

AIXTRON

AIXTRON SE is a leading provider of deposition equipment to the semiconductor industry. The Company was founded in 1983 and is headquartered in Herzogenrath (near Aachen), Germany, with subsidiaries and sales offices in Asia, United States and in Europe. AIXTRON's technology solutions are used by a diverse range of customers worldwide to build advanced components for electronic and opto-electronic applications based on compound, silicon, or organic semiconductor materials. Such components are used in a broad range of innovative applications, technologies and industries. These include LED applications, display technologies, data storage, data transmission, energy management and conversion, communication, signalling and lighting as well as a range of other leading-edge technologies.

For further information on AIXTRON please visit our website at: www.aixtron.com.

RF Matters Here

MACOM has RF Engineering Expertise, Surety of Supply and Manufacturing Scale

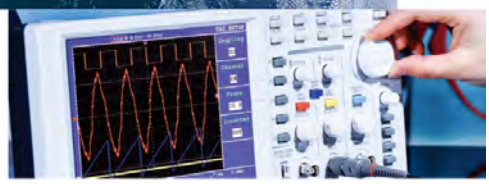

Join the Next Generation

MACOM's 65-year legacy of innovation is driving the industry's broadest portfolio of MMICs, diodes and transistors for the entire RF signal chain. These trusted high-performance RF devices enable your most critical applications including SATCOM, T&M, ISM and current 4G LTE to next-gen 5G connectivity.

With our state-of-the-art technology and high-performance products, we're helping customers achieve leading bandwidth, power, packaging and reliability.

Learn more at www.macom.com

MACOM™

Feed Your Genius

Check out our design hub

Qorvo is a Proud Sponsor of Compound Semiconductor Week 2018.

MatchCalc™
RF Design Calculator

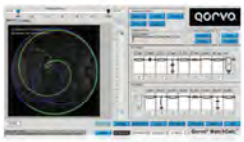

Qorvo connects the world. From the IoT and smartphones to defense and everything in between. Explore our resources to find out how.

Downloadable Software

Qorvo MatchCalc™

GaN Models

#Modelithics® Qorvo GaN Library

- Videos
- eBooks
- Whitepapers
- Blogs
- Design Tools
- Brochures
- Block Diagrams
- Published Articles

qorvo

www.qorvo.com/designhub

10 Years of MOCVD Solutions and Services

2018 marks the 10th anniversary of Agnitron Technology serving the MOCVD community. Our team is celebrating a number of notable achievements made possible by decades of collective experience in the industry.

- Expansion of Agilis MOCVD Series to include configurations for ß-Ga_2O_3, III-V and TMD materials
- Expanding Laser Diode Production MOCVD Equipment Offering
- More than 50 MOCVD Systems Operating with Imperium-MOCVD Control Software

OEM MOCVD Systems

Refurbished and Upgraded MOCVD

PLC and Control Software Upgrades

MOCVD Support & Maintenance Services, Facility Planning

Agnitron is a supplier of Original and Certified Refurbished/Upgraded MOCVD Equipment for R&D and production applications. Over the course of 10 years a comprehensive line of products has been developed and we've established a strong record supplying high-performance MOCVD equipment. Our advanced Imperium Control Software and matched PLC package solutions offer sophisticated and reliable capabilities for production users as well as flexibility for users requiring upgrades for unsupported, modified or custom equipment. Various configurations within the Agnitron Agilis MOCVD Equipment Series support growth work for standard and highly specialized III-V, oxide, TMD and many other related applications.

agnitron technology

www.agnitron.com
sales@agnitron.com
+1 952.937.7505

AIXTRON

Our technology. Your future.

YOU THINK,

GLOBAL MEGA TRENDS REQUIRE BEST PERFORMANCE III-V MATERIALS

WE THINK THAT TOO.

THE AIX 2800G4-TM

3D-SENSING
AUGMENTED REALITY
AUTONOMOUS DRIVING
CLOUD COMPUTING
INTERNET OF THINGS/5G
NEXT GENERATION DISPLAYS

DISCOVER THE AIX 2800G4-TM.

Tool of Record for all AsP-based materials for next generation applications.

Market leading technology delivering best yield combined with highest productivity in the industry.

AIXTRON SE
info@aixtron.com · www.aixtron.com

AUTHOR INDEX

Cambridge / Boston, Massachusetts

CSW2018

NOTES

NOTES

NOTES

Cambridge / Boston, Massachusetts

CSW2018

COMPOUND SEMICONDUCTOR WEEK 2018

MAY 29 - JUNE 1, 2018
Massachusetts Institute of Technology
Cambridge, MA, USA

Thank you to our Sponsors!

PLATINUM SPONSORS

GOLD SPONSORS

SILVER SPONSORS

Massachusetts Institute of Technology

MTL microsystems technology laboratories

MIT.nano

Compound Semiconductor Week (CSW 2018)
Cambridge, Massachusetts, USA

Tuesday (May 29)

DR5&6
SHORT COURSE
(Jeehwan Kim) Intro
Joshua Yang (U Mass)
Coffee Break
Ilia Valov (Aachen)
Coffee Break
Wilfried Haensch (IBM)
Lunch for Short Course Attendees
Plenary (Walker Memorial)
(Tomás Palacios)
Welcome remarks
Hiroshi Fujioka (Tokyo)
Evelyn Hu (Harvard)
Coffee Break
(Grace Huili Xing)
Mark Rodwell (UCSB)
Dario Gil (IBM)
Award Ceremony
Group Photo
Welcome Reception (MIT Museum, N51)

Wednesday (May 30)

Salon M	DR 3&4	Salon T	DR 5&6
A1-NBG (quantum)	**B1-WBG (AlGaN)**	**C1-RF (III-V)**	**D1-Power(bulk)**
(A.Liu)	(Q. Sun)	(M. Chumbes)	(E. Matioli)
A1.1 J. Shabani	B1.1 X. Liu	C1.1 T. Takahashi	D1.1 Y. Zhang
	B1.2 A. Mishima		D1.2 K. Nomoto
A1.2 E. Repiso (S)	B1.3 H.Miyaki	C1.2 D. Stoppel (S)	D1.3 S. Usami (S)
A1.3 E. Luna		C1.3 A. Vardi	D1.4 C. Gupta (S)
A1.4 Y. Zhang	B1.4 K-Hui. Li (S)	C1.4 A. Jonsson (S)	D1.5 J. Wang (S)
	B1.5 R. Blasco	C1.5 W. Lu (S)	D1.6 L. Cao (S)
Coffee Break			
A2-Lasers	**B2-WBG (GaN-Si)**	**C2-RF (RTDs)**	**D2-Power (GaN)**
(Tournie/Davannco)	(H. Miyake)	(G.Weimann)	(S. Pendharkar)
A2.1 J. Wang	B2.1 L. Zhang	C2.1 E. Wasige	D2.1 H. Fu (S)
A2.2 T. Aihara	B2.2 A. Tanaka(S)		D2.2 Abudul Khadar(S
A2.3 H. Huang	B2.3 Q. Sun	C2.2 J. Encomendero(S	D2.3 J. Ma (S)
A2.4 X. Lu		C2.3 K. Arzi (S)	D2.4 W. Choi (S)
A2.5 J. Bowers	B2.4 A. Alhassan	C2.4 M. Kim (S)	D2.5 O. Kokasaldi (S
	B2.5 D. Lee (S)	C2.5 A. Al-Khalidi	D2.6 A. Cutivet (S)
A2.6 D. Wei (S)	B2.6 T. Takeuchi	C2.6 M. Nagase	D2.7 M. Uren
A2.7 M. Nomura		C2.7 J.Inn. Chyi (S)	
Lunch			
A3-NBG	**B3-WBG**	**C3-RF (NBG)**	**D3-Power (GaN)**
(J. Bowers)	(T. Takeuchi)	(L.E. Wernersson)	(M. Uren)
A3.1 Eric Tournie	B3.1 J. Kim (S)	C3.1 J. del Alamo	D3.1 K. Fu (S)
	B3.2 A. Singh		D3.2 S. Bouchilaoun(S
A3.2 B. Shi (S)	B3.3 M. Crawford	C3.2 T. Kanazawa	D3.3 M. Yuan(S)
A3.3 G. Cole		C3.3 C. Zota	D3.4 Q. Lyu (S)
A3.4 S. Law	B3.4 S.Bharadwaj(S	C3.4 F. Lindelow (S)	D3.5 F. Brunner
	B3.5 M. Laurent	C3.5 X. Cai (S)	D3.6 C. Liu
Coffee Break			D3.7 Odnoblyudov
A4-Lasers	**B4-WBG**	**C4-Organic**	**D4-2D Materials**
(S. Law)	(M. Crawford)	(D. Gundlach)	(J. Heron)
A4.1 H. Esmaielpou	B4.1 W. Xing (S)	C4.1 D. DeLongchamp	D4.1 C. Hinkle
A4.2 A. Yangui	B4.2 F. Iucolano		
A4.3 Chang-Hasnain	B4.3 Z. Cheng (S)	C4.2 S. Engmann	D4.2 M Heilmann
	B4.4 J. Casamento	C4.3 S. Zhang	D4.3 S. Fullerton
A4.4 H.-W. Choi	B4.5 A. Sampath	C4.4 A. Takeuchi (S)	
P1: Poster Session (with hors d'oeuvres) Walker Memorial (50-140)			
Rump Session (Wong Auditorium E51, MIT)			

Thursday (May 31)

Salon M	Wong(E-51)	Salon T	DR 5&6
A5-Lasers	**B5-WBG**	**C5-Novel Materials**	**D5 RF-Power**
(N. Tansu)	(Z. Mi)	(S. Fullerton)	(S. Chowdhury)
A5.1 C. Gmachl	B5.1 R. Liu (S)	C5.1 M. Hersam	D5.1 W. Sun (S)
	B5.2 S. Goodman(S)		D5.2 J. Bergsten (S)
A5.2 H. Detz	B5.3 D. Feezell	C5.2 H. Zhao (S)	D5.3 W. Muhea (S)
A5.3 A. Rajeev(S)		C5.3 X. Yan (S)	D5.4 S. Pasayat (S)
A5.4 C. Canedy	B5.4 C. Lund	C5.4 A. Ferrari	D5.5 R. Howell
A5.5 Y. Tian(S)	B5.5 C. Haughn		
Coffee Break			
A6-Lasers	**B6-WBG-NS**	**C6-Novel Materials**	**D6 Ga2O3-WBG**
C. Gmachl/J.Shabani	(J.C. Harmand)	(C. Hinkle)	(M. Tadjer)
A6.1 A. Lyakh	B6.1 Behzadirad	C6.1 C. Palmstrom	D6.1 A. Kyrtsos (S)
	B6.2 H. Sekiguchi		D6.2 J. Zhu
A6.2 H.-H. Yuan(S)	B6.3 E. Calleja	C6.2 F. Hartmann	D6.3 K. Kaneko
A6.3 M. Lee		C6.3 Y Zhang	D6.4 H. Fu (S)
A6.4 J. Kwoen	B6.4 A. Roshko	C6.4 J. Heron	D6.5 J. Noh (S)
A6.5 S. Q. Yu	B6.5 M. Nami		D6.6 Z. Hu
	B6.6 I Rousseau(S)	C6.5 J. Han (S)	D6.7 R. Peterson
A6.6 X. Wang (S)	B6.7 X. Huang (S)	C6.6 H. Alsalman	
Lunch			
Excursion to downtown Boston (pre-registration required)			
Buses departing from Samberg Conference Center at 12:40pm and 3:10pm for 1pm and 3:30pm tours respectively.			
Conference Banquet (Fenway Park, Red Sox Stadium) (pre-registration required) Buses departing from Samberg Conference Center at 5:45pm			

Friday (June 1)

Salon M	DR3&4	Salon T	DR5&6
P2: poster session (with breakfast) Walker Memorial (50-140)			
Coffee Break			
A7-Photonics	**B7-Nanostructures**		**F1-Ga2O3 Keynotes**
(S.Q. Yu)	(C. Zota)		**(S. Fujita)**
A7.1 M. Belkin	B7.1 K. Tomioka		F1.1 M. Higashiwaki
	B7.2 G. Santoruvo (S)		F1.2 J. Speck
A7.2 M. Monavaria	B7.3 W.J. Hsueh (S)		
A7.3 A. Ajay (S)	B7.4 L.E. Wernersson		F1.3 Y. Kumagai
A7.4 X. Huang (S)			
A7.5 C. De Santi	B7.5 T. Takahashi		F1.4 S. Rajan
A7.6 P. Boucaud	B7.6 I. Rodrigues (S)		
	B7.7 S. Tommaso (S)		
Lunch			
A8-Photonics	**B8-Nanostructures**	**C7-Novel Materials**	**F2-Ga2O3 Gr&Char**
(M. Belkin)	(K. Tomioka)	(A. Khan)	**(S. Rajan)**
A8.1 A. Liu	B8.1 D. Ren	C7.1 M. Takahasi	F2.1 P. Mazzolini
	B8.2 K.W. Ng		F2.2 H. Sun
A8.2 Z. Yan (S)	B8.3 A. Bracker	C7.2 S. McKibbin	F2.3 M. Albrecht
A8.3 E. Delli (S)		C7.3 A. Devos	
A8.4 L. Megalini (S)	B8.4 T. Umezawa	C7.4 L. Lauhon	F2.4 A. Fiedler
A8.5 T. Okimoto	B8.5 Z. Zon (S)		F2.5 T. Onuma
Coffee Break			
A9-Photonics	**B9-Nanostrucures**	**C8-Novel Materials**	**F3-Ga2O3 Dev&Char**
(A. Lyakh)	(A Bracker)	(L. Lauhon)	(G. Jessen)
A9.1 M. Watts	B9.1 F. Bertram	C8.1 A. Khan	F3.1 O. Koksal(S)
	B9.2 G. Calabrese		F3.2 S. Mou
A9.2 Y. Akashi (S)	B9.3 J.C. Harmand	C8.2 A. Zubair (S)	F3.3 J. McGlone (S)
A9.3 CW Wang (S)		C8.3 R. Makin	F3.4 M Singh
A9.4 M. Davanco	B9.4 B. Connelly	C8.4 N. Samarth	F3.5 W. Li (S)
	B9.5 C.-S. Yang		F3.6 A. Koehler
A9.5 N. Grote	B9.6 L. Liborius (S)	C8.5 C. Volders	F3.7 K. Sasaki
A9.6 T. Endo	B9.7 T. Suemitsu		
A9.7 M. Diagne	B9.8 J. LaRoche		
Closing Ceremony (Samberg Salon M.I.T (7th fl.)			

Legend	
Plenary session	(S) Student Papers
Invited (30 min)	Special Events
Regular (15 min)	Focused session
Late news	Short Course

CSW 2018 Room Locations

DR 5&6 Samberg (SCC-6th floor)

DR 3&4 Samberg (SCC-6th floor)

Salon M Samberg (SCC-7th floor)

Salon T Samberg (SCC-7th floor)

CSW 2018 Room Locations

Walker Memorial 50-140 (142 Memorial Dr. Cambridge, MA)

Wong Auditorium E51 (2 Amherst St. Cambridge, MA)

CSW 2018 Off Campus Locations

MIT Museum N51 (265 Massachusetts Ave., Cambridge, MA)

Fenway Park 20 Jersey Street, Boston, MA Gate D